Participação do transporte de acetilcolina, do cálcio intracelular e do colesterol de membrana no ciclo de vesículas sinápticas em junção neuromuscular

Ernani Aloysio Amaral

Curso de Pós-Graduação em Biologia Celular
Instituto de Ciências Biológicas
Universidade Federal de Minas Gerais

Belo Horizonte, janeiro de 2010.

Participação do transporte de acetilcolina, do cálcio intracelular e do colesterol de membrana no ciclo de vesículas sinápticas em junção neuromuscular

Tese submetida ao Programa de Pós-Graduação em Biologia Celular do Instituto de Ciências Biológicas da Universidade Federal de Minas Gerais como requisito parcial para obtenção do título de Doutor em Biologia Celular

Orientadora: Profa. Dra. Cristina Guatimosim Fonseca

Belo Horizonte, janeiro de 2010.

Apoio Institucional

Este trabalho foi realizado no laboratório de Biologia da Neurotransmissão do Departamento de Morfologia do Instituto de Ciências Biológicas (ICB-UFMG) com o auxílio das seguintes instituições:

- Fundação de Amparo à Pesquisa do Estado de Minas Gerais (FAPEMIG);
- Conselho Nacional de Desenvolvimento Científico e Tecnológico (CNPq);
- Programa de Núcleos de Excelência (PRONEX);
- Coordenação de Aperfeiçoamento de Pessoal do Ensino Superior (CAPES).

Aos meus pais, José Geraldo e Cecília, pelos ensinamentos, incentivo e carinho.

À minha irmã Josane, pelo apoio constante.

À tia Dalva pela presença e acolhimento.

A Daila, pelo amor e ternura.

Agradecimentos

A Deus por iluminar e abençoar a minha vida e a minha trajetória de estudante.

À minha orientadora Cristina Guatimosim pela dedicação, compreensão, apoio e ensinamentos.

Aos meus familiares e amigos de Berilo pelo incentivo e constante aprendizado.

Aos meus amigos de lida no laboratório de Biologia da Neurotransmissão que se tornaram amigos eternos: Bento, Patrícia, Hermann, Monalise, Luciana, Débora, Lívia, Maíla, Graziele, Matheus e Matheus Castro.

Aos amigos do antigo laboratório de Neurofarmacologia: Célio, Janice, Bráulio, Cristina Martins, Fabiana e Xavier.

Aos colegas do curso de Pós-graduação em Biologia Celular por caminharem ao meu lado.

Aos Professores Marco Antônio Prado e Marcus Vinícius Gomez pelas oportunidades e ensinamentos.

Aos Professores Cristopher Kushmerick e Lígia Naves pela importante colaboração.

Ao amigo Ricardo Lima pela disponibilidade e empenho.

Aos professores da PUC-BH que muito contribuíram para minha formação acadêmica e humana: Lucília, Vânia, Antônio Mourthé, Edmundo, Stael e Raquel.

Aos professores e alunos do Instituto Metodista Izabela Hendrix pelo acolhimento e reconhecimento.

Sumário

Lista de Abreviaturas

Acetil-CoA	Acetil coenzima A
AChE	Acetilcolinesterase
2-APB	2-Aminoetoxidifenil borato
ATP	Trifosfato de Adenosina
BAPTA-AM	bis-(o-aminofenoxi)etano-N,N,N',N'-ácidotetracético
$CaCl_2$	Cloreto de cálcio
Ca^{2+}	Íon cálcio
CCCP	Carbonil cianeto *m*-clorofenildrazona
CCD	*Charge- coupled device*
CGP37147	7-Cloro-5-(2-clorofenil)-1,5-dihidro-4,1-benzotiazepina-2(3H)-um
ChAT	Colina acetiltransferase
CHT1	Transportador de colina de alta afinidade
CICR	*Calcium induced calcium release*
Cl^-	Íon cloreto
EGTA	Etilenoglicol-bis-β-aminoetil éster
EPP	*End-plate potential*
FM1-43	N-(3-*triethylammonium-propyl)-4-(4(dibutylamino)-styryl)pyridinium dibromide*
H^+	Íon hidrogênio
HEPES	Ácido N-2-hidroxietilpiperazida-N'-2-etanosulfônico
HRP	*Horseradish peroxidase*
HγCD	Hidroxi-propil-gama-ciclodextrina
Hz	Hertz
IP_3R	Receptor para inositol trifosfato
K^+	Íon potássio
KCl	Cloreto de potássio
Li^+	Íon lítio
LiCl	Cloreto de lítio
MßCD	Metil-ß-ciclodextrina
MEPPs	*Miniature end-plate potentials*
Mg^{2+}	Íon magnésio

$MgCl_2$	Cloreto de magnésio
ms	Milisegundo
nm	Nanômetro
Na^+	Íon sódio
nAChR	Receptor nicotínico para a acetilcolina
NaCl	Cloreto de sódio
Na^+/K^+ATPase	Bomba de sódio/potássio
NaOH	Hidróxido de sódio
NH_4Cl	Cloreto de amônio
NORP	*new31,5KD ouabain receptor protein*
pH	Potencial hidrogeniônico
RNA	Ácido ribonucléico
RNAm	RNA mensageiro
RyR	Receptor de rianodina
SNAP-25	*Synaptosomal-associated protein 25*
SNARE	*Soluble NSF attachment protein receptor*
TMB-8	8-(dietilamino)octil-3,4,5-trimetoxibenzoato
T-SNARE	*Target SNARE*
V	Volt
VAChT	Transportador vesicular de acetilcolina
VAChT KD	*Knockdowun* para o gene VAChT
$VAChT^{del/del}$	*Nocaute* para o gene VAChT
VAMP-2	*Vesicle associated membrane protein 2*
VGLUT	Transportador vesicular de glutamato
VH^+-ATPase	Bomba vesicular de íons hidrogênio
VMAT	Transportador vesicular de monoaminas
V-SNARE	*Vesicular SNARE*
µM	Micromolar
µm	Micrômetro

Lista de Figuras

Resumo

A biogênese e reciclagem de vesículas são etapas fundamentais para manutenção da neurotransmissão, impedindo que ocorra redução dos aglomerados vesiculares e bloqueio da função sináptica. Utilizando preparações de junção neuromuscular de camundongo e de rã, três importantes aspectos envolvendo o ciclo de vesículas sinápticas foram abordados neste trabalho de tese: 1) as conseqüências de alterações na expressão do transportador vesicular de acetilcolina (VAChT) sobre o ciclo sináptico; 2) a participação de estoques intracelulares de cálcio na exocitose de vesículas sinápticas induzida pela ouabaína; e 3) a importância do colesterol de membrana na biogênese e reciclagem de vesículas sinápticas. Os resultados obtidos mostraram que a redução na expressão do gene do VAChT não determinou alterações compensatórias no número e na área de terminações motoras presentes no diafragma de camundongos VAChT *knockdown*. Além disso, o número de vesículas aptas para a reciclagem bem como os passos de exo/endocitose estavam preservados nos animais *knockdown* homozigotos. Contudo, a ausência de expressão do VAChT leva ao aumento compensatório no número e na área de terminações motoras dos animais *nocaute*, sugerindo que a liberação de acetilcolina armazenada em vesículas via VAChT é essencial para o desenvolvimento normal de terminações motoras. Quanto à participação do cálcio intracelular na exocitose evocada pelo derivado esteróide ouabaína, os dados revelam que, embora a ouabaína iniba a endocitose, este glicosídeo cardiotônico promove liberação vesicular mobilizando cálcio armazenado no retículo endoplasmático e nas mitocôndrias via receptores de rianodina e trocador Na^{+}/Ca^{2+} mitocondrial, respectivamente. Na investigação sobre o papel do colesterol na biogênese e reciclagem de vesículas sinápticas, os resultados indicam que o seqüestro do colesterol de membrana aumenta a liberação espontânea de vesículas sinápticas, altera a amplitude e cinética de eventos em miniatura, porém inibe a exocitose evocada pelo KCl e a endocitose compensatória. Os dados obtidos com as investigações supracitadas contribuem para obtenção de princípios fundamentais sobre o funcionamento do sistema colinérgico e neurotransmissão em geral, podendo, no futuro, subsidiar meios para intervenção farmacológica em disfunções da transmissão sináptica central e periférica.

Abstract

Synaptic vesicles recycling is essential for the maintenance of neurotransmission by preventing the collapse of synaptic function. In this work, three important aspects of the synaptic vesicle cycle were investigated in preparations of mouse and frog neuromuscular junction: 1) the consequences of alterations in the expression of the vesicular acetylcholine transporter (VAChT) over synaptic vesicle cycle; 2) the involvement of intracellular calcium stores on the exocytosis evoked by the cardiotonic glycoside ouabain; and 3) the role of membrane cholesterol on the exo/endocytosis of synaptic vesicle. The results presented here indicated that the decrease in VAChT expression cause no compensatory alteration in the number and area of motor terminals at diaphragms of VAChT knockdown mice. Moreover the number of synaptic vesicles able to recycle and the steps of exo/endocytosis seemed to be preserved in knockdown homozygote animals. However the absence of VAChT expression caused an increase in the number and area of motor terminals at diaphragms of knockout mice. Data relating to ouabain-induced exocytosis showed that this glycoside promotes vesicle release recruiting calcium stored at endoplasmic reticulum and mitochondria through ryanodine receptors and mitochondrial Na^+/Ca^{2+} exchanger, respectively. As for the role of membrane cholesterol on synaptic vesicle cycle, the results indicated that cholesterol removal increased spontaneous vesicle release, modified amplitude and kinetics parameters of spontaneous events but inhibited K^+-evoked exocytosis. All aspects investigated in this work can contribute to broaden the knowledge about the cholinergic system and neurotransmission. Perhaps, in the future, the data presented here could subsidize pharmacological interventions on disturbs of peripheral and central synapses.

1 – Introdução

1.1 – Morfologia da Junção Neuromuscular

As sinapses são áreas especializadas de contato celular onde sinais são precisamente transferidos de um neurônio para uma célula alvo. Em sinapses químicas, um sinal elétrico resultante da propagação de correntes iônicas é convertido em um sinal químico, representado pela liberação de neurotransmissores que irão atuar sobre a célula alvo (Katz, 1966; revisado por Zhai & Bellen, 2004).

A junção neuromuscular é uma sinapse química colinérgica cuja função é transferir impulsos de uma terminação motora relativamente pequena para uma fibra muscular ampla e, assim, desencadear contração (Figura 1A). Portanto, ela funciona como um relé (Katz, 1966).

Em músculo esquelético de rã, o axônio motor dá origem em sua porção distal a um conjunto de ramos terminais não mielinizados de 1,5 μm de diâmetro que percorrem sulcos rasos na superfície da fibra muscular por extensões de aproximadamente 100μm (Figura 1A) (Katz, 1966). Ao longo de todo o curso da terminação, é possível observar, no plano ultraestrutural, regiões eletrondensas denominadas zonas ativas que marcam os sítios subcelulares da transmissão sináptica. Cada zona ativa pode ser identificada pela sua associação com aglomerados de vesículas sinápticas pequenas de aproximadamente 50nm de diâmetro que encerram acetilcolina em seu interior. Além das vesículas sinápticas pequenas elétronlúcidas, a terminação pré-sináptica apresenta também vesículas eletrondensas que armazenam peptídeos envolvidos com a modulação da transmissão, como o peptídeo relacionado ao gene da calcitonina (Figura 1B) (revisado por Hall & Sanes, 1993 e Burns & Augustine, 1995).

Compondo o aparato pré-sináptico estão presentes também canais para cálcio sensíveis à voltagem, dispostos em fileiras e intimamente associados à zona ativa, e que se encontram bem próximos aos aglomerados vesiculares (Harlow *et al.*, 2001). Esta disposição singular garante um rápido pico na concentração intracelular de cálcio nos sítios de exocitose durante o disparo da liberação vesicular, conferindo sincronia ao processo (Robitaille *et al*., 1990; revisado por Zhai & Bellen, 2004).

O elemento pós-sináptico, separado da membranana pré-sináptica por um espaço de aproximadamente 50nm de largura chamado de fenda sináptica, apresenta um grande número de receptores nicotínicos para a acetilcolina. Esses receptores não estão

uniformemente distribuídos pelo aparato pós-sináptico, mas sim formando agrupamentos nas dobras da membrana pós-sináptica, atingindo nesses locais densidades que podem chegar a mais de 10000 por mm^2(Figura 1B). Esse arranjo permite aos receptores detectar de forma rápida e eficiente a acetilcolina liberada durante a exocitose (revisado por Hall, 1992 e Hall & Sanes, 1993).

A junção neuromuscular de camundongo apresenta, em termos gerais, os mesmos componentes observados em junção neuromuscular de rã, tais como zonas ativas, aglomerados vesiculares, fenda sináptica e acúmulo de receptores nicotínicos na membrana pós-sináptica em aposição aos sítios de exocitose de vesículas. No entanto, as terminações axônicas não mielinizadas têm distribuição mais circunscrita e com aspecto arborizado em camundongos (Figura 1C).

Diante do que foi exposto nos parágrafos desta seção, torna-se evidente que a estrutura da junção neuromuscular garante uma excelente integração entre o sistema nervoso e as células musculares, constituindo também um excelente modelo experimental para estudo das funções sinápticas em virtude de sua simplicidade morfológica, de suas dimensões amplas e de sua fácil acessibilidade quando comparada, por exemplo, com uma sinapse entre neurônios no sistema nervoso central (revisado por Sanes & Lichtman, 2001).

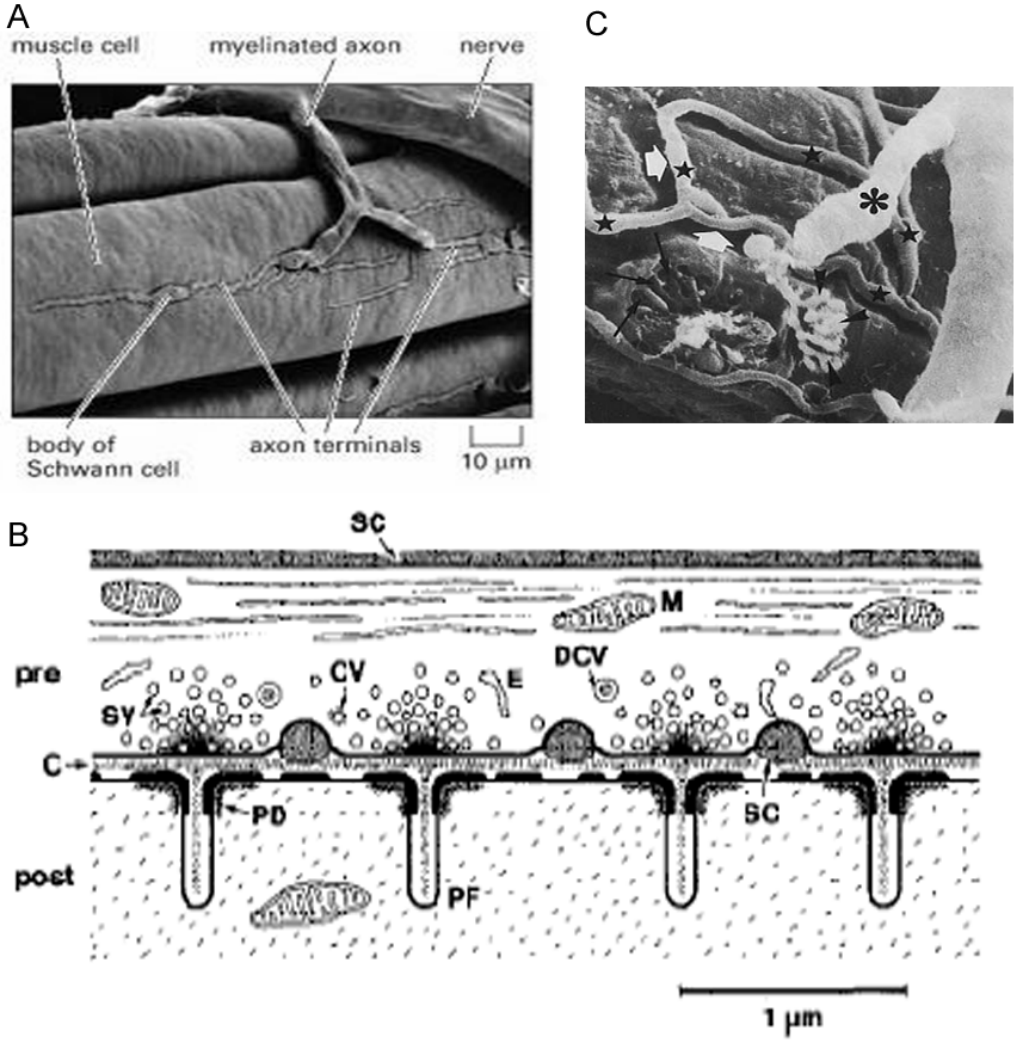

Figura 1: Junções neuromusculares de rã e camundongo. **A**) Micrografia eletrônica de varredura mostrando junções neuromusculares de rã. É possível observar terminações axônicas dispostas longitudinalmente ao longo de uma célula muscular estriada esquelética. Ao longo das terminações axônicas existem áreas de contato sináptico como evidenciado na figura 1B (Desaki & Uehara, 1981). **B**) Estrutura esquemática de junção neuromuscular de rã. O componente pré-sináptico inclui as zonas ativas associadas a vesículas sinápticas pequenas (SV), vesículas de conteúdo denso (DCV) e numerosas organelas como vesículas cobertas por clatrina (CV), endossomos (E) e mitocôndrias (M). O componente pré-sináptico é envolvido por uma Célula de Schwan (SC). O elemento pós-sináptico apresenta dobras pós-juncionais (PF), espessadas em seu ápice em virtude da alta densidade de receptores de acetilcolina na densidade pós-sináptica (PD). Os elementos pré e pós-sinápticos são separados por uma estreita fenda sináptica (C) (Burns & Augustine, 1995). **C**) Micrografia eletrônica de varredura mostrando uma junção neuromuscular de camundongo (cabeças de setas negras) (Torrejais *et al.*, 2002).

1.2 - Ciclo sináptico na junção neuromuscular

De uma maneira geral, a transmissão sináptica envolve a fusão de vesículas contendo neurotransmissores com a membrana plasmática e ativação de receptores pós-sinápticos (Heuser and Reese, 1973; revisado por Sudhof, 2004) (Figura 2). Os neurotransmissores clássicos são sintetizados na própria terminação axônica, sendo posteriormente armazenados no interior de vesículas e liberados na fenda sináptica, próximo aos seus receptores, através de áreas especializadas da membrana pré-sinaptica chamadas de zonas ativas (Ceccarelli *et al.*, 1973; Coutraux, 1974). A passagem de um potencial de ação, desencadeando a abertura de canais para cálcio sensíveis à voltagem e o influxo desse íon para o citoplasma da terminação axônica, promove o disparo da liberação de neurotransmissores (Katz & Miledi, 1965; Katz & Miledi, 1969; revisado por Murthy & De Camilli, 2003).

Na junção neuromuscular, a acetilcolina é sintetizada na terminação pré-sináptica pela enzima colina acetiltransferase (ChAT) a partir da colina e da acetil-CoA. Após sua síntese, a acetilcolina é armazenada no interior das vesículas graças a seu transportador vesicular, o VAChT, uma proteína com 12 domínios transmembrana. Para transportar acetilcolina, o VAChT utiliza um gradiente eletroquímico gerado por bombas de prótons presentes na membrana vesicular, as VH^+-ATPases (Nguyen *et al*., 1998; revisado por Prado *et al*., 2002 e Bravo & Parsons, 2002). Essas VH^+-ATPases, por meio da hidrólise do ATP, translocam prótons H^+ para o interior das vesículas sinápticas, estabelecendo duas condições: primeira, o pH no interior da vesícula torna-se mais acídico, gerando um gradiente químico de pH (ΔpH) através da membrana vesicular; segunda, o interior da vesícula torna-se abundante em cargas positivas, criando um potencial elétrico transmembrana ($\Delta\Psi$). O somatório dessas duas condições corresponde ao gradiente eletroquímico, representado pela equação $\Delta\mu H^+ = \Delta pH + \Delta\Psi$ (revisado por Liu & Edwards, 1997; Ozkan & Ueda, 1997). O VAChT realiza, então, a troca de dois íons H^+ por uma molécula de acetilcolina, preenchendo o interior das vesículas com o neurotransmissor (Nguyen & Parsons, 1995; Nguyen *et al*, 1998, Van der Kloot, *et al*., 2002).

O bombeamento de H^+ pelas VH^+-ATPases promove um acúmulo de cargas positivas no interior das vesículas sinápticas. Contudo, existem evidências de que canais para cloreto possibilitam a entrada de íons Cl^- que neutralizam o excesso de cargas positivas, reduzindo assim a influência do componente elétrico $\Delta\Psi$ na captação de

acetilcolina, mantida essencialmente pelo componente químico ΔpH do gradiente $\Delta\mu H^{+} = \Delta pH + \Delta\Psi$ (Strobawa *et al*., 2001; Van der Kloot, 2003;).

Após a exocitose e ativação dos receptores nicotínicos, a acetilcolina é hidrolisada pela acetilcolinesterase (AChE) presente na fenda sináptica, gerando colina e acetato. A colina é recaptada para o interior da terminação axônica por meio de seu transportador de membrana de alta afinidade (CHT1), podendo ser novamente utilizada para a síntese de nova acetilcolina (revisado por Ribeiro *et al*., 2006).

Cada vesícula sináptica presente na junção neuromuscular se enquadra em um de três aglomerados vesiculares: o grupo de vesículas disponíveis para liberação rápida (*Ready Releaseble Pool*), o grupo de reciclagem (*Recycling Pool*) ou o grupo de reserva (*Reserve Pool*). O grupo de vesículas disponíveis para liberação rápida está apto para a exocitose imediata e, geralmente, suas vesículas estão ancoradas na zona ativa, preparadas para a liberação. Por sua vez, o grupo de reciclagem é definido como o conjunto de vesículas que mantém a liberação de neurotransmissores em estimulação fisiológica moderada. Por último, o grupo de reserva consiste em um depósito de vesículas sinápticas cuja liberação ocorre mediante intensa estimulação (revisado por Rizzoli & Betz, 2005).

Durante a neurotransmissão, as vesículas sinápticas, organizadas em agrupamentos vesiculares, passam por um ciclo nas terminações nervosas, podendo ser dividido em passos seqüenciais (Figura 2): inicialmente os neurotransmissores são transportados para o interior das vesículas sinápticas, as quais se agrupam nas adjacências da zona ativa, onde irão ancorar-se e tornar-se-ão competentes para a fusão e liberação de seu conteúdo na fenda sináptica (revisado por Sudhof, 2004). Após a exocitose de seu conteúdo, as vesículas sinápticas sofrem endocitose e reciclagem por uma de três vias alternativas (Figura 3): (a) endocitose mediada por capa de clatrina (Heuse & Reese, 1973; Richards *et al*., 2000); (b) endocitose por meio de amplas invaginações de membrana e formação de cisternas (Takei *et al*., 1996; Richards *et al*., 2001;); (c) endocitose designada como *Kiss and Run* na qual vesículas liberam seu conteúdo sem se integrarem completamente à membrana pré-sináptica, sendo localmente reacidificadas e novamente preenchidas com neurotransmissores (Ceccarelli, *et al.*, 1973; Pyle *et al*., 2000; Gandhi & Stevens, 2003).

É importante destacar que uma série de interações moleculares está envolvida com o controle do ciclo sináptico. Nesse amplo conjunto molecular coordenador do ciclo sináptico, é bem definido o papel do complexo SNARE e da sinaptotagmina I. O

complexo SNARE é constituído pelas proteínas sintaxina, SNAP-25 e a sinaptobrevina (Sollner *et al*., 1993). A sintaxina e a SNAP-25 estão presentes na membrana pré-sináptica e, por isso, são designadas como t-SNAREs (*target SNAREs*). Já a sinaptobrevina situa-se na membrana das vesículas, sendo então designada como v-SNARE (*vesicular SNARE*). Essas três proteínas regem, por meio do seu entrelaçamento e estabelecimento de um complexo heterotrimérico, o ancoramento e fusão vesicular com a membrana pré-sináptica, possibilitando a liberação regulada de neurotransmissor (Figura 2) (Weber *et al*., 1998; revisado por Sudhof 2004). Por sua vez, a sinaptotagmina é uma proteína integral de vesículas sinápticas relacionada funcionalmente ao disparo da exocitose mediante interação com íons cálcio, elementos do complexo SNARE e fosfolipídeos de membrana (Perin *et al*., 1991; Davletov *et al*., 1993, Chapman & Davis, 1998; revisado por Chapman, 2008). Vale mencionar que outras proteínas acessórias são necessárias para acelerar e otimizar o processo de fusão de vesículas sinápticas (Rizo e Sudhof, 2002).

Nas próximas seções deste trabalho de tese, trataremos de três aspectos relacionados aos passos de exo/endocitose de vesículas sinápticas que ainda foram pouco estudados. Inicialmente, serão abordadas as relações entre o transporte de acetilcolina e o cilco de vesículas sinápticas. Em um segundo momento, discutiremos sobre a participação de cálcio intracelular na exocitose evocada pela ferramenta farmacológica ouabaína. Por fim, em uma terceira etapa, investigaremos o papel do colesterol de membrana no ciclo de vesículas sinápticas. Contudo, antes de investigarmos aspectos específicos do ciclo sináptico, no próximo tópico desta tese, discutiremos o emprego de uma sonda fluorescente vital utilizada para monitorar as etapas de endocitose e exocitose de vesículas sinápticas.

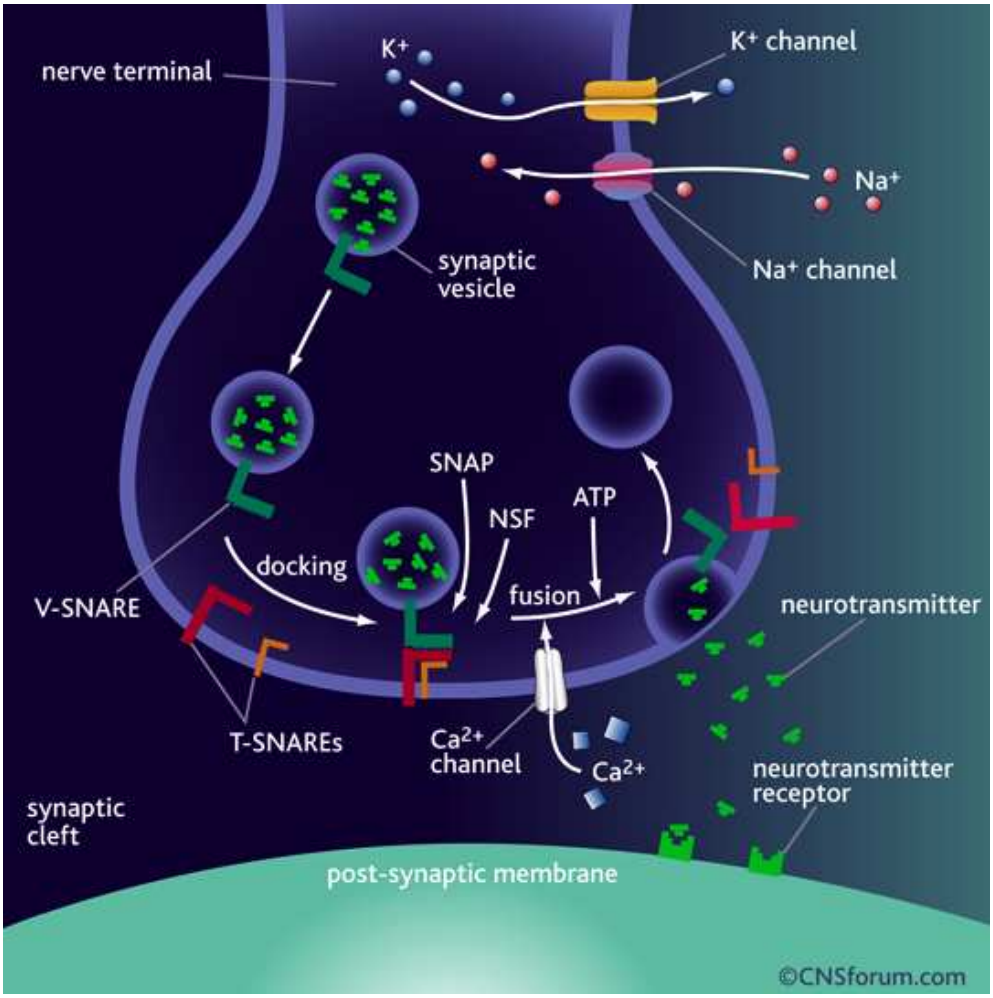

Figura 2: Etapas básicas da neurotransmissão. Durante a despolarização, após a abertura de canais de sódio sensíveis à voltagem, íons cálcio penetram na terminação pré-sináptica via canais para cálcio sensíveis à voltagem, levando a um aumento da concentração intracelular desse cátion. Vesículas sinápticas contendo neurotransmissores se acumulam nas adjacências das zonas ativas, sítios subcelulares da liberação vesicular. As vesículas que se ancoram na zona ativa (docking) sofrem uma reação de amadurecimento (priming) que as tornam competentes para a abertura de um poro de fusão (fusion) e exocitose dos neurotransmissores. Observe formação de complexo heterotrimérico entre *t-SNAREs e v-SNARE.* Após exocitose, os agrupamentos vesiculares são reconstituídos por meio de endocitose compensatória (www.cnsforum.com/hirespng/vesicle-fusion.png).

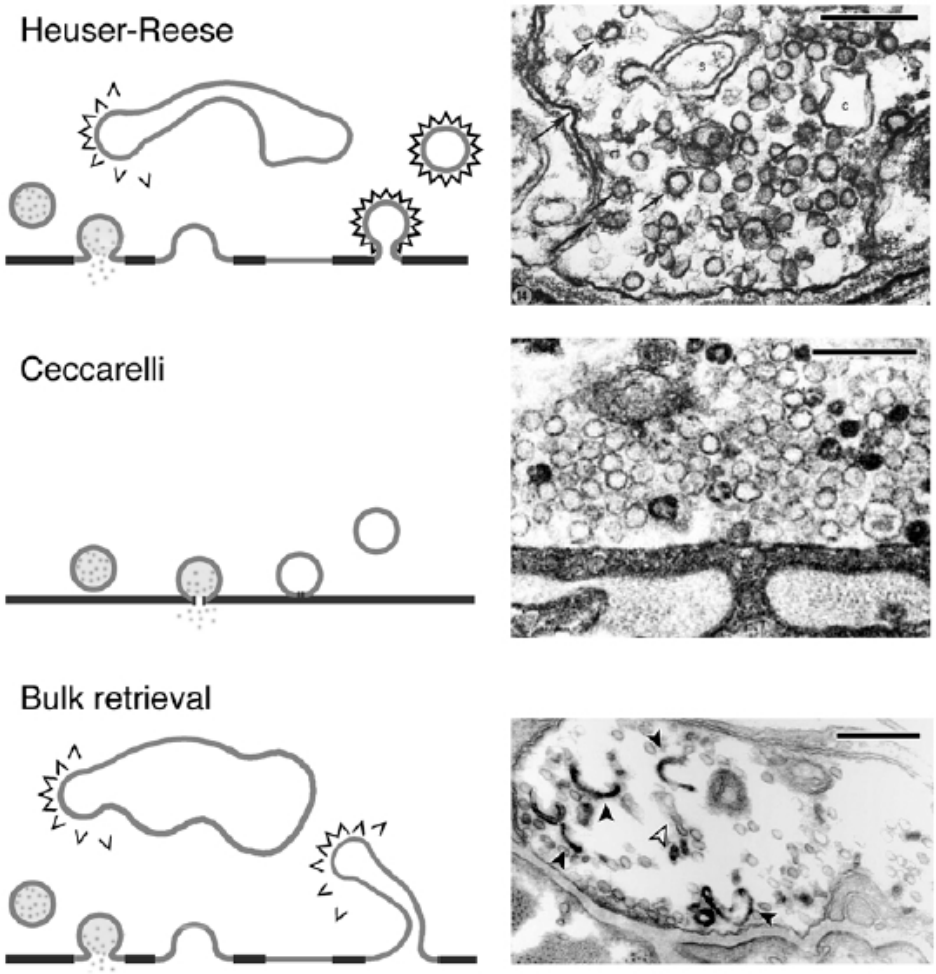

Figura 3: Modelos de endocitose de vesículas sinápticas. (**Painel Superior**) Modelo de Heuser & Reese no qual as vesículas sinápticas são completamente integradas à membrana da zona ativa durante a exocitose e são recicladas por meio de endocitose mediada por capa de clatrina. Vesículas cobertas podem também brotar a partir de grandes cisternas (diagrama à esquerda). Micrografia eletrônica (à direita) demonstrando a presença de depressões de membrana e vesículas cobertas por capa de clatrina (setas) em terminação motora submetida a estímulo elétrico. É possível observar também a presença de cisternas (c). (**Painel médio**) Diagrama representando modelo de *kiss and run* (à esquerda) proposto por Ceccarelli no qual, durante a liberação de neurotransmissores, as vesículas abrem um poro de fusão transitório, mas não se fundem completamente a membrana pré-sináptica, sendo recicladas localmente. Micrografia eletrônica (à direita) de terminação motora submetida a estímulo elétrico de baixa freqüência por duas horas. Destaca-se a ausência de vesículas cobertas por capa de clatrina e de cisternas. (**Painel inferior**) Diagrama representando endocitose via grandes invaginações de membrana (à esquerda) após liberação vesicular. Micrografia eletrônica (à direita) indicando invaginações de membrana contendo FM1-43 fotoconvertido (setas negras) ou desprovidas do marcador (seta clara) (revisado por Royle & Lagnado, 2003).

1.3 – Monitoramento do ciclo de vesículas sinápticas utilizando o marcador fluorescente FM1-43

Em estudos do ciclo sináptico, é possível visualizar os passos de exocitose e endocitose utilizando marcadores fluorescentes vitais captados durante a endocitose e liberados durante a exocitose. (Lichtman *et al*., 1985; Betz *et al*., 1992; Ribchester, *et al.*, 1994).

Entre as sondas fluorescentes disponíveis para monitoramento do ciclo de vesículas sinápticas, tornou-se muito divulgado o uso de marcadores do tipo "FM". Marcadores do tipo FM, como o FM1-43, são moléculas anfipáticas nas quais uma cauda lipofílica está ligada a uma cabeça carregada positivamente via ligações duplas (Figura 4A). A cabeça carregada positivamente impede o marcador de atravessar livremente as membranas celulares, mantendo-o preso no interior de endossomas ou vesículas. Por sua vez, o comprimento da cauda lipofílica determina a afinidade da molécula por membranas biológicas. Finalmente, o número de duplas ligações unindo a cabeça à cauda determina as propriedades espectrais da sonda. Por exemplo, o FM1-43 tem uma dupla ligação e pode ser excitado no espectro da fluoresceína enquanto o FM4-64 apresenta 3 ligações duplas entre cabeça e cauda, sendo excitado no espectro da rodamina (Betz, *et al.,* 1996; Brumback *et al.*, 2004).

A família de marcadores do tipo FM apresenta três propriedades que a tornam muito útil para estudo do tráfego de vesículas: (1) marcadores do tipo FM se ligam reversivelmente à membrana celular. Portanto, quando a sonda é aplicada à preparação, toda superfície de membrana exposta ao meio contendo FM torna-se marcada (Figura 4B). Quando a preparação é lavada em meio desprovido de FM, as moléculas do marcador são removidas da superfície celular (Figura 4C). (2) Moléculas de FM marcam seletivamente o folheto externo da bicamada lipídica. Isto possibilita que as vesículas em reciclagem nos sítios de endocitose capturem o marcador e o mantenham aprisionado em seu interior (Figura 4B). Além disso, as moléculas de FM estão permanentemente carregadas (cabeça com valência +2), impedindo que elas se difundam através das membranas e se tornem livres no citoplasma. (3) Sondas do tipo FM são menos fluorescentes quando estão em ambiente aquoso, mas sua fluorescência aumenta aproximadamente 350 vezes quando estão agregadas ao ambiente hidrofóbico das membranas (Betz *et al*.,1996; Brumback *et al.*, 2004). Portanto, em meio contendo FM1-43, após fusão e incorporação da membrana das vesículas à membrana da zona

ativa durante a exocitose, a endocitose compensatória promoverá reciclagem dos grupos vesiculares com membrana marcada com FM de modo que as vesículas recicladas apresentarão o marcador aprisionado em seu interior e aderido a sua membrana (Figura 4B). Isto possibilitará a visualização de aglomerados vesiculares marcados com a sonda em microscópio de fluorescência sob a forma de pontos fluorescentes (Figura 5A). O excesso de FM ligado à membrana das células musculares ou à mielina dos nervos será removido durante lavagem da preparação em meio desprovido do marcador (Figura 4C). Caso a preparação seja estimulada por algum agente que desencadeie exocitose, como estímulo elétrico, ocorrerá uma nova etapa de liberação de neurotransmissores e exposição da sonda ao meio aquoso, possibilitando difusão do FM1-43 para a solução salina na qual se encontra a preparação (Figura 4D). Isso determinará redução do sinal fluorescente e desmarcação dos pontos que representavam os aglomerados vesiculares que continham o marcador (Figura 4E).

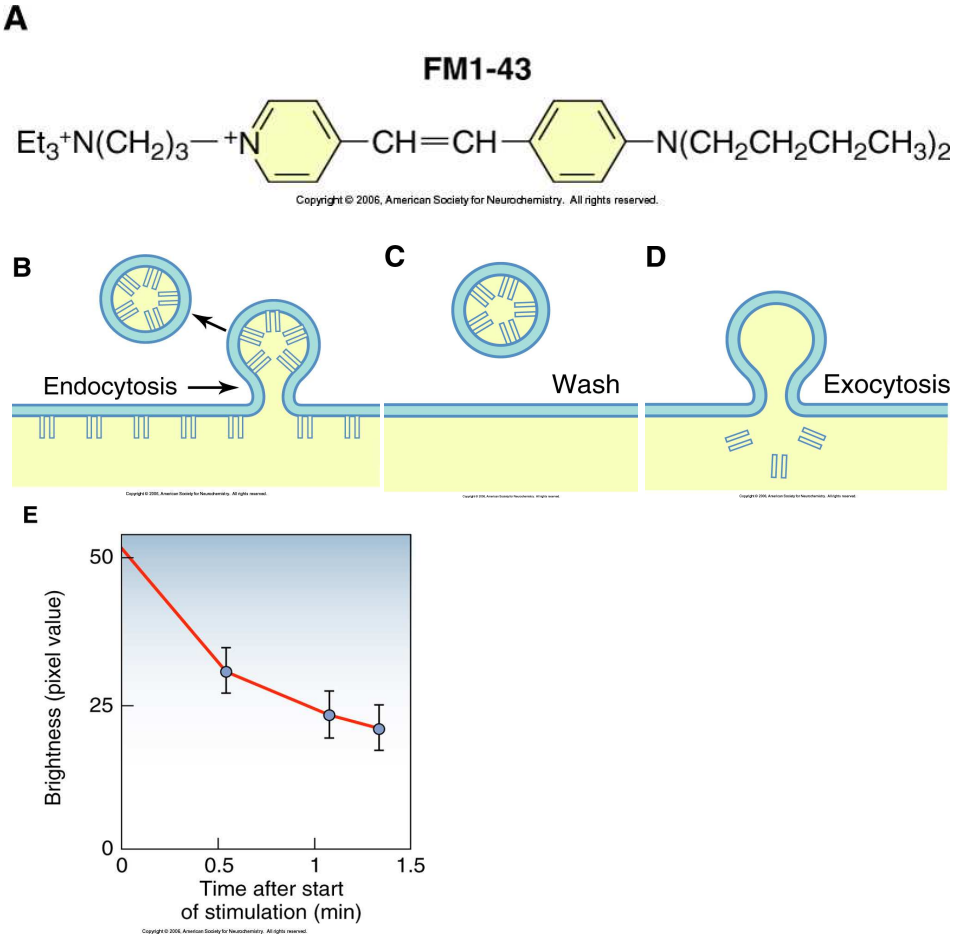

Figura 4: O marcador fluorescente FM1-43 é utilizado para monitoramento dos passos de endocitose e exocitose de vesículas sinápticas em neurônios. A) Estrutura da sonda fluorescente FM1-43. **B**) Marcação da membrana da terminação pré-sináptica com o FM1-43 adicionado à solução salina. O neurônio foi estimulado eletricamente na presença de FM1-43. Notar que a membrana que originou uma nova vesícula sináptica está marcada com a sonda. **C**) Uma breve lavagem remove as moléculas de FM que não foram internalizadas. **D**) Um segundo ciclo de exocitose induzido por estímulo elétrico resulta na liberação da sonda que foi internalizada durante a endocitose. **E**) Declínio da fluorescência da sonda FM1-43 durante exocitose de vesículas induzida por estímulo elétrico. Essa perda de fluorescência resulta da passagem da sonda de um meio hidrofóbico (membrana da vesícula sináptica) para um meio aquoso (solução salina) durante a exocitose (*Basic Neurochemistry*, *seventh edition. Edited by Siegel et. al., 2006).*

1.4 - Ciclo de vesículas sinápticas em junção neuromuscular de animais com expressão reduzida ou com ausência de expressão do gene do transportador vesicular da acetilcolina (VAChT)

Como anteriormente mencionado, a síntese de acetilcolina requer a captação da colina disponível na fenda sináptica para o interior da terminação axônica por meio de seu transportador de alta afinidade (CHT1). Contudo, uma eficiente liberação de acetilcolina depende do armazenamento deste neurotransmissor em vesículas sinápticas, passo controlado pelo VAChT, o transportador vesicular de acetilcolina (Nguyen & Parsons, 1995; Nguyen *et al*, 1998; Parsons, 2000; Ribeiro *et. al*., 2006).

Para avaliar a participação e a importância funcional do VAChT na neurotransmissão colinérgica, um grupo de pesquisadores coordenados pelo Prof. Marco Antônio Prado, do Departamento de Farmacologia da UFMG, gerou, por recombinação homóloga, uma linhagem de camundongos que apresenta expressão reduzida (*knockdown)* do gene do transportador vesicular da acetilcolina. Análises por *imunoblot* revelaram uma redução de 45% na expressão do VAChT em camundongos heterozigotos enquanto nos homozigotos a redução foi de 65% (artigo nº1 - Prado *et al.*, 2006). A menor expressão de VAChT não determinou inviabilidade dos animais geneticamente modificados de modo que mesmo as linhagens homozigotas tinham longevidade aparentemente normal, permitindo que as cobaias atingissem a idade adulta e possibilitando inclusive a realização de análise comportamental desse animais. A viabilidade dos camundongos *knockdown* homozigotos é um importante aspecto desse modelo experimental, pois em outras abordagens com animais homozigotos para mutações que anulavam a expressão da colina acetiltransferase e do CHT1 determinavam a morte pós-natal precoce dos camundongos homozigotos por colapso respiratório (Brandon *et. al*., 2004; Misgeld *et. al.*, 2002; Ferguson *et. al*, 2004).

Em análises eletrofisiológicas realizadas em placas motoras do músculo diafragama, camundongos *Knockdown* homozigotos apresentavam uma redução de 20% no conteúdo quântico de vesículas sinápticas quando comparados aos selvagens. Além disso, a freqüência de eventos pós-sinápticos em miniatura (MEPPs) sofria uma redução significativa nestes animais. Por sua vez, os resultados obtidos com os animais *knockdown* heterozigotos eram intermediários entre os dados obtidos com os *knockdown* homozigotos e os selvagens (artigo nº1 - Prado *et. al.,* 2006).

Em virtude das alterações observadas na transmissão neuromuscular, testes de avaliação da força muscular foram realizados. Os animais *Knockdown* heterozigotos tinham desempenho semelhante ao selvagem. Contudo, os *Knockdown* homozigotos apresentavam importante déficit de força muscular, reversível à aplicação do inibidor da acetilcolinesterase galatamina (artigo nº1 - Prado *et. al.,* 2006).

Aliando-se às alterações eletrofisiológicas e de força muscular, os *Knockdown* homozigotos também apresentavam déficits na liberação de acetilcolina no cérebro e obtinham piores resultados em testes de aprendizado e desempenho motor que exigiam atividade física sustentada. Portanto, estes animais apresentavam um quadro de síndrome miastênica (artigo nº1 - Prado *et. al.,* 2006).

A mesma equipe do professor Marco Antônio Prado gerou também uma linhagem de camundongos incapazes de expressar o VAChT. Os camundongos *nocaute* para o transportador vesicular de acetilcolina morrem logo após o nascimento indicando que a liberação de acetilcolina armazenada em vesículas sinápticas pelo VAChT é essencial à sobrevivência. Entretanto, registros eletrofisiológicos mostraram, surpreendentemente, que os camundongos *nocaute* para o VAChT apresentavam eventos espontâneos (MEPPs) com amplitude e freqüência reduzidas (artigo nº2 - de Castro *et al.*, 2009). De forma bastante interessante, os camundongos nos quais a expressão do VAChT foi abolida apresentavam níveis elevados de RNAm para a colina acetiltransferase e para o transportador de alta afinidade de colina (CHT1). Apresentavam também um aumento de 5 vezes no conteúdo de acetilcolina citoplasmática, o que poderia contribuir para uma possível liberação desse neurotransmissor independentemente do VAChT (artigo nº2 - de Castro *et al.,* 2009). Com relação ao elemento pós-sináptico, análise dos receptores nicotínicos para a acetilcolina (nAChR) utilizando bungarotoxina revelaram uma distribuição desorganizada dos agrupamentos desses receptores em preparações de junção neuromuscular de diafragma. Além disso, foi observado um aumento na área dos agrupamentos de receptores nicotínicos nos animais com abolição da expressão do VAChT (artigo nº2 - de Castro *et al.*, 2009).

Diante das observações e resultados relatados nesta seção, tornou-se de grande relevância investigar quais são as implicações da expressão reduzida ou total ausência da expressão do VAChT sobre a biogênese e ciclo de vesículas sinápticas. Também tornou-se importante investigar a possibilidade de modificações compensatórias no componente pré-sináptico como alterações na quantidade de vesículas sinápticas, no

número ou na área de terminações motoras. Portanto, em um primeiro momento nesse trabalho de tese, investigou-se o ciclo de vesículas sinápticas em junções neuromusculares de animais com alteração na expressão do transportador vesicular de acetilcolina (VAChT *knockdown* e VAChT *nocaute*).

1.5 – Influência da Ouabaína sobre o ciclo de vesículas sinápticas

A Ouabaína é um potente derivado esteróide, cardiotônico, obtido a partir de sementes maduras de *Strophantus gratus* e *Acokanthera ouabaio*, plantas de origem africana. No entanto, alguns trabalhos indicam possível síntese endógena e também apontam a existência de esteróides semelhantes à ouabaína em tecidos de mamíferos. Em 1991, um isômero da ouabaína foi identificado como um hormônio endógeno sintetizado pela glândula adrenal e também pelo hipotálamo, contudo o seu mecanismo de ação e sua significância fisiológica não foram ainda precisamente determinados (Hamlyn *et al*., 1991; Hamlyn *et al.*, 2003; Boulanger *et al*., 1993; Scheneider *et al*., 1998; Kawamura *et al.,* 2001).

O glicosídeo ouabaína é usado freqüentemente em pesquisas biomédicas como inibidor específico da Na^+,K^+-ATPase da membrana plasmática, proteína que catalisa o transporte ativo acoplado de Na^+ e K^+, estabelecendo um gradiente eletroquímico através da membrana plasmática. Portanto, diferentemente de outros esteróides, a ouabaína liga-se a uma proteína de membrana. Considerando que a Na^+,K^+-ATPase é o principal sistema de transporte ativo na maioria das células animais, promovendo a extrusão de três íons Na^+ e a entrada de dois íons K^+, sua inibição gera uma condição que favorece o acúmulo intracelular de Na^+ (Birks & Cohen, 1968; Gomez *et al.*, 1975; Aizman *et al.,* 2001; McFadden *et al.,* 2001).

Birks (1962) demonstrou que preparações de gânglio simpático de gato submetidas a tratamento com digoxina, um glicosídeo cardíaco assim como a ouabaína, apresentavam importantes modificações ultraestruturais quando visualizadas ao microscópio eletrônico de transmissão. No gânglio, as células neuronais apresentavam-se dilatadas, ocorria uma redução das dimensões mitocondriais com pronunciado aumento da eletrondensidade dessas organelas. Era possível também observar um aumento de volume da substância de *Nissl* e que o citoplasma tinha aspecto mais claro do que em células não tratadas. As terminações axônicas também se apresentavam dilatadas, possuíam mitocôndrias com estrutura alterada e as vesículas sinápticas eram

praticamente ausentes. Algo semelhante era observado com as junções neuromusculares tratadas com ouabaína (Haimann *et al*.,1985). Em ambos os modelos experimentais, a redução dos níveis de sódio extracelular inibia o aparecimento das alterações morfológicas descritas.

Vários trabalhos demonstraram que a ouabaína induz uma liberação pronunciada de neurotransmissores. Experimentos realizados com o modelo de fatias corticais de cérebro de rato indicaram que a ouabaína promove liberação de acetilcolina marcada radioativamente, independentemente da presença de Ca^{2+} no meio extracelular e da ativação de canais para Na^{+} e Ca^{2+} sensíveis à voltagem (Vizi, 1972; Gomez *et al.*, 1975; Casali, *et al.*, 1995). Contudo, a liberação de neurotransmissores induzida pelo glicosídeo mostrou-se dependente da presença de Na^{+} no meio extracelular e mediada pelo recrutamento de estoques intracelulares de Ca^{2+} (Elmqvist & Feldman 1965a and b; Baker & Cawford, 1975; Deri & Adam-Vizi, 1993; Lomeo *et al*, 2003). Apesar das evidências indicando que a liberação de neurotransmissores evocada pela ouabaína tenha precisa relação com os níveis de sódio e determine recrutamento de estoques intracelulares de cálcio, experimentos utilizando preparações de gânglio simpático de gato demonstraram que a liberação de neurotransmissor evocada pela ouabaína mostrou-se dependente do cálcio extracelular (Prado *et al.,*1993).

Em junção neuromuscular de rã, análises eletrofisiológicas demonstraram que a ouabaína determina um aumento da amplitude de potenciais pós-sinápticos evocados (EPPs) e aumento da freqüência de potenciais pós-sinápticos em miniatura (MEPPs). Por sua vez, análise ultraestrutural das junções neuromusculares após incubação com ouabaína evidenciou depleção dos agrupamentos de vesículas sinápticas, comprometimento da endocitose e dilatação mitocondrial (Birks & Cohen, 1968; Baker & Crawford, 1974; Haimann *et al*.,1985).

Com a utilização do marcador FM1-43 para monitorar o ciclo sináptico em junção neuromuscular de rã, foi possível observar que a ouabaína promovia liberação vesicular com conseqüente desmarcação de junções contendo FM1-43 (artigo nº 3 - Amaral *et al*., 2009). Observou-se, também, que a liberação vesicular induzida pela ouabaína ocorreu independentemente da presença de íons cálcio no meio extracelular (artigo nº 3 - Amaral *et al.*, 2009) um mecanismo distinto da descrição clássica de exocitose mediada pelo influxo de íons cálcio após passagem de um potencial de ação pela terminação axônica. Contudo, a cinética de liberação vesicular evocada pela ouabaína é bem mais lenta que a cinética da exocitose evocada por estímulo elétrico.

Além disso, a exocitose evocada pela ouabaína mostrou-se dependente da presença de íons Na^+ na solução salina (artigo nº 3 - Amaral *et al*., 2009) já que o glicosídeo exerce seus efeitos através da inibição da Na^+,K^+-ATPase, favorecendo o acúmulo intracelular de sódio. Contudo, apesar de promover exocitose, a incubação com a ouabaína inibiu a endocitose compensatória (artigo nº 3 - Amaral *et al.*, 2009). A liberação vesicular independente de cálcio extracelular promovida pela ouabaína sugere a ocorrência de recrutamento de estoques intracelulares de cálcio no mecanismo de ação desse glicosídeo. Investigar essa possibilidade constituiu um dos objetivos desta tese.

1.6 – Colesterol e ciclo de vesículas sinápticas

Segundo o modelo do mosaico fluído proposto por Singer e Nicolson (1972), os fosfolipídeos e proteínas de membrana estavam globalmente distribuídos pelas membranas celulares. Contudo, nas últimas duas décadas, muitos trabalhos apontam a existência de microdomínios de membrana ricos em colesterol, glicolipídeos e esfingolipídeos (para uma revisão veja Lingwood *et al.*, 2009). Estes microdomínios foram designados como balsas lipídicas (*lipid rafts)*. Nas balsas lipídicas, esfingolipídeos se associam lateralmente um ao outro, provavelmente através de interações fracas entre as cabeças de carboidratos de glicoesfingolipídeos. As cabeças globulares dos esfingolipídeos ocupam maiores áreas no folheto de membrana que suas finas caudas constituídas predominantemente por cadeias de hidrocarbonetos saturados. Portanto, os espaços existentes entre as caudas dos esfingolipídeos são ocupados por moléculas de colesterol. O arranjo apertado entre as moléculas de colesterol e os esfingolipídeos faz com que o conjunto se comporte como bloco dentro da monocamada externa das membranas enquanto as regiões fluídas entre as plataformas lipídicas são constituídas por moléculas insaturadas de fosfatidilcolina (Simons & Ikonen, 1997). Glicoesfingolipídeos normalmente apresentam uma longa cauda de ácido graxo que pode se interdigitar com os esfingolipídeos da monocamada interna da membrana. Como o colesterol está presente em ambos os folhetos, ele funciona como um espaçador também no folheto citoplasmático, preenchendo áreas vazias criadas pela interdigitação das cadeias carbônicas dos ácidos graxos (Simons & Ikonen, 1997). Embora a natureza dos fosfolipídeos ocupando o lado citoplasmático das balsas não seja totalmente conhecida, eles provavelmente também possuem longas cadeias de ácidos graxos saturados para otimizar a agregação do microdomínio (Simons & Ikonen, 1997).

Os microdomínios ricos em esfingolipídeos e colesterol são insolúveis ao detergente Triton X-100 a 4^{o}C. Em virtude do seu elevado conteúdo lipídico, esses complexos insolúveis a detergentes flutuam para uma região de baixa densidade durante centrifugação por gradiente de densidade, fato que possibilita a separação de proteínas associadas às balsas lipídicas (Simons & Ikonen, 1997).

Entre as proteínas que podem se associar às plataformas lipídicas podemos citar, por exemplo, proteínas com âncora de glicosilfosfatidilinositol (GPI) e tirosinas cinases da família Src (Simons & Ikonen, 1997). Algumas proteínas relacionadas ao controle do ciclo de vesículas sinápticas também mantêm íntima associação com microdomínios de membrana ricos em colesterol. Em experimentos realizados com o modelo de células neurosecretórias PC12, Chamberlain *et. al*. (2001) demonstraram que SNAP-25, sintaxina-1 e sinaptobrevina/VAMP-2, proteínas do complexo SNARE, estão associadas às plataformas lipídicas. Além disso, o seqüestro de colesterol da membrana por metil-β-ciclodextrina determinava redução da liberação exocítica de dopamina pelas células PC12. Esta constatação fornece forte evidência de que balsas lipídicas desempenham importante função na fusão de membranas e exocitose regulada. Estes microdomínios ricos em colesterol parecem organizar proteínas do complexo SNARE em sítios específicos da membrana, criando condições mais favoráveis à fusão vesicular.

Lang *et. al*. (2001), em experimentos com células PC12, relataram que sintaxinas estavam concentradas em agregados dependentes de colesterol com aproximadamente 200nm de largura. Nestes locais ocorriam preferencialmente o ancoramento e fusão vesicular. Eles demonstraram também que agregados de SNAP-25 tinham co-localização parcial com os microdomínios ricos em sintaxina. A redução do colesterol de membrana por metil-β-ciclodextrina desencadeava a dispersão dos agregados de SNAP-25 e sintaxina com conseqüente redução dos níveis de exocitose, sugerindo que altas concentrações de t-SNAREs em áreas específicas da membrana plasmática são necessárias para eficiente liberação vesicular.

Lafont *et. al*. (1999) observaram que a sintaxina-3 e a sinaptobrevina estavam associadas a balsas lipídicas em células MDCK, sugerindo que a associação de SNAREs com microdomínios ricos em colesterol não é algo restrito às células PC12. Somando-se a esta observação, trabalhos recentes demonstraram a presença de SNAREs em balsas lipídicas em adipócitos, mastócitos, células HeLa e sinaptossomos de córtex cerebral (revisado por Salaün *et. al*., 2004).

Thiele *et. al*. (1999) descrevaram a existência de interação entre o colesterol e a sinaptofisina, uma proteína da membrana de vesículas sinápticas e grânulos secretórios. Eles observaram que, após remoção parcial do colesterol de membrana, ocorria bloqueio da reciclagem e biogênese de vesículas a partir da membrana plasmática em células PC12. Diante disso, eles propuseram que interações específicas entre colesterol e proteínas de vesículas sinápticas, como a sinaptofisina, devem contribuir para o mecanismo de endocitose.

Rodal *et. al*. (1999) investigaram o papel do colesterol para a endocitose em diferentes linhagens celulares. Eles constataram que, após tratamento com metil-β-ciclodextrina, a endocitose de ricina-I^{125} e transferrina-I^{125}, mediadas por capa de clatrina, eram fortemente inibidas. Por outro lado, a endocitose de fator de crescimento endotelial (EGF-I^{125}), processada por mecanismo independente de clatrina, era menos afetada. A inibição da endocitose de transferrina e ricina era reversível ao longo do tempo após remoção da metil-β-ciclodextrina, contudo a adição de lovastatina para impedir síntese de novo colesterol bloqueava a recuperação da endocitose. Análise ultra-estrutural revelou comprometimento na formação de invaginações de membrana durante reciclagem vesicular, resultando no acúmulo de depressões rasas cobertas por clatrina ao longo da superfície da membrana plasmática. Subtil *et. al*., (1999) também observaram comprometimento da endocitose de transferrina após seqüestro de colesterol da membrana. Os dois grupos citados neste parágrafo sugerem um papel essencial do colesterol na reciclagem de vesículas por endocitose mediada por capa de clatrina.

Zamir & Charlton (2006) observaram, em placa motora de lagostim, falha na transmissão neuromuscular por bloqueio da propagação do potencial de ação após seqüestro de colesterol. Eles constataram também um aumento na freqüência de potenciais em miniatura (MEEPs). Estas alterações decorrentes do tratamento com metil-β-ciclodextrina são reversíveis após reposição do colesterol de membrana com o conjugado MβCD-colesterol. Estes achados indicam que os níveis de colesterol na membrana da terminação pré-sináptica podem modular passos essenciais na liberação de neutortransmissor.

Tendo em vista a associação de proteínas que regulam o ciclo sináptico com microdomínios ricos em colesterol e as alterações na transmissão neuromuscular após tratamento com metil-β-ciclodextrina, investigou-se, em um terceiro momento deste trabalho de tese, o papel do colesterol na biogênese e ciclo de vesículas sinápticas em

preparação de junção neuromuscular de rã (artigo nº 4 - Amaral *et al.*, em preparação). Para tanto, foram utilizadas preparações *ex-vivo* marcadas com FM1-43. Essa ferramenta possibilitou monitorar dinamicamente as implicações do seqüestro de colesterol sobre as etapas de exocitose e endocitose. Experimentos utilizando microscopia eletrônica e técnicas de eletrofisiologia também foram utilizados nessa etapa do trabalho de tese.

2 – Artigos

2.1.1 – Artigo número 1*

Mice deficient for the vesicular acetylcholine transporter are myasthenic and have deficits in object and social recognition*

PRADO, V. F.; MARTINS-SILVA, C.; DE CASTRO, B. M.; LIMA, R. F.; BARROS, D. M.; AMARAL, E.; RAMSEY, A. J.; SOTNIKOVA, T.D.; RAMIREZ, M. R.; KIM, H. G.; ROSSATO, J.I.; KOENEN, J.; QUAN, H.; COTA, V. R.; MORAES, M. F.; GOMEZ, M. V.; GUATIMOSIM, C.; WETSEL, W. C.; KUSHMERICK, C.; PEREIRA, G. S.; GAINETDINOV, R. R.; IZQUIERDO, I.; CARON, M. G.; PRADO, M. A.

Neuron, v. 51, n. 5, p. 601-12, 2006.

* Os dados referentes ao monitoramento do ciclo sináptico apresentados nesse artigo foram obtidos pelo autor durante transição entre o mestrado e o doutorado. Os resultados serão apresentados nessa seção por terem relação com o material suplementar descrito na página 26 da tese e com artigo número 2 apresentado na página 28.

Neuron 51, 601–612, September 7, 2006 ©2006 Elsevier Inc. DOI 10.1016/j.neuron.2006.08.005

Mice Deficient for the Vesicular Acetylcholine Transporter Are Myasthenic and Have Deficits in Object and Social Recognition

Vania F. Prado,[1] Cristina Martins-Silva,[2] Braulio M. de Castro,[2] Ricardo F. Lima,[3] Daniela M. Barros,[5] Ernani Amaral,[4] Amy J. Ramsey,[6] Tatyana D. Sotnikova,[6] Maria R. Ramirez,[5] Hyung-Gun Kim,[7,8] Janine I. Rossato,[5] Janaina Koenen,[1] Hui Quan,[6] Vinicius R. Cota,[3] Marcio F.D. Moraes,[3] Marcus V. Gomez,[2] Cristina Guatimosim,[4] William C. Wetsel,[7] Christopher Kushmerick,[3] Grace S. Pereira,[2] Raul R. Gainetdinov,[6] Ivan Izquierdo,[5] Marc G. Caron,[6,*] and Marco A.M. Prado[2,*]

[1] Departamento de Bioquímica-Imunologia
[2] Departamento de Farmacologia
[3] Departamento de Fisiologia-Biofísica
[4] Departamento de Morfologia
Instituto de Ciências Biológicas
Universidade Federal de Minas Gerais
Avenida Antônio Carlos 6627
Belo Horizonte, MG
Brazil, 31270-901
[5] Centro de Memória
Instituto de Pesquisas Biomédicas
Pontificia Universidade Católica
de Rio Grande do Sul
Hospital São Lucas da PUC-RS
Av. Ipiranga 6690 2 andar
90610-000 Porto Alegre, RS
Brazil
[6] Department of Cell Biology
[7] Department of Psychiatry and Behavioral Sciences
Duke University Medical Center
Durham, North Carolina, 27710

Summary

An important step for cholinergic transmission involves the vesicular storage of acetylcholine (ACh), a process mediated by the vesicular acetylcholine transporter (VAChT). In order to understand the physiological roles of the VAChT, we developed a genetically altered strain of mice with reduced expression of this transporter. Heterozygous and homozygous VAChT knockdown mice have a 45% and 65% decrease in VAChT protein expression, respectively. VAChT deficiency alters synaptic vesicle filling and affects ACh release. Whereas VAChT homozygous mutant mice demonstrate major neuromuscular deficits, VAChT heterozygous mice appear normal in that respect and could be used for analysis of central cholinergic function. Behavioral analyses revealed that aversive learning and memory are not altered in mutant mice; however, performance in cognitive tasks involving object and social recognition is severely impaired. These observations suggest a critical role of VAChT in the regulation of ACh release and physiological functions in the peripheral and central nervous system.

*Correspondence: m.caron@cellbio.duke.edu (M.G.C.); mprado@icb.ufmg.br (M.A.M.P.)
[8] Present address: Department of Pharmacology, College of Medicine, Dankook University, San-29, Anseo-dong, Cheonan, Choongnam 330-714, Korea.

Introduction

Acetylcholine (ACh) plays a crucial role in controlling a number of physiological processes in both the peripheral and central nervous system. Synthesis of ACh requires efficient uptake of choline by the high-affinity choline transporter and choline acetylation by the enzyme choline acetyltransferase (ChAT) (Ribeiro et al., 2006). Efficient release of ACh from nerve endings depends on its storage in synaptic vesicles, a step reliant on the activity of a vesicular acetylcholine transporter (VAChT) (Parsons, 2000). VAChT is a twelve-transmembrane domain protein that uses the electrochemical gradient generated by a V-type proton ATPase to accumulate ACh in synaptic vesicles. VAChT and the vesicular monoamine transporters (VMATs) share a high degree of homology in their transmembrane domains and belong to the SLC18 (or solute carrier) family of proton/neurotransmitter antiporters (Erickson et al., 1994; Reimer et al., 1998; Roghani et al., 1994).

The ACh transporter is likely to provide stringent control of the amount of neurotransmitter stored and released by cholinergic nerve endings (Prado et al., 2002). VAChT trafficking to secretory vesicles appears to be the target of cellular regulation, and phosphorylation by protein kinase C (PKC) influences delivery of VAChT to synaptic-like microvesicles in PC12 cells (Cho et al., 2000; Krantz et al., 2000). However, the consequences of reduced targeting of VAChT to synaptic vesicles for ACh output in vivo are unknown.

Deficits in central or peripheral ACh neurotransmission have been described in several human disorders, including Alzheimer's disease (AD), in which certain behavioral and cognitive abnormalities have been related to brain cholinergic dysfunction (Bartus et al., 1982; Mesulam, 2004). However, the relationship between cholinergic decline and specific behavioral deficits is still not completely appreciated. Basal forebrain lesions in rats, with immunotoxins targeting the p75 neurotrophin receptor, indicate that ACh plays an essential role in attention (Sarter and Parikh, 2005), whereas it seems to participate, but it is not essential, in hippocampal-dependent spatial learning and memory (Parent and Baxter, 2004).

To investigate the consequences of reduced expression of VAChT on ACh neurotransmission and function, we genetically modified mice to produce a knockdown (KD) of VAChT gene expression. We observed a strong relationship between the levels of VAChT expression and ACh release in both the peripheral and central nervous systems. A marked reduction of VAChT expression was necessary to affect neurotransmission at the neuromuscular junction, while even modest deficiency was sufficient to interfere with brain ACh release and affect

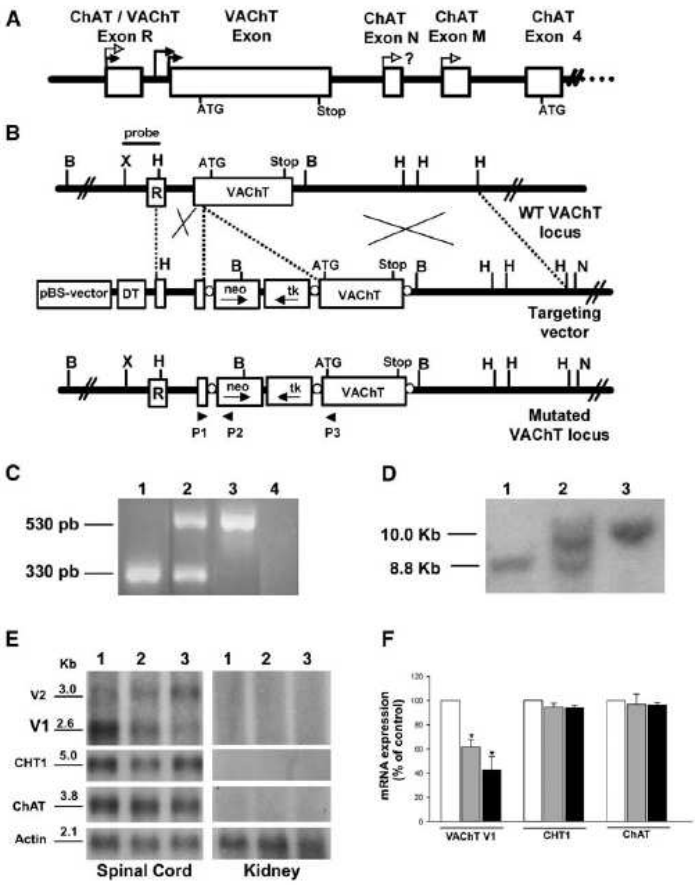

Figure 1. Schematic Drawing of the Cholinergic Gene Locus and Generation of VAChT-Deficient Mice

(A) Boxes represent the different exons of ChAT or VAChT. The position of the initiation codon (ATG) for VAChT and ChAT and the stop codon (stop) of VAChT are indicated. Potential transcription initiation sites are indicated for VAChT (filled arrowheads) and ChAT (open arrowheads). Note that the VAChT gene is within the first intron of ChAT.

(B) Schematic representation of the VAChT gene locus, the targeting construct, and the recombinant DNA. P1, P2, and P3 indicate position of PCR primers used for genotyping. Open white circles indicate loxP sites.

(C) PCR analysis of wild-type (lane 1), heterozygous VAChT KD mice (lane 2), and homozygous VAChT KD mice (lane 3). Lane 4 is a negative control without DNA.

(D) Southern analysis of wild-type (lanes 1), VAChT KD^{HET} (lane 2), and VAChT KD^{HOM} mice (lane 3).

(E) Northern blot analysis of VAChT, ChAT, and CHT1 in spinal cord for wild-type (lane 1), VAChT KD^{HET} (lane 2), and VAChT KD^{HOM} mice (lane 3). Kidney mRNA was isolated, and Northern analysis detected no signal for VAChT, ChAT, and CHT1 transcripts.

(F) Quantification of cholinergic transcripts. Blots were scanned and densitometric analysis was performed using the actin signal to normalize mRNA levels. Data are presented as a percentage of wild-type levels. (*) indicates statistical significant differences as described in the text.

behavior. Moreover, these investigations revealed a role for cholinergic tone in processing complex cues, which manifested as cognitive deficits in mutant mice for object and social memory.

Results

Molecular Analysis

To investigate the physiological consequences of altered expression of VAChT as related to vesicle filling and ACh release, we generated a mouse line with decreased expression rather than complete deletion, of this transporter, so we could investigate the consequences of reduced cholinergic tone in vivo (Figures 1A and 1B for wild-type and mutant alleles, respectively). PCR and Southern analyses confirmed homologous recombination and targeting of the 5′ untranslated region of the VAChT gene in genetically altered mice (Figures 1C and 1D). Mutant mice were born at the expected Mendelian frequency, survived, and exhibited no gross abnormalities.

Northern analysis of spinal cord indicated that the major mRNA species for VAChT (V1, 2.6 kb) was significantly reduced by 40% and 62% in VAChT KD^{HET} and KD^{HOM} mice, respectively [$F(2,11) = 11.09$, $p < 0.005$, one-way ANOVA, Figures 1E and 1F]. Surprisingly, a second VAChT species of 3.0 kb, which was especially apparent in spinal cord, was significantly increased in VAChT KD mice, suggesting that compensatory transcriptional mechanisms operate in response to changes in VAChT expression. The changes in mRNA were specific for VAChT transcripts, as we detected no significant changes in mRNA levels for ChAT [$F(2,3) = 0.0311$, $p = 0.970$] and CHT1 [$F(2,12) = 0.0921$, $p = 0.9127$] in mutant mice (Figures 1E and 1F). These results agree with the lack of significant alterations found in ChAT activity and high-affinity choline transport in mutant mice (see Figure S1 in the Supplemental Data). Control experiments using kidney mRNA demonstrated the specificity of the probes (Figure 1E).

We investigated the consequences of altered expression of VAChT mRNA in VAChT KD mice by probing protein expression by immunoblot analysis. These experiments show a reduction of close to 50% in immunoreactivity for VAChT in the hippocampus [two-way ANOVA followed by Bonferroni post hoc, $F(2,23) = 70.95$, $p < 0.001$, Figures 2D and 2E] and in other brain regions (Figures 2A–2E) of VAChT KD^{HET} mice compared to wild-type control mice. In contrast, levels of other presynaptic proteins were not altered (Figures 2A–2E). Results were similar in all brain regions and in spinal cord (Figure 2E, overall decrease in all tissues was 56% ± 4% of the wild-type levels, n = 20). These results indicate a significant reduction in VAChT protein in VAChT KD^{HET}

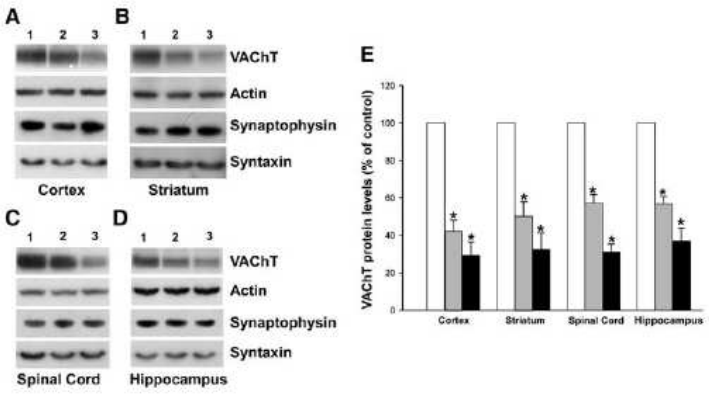

Figure 2. Gene Targeting Alters VAChT Protein Levels

Western blot analysis of VAChT, synaptophysin, and syntaxin in the cortex (A), striatum (B), spinal cord (C), and hippocampus (D) of wild-type (lane 1), VAChT KD^{HET} (lane 2), and VAChT KD^{HOM} mice (lane 3). (E) Quantification of protein levels. Actin immunoreactivity was used to correct for protein loading between experiments. Data are presented as a percentage of wild-type levels. (*) indicates statistical significant difference (one-way Anova with Bonferroni post hoc [cortex, $F(2,9) = 49.11$, $p < 0.001$; striatum, $F(2,6) = 27.24$, $p < 0.001$; spinal cord, $F(2,9) = 95.75$, $p < 0.001$; Hippocampus, $F(2,23) = 70.95$, $p < 0.001$]).

mice. VAChT KD^{HOM} mice showed further decrease in VAChT protein levels (65% to 70%, Figures 2A–2E). Thus, VAChT KD^{HOM} mice present an even larger decrease in levels of transporter than VAChT KD^{HET} mice, but VAChT expression in homozygous mutant mice is sufficient for survival.

Electrophysiological Analysis and Neuromuscular Function

In order to evaluate the impact of reduced VAChT expression on quantal ACh release, we examined neuromuscular transmission. Miniature end-plate potentials (MEPPs) were readily recorded at neuromuscular junctions from either wild-type, VAChT KD^{HET}, or VAChT KD^{HOM} mice. To compare quantal size we recorded at least 100 MEPPs from each of five fibers from five to seven animals of each genotype. MEPPs from mutant mice were smaller than those from wild-type, as can be seen in histograms of MEPP amplitudes (Figure 3A). To avoid possible histogram binning artifacts, we also analyzed the cumulative distribution of MEPP amplitudes, which showed a similar shift to smaller MEPPs in mutant animals (Figure 3B, $p < 0.001$ for VAChT KD^{HOM}, $p < 0.05$ for VAChT KD^{HET}, Kolmogorov-Smirnoff test). Further statistical analysis using ANOVA on averages of either the peak amplitude or the area of MEPPs confirmed the statistical significance of the differences in quantal sizes between wild-type and VAChT KD^{HOM} animals [$F(1,71) = 8.7$, $p < 0.005$]. Therefore, mutant mice appear to pack less ACh in each synaptic vesicle.

In addition to quantal size, MEPP frequency was also strongly reduced in VAChT KD^{HOM} animals, as shown in Figure 3C. The frequency of MEPPs was $0.69 \pm 0.08\ s^{-1}$ in wild-type animals (40 synapses from seven animals), $0.79 \pm 0.18\ s^{-1}$ in VAChT KD^{HET} animals (30 synapses from five animals), and $0.37 \pm 0.05\ s^{-1}$ in VAChT KD^{HOM} mice (41 synapses from seven animals). The difference in MEPP frequency between wild-type and VAChT KD^{HOM} mice was statistically significant [two-way ANOVA followed by Bonferroni post hoc, $F(1,18) = 10.3$, $p < 0.005$].

The observed decrease in MEPP frequency at junctions from KD^{HOM} mice could be due to a reduction in the number of synaptic vesicles available for release, a reduction in vesicle release probability, or a population of synaptic vesicles whose ACh load is below our detection limit. To investigate these possibilities, we measured evoked end-plate potentials (EPPs) during 100 Hz trains after cutting the muscle fibers to avoid contraction. Under these conditions, EPP amplitudes during a train rapidly fell from their initial level to a depressed steady state over the course of the first ten stimuli (Figure 3D). Overall, initial depression of normalized EPPs was similar in recordings from wild-type and KD^{HOM} animals, suggesting similar release probabilities. Quantal content of each EPP during a train was calculated based on measured MEPP amplitudes, thus permitting an estimate of the size of the readily releasable pool of vesicles as described (Elmqvist and Quastel, 1965). This analysis considered only the first eight responses during a train for which the relationship between EPP versus cumulative EPP was linear. With this method, the readily releasable pool was similar for both genotypes and estimated at 439 ± 73 vesicles in synapses from wild-type animals and 550 ± 59 vesicles in VAChT KD^{HOM} synapses ($p = 0.52$, two-tailed Student's t test). In contrast, the extent of steady-state depression of EPPs was significantly greater in VAChT KD^{HOM} animals compared with wild-type [one-way ANOVA, $F(1,70) = 197$, $p < 0.001$].

Assuming constant quantal size, the increase in depression uncovered in the above experiments would suggest a defect in mobilizing or recycling of ACh-filled vesicles; however, the assumption of constant quantal size during the stimulus train may not be valid for mutant animals. Therefore, we attempted to directly test whether synaptic vesicle exo- and endocytosis would be altered in mutant mice. For this we performed experiments with the vital dye FM1-43 (Richards et al., 2000), which provides the opportunity for optical detection of both exocytosis and endocytosis of synaptic vesicles.

Labeling of nerve terminals in junctions from both wild-type and KD^{HOM} animals in response to 60 mM KCl (10 min) was indistinguishable, and no differences were detected upon quantification of fluorescent spots (Figure 3E), suggesting that endocytosis occurs to the same extent in both genoytypes. Destaining of fluorescent spots in response to 60 mM KCl was calcium dependent (not shown), and was not different between wild-type and KD^{HOM} animals (Figure 3F), indicating that synaptic vesicle exocytosis is not changed in VAChT KD^{HOM} mice. Thus, taken together, our observations would suggest that the alterations in MEPP frequency and EPP

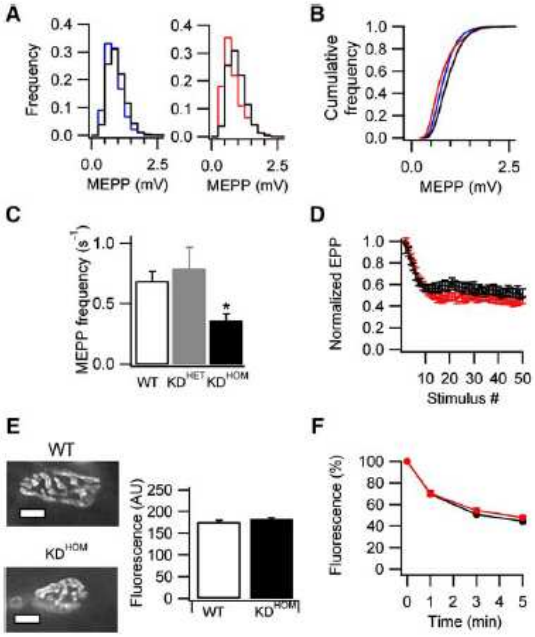

Figure 3. Neuromuscular Transmission in VAChT KD^{HET} and VAChT KD^{HOM} Mice

(A) Normalized histogram of MEPP amplitudes for wild-type (black line, 3302 MEPPs), VAChT KD^{HET} (blue line, 4319 MEPPs), and VAChT KD^{HOM} (red line, 3690 MEPPs) mice. Data are from five synapses from five to seven animals for each genotype.

(B) Quantal size of the three genotypes quantified by plotting the cumulative frequency of MEPP amplitudes. Black line, wild-type; blue line, VAChT KD^{HET}; red line, VAChT KD^{HOM}.

(C) Frequency of MEPPs at synapses from the three genotypes. (*) indicates statistically significant difference from control wild-type mice (two-way ANOVA followed by Bonferroni post hoc; $F(1,18) = 10.3$, $p < 0.005$).

(D) Normalized EPP amplitude (to the first stimulus) for wild-type (black line) and VAChT KD^{HOM} (red line) mice in response to a train of 100 Hz (0.5 s). Data are from ten synapses from three wild-type animals and 16 synapses from three KD^{HOM} animals.

(E) Nerve terminals from wild-type and VAChT KD^{HOM} mice were labeled with FM1-43 and show similar patterns of staining. Data are mean ± SEM of 109 fluorescent spots from 21 nerve terminals of wild-type mice and 111 fluorescent spots from 26 nerve terminals from VAChT KD^{HOM}. Scale bar, 10 μm.

(F) Destaining of FM1-43-labeled nerve endings from wild-type (black line) and VAChT KD^{HOM} (red line). Data are mean ± SEM of 26 fluorescent spots (wild-type mice) and 21 fluorescent spots (VAChT KD^{HOM}) from four mice per genotype.

depression in VAChT KD^{HOM} are more than likely a consequence of decreased transport of ACh by synaptic vesicles.

To evaluate whether the alterations detected in neuromuscular transmission may affect neuromuscular function, we tested the performance of wild-type and mutant mice in motor tasks (Figure 4). In the wire-hang test (Figure 4A), wild-type and VAChT KD^{HET} mice show no differences in performance; however, VAChT KD^{HOM} mice were significantly impaired [$F(2,37) = 28.77$, $p < 0.001$]. This altered performance of VAChT KD^{HOM} animals is likely the result of altered neuromuscular force, since these mutants were also severely impaired in a grip strength test when compared with wild-type mice [Figure 4B, $F(3,48) = 9.52$, $p < 0.001$]. By comparison, VAChT KD^{HET} mice present no deficit in neuromuscular function as assessed in this test. Importantly, reduced grip strength in VAChT KD^{HOM} mice was improved by prior injection of one of three cholinesterase inhibitors: pyridostigmine (i.p., 1 mg/kg), galantamine (s.c., 1 mg/kg) or physostigmine (i.p., 0.3 mg/kg) [Figure 4B, $F(3,47) = 8.323$, $p < 0.05$]. No change in grip force was observed in wild-type mice treated similarly with any of the above cholinesterase inhibitors at the doses used (not shown). Since pyridostigmine is charged and should not cross the blood-brain barrier, its efficacy in improving grip force observed in homozygous mutant mice directly implicates peripheral cholinergic transmission in this effect.

To further study neuromuscular output, we examined performance of VAChT mice on the rotarod. This test depends not only on the ability of mice to learn motor skills, but also on their ability to maintain prolonged motor function. Wild-type mice were able to learn this motor task, and after five trials their performance was significantly better than their performance during the first trial [Figure 4C, repeated measures ANOVA, $F(13,195) = 16.9$, $p < 0.05$]. The performance of VAChT KD^{HET} mice improved significantly only after 12 trials on the rotarod [repeated measures ANOVA, $F(13,117) = 4.63$, $p < 0.05$]. In contrast, VAChT KD^{HOM} mice never learned this motor task [Figure 4C, $F(13,91) = 0.653$] and their performance was significantly worse than those of wild-type and VAChT KD^{HET} mice [$F(2,434) = 60.16$, $p < 0.05$ on trials 12, 13, and 14, two-way ANOVA followed by Bonferroni post hoc tests].

The performance of VAChT KD^{HOM} mice may indicate either motor learning deficits on the rotarod or that mutant mice are incapable of sustained physical activity. To evaluate the latter possibility, we used a treadmill to evaluate the performance of wild-type, VAChT KD^{HET}, and VAChT KD^{HOM} mice in exhaustive physical activity. Figure 4D shows that VAChT KD^{HOM} mice were not able to maintain long periods of physical activity and performed poorly compared with wild-type or VAChT KD^{HET} mice [one-way ANOVA followed by Bonferroni post hoc, $F(2,28) = 22.09$, $p < 0.001$]. Indeed, VAChT KD^{HOM} mice could run for no more than 5 min on the treadmill, whereas wild-type or VAChT KD^{HET} mice could usually run for longer than 60 min. These results indicate that VAChT KD^{HOM} mice are unable to perform on the rotarod due to their decreased capacity to maintain physical activity. They also indicate that VAChT KD^{HET} mice appear as physically fit as wild-type control mice under the conditions tested.

Neurochemical Analysis

VAChT KD^{HOM} mice display significant neuromuscular deficiency, which may confound the outcomes of complex behavioral tests aimed at assessing consequences of central ACh deficiency. In contrast, VAChT KD^{HET} mice have essentially normal neuromuscular transmission, thereby indicating their potential usefulness as test subjects for investigating the behavioral consequences of mild reductions of central cholinergic function.

To investigate the functional consequences of reduced VAChT expression, we first used brain microdialysis to

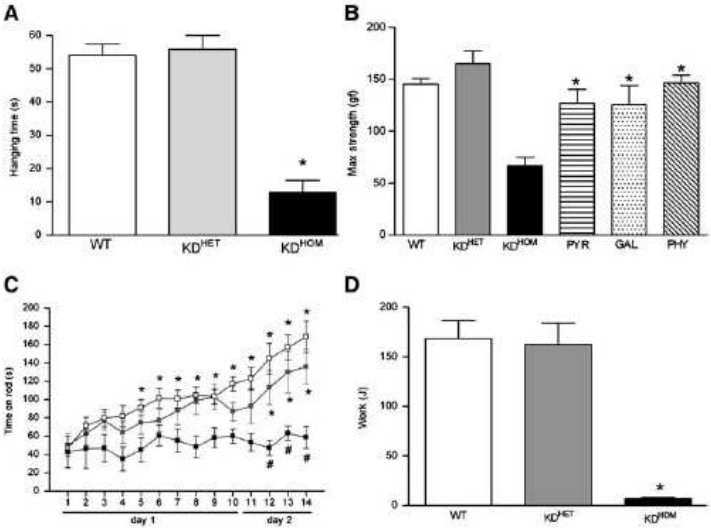

Figure 4. Neuromuscular Function of VAChT KD^{HET} and VAChT KD^{HOM} Mice

(A) Time spent hanging upside-down from a cage by wild-type, VAChT KD^{HET}, and VAChT KD^{HOM} mice. *$p < 0.05$ from wild-type controls (one-way ANOVA followed by Bonferroni post hoc; $F[2,37] = 28.77$, $p < 0.05$, n = 20 wild-type, n = 12 VAChT KD^{HET}, and n = 8 VAChT KD^{HOM}).

(B) Grip force measured for wild-type, VAChT KD^{HET}, VAChT KD^{HOM}, and VAChT KD^{HOM} mice treated with pyridostigmine (i.p., 1 mg/kg), galantamine (s.c., 1 mg/kg) and physostigmine (i.p., 0.3 mg/kg) 30 min prior to the test. (*) indicates statistical difference when compared with VAChT KD^{HOM} mice without cholinesterase treatment.

(C) Performance of wild-type (clear squares), VAChT KD^{HET} (gray squares), and VAChT KD^{HOM} mice (black squares) on the rotarod task. (*) indicates statistically significant differences compared with the first trial for each genotype (repeated measures ANOVA, $p < 0.05$). (#) indicates statistically different performance when compared with wild-type mice [two-way ANOVA shows an effect of genotype; $F(2,434) = 60.16$, $p < 0.05$].

(D) Exercise capacity of wild-type, VAChT KD^{HET}, and VAChT KD^{HOM} mice. Mice were trained on the treadmill with a protocol that evaluated physical capacity (see Experimental Procedures). After training mice, were tested for performance, and the work (in J) done was calculated.

establish extracellular levels of ACh in freely moving VAChT KD^{HET} mice. Because all brain regions examined appeared to show similar reductions in VAChT expression, we chose to determine extracellular ACh levels in frontal cortex and striatum. Frontal cortex was selected because this brain region receives innervation from nucleus basalis and substantia innominata, areas known to be affected in Alzheimer's disease. Striatum was chosen because it contains the largest concentration of cholinergic nerve endings and is therefore particularly suitable to evaluate possible decreases in extracellular ACh. The quantitative "low perfusion rate" microdialysis approach, which allows precise determination of a given extracellular neurotransmitter (Gainetdinov et al., 2003), revealed that levels of extracellular ACh were depressed by more than 35% in frontal cortex [$t(1,19) = 2.642$, $p < 0.016$] and by approximately 31% in striatum [$t(1,18) = 2.560$, $p < 0.020$] of VAChT KD^{HET} mice (Figure 5A). Next, by using the conventional microdialysis approach, we examined the dynamic responses to KCl-stimulated ACh release in the striatum. After establishing basal extracellular ACh levels, artificial cerebrospinal fluid (CSF) containing 60 mM [K^+] was perfused through the microdialysis probe over the next 40 min, and the probe was returned to normal artificial CSF for the remaining 40 min of the experiment (Figure 5B). A repeated measures ANOVA revealed a significant main effect of time [$F(5,60) = 31.541$, $p < 0.001$] and a significant time by genotype interaction [$F(5,60) = 7.502$, $p < 0.001$]. Bonferroni-corrected pairwise comparisons showed genotype effects at 40 ($p < 0.044$), 60 ($p < 0.023$), and 80 min ($p < 0.026$). Hence, both genotypes responded to KCl depolarization; however, stimulated release in KD^{HET} striatum was reduced relative to that of the wild-type controls.

Since VAChT is responsible for sequestering ACh into secretory vesicles, we evaluated the effects of decreased VAChT expression on total ACh levels in brain tissue. When tissue concentrations of ACh were measured by high-performance liquid chromatography (HPLC) with eletrochemical detection (HPLC-EC), levels in frontal cortex and striatum of VAChT KD^{HET} mice were significantly increased by approximately 49% [$t(1,25) = 4.082$, $p < 0.001$] and 30% [$t(1,10) = 3.408$, $p < 0.007$], respectively, over that of the wild-type controls (Figure 5C). These data were replicated in a complementary chemiluminescence assay in a separate group of mice using both striatum and hippocampus (Figure 5D; $p < 0.05$). Moreover, VAChT KD^{HOM} mice show an even larger increase in ACh content in the brain, and this increase was statistically different from that of VAChT KD^{HET} mice or wild-type mice (Figure S1C; $p < 0.05$). This increase in ACh content for mutant mice cannot be attributed to an increase in ChAT activity (Figure S1A), high-affinity choline transporter activation (Figure S1D), or increased levels of expression of ChAT (Figures S1B and S1E) or CHT1 (Figure 1E). Whereas the mechanism of such an increase in total tissue ACh content it is not immediately apparent, it is important to emphasize that the functional "releasable" ACh pool seems to be decreased, as evidenced by in vivo microdialysis experiments and quantal analysis at the neuromuscular junction. All together, these results demonstrate that a reduction of approximately 50% in the levels of VAChT expression in the brain results in a significant decrease in the release of ACh in vivo, despite enhanced intracellular content of neurotransmitter. These observations suggest a complex relationship between the control of storage and release of ACh in CNS neurons.

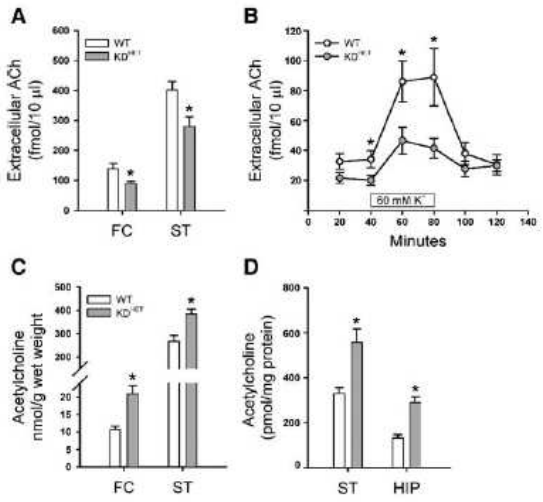

Figure 5. Neurochemical Alterations in VAChT KD^{HET} Mice

(A) Extracellular ACh levels as determined by quantitative low perfusion rate microdialysis in frontal cortex and striatum. n = 10 mice per genotype per brain region.

(B) KCl-stimulated release of ACh in striatum of freely moving mice. Following 40 min of baseline collection of ACh, 60 mM [K$^+$] was infused through the microdialysis probe for 40 min, and artificial CSF was infused over the last 40 min of the experiment. n = 7 mice per genotype. *p < 0.05 for wild-type controls.

(C) Tissue ACh contents in frontal cortex (FC) and striatum (ST) of wild-type and KD^{HET} mice measured by HPLC with electrochemical detection. FC: n = 14 (wild-type), n = 13 (KD^{HET}); ST: n = 6 mice per genotype.

(D) Striatal (ST) and hippocampal (HIP) tissue ACh levels assayed by chemiluminescent detection in wild-type (open bars) and VAChT KD^{HET} (gray bars) mice (n = 5). In all panes, data are mean ± SEM. *p < 0.05 for wild-type controls.

Behavioral Evaluation

After documenting normal performance of VAChT KD^{HET} mice in tests of neuromuscular strength, despite reduced cholinergic tone in the brain, we proceeded to evaluate performance of mutants in behavioral tasks reflecting CNS cholinergic function. VAChT KD^{HET} mice were tested for performance in the step-down inhibitory avoidance task, a task that depends upon hippocampal and amygdala networks and may be sensitive to manipulations in central cholinergic function (Izquierdo and Medina, 1997). Both genotypes exhibited learning, as latency to step-down from the platform increased from 10 to 15 s to approximately 80 to 100 s after training. In parallel experiments, we determined in another cohort of mice that the unconditioned stimulus was essential for both genotypes to learn the task (data not shown). VAChT KD^{HET} performed as well as wild-type littermates on this task on a short-term (1.5 hr after learning) and long-term (24 hr after learning) memory test, suggesting that this specific aspect of learning and memory is preserved in animals with a mild decrease in cholinergic tone (Figure 6A).

A second test for memory, based on the ability to discriminate novel objects, was used to evaluate the performance of mutant mice. In the object recognition task, mice explore two objects, and after a latency of 1.5 or 24 hr they are presented with one of the familiar objects and a nonfamiliar object. Initial exploration time of two objects was identical for both genotypes, indicating that they both show preference for novelty (data not shown). However, whereas wild-type mice exhibited a significant increase in the exploration of the unfamiliar object, mutant mice performed poorly compared to wild-type mice in their ability to remember the familiar object both 1.5 and 24 hr after learning (Figure 6B, $p < 0.05$, Kruskal-Wallis analysis of variance and Mann-Whitney U tests, n = 12–18). Thus, VAChT KD^{HET} mice appear to have a cognitive deficit that impacts behavior in this test.

Recognition of a familiar conspecific is the basis of several social interactions, including hierarchical social relationship and mate choice (Winslow and Insel, 2004). There is evidence for the participation of nicotinic and muscarinic central systems in social recognition in rodents (Prediger et al., 2006; van Kampen et al., 2004; Winslow and Camacho, 1995), and social recognition deficits may relate to cholinergic decline in a mouse model of AD (Ohno et al., 2004). We evaluated social interactions of VAChT KD^{HET} mice in a habituation-dishabituation paradigm using a mouse intruder (Choleris et al., 2003). Wild-type control mice showed extensive exploration of the intruder (e.g., sniffing) during first contact. This response decreased with subsequent exposure to the same juvenile [$F(4,11) = 60.93$, $p < 0.01$], indicating that wild-type control mice readily habituated to the conspecific (Figure 6C). Hence, after four exposures to the same juvenile, wild-type mice explored the intruder for only one-third of the length of time of the initial exploration. Upon changing to an unfamiliar mouse, wild-type animals showed a renewed interest in investigation, and explored the new mice as much as they explored the original intruder during the first contact (Figure 6C). These results indicate that lack of interest in exploring the first intruder upon recurring exposure was not attributable to lack of motivation, but appears to be due to habituation, i.e., learning. Exploration of the intruder mice by VAChT KD^{HET} mice on the first contact was slightly less than that observed for wild-type animals ($p < 0.05$, two-way ANOVA with Bonferroni post hoc). Upon subsequent exposures, VAChT KD^{HET} mice show statistically significant differences in exploration of the intruder mice as compared with wild-type mice ($p < 0.001$, two-way ANOVA with Bonferroni post hoc). In sharp contrast to wild-type littermates, VAChT KD^{HET} mice failed to habituate to the juvenile intruder in the subsequent exposures after the initial contact, and only after the fourth contact was there a significant difference in exploratory behavior compared with the first encounter [$F(4,10) = 5.293$, Figure 6C)]. Introduction of an unfamiliar mouse led VAChT KD^{HET} mice to increase their exploration, indicating that the decrease in exploration during the fourth exposure for the first intruder was not due to nonspecific effects such as physical exhaustion or motivation.

One possible explanation for the inability of VAChT KD^{HET} mice to habituate to a conspecific is that mutant mice have olfactory deficits. In a control experiment, we evaluated olfactory responses in these mice. However, both wild-type and VAChT KD^{HET} mice showed similar abilities in finding a hidden food reward (data not shown), suggesting that the differences observed

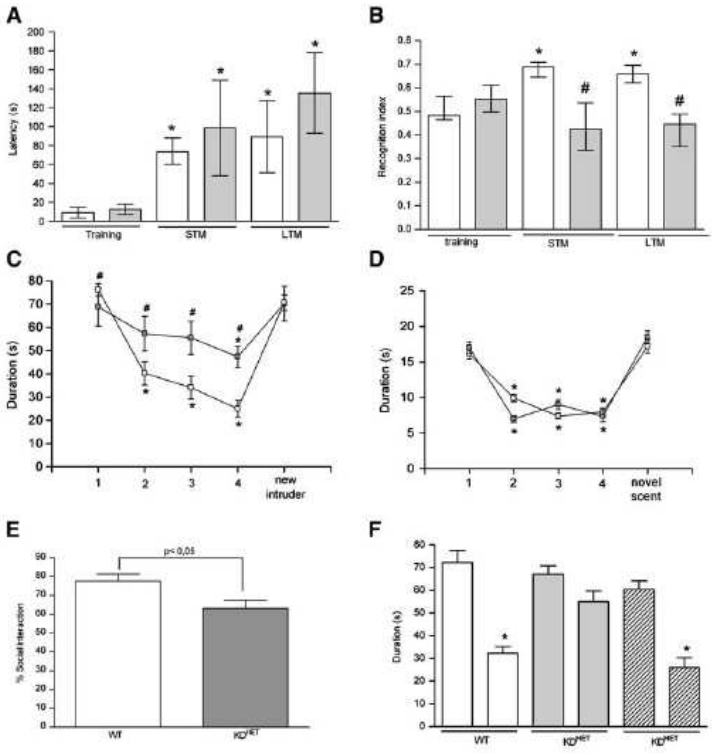

Figure 6. Behavioral Alterations of VAChT KD^{HET} Mice

(A) Step-down inhibitory avoidance task. Retention test latency measured 90 min after training (STM) and again at 24 hr (LTM). Ordinates express median (interquartile range) test session latency, in seconds. Open bars represent the performance of wild-type mice and shadowed bars represent that of VAChT KD^{HET} mice (n = 13–18 per group). *p < 0.05 compared with performance of mice during training.

(B) Object recognition test. Results are shown as median (interquartile ranges) recognition indexes of short-term (STM) and long-term (LTM) retention test trials. Clear bars represent data from wild-type mice and shadow bars are the data from VAChT KD^{HET} mice. (#) indicates a significant difference from wild-type; p < 0.05, n = 12–18. *p < 0.05 compared with performance of mice during training.

(C) Social memory of wild-type (open squares) and KD^{HET} (gray squares) mice was measured as olfactory investigation during each of four successive 5 min trials with an intertrial interval of 15 min. A fifth dishabituation trial depicts the response of mice to the presentation of a new intruder in a 5 min pairing, 15 min after the fourth trial. *p < 0.05 compared with performance on the first trial within the genotype, and #p < 0.05 when compared with wild-type control mice; n = 10–12.

(D) Olfactory function of wild-type and VAChT KD^{HET} mice. Mice were presented a strawberry essence for 1 min in 4 sequential trials with an intertrial interval of 10 min. On the 5th trial, vanilla essence was presented. *p < 0.05 from the first trial within genotype. No between group differences were observed.

(E) Social preference of wild-type (open bar) and VAChT KD^{HET} mice. Only the percentage of exploration for the social stimulus is shown.

(F) Social memory of wild-type (open bars, n = 14), VAChT KD^{HET} (gray bars, n = 14), and VAChT KD^{HET} mice treated with galantamine (s.c., 1 mg/kg) 30 min prior to the first exposure to an intruder (hatched bars, n = 8). The intruder is presented in each of two 5 min trials with an intertrial interval of 30 min. *p < 0.05 for the first trial within the genotype. Unless otherwise stated, data are mean ± SEM.

in social recognition do not relate to deficits in olfactory function. In addition, wild-type and VAChT KD^{HET} mice habituated to a test odor similarly [wild-type, $F(4,6) = 11.35$, and VAChT KD^{HET} mice, $F(4,6) = 18.11$, $p < 0.05$ by repeated measures ANOVA]. There were no differences between the two genotypes in olfactory habituation or in their ability to discriminate between two test odors (Figure 6D).

A second possibility to explain the deficit in social habituation is that VAChT KD^{HET} mice are more social than wild-type mice, i.e., they prefer the company of intruder mice more than wild-type mice do. This would be the converse of the autistic-like behavior found in PTEN mutant mice (Kwon et al., 2006). To specifically test this possibility, we evaluated the choice of wild-type and VAChT KD^{HET} mice for a social stimulus (an adult mouse in an acrylic cage that allowed minimum tactile exploration but allowed olfactory exploration) against a nonsocial stimulus (an identical acrylic cage which was never previously presented to the mice). This experiment was done in specially designed boxes containing two separate rooms, each of which the mice had to enter to explore the social or nonsocial target, respectively (Kwon et al., 2006). As expected from the previous experiment, both genotypes had a stronger preference for the social against the nonsocial stimuli (Figure 6F); however, VAChT KD^{HET} mice expended significantly less time with the social stimulus and consequently more time with the nonsocial stimulus than wild-type control mice did ($p < 0.05$, Student's t test). Therefore, increased social preference of VAChT KD^{HET} mice cannot explain the lack of habituation observed in the social recognition test. If anything, the data indicate that VAChT KD^{HET} mice are less social than control mice.

The results above suggest that VAChT KD^{HET} mice have a deficit in social memory. This deficit could be a consequence of decreased ACh release, or it could result from adaptative changes in brain neurochemistry during development in response to the decreased expression levels of VAChT. If the deficits in social recognition are related to decreased acetylcholine output, acute inhibition of cholinesterase, which preserves ACh in the synapse, might rescue the phenotype. Therefore, we retested mice in the social memory task using a paradigm that allowed us to treat mice with a cholinesterase inhibitor prior to the experiment. The social recognition memory lasted at least 30 min, as wild-type mice exposed to an intruder for 5 min twice, with an intertrial interval of 30 min, explored the intruder significantly less in the second exposure [$F(5,70) = 17.21$, $p < 0.001$] (Figure 6F). In contrast, there was no difference for VAChT KD^{HET} mice between the first and second

exposure to intruder mice with this protocol (Figure 6E). We repeated these experiments after injecting mice with either saline or galantamine (Figure 6F). The dose of galantamine used (s.c., 1 mg/kg) has been shown to be effective in improving cholinergic function in mice (Csernansky et al., 2005), and it was sufficient to improve the performance of VAChT KD^{HET} in this social recognition task (Figure 6F). Injection of saline had no effect on the performance of wild-type or VAChT KD^{HET} mice, ruling out that prior manipulation of mice affected the outcome of these experiments (data not shown). In addition, galantamine did not alter the response of wild-type mice (data not shown). It should be noted that the deficit in social recognition memory was also observed in a small number of VAChT KD^{HOM} mice studied with an identical protocol (Figure S2), thus confirming this phenotype for the two mutant genotypes. Hence, it appears that VAChT KD^{HET} mice have a deficit in social memory due to decreased cholinergic tone.

Discussion

To define the role of VAChT and ACh in physiological functions and behavior, we generated a mouse line with reduced expression of this transporter. The partial decrease in VAChT expression is essential in these investigations as complete lack of the vesicular transporter is likely to be incompatible with life, as shown for other presynaptic cholinergic genes (Brandon et al., 2004; Ferguson et al., 2004; Misgeld et al., 2002). Thus, this reduced expression mouse line allowed us to examine the consequences of reduced cholinergic tone in function, behavior, and cholinergic neurochemistry.

It has been demonstrated that several putative mRNA species exist for VAChT, although V1 is predominant in cholinergic tissues (Bejanin et al., 1994). In the present experiments, we show that VAChT KD^{HET} and KD^{HOM} mice have reduced levels of this major VAChT mRNA, whereas an increase in a less common mRNA for VAChT was detected, suggesting the existence of a compensatory mechanism in mutant mice. The open reading frame of VAChT is within the first intron of the ChAT gene. Interestingly, we detected no changes in ChAT mRNA levels in all CNS regions investigated, even though ChAT and VAChT transcripts might be, under certain conditions, coregulated (Eiden, 1998). In vertebrates, regulation of the cholinergic gene locus expression is complex; ChAT- and VAChT-specific mRNAs can be produced either from different promoters or by alternative RNA splicing (Oda, 1999).

In addition to the decrease in VAChT transcript, we detected a 45% reduction in VAChT protein levels in several CNS regions in VAChT KD^{HET} mice, whereas the reduction of VAChT protein levels in homozygous mutant mice was 65%–70% of that found in wild-type littermates. Therefore, the data indicate that protein levels of VAChT closely follow the reduction of the major VAChT mRNA species.

To evaluate how a decrease in VAChT levels affects transmitter release, we examined quantal secretion of ACh at the neuromuscular junction. Surprisingly, we observed relatively mild alterations in the distribution of quantal sizes in VAChT KD^{HET} mice. A robust change in quantal size distribution for VAChT KD^{HOM} mice was detected; however, a very pronounced decrease in the frequency of MEPPs was also observed. This decrease in MEPP frequency is not the result of alterations in the readily releasable pool of vesicles. It also seems unlikely that the alteration in MEPP frequency is the result of decreased exocytosis, endocytosis, and total pool of vesicles, as FM1-43 experiments have shown no difference in these parameters between wild-type and VAChT KD^{HOM} mice. We hypothesized that, if in synapses, the number of copies of VAChT per synaptic vesicles is low (Parsons et al., 1993; Van der Kloot, 2003), a reduction in VAChT abundance could result in electrophysiologically "silent" vesicles, and thus a decrease in MEPP frequency. Prior experiments have demonstrated that overexpression of VAChT in immature *Xenopus* spinal neurons increases not only the amplitude but also the frequency of miniature excitatory postsynaptic currents (Song et al., 1997), indicating that, at least under certain conditions, VAChT expression levels can affect electrophysiological detection of exocytosis. Similarly, in *Drosophila* mutants with decreased neuromuscular expression of the vesicular glutamate transporter, there are major deficits in frequency of miniature end-plate currents, but no alterations in quantal size (Daniels et al., 2006). Remarkably, VAChT phosphorylation by PKC affects its trafficking to secretory vesicles, suggesting that alterations in VAChT expression in synaptic vesicles could occur physiologically (Krantz et al., 2000).

The results herein with VAChT mutant mice also indicate that synaptic vesicle exocytosis is not altered by decreased levels of the transporter; in this regard, these results agree with similar observations in VMAT2-deficient mice (Croft et al., 2005), which also present no deficits in monoaminergic vesicle exocytosis. Nonetheless, the data show that VAChT KD^{HET} mice have mild changes in ACh release at the neuromuscular junction, whereas VAChT KD^{HOM} mice have a more profound deficit in transmitter release.

Analysis of neuromuscular function in the three genotypes corroborated these electrophysiological data. VAChT KD^{HET} mice performed as well as wild-type mice in tests of motor function, whereas VAChT KD^{HOM} mice were significantly impaired in grip strength and ability to hold their weight. Importantly, the deficit in grip strength could be ameliorated by prior treatment of mutant mice with cholinesterase inhibitors. The effect of pyridostigmine, which is used to treat myasthenia, is of particular importance, as it indicates that a peripheral cholinergic deficit due to alteration in neuromuscular transmission is the cause of neuromuscular dysfunction.

Investigation of VAChT KD mice on the rotarod, a task that depends upon motor learning and physical endurance, reveals that VAChT KD^{HET} are slower to learn this motor task than wild-type control mice, but the former are able to reach the same level of performance in time. In contrast, VAChT KD^{HOM} mice are significantly impaired and never improve their performance. That VAChT KD^{HOM} mice have limited capacity for exercise is clearly observed on the treadmill, indicating that performance of the homozygous mutants on the rotarod also reflects their inability to maintain prolonged physical activity. These results suggest that VAChT KD^{HOM} mice may provide a model for study of the effects of markedly reduced ACh release on neuromuscular

function, such as the ones observed in certain types of congenital presynaptic myasthenia (Ohno et al., 2001).

In contrast, we were unable to detect any alteration in neuromuscular function in VAChT KD^{HET} mice. Release of ACh accompanied the reduction of protein expression in the brain for VAChT KD^{HET} mice, and both basal and stimulated extracellular levels were affected. This decrease in ACh release appears to be related to the reduction of VAChT expression, as ChAT activity was not decreased in these mutants. Overall, the approximately 45% reduction in VAChT expression appears to decrease ACh secretion to a similar extent in the brain. Unexpectedly, tissue ACh was significantly increased in several brain regions from VAChT KD^{HET} and VAChT KD^{HOM} mice, indicating a previously unrecognized connection between ACh storage, nonvesicular ACh pools, and tissue content. Molecular mechanisms responsible for this increased tissue ACh content have not been uncovered yet, but it does not seem to be due to altered ChAT activity or high-affinity choline uptake. It is interesting that pharmacological experiments with vesamicol, an inhibitor of VAChT, have revealed a similar relationship, whereby decreased secretion of ACh leads to accumulation of intracellular transmitter during nerve stimulation (Collier et al., 1986).

Whereas VAChT KD^{HET} mice present only mild defects in neuromuscular neurotransmission, there is a relatively larger deficiency in central ACh release in vivo. Neuromuscular transmission has a high safety margin, and neuromuscular weakness is not observed until a significant proportion of neuromotor units are compromised (Paton and Waud, 1967; Waud and Waud, 1975). Therefore, it is reasonable to envision that a partial decrease in VAChT expression will cause more profound consequences on cholinergic transmission in the brain, where a relatively small number of synaptic vesicles (100–200 vesicles) need to be constantly recycled and refilled with neurotransmitter. In contrast, at neuromuscular synapses, there is a very large population of vesicles; fast refilling of vesicles may not be as crucial for neurotransmission at the neuromuscular junction as it is for brain synapses, at least when under low neuromuscular demand.

The VAChT KD^{HET} mice present a unique opportunity to investigate the consequences of homogeneous decrease of ACh tone in cognitive tasks, as the results show that these mice represent a model of moderate, predominantly central cholinergic dysfunction. We observed no deficits in performance of VAChT KD^{HET} mice in the step-down inhibitory avoidance test. A number of experiments have demonstrated that inhibition of nicotinic and muscarinic central receptor activity can affect performance of rats in this paradigm (Barros et al., 2002), indicating an important cholinergic contribution toward performance in this test. It is likely that the reduction of cholinergic function in VAChT KD^{HET} mice was below the threshold for detecting a learning or memory impairment for this task. This result supports the notion that ACh participates in, but is not essential for, some hippocampal-dependent paradigms of learning and memory (Parent and Baxter, 2004).

Interestingly, VAChT KD^{HET} mice performed worse than wild-type mice in an object recognition test, suggesting that even mild decline of cholinergic function can affect cognitive processes required for this task. Indeed, rats treated with 192 IgG-saporin, which leads to cholinergic degeneration in the basal forebrain, also present object recognition deficits (Paban et al., 2005), and object recognition alterations are observed in certain mouse models of AD (Dewachter et al., 2002). It is likely that VAChT KD^{HET} present such deficits because they have impairments in their ability to learn or remember the intricate cues necessary for discriminating the novel object.

Our data also revealed an important role of cholinergic tone in recognition of mouse conspecifics. In these experiments, the KD^{HET} mice explore unfamiliar mice; however, their preference for a social stimuli is somewhat decreased compared with wild-type mice. Nonetheless, the mutant mice are not socially deficient, but they are clearly impaired in remembering intruder mice when compared with wild-type mice. Absence of deficits in olfactory discrimination in VAChT KD^{HET} mice supports the notion that the decreased social memory is due to cognitive impairments rather than a simple incapacity to process olfactory cues. An important role of cholinergic tone in social recognition is supported by reversal of this phenotype in mice treated with a cholinesterase inhibitor and by the fact that VAChT KD^{HOM} mice also present a significant deficit in social recognition.

Social memory in rodents depends upon the activity of vasopressin on V1A receptors in the lateral septum (Bielsky et al., 2005) and upon the activity of oxytocin (Bielsky and Young, 2004; Ferguson et al., 2000; Winslow and Insel, 2004). However, central muscarinic and $\alpha 7$ nicotinic receptors have also been suggested to play a role in social memory (Prediger et al., 2006; van Kampen et al., 2004; Winslow and Camacho, 1995), indicating a potential mechanism for ameliorating social memory deficits in response to cholinergic decline. Our observations support the notion that reduced cholinergic tone in AD mouse models can indeed cause deficits in social memory. However, based on somewhat similar impairments found in the object and social recognition tasks, it is possible that mild cholinergic deficits may cause a more general memory deficit for recognizing previously learned complex cues, whether social or not. Future detailed investigations will be necessary to further define the specific type of cognitive processing affected by cholinergic deficits in these mutants. Such studies in mouse models of reduced cholinergic tone may be particularly informative for understanding the contribution of cholinergic decline to specific behavioral alterations observed in certain pathologies of the CNS, and may even be helpful in understanding physiological aging (Cummings, 2004).

In conclusion, we have generated an animal model to study the impact of decreased VAChT expression on peripheral and central ACh neurotransmission and function. The present results illuminate the role of VAChT in vesicular ACh release and reveal that deficits in VAChT-mediated filling of synaptic vesicles may have important behavioral consequences. Furthermore, these observations indicate an important role for ACh in cognitive processes involved in object and social recognition and memory. In this respect, a decrease in VAChT expression is much less tolerated than a decrease in

ChAT activity, a parameter that is used extensively to evaluate cholinergic deficits in AD.

Experimental Procedures

Animal Care

Heterozygous mutant VAChT mice were backcrossed with C57BL/6J animals for three generations; the N3 mice were used in most experiments. Homozygous mutant VAChT mice were obtained by intercrossing N3 heterozygous animals. Control animals were wild-type age- and sex-matched littermates, and all behavioral and most of the biochemical studies were conducted with researchers "blind" to the genotypes of the mice. For all behavioral experiments, male mice were used.

Animals were housed in groups of three to five animals per cage in a temperature-controlled room with a 12:12 light-dark cycles, and food and water were provided ad libitum. All studies were conducted in accordance with NIH guidelines for the care and use of animals and with approved animal protocols from the Institutional Animal Care and Use Committees at the Federal University of Minas Gerais in Brazil, Pontificia Universidade Catolica de Rio Grande do Sul in Brazil, and Duke University in the United States.

Wire-Hang, Grip Force, Rotarod, and Treadmill Tests

The wire-hang experiments were conducted as described (Sango et al., 1996) and time spent hanging upside down was determined with a cutoff time of 60 s.

To measure grip force, we used a custom-built force transducer connected to a small support that could be grasped by the mouse as described (Fowler et al., 2002). Five tests were performed per mouse with a maximum period of 50 s for each animal over 2 different days. The force transducer was coupled to a computer and a routine was developed to record the maximal grip force exerted.

For the rotarod task, we followed the protocol described by Brandon et al. (1998). Mice were placed on the rotarod apparatus (Insight Equipments, Ribeirão Preto, Brazil) and rotation was increased from 5 to 35 rpm. Latency to fall was recorded automatically. The test was run within the last 4 hr of the light phase of the 12:12 cycle. Ten trials were given on the first day and four trials on the second day, with a 10 min intertrial interval. In the time between trials, mice were placed in their home cage.

For the treadmill test (Insight Equipments, Ribeirão Preto, Brazil), mice were trained for 4 days (3 min a day). On the first day, inclination was set to 5°. The inclination was increased by 5° for each training day until reaching 20°. The initial training speed was 8 m/min, and the treadmill was accelerated by 1 m/min. In the second training session, the initial speed was 10 m/min increased to 11 and 12 m/min in the third and fourth training days, respectively. During testing, the initial speed was set to 12 m/min, which was increased by 1 m/min at 2, 5, 10, 20, 30, 40, 50, and 60 min after starting the exercise, essentially as described by Pederson et al. (2005). The work performed (in J) was calculated with the following formula: W(J) = body weight (kg) × cos 20° × 9.8 (J/kg × m) × distance (m).

Step-Down Inhibitory Avoidance

The step-down inhibitory avoidance apparatus was a 50 × 25 × 25 cm acrylic box which had a floor consisting of a grid of parallel stainless steel bars 1 mm in diameter spaced 1 cm apart. A 10 cm^2 wide, 2 cm high acrylic platform was placed in the center of the floor. Animals were placed on the platform and their latency to step down on the grid with all four paws was measured with an automatic device. In the training session, immediately after stepping down on the grid, the animals received a 2.0 s, 0.3 mA scrambled foot-shock. Retention test sessions were procedurally identical, except that no foot-shock was given. The latency to step down during testing was taken as a measure of retention. A ceiling of 180 s was imposed in this measure, i.e., animals whose test latency was over than 180 s were counted as 180 s. Each animal was tested twice, once at 1.5 hr after training, to measure short-term retention, and once at 24 hr after training, to measure long-term retention (Izquierdo et al., 2002; Lorenzini et al., 1996). Since the variable being analyzed (step-down latency) does not follow a normal distribution, the data were analyzed by Mann-Whitney U or Kruskal-Wallis nonparametric tests, followed by Dunn's post hoc comparisons where appropriated.

Object Recognition

All animals were given a single 5 min habituation session with no objects in the open-field arena (as described above). Twenty-four hours after habituation, training was conducted by placing individual mice for 5 min into the field, in which two identical objects (objects A1 and A2; Duplo Lego toys) were positioned in two adjacent corners, 10 cm from the walls. A minimum of 30 s exploration time for objects was allowed in this first exposure. In a short-term memory (STM) test given 1.5 hr after training, the mice explored the open field for 5 min in the presence of one familiar (A) and one novel (B) object. All objects presented similar textures, colors, and sizes, but distinctive shapes. A recognition index calculated for each animal was expressed by the ratio $T_B/(T_A + T_B)$ [T_A = time spent exploring the familiar object A; T_B = time spent exploring the novel object B]. Between trials the objects were washed with 10% ethanol solution and air-dried. In a long-term memory (LTM) test given 24 hr after training, the same mice explored the field for 5 min in the presence of familiar object A and a novel object C. Recognition memory was evaluated as for the short-term memory test. Exploration was defined as sniffing or touching the object with nose and/or forepaws (de Lima et al., 2005). Data for recognition indexes are expressed as median (interquartile ranges). Comparisons among groups were performed using a Kruskal-Wallis analysis of variance and Mann-Whitney U tests. Recognition indexes within individual groups were analyzed with Wilcoxon tests.

Social Recognition

Mice were housed in individual cages in a quiet room for 4 days to establish territory dominance. Swiss juvenile male mice were used as the intruder. To test for social interaction, the intruder was placed inside a transparent acrylic chamber containing several holes and introduced into the test cage exactly as described (Choleris et al., 2003). Time spent sniffing was measured as the amount of time that VAChT KD^{HET} mice or wild-type littermates spent poking their noses into the holes of the chamber. Initially, the subject tested (wild-type or VAChT KD^{HET} mouse) was exposed to an empty acrylic chamber for 10 min; subsequently, this chamber was exchanged by one containing the intruder and left for 5 min. The entire procedure was repeated four times. After the fourth exposure to the same intruder, a novel intruder was added to the acrylic chamber. The experiment was videotaped and a trained researcher, blind to genotype, evaluated time spent sniffing in each condition.

A second experiment consisted of exposing the subject to the same intruder twice with an intertrial interval of 30 min. The standard measure for the statistical analysis in social recognition tests was the time spent exploring the juvenile intruder. To evaluate the contribution of acute cholinergic deficits, saline or 1 mg/kg galantamine (s.c.) was injected 30 min before beginning of the tests.

For evaluation of sociability, we followed the protocol described by Kwon et al. (2006). Testing was done in a three-chambered apparatus (15 × 90 × 18.5 cm divided into three chambers of 15 × 29 cm and separated by dividers with a central 3.8 × 3.8 cm door) that offers the subject a choice between a social stimulus and an inanimate target. In the habituation session, mice were allowed to explore the entire box for 10 min. Subsequently, mice stayed 5 min in the center and were then allowed to interact for 10 min with an empty cage in one chamber versus a caged social target in the opposite chamber. Social and nonsocial stimuli were varied among the chambers and the box was cleaned between tests. Results are presented as percentage of total exploration time.

Two tests to evaluate the olfactory responses of the mice were conducted (Bielsky et al., 2005; Ferguson et al., 2000). The first consisted of measuring the time that both genotypes took to find a candy located on the surface of bedding or hidden within the bedding (Ferguson et al., 2000). The second test investigated whether VAChT KD^{HET} mice presented olfactory habituation and discrimination. Experiments were performed 7 days after completing the social recognition tests in the same groups of mice. For this test, a microtube, with a piece of cotton containing 10 μl of strawberry essence, was presented to mice four times for 1 min with a 10 min intertrial interval. On the fifth trial, the microtube was exchanged with one containing

vanilla essence. The significance of differences between the groups was determined by Student's t test or two-way ANOVA, and a post hoc Bonferroni test was performed when appropriate. Changes across trials were assessed with repeated measures ANOVA with Bonferroni's post hoc analysis.

For all other methods, see the Supplemental Data.

Supplemental Data

The Supplemental Data for this article can be found online at http://www.neuron.org/cgi/content/full/51/5/601/DC1/.

Acknowledgments

We thank W. Roberts and S. Suter (Duke University Medical Center) as well as D.A. Guimaraes and D.M. Diniz (Universidade Federal de Minas Gerais) for outstanding help in caring for mouse colonies, L.F.L. Reis and E. Abrantes (Ludwig Institute, Sao Paulo) for help with genomic library screening, A.M. Carneiro for initial help with the targeting construct, C. Bock for transgenic service (Duke University Medical Center), B. Collier (McGill University), W. Van der Kloot (SUNY) and S. Parsons (UCSB) for discussions, and R.M. Rodriguiz (Duke University Medical Center) for assisting with the statistical analyses of the neurochemistry experiments. This work was partially supported by CAPES Fellowships for a sabbatical period at Duke University (M.A.M.P., V.F.P.), an IBRO grant (M.A.M.P.), a Center for excellence grant (FAPEMIG, CNPq, and PRONEX-MG to M.A.M.P. and V.F.P.), the Millenium Institute (M.V.G.), a Fogarty International Collaboration Award (FIC-NIH, R03 TW007025-01A1 to M.G.C., M.A.M.P., and V.F.P.), and NIH grants DA13551, NS19576 and MH60451 to M.G.C. Establishment of mouse colonies in Brazil received support from a pilot grant from the Alzheimer's Program of the American Health Assistance Foundation (M.A.M.P.).

Received: March 29, 2006
Revised: June 27, 2006
Accepted: August 3, 2006
Published: September 6, 2006

References

Barros, D.M., Pereira, P., Medina, J.H., and Izquierdo, I. (2002). Modulation of working memory and of long- but not short-term memory by cholinergic mechanisms in the basolateral amygdala. Behav. Pharmacol. *13*, 163–167.

Bartus, R.T., Dean, R.L., III, Beer, B., and Lippa, A.S. (1982). The cholinergic hypothesis of geriatric memory dysfunction. Science *217*, 408–414.

Bejanin, S., Cervini, R., Mallet, J., and Berrard, S. (1994). A unique gene organization for two cholinergic markers, choline acetyltransferase and a putative vesicular transporter of acetylcholine. J. Biol. Chem. *269*, 21944–21947.

Bielsky, I.F., and Young, L.J. (2004). Oxytocin, vasopressin, and social recognition in mammals. Peptides *25*, 1565–1574.

Bielsky, I.F., Hu, S.B., Ren, X., Terwilliger, E.F., and Young, L.J. (2005). The v1a vasopressin receptor is necessary and sufficient for normal social recognition: a gene replacement study. Neuron *47*, 503–513.

Brandon, E.P., Logue, S.F., Adams, M.R., Qi, M., Sullivan, S.P., Matsumoto, A.M., Dorsa, D.M., Wehner, J.M., McKnight, G.S., and Idzerda, R.L. (1998). Defective motor behavior and neural gene expression in RIIbeta-protein kinase A mutant mice. J. Neurosci. *18*, 3639–3649.

Brandon, E.P., Mellott, T., Pizzo, D.P., Coufal, N., D'Amour, K.A., Gobeske, K., Lortie, M., Lopez-Coviella, I., Berse, B., Thal, L.J., et al. (2004). Choline transporter 1 maintains cholinergic function in choline acetyltransferase haploinsufficiency. J. Neurosci. *24*, 5459–5466.

Cho, G.W., Kim, M.H., Chai, Y.G., Gilmor, M.L., Levey, A.I., and Hersh, L.B. (2000). Phosphorylation of the rat vesicular acetylcholine transporter. J. Biol. Chem. *275*, 19942–19948.

Choleris, E., Gustafsson, J.A., Korach, K.S., Muglia, L.J., Pfaff, D.W., and Ogawa, S. (2003). An estrogen-dependent four-gene micronet regulating social recognition: a study with oxytocin and estrogen receptor-alpha and -beta knockout mice. Proc. Natl. Acad. Sci. USA *100*, 6192–6197.

Collier, B., Welner, S.A., Ricny, J., and Araujo, D.M. (1986). Acetylcholine synthesis and release by a sympathetic ganglion in the presence of 2-(4-phenylpiperidino) cyclohexanol (AH5183). J. Neurochem. *46*, 822–830.

Croft, B.G., Fortin, G.D., Corera, A.T., Edwards, R.H., Beaudet, A., Trudeau, L.E., and Fon, E.A. (2005). Normal biogenesis and cycling of empty synaptic vesicles in dopamine neurons of vesicular monoamine transporter 2 knockout mice. Mol. Biol. Cell *16*, 306–315.

Csernansky, J.G., Martin, M., Shah, R., Bertchume, A., Colvin, J., and Dong, H. (2005). Cholinesterase inhibitors ameliorate behavioral deficits induced by MK-801 in mice. Neuropsychopharmacology *30*, 2135–2143.

Cummings, J.L. (2004). Alzheimer's disease. N. Engl. J. Med. *351*, 56–67.

Daniels, R.W., Collins, C.A., Chen, K., Gelfand, M.V., Featherstone, D.E., and DiAntonio, A. (2006). A single vesicular glutamate transporter is sufficient to fill a synaptic vesicle. Neuron *49*, 11–16.

de Lima, M.N., Laranja, D.C., Caldana, F., Grazziotin, M.M., Garcia, V.A., Dal Pizzol, F., Bromberg, E., and Schroder, N. (2005). Selegiline protects against recognition memory impairment induced by neonatal iron treatment. Exp. Neurol. *196*, 177–183.

Dewachter, I., Reverse, D., Caluwaerts, N., Ris, L., Kuiperi, C., Van den, H.C., Spittaels, K., Umans, L., Serneels, L., Thiry, E., et al. (2002). Neuronal deficiency of presenilin 1 inhibits amyloid plaque formation and corrects hippocampal long-term potentiation but not a cognitive defect of amyloid precursor protein [V717I] transgenic mice. J. Neurosci. *22*, 3445–3453.

Eiden, L.E. (1998). The cholinergic gene locus. J. Neurochem. *70*, 2227–2240.

Elmqvist, D., and Quastel, D.M. (1965). Presynaptic action of hemicholinium at the neuromuscular junction. J. Physiol. *177*, 463–482.

Erickson, J.D., Varoqui, H., Schafer, M.K., Modi, W., Diebler, M.F., Weihe, E., Rand, J., Eiden, L.E., Bonner, T.I., and Usdin, T.B. (1994). Functional identification of a vesicular acetylcholine transporter and its expression from a "cholinergic" gene locus. J. Biol. Chem. *269*, 21929–21932.

Ferguson, J.N., Young, L.J., Hearn, E.F., Matzuk, M.M., Insel, T.R., and Winslow, J.T. (2000). Social amnesia in mice lacking the oxytocin gene. Nat. Genet. *25*, 284–288.

Ferguson, S.M., Bazalakova, M., Savchenko, V., Tapia, J.C., Wright, J., and Blakely, R.D. (2004). Lethal impairment of cholinergic neurotransmission in hemicholinium-3-sensitive choline transporter knockout mice. Proc. Natl. Acad. Sci. USA *101*, 8762–8767.

Fowler, S.C., Zarcone, T.J., Vorontsova, E., and Chen, R. (2002). Motor and associative deficits in D2 dopamine receptor knockout mice. Int. J. Dev. Neurosci. *20*, 309–321.

Gainetdinov, R.R., Bohn, L.M., Sotnikova, T.D., Cyr, M., Laakso, A., Macrae, A.D., Torres, G.E., Kim, K.M., Lefkowitz, R.J., Caron, M.G., and Premont, R.T. (2003). Dopaminergic supersensitivity in G protein-coupled receptor kinase 6-deficient mice. Neuron *38*, 291–303.

Izquierdo, I., and Medina, J.H. (1997). Memory formation: the sequence of biochemical events in the hippocampus and its connection to activity in other brain structures. Neurobiol. Learn. Mem. *68*, 285–316.

Izquierdo, I., Vianna, M.R., Medina, J.H., and Viola, H. (2002). Repetition of memories lost or never acquired. Trends Neurosci. *25*, 77–78.

Krantz, D.E., Waites, C., Oorschot, V., Liu, Y., Wilson, R.I., Tan, P.K., Klumperman, J., and Edwards, R.H. (2000). A phosphorylation site regulates sorting of the vesicular acetylcholine transporter to dense core vesicles. J. Cell Biol. *149*, 379–396.

Kwon, C.H., Luikart, B.W., Powell, C.M., Zhou, J., Matheny, S.A., Zhang, W., Li, Y.J., Baker, S.J., and Parada, L.F. (2006). Pten regulates neuronal arborization and social interaction in mice. Neuron *50*, 377–388.

Lorenzini, C.A., Baldi, E., Bucherelli, C., Sacchetti, B., and Tassoni, G. (1996). Role of dorsal hippocampus in acquisition, consolidation

and retrieval of rat's passive avoidance response: a tetrodotoxin functional inactivation study. Brain Res. *730*, 32–39.

Mesulam, M. (2004). The cholinergic lesion of Alzheimer's disease: pivotal factor or side show? Learn. Mem. *11*, 43–49.

Misgeld, T., Burgess, R.W., Lewis, R.M., Cunningham, J.M., Lichtman, J.W., and Sanes, J.R. (2002). Roles of neurotransmitter in synapse formation: development of neuromuscular junctions lacking choline acetyltransferase. Neuron *36*, 635–648.

Oda, Y. (1999). Choline acetyltransferase: the structure, distribution and pathologic changes in the central nervous system. Pathol. Int. *49*, 921–937.

Ohno, K., Tsujino, A., Brengman, J.M., Harper, C.M., Bajzer, Z., Udd, B., Beyring, R., Robb, S., Kirkham, F.J., and Engel, A.G. (2001). Choline acetyltransferase mutations cause myasthenic syndrome associated with episodic apnea in humans. Proc. Natl. Acad. Sci. USA *98*, 2017–2022.

Ohno, M., Sametsky, E.A., Younkin, L.H., Oakley, H., Younkin, S.G., Citron, M., Vassar, R., and Disterhoft, J.F. (2004). BACE1 Deficiency Rescues Memory Deficits and Cholinergic Dysfunction in a Mouse Model of Alzheimer's Disease. Neuron *41*, 27–33.

Paban, V., Jaffard, M., Chambon, C., Malafosse, M., and Alescio-Lautier, B. (2005). Time course of behavioral changes following basal forebrain cholinergic damage in rats: Environmental enrichment as a therapeutic intervention. Neuroscience *132*, 13–32.

Parent, M.B., and Baxter, M.G. (2004). Septohippocampal acetylcholine: involved in but not necessary for learning and memory? Learn. Mem. *11*, 9–20.

Parsons, S.M. (2000). Transport mechanisms in acetylcholine and monoamine storage. FASEB J. *14*, 2423–2434.

Parsons, S.M., Prior, C., and Marshall, I.G. (1993). Acetylcholine transport, storage, and release. Int. Rev. Neurobiol. *35*, 279–390.

Paton, W.D., and Waud, D.R. (1967). The margin of safety of neuromuscular transmission. J. Physiol. *191*, 59–90.

Pederson, B.A., Cope, C.R., Schroeder, J.M., Smith, M.W., Irimia, J.M., Thurberg, B.L., Depaoli-Roach, A.A., and Roach, P.J. (2005). Exercise capacity of mice genetically lacking muscle glycogen synthase: in mice, muscle glycogen is not essential for exercise. J. Biol. Chem. *280*, 17260–17265.

Prado, M.A., Reis, R.A., Prado, V.F., de Mello, M.C., Gomez, M.V., and de Mello, F.G. (2002). Regulation of acetylcholine synthesis and storage. Neurochem. Int. *41*, 291–299.

Prediger, R.D.S., De Mello, N., and Takahashi, R.N. (2006). Pilocarpine improves olfactory discrimination and social recognition memory deficits in 24 month-old rats. Eur. J. Pharmacol. *531*, 176–182.

Reimer, R.J., Fon, E.A., and Edwards, R.H. (1998). Vesicular neurotransmitter transport and the presynaptic regulation of quantal size. Curr. Opin. Neurobiol. *8*, 405–412.

Ribeiro, F.M., Black, S.A., Prado, V.F., Rylett, R.J., Ferguson, S.S., and Prado, M.A. (2006). The "ins" and "outs" of the high-affinity choline transporter CHT1. J. Neurochem. *97*, 1–12.

Richards, D.A., Guatimosim, C., and Betz, W.J. (2000). Two endocytic recycling routes selectively fill two vesicle pools in frog motor nerve terminals. Neuron *27*, 551–559.

Roghani, A., Feldman, J., Kohan, S.A., Shirzadi, A., Gundersen, C.B., Brecha, N., and Edwards, R.H. (1994). Molecular cloning of a putative vesicular transporter for acetylcholine. Proc. Natl. Acad. Sci. USA *91*, 10620–10624.

Sango, K., McDonald, M.P., Crawley, J.N., Mack, M.L., Tifft, C.J., Skop, E., Starr, C.M., Hoffmann, A., Sandhoff, K., Suzuki, K., and Proia, R.L. (1996). Mice lacking both subunits of lysosomal beta-hexosaminidase display gangliosidosis and mucopolysaccharidosis. Nat. Genet. *14*, 348–352.

Sarter, M., and Parikh, V. (2005). Choline transporters, cholinergic transmission and cognition. Nat. Rev. Neurosci. *6*, 48–56.

Song, H., Ming, G., Fon, E., Bellocchio, E., Edwards, R.H., and Poo, M. (1997). Expression of a putative vesicular acetylcholine transporter facilitates quantal transmitter packaging. Neuron *18*, 815–826.

Van der Kloot, W. (2003). Loading and recycling of synaptic vesicles in the Torpedo electric organ and the vertebrate neuromuscular junction. Prog. Neurobiol. *71*, 269–303.

van Kampen, M., Selbach, K., Schneider, R., Schiegel, E., Boess, F., and Schreiber, R. (2004). AR-R 17779 improves social recognition in rats by activation of nicotinic alpha(7) receptors. Psychopharmacology (Berl.) *172*, 375–383.

Waud, D.R., and Waud, B.E. (1975). In vitro measurement of margin of safety of neuromuscular transmission. Am. J. Physiol. *229*, 1632–1634.

Winslow, J.T., and Camacho, F. (1995). Cholinergic modulation of a decrement in social investigation following repeated contacts between mice. Psychopharmacology (Berl.) *121*, 164–172.

Winslow, J.T., and Insel, T.R. (2004). Neuroendocrine basis of social recognition. Curr. Opin. Neurobiol. *14*, 248–253.

2.1.2 - Material suplementar ao artigo nº 1 – Redução da expressão do VAChT não determina alterações pré-sinápticas compensatórias em animais *knockdown* homozigotos

A redução da expressão do VAChT não interferiu com o ciclo exo/endocitose e aparentemente não determinou redução do número de vesículas sinápticas aptas para a reciclagem (artigo nº1 - Prado *et al.*,2006). Entretanto, em busca de possíveis alterações pré-sinápticas compensatórias em resposta a redução na expressão do VAChT, foram feitas análises do número, da densidade e da área de terminações motoras marcadas com FM1-43 por hemidiafragma, utilizando o marcador fluorescente FM1-43fx, versão fixável do FM1-43. Após marcação, as preparações contendo FM1-43fx eram embebidas em solução de paraformaldeído 4% a 4ºC durante 40min (veja descrição do método no artigo 2 – de Castro *et al.*, 2009). Contudo, nenhuma diferença estatisticamente significativa foi encontrada entre camundongos *knockdown* homozigotos e camundongos selvagens (Figura Suplementar 1 em seqüência).

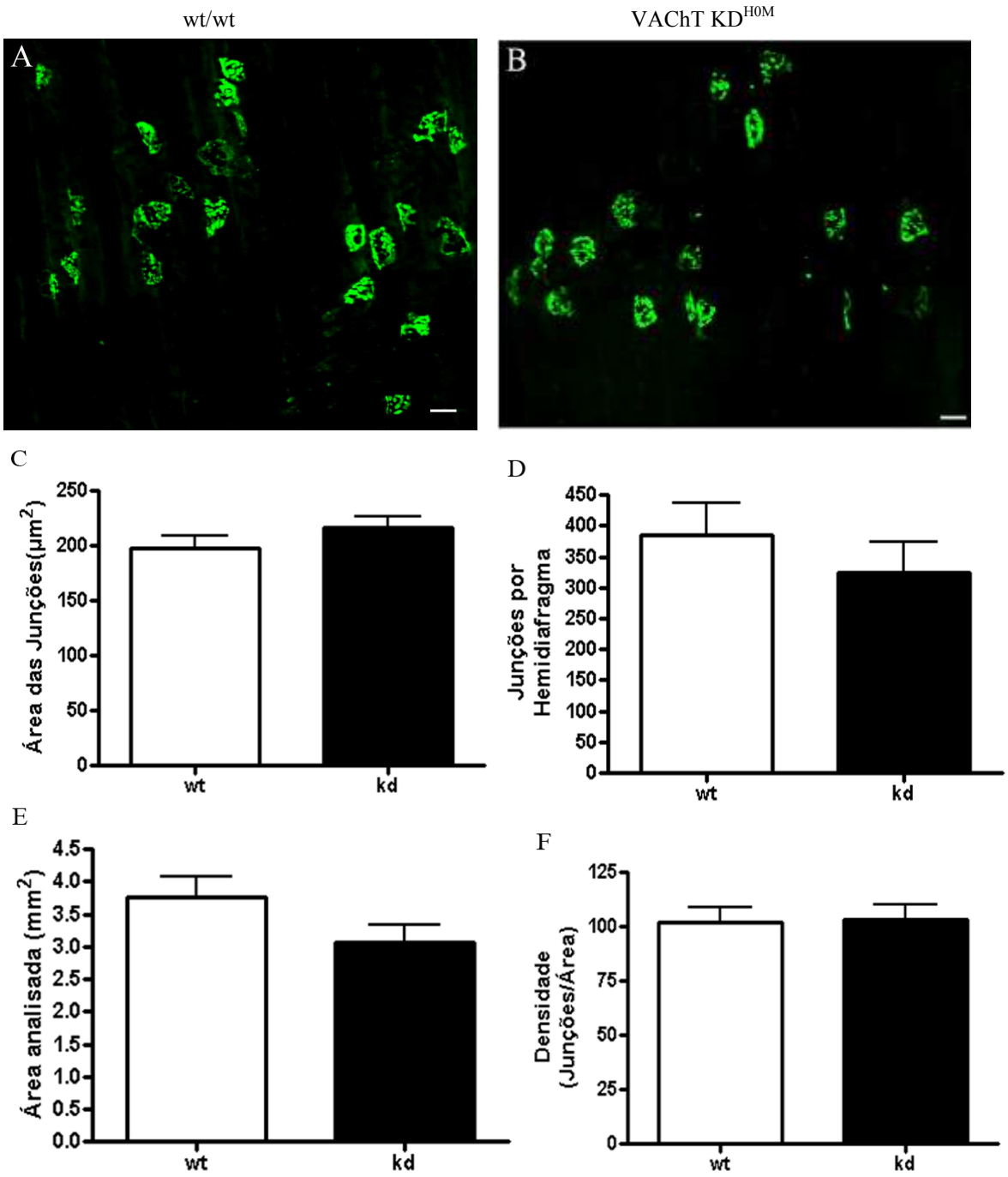

Figura Suplementar 1: Expressão reduzida do gene VAChT não determina alterações compensatórias no número e na área de terminações motoras em animais *knockdown* homozigotos. A e B) Junções neuromusculares marcadas com FM1-43fx (análogo fixável do FM1-43) em diafragma de camundongos selvagem e *knockdow* homozigoto, respectivamente (Barra de escala: 10µm). As imagens foram obtidas em microscópio de fluorescência Zeiss Axiovert 200M equipado com sistema ApoTome utilizando-se filtros apropriados para a fluoresceína **C)** Redução da expressão do VAChT não altera a área das junções. **D)** Expressão reduzida do VAChT não determina alteração no número de junções por hemidiafragma. **E)** Histograma indicando a área do músculo diafragma percorrida durante a coleta de imagens. Observe que não há diferença estatística significativa entre as áreas analisadas. **F)** Redução na expressão do VAChT não alterou a densidade de junções no músculo diafragma de camundongos. (n=6. Barra de erro: ±EPM)

2.2 – Artigo número 2

The vesicular acetylcholine transporter is required for neuromuscular development and function

DE CASTRO, B. M.; DE JAEGER, X.; MARTINS-SILVA, C.; LIMA, R. D.; AMARAL, E.; MENEZES, C.; LIMA, P; NEVES, C. M.; PIRES, R. G; GOULD, T. W.; WELCH, I.; KUSHMERICK, C.;, GUATIMOSIM, C.; IZQUIERDO, I.; CAMMAROTA, M; RYLETT, R. J.; GÓMEZ, M. V.; CARON, M. G.; OPPENHEIM, R. W.; PRADO, M. A.; PRADO, V. F. .

Molecular and Cellular Biology, v.29, n.19, p. 5238-50, 2009.

MOLECULAR AND CELLULAR BIOLOGY, Oct. 2009, p. 5238–5250 Vol. 29, No. 19
0270-7306/09/$08.00+0 doi:10.1128/MCB.00245-09

The Vesicular Acetylcholine Transporter Is Required for Neuromuscular Development and Function▽

Braulio M. de Castro,[1]† Xavier De Jaeger,[1,2,3]† Cristina Martins-Silva,[2,3]† Ricardo D. F. Lima,[4] Ernani Amaral,[5] Cristiane Menezes,[2,3] Patricia Lima,[5] Cintia M. L. Neves,[6] Rita G. Pires,[2] Thomas W. Gould,[8]‡ Ian Welch,[9] Christopher Kushmerick,[4] Cristina Guatimosim,[5] Ivan Izquierdo,[10] Martin Cammarota,[10] R. Jane Rylett,[2,3] Marcus V. Gomez,[1,11] Marc G. Caron,[12] Ronald W. Oppenheim,[8] Marco A. M. Prado,[1,2,3,7]* and Vania F. Prado[1,2,3,6,7]*

Programa de Farmacologia Molecular, UFMG, Belo Horizonte, Minas Gerais, Brazil[1]; Molecular Brain Research Group, Robarts Research Institute,[2] and Department of Physiology and Pharmacology,[3] University of Western Ontario, London, Ontario, Canada; Departamento de Fisiologia e Biofísica,[4] Departamento de Morfologia,[5] and Departamento de Bioquímica-Imunologia,[6] UFMG, Belo Horizonte, Minas Gerais, Brazil; Department of Anatomy and Cell Biology, University of Western Ontario, London, Ontario, Canada[7]; Department of Neurobiology and Anatomy, Wake Forest University, Winston-Salem, North Carolina[8]; Animal Care and Veterinary Services, University of Western Ontario, London, Ontario, Canada[9]; Centro de Memoria, Instituto de Pesquisas Biomedicas, PUC-RS, Porto Alegre, Brazil[10]; Nucleo de Neurociencias, Faculdade de Medicina, UFMG, Belo Horizonte, Minas Gerais, Brazil[11]; and Department of Cell Biology, Duke University, Durham, North Carolina[12]

Received 24 February 2009/Returned for modification 19 March 2009/Accepted 8 July 2009

The vesicular acetylcholine (ACh) transporter (VAChT) mediates ACh storage by synaptic vesicles. However, the VAChT-independent release of ACh is believed to be important during development. Here we generated VAChT knockout mice and tested the physiological relevance of the VAChT-independent release of ACh. Homozygous VAChT knockout mice died shortly after birth, indicating that VAChT-mediated storage of ACh is essential for life. Indeed, synaptosomes obtained from brains of homozygous knockouts were incapable of releasing ACh in response to depolarization. Surprisingly, electrophysiological recordings at the skeletal-neuromuscular junction show that VAChT knockout mice present spontaneous miniature end-plate potentials with reduced amplitude and frequency, which are likely the result of a passive transport of ACh into synaptic vesicles. Interestingly, VAChT knockouts exhibit substantial increases in amounts of choline acetyltransferase, high-affinity choline transporter, and ACh. However, the development of the neuromuscular junction in these mice is severely affected. Mutant VAChT mice show increases in motoneuron and nerve terminal numbers. End plates are large, nerves exhibit abnormal sprouting, and muscle is necrotic. The abnormalities are similar to those of mice that cannot synthesize ACh due to a lack of choline acetyltransferase. Our results indicate that VAChT is essential to the normal development of motor neurons and the release of ACh.

Cholinergic neurotransmission has key functions in life, as it regulates several central and peripheral nervous system outputs. Acetylcholine (ACh) is synthesized in the cytoplasm by the enzyme choline acetyltransferase (ChAT) (16). Choline supplied by the high-affinity choline transporter (CHT1) is required to maintain ACh synthesis (52). A lack of ChAT (4, 35) or the high-affinity choline transporter (21) in genetically modified mice is incompatible with life. ACh plays an important role in wiring the neuromuscular junction (NMJ) during development (38, 43). Embryonic synthesis of ACh is fundamental for the development of proper nerve-muscle patterning at the mammalian NMJ, as ChAT-null mice present aberrant nicotinic ACh receptor (nAChR) localization and increased motoneuron (MN) survival, axonal sprouting, and branching (4, 35).

The vesicular ACh transporter (VAChT) exchanges cytoplasmic ACh for two vesicular protons (37, 41). Previously reported electrophysiological studies showed that quantal size is decreased by vesamicol, an inhibitor of VAChT, but only in nerve terminals that have been electrically stimulated (19, 59, 60, 63). VAChT overexpression in developing *Xenopus* MNs increases both the size and frequency of miniature-end-plate currents (54). In *Caenorhabditis elegans*, mutations in VAChT affect behavior (65). Moreover, a decrease in VAChT expression has functional consequences for mammals, as mutant mice with a 70% reduction in the expression levels of this transporter (VAChT knockdown [KD^{HOM}] mice) are myasthenic and have cognitive deficits (47). Hence, vesicular transport activity is rate limiting for neurotransmission "in vivo" (18, 47).

Exocytosis of synaptic vesicle contents is the predominant mechanism for the regulated secretion of neurotransmitters (55). However, alternative mechanisms of secretion have been proposed (20, 56, 61). Quantal ACh release, comparable to that seen in developing nerve terminals, has been detected in

* Corresponding author. Mailing address: Molecular Brain Research Group, Robarts Research Institute, University of Western Ontario, P.O. Box 5015, 100 Perth Drive, London, Ontario N6A 5K8, Canada. Phone: (519) 663-5777, ext. 24888. Fax: (519) 663-3789. E-mail for Marco A. M. Prado: mprado@robarts.ca. E-mail for Vania F. Prado: vprado@robarts.ca.

† B.M.D.C., X.D.G., and C.M.-S. contributed equally to this work.

‡ Present address: Department of Basic Medical Sciences, Oceania University of Medicine, P.O. Box 232, Apia, Samoa.

▽ Published ahead of print on 27 July 2009.

myocytes and fibroblasts in culture, which presumably do not express VAChT (14, 24). More recently, it was found that the correct targeting of *Drosophila* photoreceptor axons is disrupted in flies with null mutations in ChAT (64). Remarkably, the inactivation of VAChT did not produce the same result (64). The result suggests that the release of ACh during development is not dependent on VAChT, perhaps because it is nonvesicular or because vesicular storage can occur without VAChT.

To test if the VAChT-independent secretion of ACh has any physiological role in the mammalian nervous system, we generated a mouse line in which the VAChT gene is deleted. These mice lack the stimulated release of ACh from synaptosomes, die after birth, and show several alterations in neuromuscular wiring consistent with a severe decrease in the cholinergic input to muscles during development. These experiments indicate that VAChT has an important role in maintaining activity-dependent ACh release that supports life and the correct patterning of innervation at the NMJ.

MATERIALS AND METHODS

Generation of VAChT knockout mice. The isolation of a VAChT genomic clone was described elsewhere previously (47). This genomic clone was used to construct a gene-targeting vector in which we added LoxP sequences flanking the VAChT open reading frame (ORF) and the TK-Neo cassette. One LoxP sequence was added 260 bp upstream from the VAChT translational initiation codon, and a second LoxP was added approximately 1.5 kb downstream from the stop codon. The TK-Neo cassette was added immediately after the second LoxP and was followed by a third LoxP (S1). Note that this is a vector distinct from what we previously reported for the localization of the TK-Neo cassette (47). The linearized targeting vector was electroporated into J1 embryonic stem cells derived from 129/terSv mice, and selected embryonic stem cell clones harboring homologous recombination (determined by PCR and Southern blotting [not shown]) were injected into C57BL/6J blastocysts to produce chimeric mice. Germ line transmission was achieved, and mice were bred to C57BL/6J mice to produce heterozygote mutant mice ($VAChT^{wt/flox}$). Prior to breeding $VAChT^{flox}$ mice to transgenic mice constitutively expressing Cre, we bred $VAChT^{flox}$ mice with CaMKIIalpha-Cre mice (Cre expression is driven by a fragment of the CaMKIIalpha promoter, kindly donated by Scott Zeitlin [17]) in an attempt to generate brain region-specific conditional knockout mice (these will be reported elsewhere). However, we noted that the progeny of mating between $VAChT^{wt/flox,cre+\text{-}CaMKIIalpha}$ males and $VAChT^{wt/flox}$ females inherited a recombined floxed allele (VAChT-deleted allele, or $VAChT^{del}$). This allele would be identical to that obtained by crossing the $VAChT^{flox}$ mice to Cre mice that constitutively express Cre. This recombination happened because there is ectopic expression of CaMKIIalpha-Cre in the testes, which can be detected by quantitative reverse transcription-PCR (data not shown). The presence of Cre within the testes allows the recombination of the floxed allele, probably during spermatogenesis, and therefore, the $VAChT^{del}$ allele is transmitted to the progeny. The ectopic expression of Cre in the testes was also previously described for other Cre lines (e.g., synapsin-Cre [49]), indicating that this is likely to be a common phenomenon. We backcrossed the progeny ($VAChT^{wt/del}$) to C57BL/6J mice (N4) and confirmed that they were capable of germ line transmission for the $VAChT^{del}$ allele. We then intercrossed $VAChT^{wt/del}$ mice to generate $VAChT^{del/del}$ mice, i.e., a potential homozygous VAChT-null mutant (see below). For comparison purposes, we also obtained ChAT-null mice as a kind gift from Kuo-Fen Lee and Fred H. Gage, Salk Institute (4).

Animals were housed in groups of three to five mice per cage in a temperature-controlled room with 12-h light–12-h dark cycles, and food and water were provided ad libitum. Unless otherwise stated, the experiments were always done using embryonic day 18.5 (E18.5) embryos. All studies were conducted in accordance with NIH guidelines for the care and use of animals and with approved animal protocols from the Institutional Animal Care and Use Committees at the Federal University of Minas Gerais and the University of Western Ontario.

Genotyping, Southern blotting, and sequencing. Genotyping by PCR was performed using tail DNA as a template. The set of three primers used were P1 (5′-TACTTGTCTGTCTGCCTGCCTGTC-3′), P2 (5′-AAGGAGTTGGTTGG CCACAGTAAG-3′), and P4 (5′-TCATAGCCCCAAGTGGAGGG AGA-3′). Oligonucleotides P1 and P2 amplified a 247-bp fragment in the wild-type (wt) allele, while primers P4 and P2 amplified a 329-bp fragment in the *del* allele. The 329-bp fragment amplified by primers P4 and P2 was purified from agarose gel using the QIAquick gel extraction kit (Qiagen) and cloned into the pCR 2.1 vector using the TA cloning kit (Invitrogen). The sequence of the cloned fragment was determined by automated DNA sequencing.

For Southern blot analysis, genomic DNA was digested with the enzymes BamHI and SacI. Digested DNA was subjected to electrophoresis in a 1.5% agarose gel and transferred onto a nylon membrane. After UV cross-linking, DNA on the membrane was hybridized to the NdeI/PmeI VAChT DNA fragment (see Fig. 1 for the position of the probe fragment). Detection was done using the Alkphos direct labeling and detection system kit (GE) according to the manufacturer's instructions.

qPCR. For real-time quantitative PCR (qPCR), total RNA was extracted using Trizol (Invitrogen, São Paulo, Brazil) treated with DNase I (Ambion, Austin, TX), and first-strand cDNA was synthesized using a High Capacity cDNA transcription kit (Applied Biosystems, CA) according to the manufacturer's instructions. cDNA was subsequently subjected to qPCR on a 7500 real-time PCR system (Applied Biosystems, CA) using Power SYBR green PCR master mix (Applied Biosystems, CA). For each experiment, a nontemplate reaction was used as a negative control. In addition, the absence of DNA contaminants was assessed in reverse transcription-negative samples and by melting-curve analysis. The specificity of the PCRs was also confirmed by size verification of the amplicons by electrophoresis in acrylamide gels. Relative quantification of gene expression was done with the $2^{-\Delta\Delta CT}$ method using β-actin gene expression to normalize the data. The sequences of the primers used are available upon request.

Western blotting. Immunoblot analysis was carried out as described previously using spinal cord extracts from E18.5 mice (47). Antibodies used were anti-VAChT (Synaptic Systems Gottingen, Germany, and Sigma Chemical Co., São Paulo, Brazil), anti-CHT1 (51), anti-synaptophysin (Sigma Chemical Co.), and anti-actin (Chemicon, CA). Images were acquired and analyzed using ImageQuant TL (GE Healthcare).

Recombinant cDNA construct preparation, cell culture, and transfection. Rat CHT1 subcloned into the expression vector pcDNA3.1(−) and mutated in dileucine-like motif L531A was described previously (51). Human embryonic kidney HEK293 cells were acquired from the Cell Bank, Rio de Janeiro, Brazil. HEK293 cells were grown in Dulbecco's modified Eagle's medium (Gibco) supplemented with 10% (vol/vol) heat-inactivated fetal bovine serum (Gibco) and 1% penicillin-streptomycin (Gibco). For transient transfections with empty vector (pcDNA3.1) or mutant CHT1 (L531A), HEK293 cells were seeded into 60-mm dishes (Falcon) and transfected using a modified calcium phosphate method (23). Choline and ACh uptake assays were performed at 48 h after transfection.

Choline and ACh uptake assays and ACh release. Choline and ACh uptake assays were performed as described previously (50). Briefly, cells plated into 60-mm dishes were washed twice with Krebs-HEPES medium (124 mM NaCl, 4 mM KCl, 1.2 mM $MgSO_4$, 1 mM $CaCl_2$, 10 mM glucose, 25 mM HEPES [pH 7.4]) containing 10 mM paraoxon to inhibit acetylcholinesterase. Cells were then incubated with Krebs-HEPES containing 10 μM paraoxon and [^{3}H]choline chloride (1 μM; diluted to 1 mCi/μmol) or [^{3}H]ACh (1 mCi/μmol) for 10 min at 37°C. When hemicholinium-3 (1 μM) was used, the drug was added during this incubation step and maintained during the course of the experiment. Subsequently, cells were washed three times with 1.0 ml of cold Krebs-HEPES with paraoxon (10 μM) and lysed with 500 μl of 5% trichloroacetic acid (TCA) solution. Lysates were centrifuged for 10 min at 10,000 × *g* at 4°C. Pellets were used to measure protein content (3), and radioactivity was measured in the supernatants (100 μl) by liquid scintillation spectrometry to determine choline and ACh uptakes. In the competition assay, choline uptake was performed in the presence of crescent amounts of ACh (3 mM, 10 mM, or 30 mM).

The TCA supernatants obtained as described above were used to determine the [^{3}H]ACh content (45). Briefly, TCA was removed with ether, and quaternary amines were extracted using sodium tetraphenylboron in butyronitrile (10 mg/ml), the organic phase separated by centrifugation was reserved, and tetraphenylboron was precipitated with $AgNO_3$ in water. The suspension was homogenized and centrifuged. The organic phase was transferred into a new plastic tube containing $MgCl_2$ in water to precipitate excess Ag^+. After centrifugation, the solution containing quaternary amines was taken to dryness under a vacuum. The [^{3}H]choline present in dried samples was resuspended and oxidized using choline oxidase (Sigma-Aldrich) in glycylglycine buffer (pH 8). [^{3}H]ACh was extracted using tetraphenylboron in butyronitrile similarly to the procedure described above. Tritium in the organic (predominantly ACh) and aqueous (corresponding predominantly to choline) phases was measured by liquid scintillation spectrom-

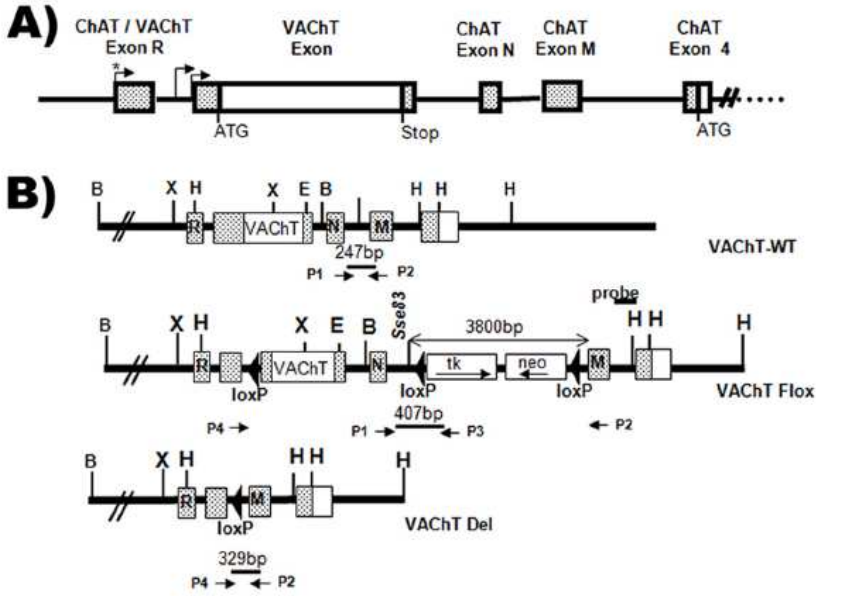

C)

```
1   TCATAGCCCC AAGTGGAGGG AGAAAAAAAA AAAAAAAGAG AGGCGGCGGT GGAGGAAGAG
                              P4
61  GCAAGAGCGG ACGCGCGGGG AGGGCTGGAG AGACGGCGGG CGGCGGCAGC ATGCCCCTGG

121 GCGGGTGCAC ACGGCCTCTC TGCGCGGCAG GGGCGGGCAG GGGCTGCTCC TGCTCTCTCT

181 GGGCACCGCG CGTCCAGTCT CCCGCCTCAG CCCCTCGGCT TGCCGGCCTA CTAGCATAAC
                                                    NheI/SpeI
241 TTCGTATAAT GTATGCTATA CGAAGTTATG GCGCGCCCCT GCAGGAATTG GATGGTAAAA
        loxP                    AscI
301 GAAAACAAGG GAGGTCTTAC TGTGGCCAAC CAACTCCTT
                              P2
```

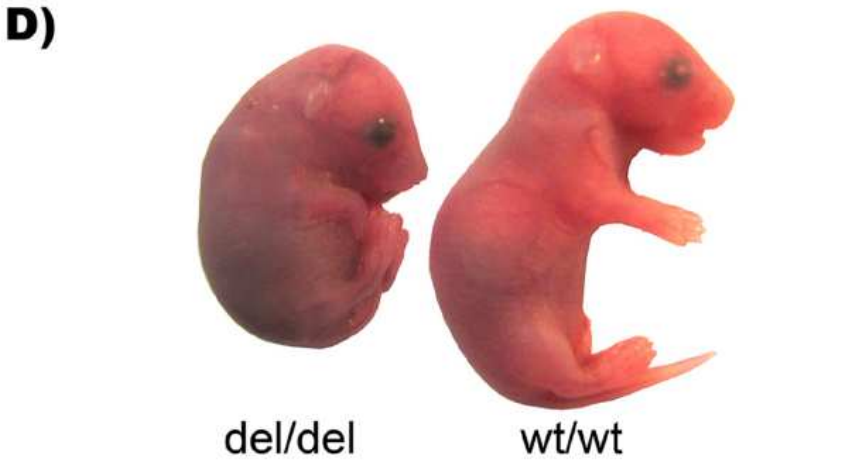

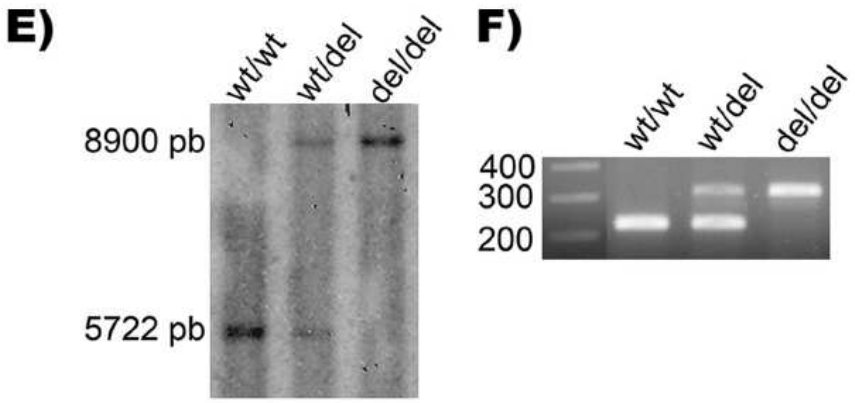

etry. Choline and ACh standards (0.1 to 0.5 μCi/ml) were processed in parallel with the samples to assess yield and cross-contamination. The later values were used to correct results of sample analyses. Protein content determined by the method of Bradford was used to normalize the data (3). Choline or ACh uptake into cells that was dependent on CHT1 was measured as a percentage of transport in cells transfected with empty vector. Each *n* value represents the average of data for triplicate samples.

KCl-induced release of [^{3}H]ACh in brain synaptosomes. Crude synaptosomes from whole brains of individual mice were homogenized in ice-cold buffer (0.32 M sucrose, 10 mM EDTA, Tris-HCl [pH 7.4]), and P2 pellets were obtained as described previously (2), washed, and then incubated in a depolarizing solution (90 mM NaCl, 50 mM KCl, 5 mM $NaHCO_3$, 1 mM $MgCl_2$, 1.2 mM Na_2HPO_4, 10 mM glucose, 20 mM HEPES, 2 mM $CaCl_2$, 0.02 mM paraoxon [pH 7.4]) for 5 min at 30°C. Subsequently, samples were centrifuged at 5,500 × *g* for 5 min at 4°C, and pellets were incubated in Krebs-HEPES medium (140 mM NaCl, 5 mM KCl) containing 100 nM of [^{3}H]choline, 5 mM $NaHCO_3$, 1 mM $MgCl_2$, 1.2 mM Na_2HPO_4, 10 mM glucose, 20 mM HEPES, 2 mM $CaCl_2$, and 0.02 mM paraoxon (pH 7.4) for 15 min at 30°C for choline uptake. After centrifugation, synaptosomes were washed three times with choline in ice-cold buffer (50 μM), and pellets were resuspended in ice-cold buffer. Each sample was separated into four aliquots. Two aliquots were incubated in Krebs-HEPES medium, and the other two aliquots were incubated in depolarizing solution containing hemicholinium-3 (1 μM) for 5 min at 30°C. The [^{3}H]ACh released was collected after centrifugation, pellets were digested with 5% TCA, and the radioactivity of both samples was measured using liquid scintillation counting. Total radioactivity (supernatant and pellet) was calculated and then normalized by protein content. For each sample, the average values obtained under depolarizing or nondepolarizing conditions was divided for the total radioactivity. The release of newly synthesized [^{3}H]ACh is predominant under this condition (2); the results are shown as fractional release above baseline release obtained under nondepolarizing conditions.

Tissue ACh measurements. Brains were dissected rapidly, homogenized in 5% TCA, and centrifuged (10,000 × *g* for 10 min) at 4°C. Supernatants were frozen at −80°C until use. For ACh determinations, TCA was removed with ether, and a chemiluminescent assay was done with choline oxidase as described previously (44). The data are presented as means and standard errors of the means (SEM). One-way analysis of variance (ANOVA), followed by Bonferroni's test, was used to analyze the differences in tissue ACh concentrations in $VAChT^{wt/wt}$, $VAChT^{wt/del}$, and $VAChT^{del/del}$ mice; a *P* value of <0.05 was considered to be statistically significant.

Electrophysiology. Electrophysiology experiments were performed similarly to methods described elsewhere previously (47). Hemidiaphragms were isolated from E18.5 embryos, and the muscle with attached nerve was pinned to a Sylgard pad in a 5-ml acrylic chamber continuously perfused at a rate of 1 ml/min with Tyrodes solution containing 137 mM NaCl, 26 mM $NaHCO_3$, 5 mM KCl, 1.2 mM NaH_2PO_4, 1.3 mM $MgCl_2$, 2.4 mM $CaCl_2$, and 10 mM glucose equilibrated with 95% O_2–5% CO_2 at pH 7.4. During recording, tetrodotoxin (3 μM) was included to avoid contractions. Microelectrodes were fabricated from borosilicate glass and had resistances of 8 to 15 MΩ when filled with 3 M KCl. Standard intracellular recording techniques were used to record miniature end plate potentials with an Axoclamp-2A amplifier. Recordings were band-pass filtered (0.1 Hz to 10 KHz) and amplified 200 times prior to digitization and acquisition on an IBM computer running WinEDR (John Dempster, University of Strathclyde). The membrane potential was recorded and used to correct MEPP amplitudes and areas to a standard resting potential of −60 mV. At the end of experiments, 5 μM *d*-tubocurarine was applied to verify that the observed events were due to nicotinic receptors.

FM1-43 imaging. FM1-43 imaging experiments were performed as described previously (47) except that a fixable FM1-43 analog was used. Briefly, diaphragms from E18.5 mice were dissected and mounted onto a Sylgard-lined chamber containing mouse Ringer solution with the following composition: 135 mM NaCl, 5 mM KCl, 2 mM $CaCl_2$, 1 mM $MgCl_2$, 12 mM $NaHCO_3$, 1 mM Na_2HPO_4, and 11 mM D-glucose. Solutions were aerated with 95% CO_2–5% O_2, and the pH was adjusted to 7.4. FM1-43fx (8 μM) was used to stain recycling synaptic vesicles during stimulus with a high-K^+ solution (60 mM KCl) for 10 min with 16 μM *d*-tubocurarine to prevent contractions. After stimulation, the preparation was maintained in normal K^+ solution for 10 min to guarantee maximal FM1-43fx uptake. Excess FM1-43fx adhering to the muscle cell plasma membrane was removed during a washing period in mouse Ringer solution not containing FM1-43fx for at least 40 min; 16 μM *d*-tubocurarine was present to prevent muscle contraction. Advasep-7 (1 mM) was added during the washing period after FM1-43fx staining to reduce background fluorescence. Diaphragms stained with FM1-43fx were fixed with 4% paraformaldehyde for 40 min and then mounted onto slides and examined by fluorescence microscopy on either an Axiovert 200 M microscope equipped with a 40× water immersion objective using the Apotome system or a Leica SP5 confocal microscope using a 63× water immersion objective and an argon laser (488 nm) for excitation. The spectrum emission was set from 510 to 620 nm. During image acquisition, whole hemidiaphragms were scanned, and the images were obtained from muscle areas with stained NMJs. The total number of junctions per hemidiaphragm was defined by the sum of junctions observed in each image after scanning the entire muscle. The density of junctions was determined by the ratio of the number of junctions/total area (mm^2). The nerve terminal area was measured using Image J, and the size of each terminal was expressed in $pixels^2$. Data were analyzed using an unpaired *t* test. A *P* value of <0.05 was considered to be statistically significant.

Immunofluorescence. Immunofluorescence was performed as described previously (4). Briefly, whole-mount diaphragms from embryos were rapidly dissected and fixed in 4% paraformaldehyde–phosphate-buffered saline (PBS) (pH 7.4) for approximately 3 days. Tissues were cryoprotected with 10% sucrose–4% paraformaldehyde, frozen with isopentane over dry ice, and kept at −80°C until use. Muscles were rinsed two times in PBS, incubated with a 0.1 M glycine–PBS solution for 1 h, and blocked in incubation buffer (150 mM NaCl, 0.01 M phosphate buffer, 3% bovine serum albumin, 5% goat serum, and 0.01% thimerosal) overnight at 4°C. Tissues were immunostained with anti-VAChT (rabbit polyclonal; Sigma Chemical Co.), anti-CHT1 (51), or anti-neurofilament 150 (rabbit polyclonal; Chemicon) in incubation buffer overnight at 4°C. Following three washes of 1 h each with PBS–0.5% Triton X-100, muscles were incubated with Alexa Fluor 546-conjugated goat anti-rabbit antibody (Molecular Probes) and Alexa Fluor 488-conjugated α-bungarotoxin (Molecular Probes) in the buffer described above overnight at 4°C, and the washing step was repeated. Diaphragms were flat mounted in Hydromount medium, and images were collected with an Axiovert 200 M microscope using the Apotome system or a Leica SP5 confocal microscope to acquire optical sections of the tissues. Quantitative analyses of nAChR or CHT1 fluorescence were carried out with Metamorph software (Molecular Devices, Downingtown, PA). For each set of experiments, a threshold was calculated by using a background area of the image. This threshold value determined for $VAChT^{wt/wt}$ was applied to images obtained with other genotypes, and the total fluorescence intensity (integrated intensity) for bungarotoxin-labeled nAChR or terminals labeled by CHT1 antibody was then detected automatically. To count the number of positive terminals or junctions, adjacent sections of the entire muscle were obtained, and the numbers of positive labeled structures were counted with Metamorph similarly to the above-described experiments with FM1-43.

MN quantification. Adult pregnant females were anesthetized with ketamine-xylazine (70 mg/kg and 10 mg/kg, respectively) intraperitoneally and sacrificed by cervical dislocation. Embryos were removed quickly, and spinal cords were removed and immersed in Bouins fixative for 24 h prior to being processed for paraffin embedding. Paraffin blocks were serially sectioned, with sections placed onto microscope slides and stained with thionin. MNs were counted as described previously (12).

In vivo analysis of muscle function. Locomotor activity, grip force, and wire hang tests were performed essentially as described previously (15, 47).

FIG. 1. Generation of $VAChT^{del/del}$ mice. (A) Generation of VAChT *del* mice using the Cre-LoxP system. Boxes represent the different exons of ChAT or VAChT. Open boxes represent the ORF of VAChT and ChAT. Note that the VAChT gene is within the first intron of ChAT. (B) Schematic representation of the VAChT gene locus, the *floxed* allele, and the *del* allele. P1, P2, P3, and P4 indicate the positions of PCR primers used for genotyping. (C) Sequence analysis of the 329-bp fragment amplified with primers P2 and P4. Restriction sites and LoxP sequences are indicated. (D) VAChT mutant mice ($VAChT^{del/del}$) died rapidly after birth in cyanosis (not shown). Embryos from E18.5 exhibited flaccid limbs and kyphosis (hunchback). (E) Southern blot analysis confirmed the presence of the *del* allele in VAChT mutant mice. (F) Genotype of VAChT mutant mice by PCR.

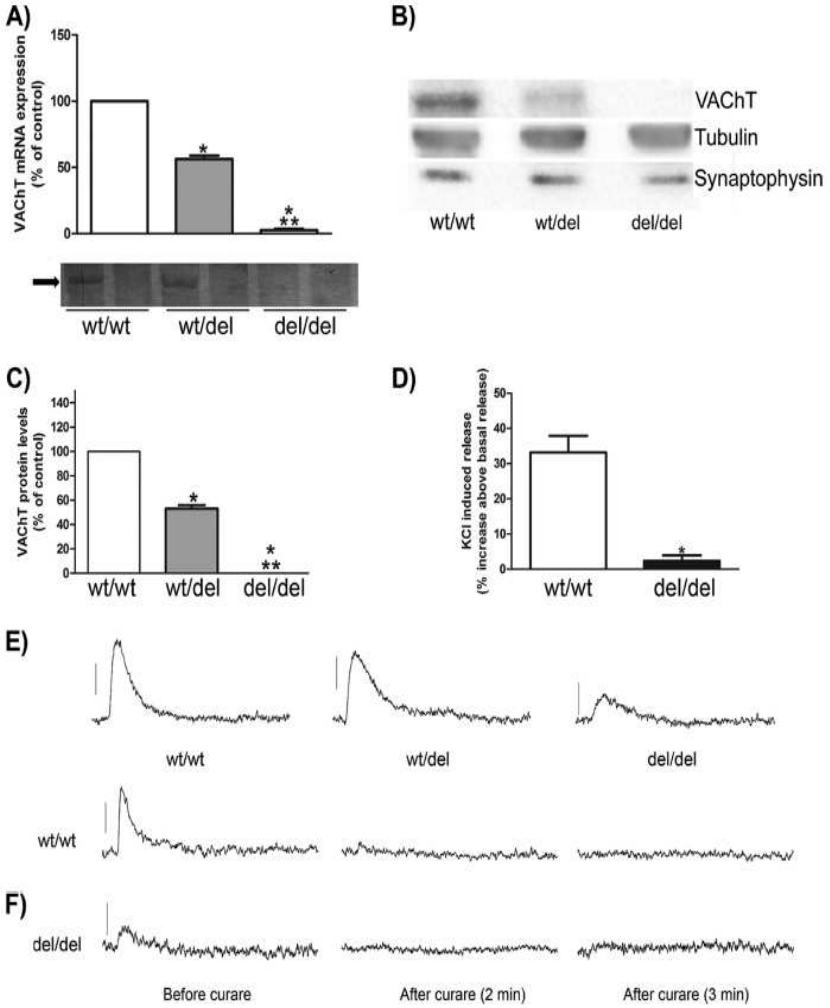

FIG. 2. VAChT expression and ACh release in VAChT$^{del/del}$ E18.5 mice. (A) Quantitative analysis of VAChT mRNA levels by qPCR. PCR products were run in a polyacrylamide gel. *, statistically different from wt; **, statistically different from wt/del {one-way ANOVA with Bonferroni post hoc [$F(2,6 = 920)$]; $P < 0.0001$; $n = 4$}. Lanes labeled with a − show the respective negative control without the sample. (B) Western blot analysis of VAChT, synaptophysin, and tubulin in spinal cord extracts. (C) Average values for the amount of VAChT from densitometric analyses of several Western blots. Tubulin immunoreactivity was used to normalize protein loading. Data are presented as percentages of VAChT$^{wt/wt}$ levels. *, statistically different from wt; **, statistically different from wt/del {one-way ANOVA with Bonferroni post hoc [$F(2,9 = 927.9)$]; $P < 0.0001$; $n = 4$}. (D) Effects of KCl-induced depolarization on [^{3}H]ACh release from synaptosomes. *, statistically different from wt/wt ($P < 0.05$ by t test). (E) MEPPs from the NMJ. MEPPs recorded in VAChT$^{wt/del}$ muscle show no significant change in amplitude compared to VAChT$^{wt/wt}$ mice. VAChT-null mice showed the existence of scarce MEPPs with decreased amplitude compared to VAChT$^{wt/wt}$ and VAChT$^{wt/del}$ mice. (F) *d*-Tubocurarine abrogated MEPPs in both VAChT$^{wt/wt}$ and VAChT$^{del/del}$ mice.

RESULTS

Generation of mice null for VAChT. We have generated mice in which the VAChT ORF was deleted using Cre-Lox technology (Fig. 1A and B). The deletion of the VAChT ORF was confirmed by DNA sequencing (Fig. 1C), and we named the VAChT-deleted allele VAChT^{del}. The posture of VAChT$^{del/del}$ mice at E18.5 resembles that of ChAT-null mice, with flaccid limbs and signs of slight kyphosis (Fig. 1D). VAChT$^{del/del}$ mice die rapidly in cyanosis within 2 to 5 min after birth. Southern analysis (Fig. 1E) and PCR genotyping (Fig. 1F) confirmed the presence of the *del* allele in heterozygous and homozygous VAChT mutant mice. These mice are a novel mutant line distinct from the one that we have previously described and that presents close to 70% and 45% reductions in VAChT expression (VAChT KD^{HOM} and VAChT KD^{HET}, respectively). Contrary to the mouse line reported here (VAChT$^{del/del}$), the VAChT KD lines survive to adulthood (47).

To confirm that the genetic manipulation that putatively deleted the VAChT ORF indeed suppresses VAChT mRNA expression, we used qPCR and E18.5 embryos (Fig. 2A). VAChT$^{wt/del}$ mouse brain presented a 50% decrease in the VAChT mRNA level compared to VAChT$^{wt/wt}$ littermate controls. No VAChT mRNA was detected in VAChT$^{del/del}$ mouse brain. The reverse transcription-PCR amplicons were also separated by electrophoresis in a polyacrylamide gel. VAChT$^{del/del}$ mice generated no DNA fragment corresponding to VAChT (Fig. 2A, inset gel). VAChT$^{wt/del}$ mice exhibited

a 50% decrease and VAChT$^{del/del}$ mice exhibited a 100% decrease in VAChT protein levels assayed by Western blotting of spinal cord extracts (Fig. 2B and C). The amount of synaptophysin, a protein present in synaptic vesicles, was unchanged in the spinal cord of VAChT$^{del/del}$ mice (Fig. 2B).

To investigate the importance of VAChT for the evoked secretion of ACh, we prepared crude synaptosomes from the forebrain of E18.5 wt and homozygous mutant mice. We labeled ACh in these synaptosomes with the precursor [^{3}H]choline and monitored the release of labeled neurotransmitter as previously described (2, 26, 27, 32). VAChT$^{del/del}$ mice are capable of producing ACh (see Fig. 5). KCl depolarization was able to increase the release of [^{3}H]ACh in synaptosomes obtained from wt mice but not from VAChT$^{del/del}$ mice (Fig. 2D). Therefore, this experiment indicates that in the absence of VAChT, depolarization-evoked ACh release is hindered.

In order to analyze ACh secretion under nondepolarizing conditions, we performed electrophysiological analysis of the nerve-muscle diaphragm preparation. Figure 2E shows MEPPs recorded from NMJs of VAChT$^{wt/wt}$, VAChT$^{wt/del}$, and VAChT$^{del/del}$ E18.5 mice. VAChT$^{wt/del}$ mice presented no change in the amplitude of MEPPs compared to control mice (0.99 ± 0.09 mV for wt/wt and 0.92 ± 0.09 for wt/del for 31 MEPPs in three and four mice, respectively). Surprisingly, we could detect small-amplitude MEPPs in the NMJ from E18.5 embryos of VAChT$^{del/del}$ mice (Fig. 2E). These experiments were difficult to perform, as the frequency of MEPPs in VAChT$^{del/del}$ mice was noticeably low compared to that of VAChT$^{wt/wt}$ embryos (del/del = 0.0072 ± 0.0009 Hz [11 MEPPs obtained from four fibers from two mice]; wt/wt = 0.0308 ± 0.002 Hz [three fibers from three mice]; wt/del = 0.0364 ± 0.008 Hz [six fibers from four mice]). MEPPs from VAChT$^{del/del}$ mice were of smaller amplitude (0.54 ± 0.07 mV). However, given the overt morphological changes at the NMJs from E18.5 VAChT$^{del/del}$ mice (see Fig. 6, 7, and 8), both pre- and postsynaptic contributions to these changes are likely. Treatment of NMJs from control littermates and homozygous VAChT mutants with *d*-tubocurarine (5 μM) abolished miniature detection, indicating that the MEPPs were likely recorded due to the activation of nAChR (Fig. 2F). In agreement with the fact that VAChT$^{wt/del}$ mice presented no alteration in MEPPs at the NMJ, adult VAChT$^{wt/del}$ mice presented no overt neuromuscular dysfunction that could be detected in a test of fatigue or grip force (Fig. 3A and B). In addition, spontaneous locomotor activity was unchanged in VAChT$^{wt/del}$ mice (Fig. 3C).

We considered whether ACh uses another type of transporter to load synaptic vesicles in the absence of VAChT. One candidate is CHT1, which has been found to reside predominantly in synaptic vesicles by us (15, 50–52) and others (22, 36). Like other secondary active transporters for aqueous solutes, CHT1 probably functions bidirectionally (33). "Reverse transport" by CHT1 would be required to mediate ACh uptake by synaptic vesicles. We tested the possibility that CHT1 transports ACh in addition to choline by using a cell line expressing recombinant CHT1. We were not able to do the test in nerve terminals per se, as the pharmacological blockade of CHT1 would decrease ACh synthesis and potentially produce effects on small MEPPs not due to the inhibition of vesicular CHT1. To untangle the multiple possible roles of CHT1, we used a

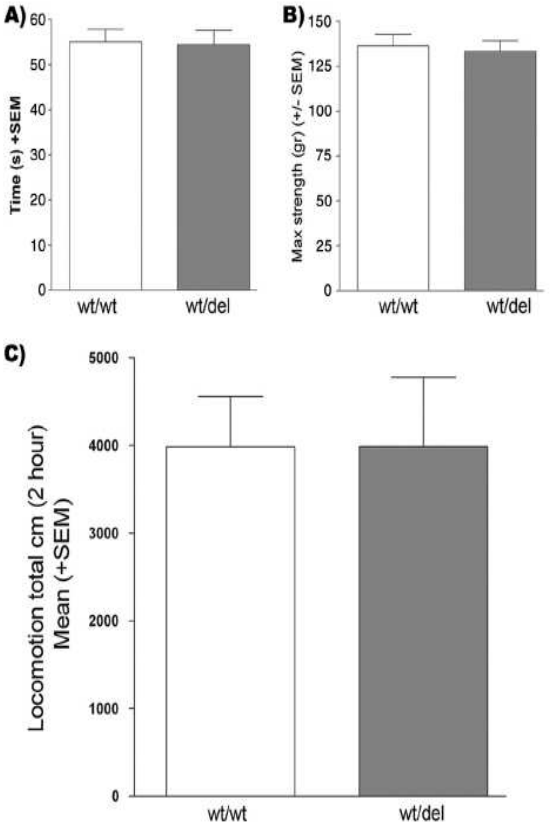

FIG. 3. Neuromuscular function in VAChT$^{wt/del}$ mice. (A) Grip force measured for VAChT$^{wt/wt}$ and VAChT$^{wt/del}$ mice. There is no significant difference between the two genotypes. (B) Time spent hanging upside down from a wire netting for VAChT$^{wt/wt}$ and VAChT$^{wt/del}$ mice. No significant difference was observed. (C) Spontaneous locomotor activity is not changed between the genotypes.

mutant form of CHT1 (L531A) that does not undergo endocytosis, and which remains predominantly on the cell surface, to transfect HEK293 cells. The strategy is expected to maximize ACh uptake by transfected cells should CHT1 be able to transport ACh (51). As expected, transfected cells took up fourfold-more choline than did nontransfected cells (Fig. 4A) (51). ACh in concentrations similar to those found in the cytoplasm of cholinergic terminals (41) inhibited choline uptake, indicating a good likelihood that ACh competes with choline for binding to CHT1 (Fig. 4B). However, the transfected cells took up no more ACh than did nontransfected cells (Fig. 4C). The results demonstrate that CHT1 does not significantly transport ACh, and thus, they do not support the possibility that CHT1 mediates the uptake of ACh by synaptic vesicles.

The results leave open the possibility that a passive transport system similar to that described previously for isolated cholinergic vesicles of *Torpedo* is present in mammalian synaptic vesicles (8). In the right circumstances, even the passive uptake of ACh by synaptic vesicles might be sufficient to generate the small MEPPs observed here. Indeed, recent experiments by Parsons and collaborators using synapse-like microvesicles from rat PC12 cells found that intact vesicles loaded with ACh lose their neurotransmitter content even when a high-affinity analog of vesamicol completely blocks VAChT. The result demonstrates an ACh leakage

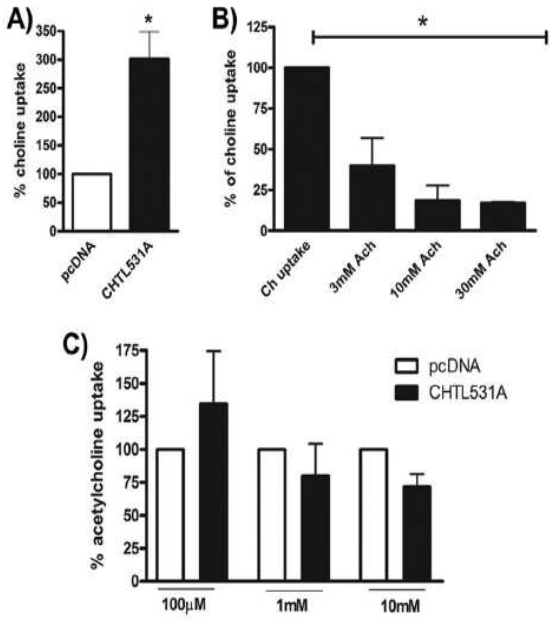

FIG. 4. (A) Choline uptake in HEK293 cells transiently transfected with empty vector (pcDNA3.1) or L531A CHT1 cDNAs. The data represent the means ± SEM of data from five independent experiments (in duplicates) and are normalized to data for cells expressing empty vector (pcDNA3.1). *, significant difference ($P < 0.05$ by t test). (B) ACh competition assay using HEK293 cells transiently transfected with empty vector (pcDNA3.1) or L531A CHT1 cDNAs. The data represent the means ± SEM of data from four independent experiments and are normalized to data for cells expressing the empty vector (pcDNA3.1). *, significantly different from control uptake. (C) ACh uptake in HEK293 cells transiently transfected with empty vector (pcDNA3.1) or L531A CHT1 cDNAs. The data represent the means ± SEM of data from three independent experiments and are normalized to data for cells expressing the empty vector (pcDNA3.1).

mechanism in synapse-like microvesicles that might be bidirectional (S. M. Parsons, personal communication).

However, in order for the passive uptake of ACh by synaptic vesicles to be possible in VAChT$^{del/del}$ mice, cytoplasmic stores of ACh must be maintained. In the absence of vesicular storage, many neurotransmitters are degraded (62), but in *C. elegans*, the mutational inactivation of VAChT leads to an increase in the ACh content of the worm (29). Therefore, we measured the amount of intracellular ACh in the brains of mutant mice. In E18.5 embryos, the amount in VAChT$^{del/del}$ mice was more than fivefold greater than that in VAChT$^{wt/wt}$ mice (Fig. 5A). There was also a clear tendency for the level of ACh in the brain of VAChT$^{wt/del}$ embryos to be increased compared to that of control wt mice (Fig. 5A). In adult VAChT$^{wt/del}$ mice, the ACh content was significantly increased compared to that of control wt mice (Fig. 5B). Because vesicles in VAChT$^{del/del}$ mice are likely depleted of ACh, the concentration increase for ACh in the cytoplasm of cholinergic terminals is probably greater than what the bulk analysis indicates. Hence, an increased concentration of cytoplasmic ACh in VAChT$^{del/del}$ mice might support the passive uptake of ACh into synaptic vesicles and produce small MEPPs.

Why is there so much more ACh in VAChT$^{del/del}$ mice? One possible explanation is increases in the amounts of either ChAT or CHT1, which are involved in the synthesis of ACh. To test for this possibility, we performed qPCR analysis of E18.5 embryos. Transcript levels for ChAT were increased in a gene dosage-dependent way (Fig. 5C). VAChT$^{wt/del}$ mice had nearly twofold-more ChAT mRNA than their control littermates, whereas VAChT$^{del/del}$ mice had nearly fourfold more (Fig. 5C). In addition, we found that VAChT$^{del/del}$ mice had nearly twofold-more CHT1 mRNA than control littermates, whereas VAChT$^{wt/del}$ mice had no significant change (Fig. 5D). At the protein level, we also detected an increase in the amounts of ChAT and CHT1 in homozygous mutant animals (Fig. 5E and F). These observations suggest that increases in ChAT and CHT1 expression levels likely underlie the increase in the amount of ACh in VAChT$^{del/del}$ mice.

Abnormal neuromuscular patterning is a major feature of NMJ developed in the absence of ACh (4, 35). In VAChT$^{del/del}$ mice, nerve terminals have fivefold-more ACh but lack the protein responsible for the active storage of the transmitter in vesicles. Does a lack of VAChT affect NMJ development? Can the lack of VAChT be compensated by the excess intraterminal ACh in VAChT mutants? In order to answer these questions, we evaluated nerve branching, nAChR localization, and the genesis of nerve terminals by labeling the NMJ of wt, VAChT$^{wt/del}$, and VAChT$^{del/del}$ mice with distinct markers. To begin, we tested whether NMJs of VAChT$^{del/del}$ mice showed immunoreactivity for VAChT. We found no VAChT immunoreactivity, as expected (Fig. 6A); in comparison, CHT1 immunolabeling was easily detected (Fig. 6B). Interestingly, analysis of nAChR labeling using fluorescent α-bungarotoxin–Alexa Fluor 543 (BTX-543) (Fig. 6, red) suggested an altered nAChR distribution (Fig. 6A and B and higher magnification in C). Indeed, clusters of nAChR labeled with BTX-543 showed stronger labeling and a larger area in VAChT$^{del/del}$ mice than the corresponding labeling in control and VAChT$^{wt/del}$ mice (Fig. 6C and D) (the increase in labeling was close to 70%).

The rescue of MNs from physiologically programmed cell death that follows the blockade of neuromuscular activity during development is a well-known phenomenon (38, 39). The disturbance of ACh synthesis also affects MN apoptosis (4). In order to test if in the absence of VAChT MNs went through the normal wave of apoptosis, we counted lumbar MNs from wt and VAChT$^{del/del}$ E18.5 embryos (Fig. 6E). Of note, there was a significant increase in the number of MNs in VAChT mutant mice compared to wt controls (36%), suggesting that VAChT-independent ACh secretion did not generate the muscle activity necessary for the programmed cell death of MNs during development. The increase in MN survival was similar to but somewhat less severe than that observed for ChAT-null mice (Fig. 6E) (51% increase in the number of neurons compared to wt controls).

To examine if the enhanced nAChR labeling and enhanced MN numbers are accompanied by an increase in the number of nerve terminals in VAChT$^{del/del}$ mice, we quantified the number of CHT1-positive nerve terminals. Immunoreactivity for CHT1 (Fig. 7A) was increased at the NMJ, confirming the biochemical data shown in Fig. 5D and F. We also quantified the number of CHT1-positive nerve terminals, and we detected a significant increase in the number of CHT1-positive nerve

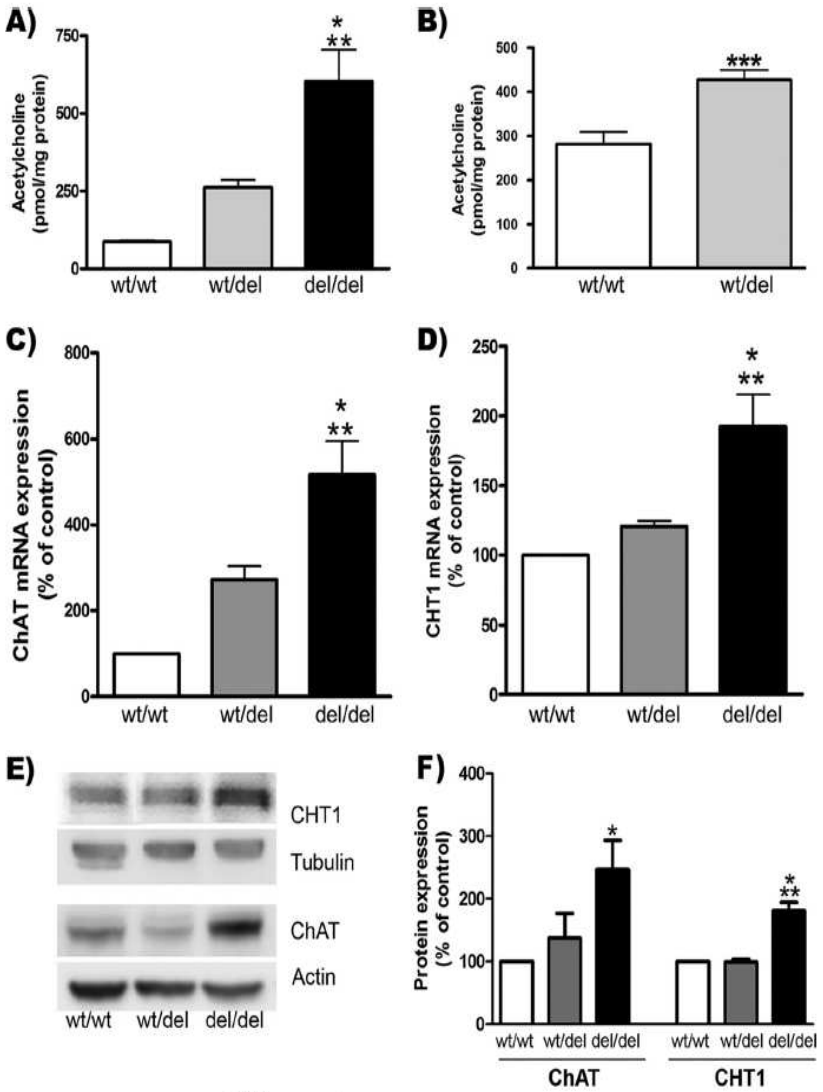

FIG. 5. Neurochemical alterations in VAChT$^{del/del}$ mice. (A) Intracellular ACh contents in brains of VAChT mutant mouse embryos. Data are means ± SEM (three to five mice). An asterisk indicates a statistically significant difference by one-way ANOVA with Bonferroni post hoc test [$F(2,10 = 12.72)$]. (B) Intracellular ACh content in brains from adult VAChT$^{wt/wt}$ and VAChT$^{wt/del}$ mice (n = 4 to 6 brains) (***, $P < 0.001$). (C) ChAT mRNA levels detected by qPCR from E18.5 mouse brains [$F(2,9 = 18.28)$] (n = 4). (D) CHT1 mRNA levels detected by qPCR from E18.5 mouse brains. *, statistically different from VAChT$^{wt/wt}$ mice; **, statistically different from VAChT$^{wt/del}$ mice [$F(2,11 = 12.52)$] (n = 5). (E) ChAT and CHT1 protein expression in E18.5 spinal cords. (F) Quantification of protein expression (three to four animals) ($P < 0.05$) [CHT1 $F(2,6) = 35.21$; ChAT $F(2,15) = 4.599$]. *, statistically different from wt/wt; **, statistically different from wt/del.

endings in VAChT-null mutants (Fig. 7B). To further test if the nerve endings in the diaphragm of VAChT$^{del/del}$ mice were able to undergo exocytosis-endocytosis, we used a form of the activity-dependent dye FM1-43, FM1-43fx, that can be used for protocols requiring tissues to undergo fixation. Preparations to be stained with FMI-43fx underwent KCl-mediated depolarization as described previously (47, 53) and were then washed and fixed prior to the quantification of fluorescently labeled nerve terminals. The results show that synaptic vesicles in VAChT$^{del/del}$ mice undergo exocytosis-endocytosis. Moreover, muscles from homozygous mutants have an increased density of stained nerve terminals compared to control wt mice (40% increase) (Fig. 7C and D). Figure 7E shows an example of terminals labeled with FM dye, and Fig. 7F indicates that in addition to an increase in the number of terminals, the area of the individual terminals labeled with FM1-43 from VAChT$^{del/del}$ mice is also increased compared to that from VAChT$^{wt/wt}$ mice ($P = 0.0018$). The increase in the number of nerve terminals appears to be a consequence of the complete loss of VAChT, as VAChT KD^{HOM} mice that preserve 30% of normal levels of the transporter show no such increase (48; data not shown). VAChT KD^{HOM} mice also did not show an increase in the number of MNs, suggesting that reducing VAChT levels by up to 70% can still support enough release of neurotransmitter during development to maintain the program of MN cell death (data not shown).

To further examine axonal targeting at the NMJ in the absence of VAChT, we labeled diaphragms from wt,

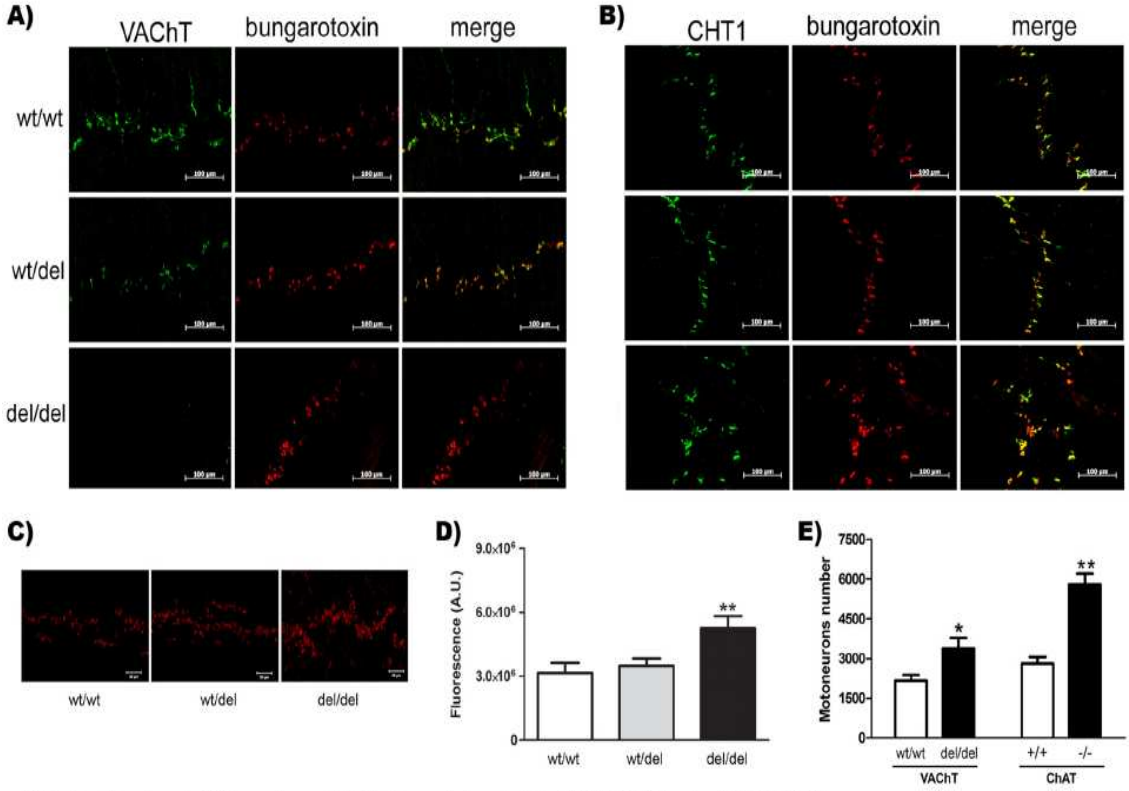

FIG. 6. Alterations in MN number and in NMJ morphology in VAChT$^{del/del}$ E18.5 mice. (A) VAChT immunoreactivity was easily detected in presynaptic termini of VAChT$^{wt/wt}$ and VAChT$^{wt/del}$ diaphragms but was absent in VAChT$^{del/del}$ mice. (B) CHT1 immunoreactivity was detected in all genotypes, although VAChT$^{del/del}$ mice showed an altered distribution of nerve endings (see below and Fig. 5). (C) Abnormal distribution of nAChR in VAChT$^{del/del}$ NMJs. Images show that nAChRs from VAChT$^{del/del}$ mice present stronger labeling and are distributed over a broader region than those from wt and VAChT$^{wt/del}$ mice. (D) Quantification of nAChR fluorescence. Four independent experiments were performed, and the results are expressed as means ± SEM. An asterisk indicates a statistically significant difference (one-way ANOVA with Bonferroni post hoc) [$F(2,20 = 5.632)$]. A.U., arbitrary units. (E) The number of lumbar MNs was significantly increased in VAChT and ChAT-null mice. Clear bars, wt mice; dark bars, homozygous mutant mice.

VAChT$^{wt/del}$, and VAChT$^{del/del}$ mice with an anti-neurofilament antibody (Fig. 8, red) and nAChR with BTX-Alexa Fluor 488 (Fig. 8, green). These experiments show that there is no difference in axonal branching between wt and VAChT$^{wt/del}$ mice. Axon branches from the nerves labeled with the anti-neurofilament antibody were of the characteristic size and generally contacted a cluster of nAChR (Fig. 8). In contrast, VAChT$^{del/del}$ mice had an increase in axonal sprouting and branching that contacted improperly arranged nAChR clusters (Fig. 8). The morphology of the NMJ from VAChT$^{del/del}$ mice was remarkably similar to that reported for ChAT-deficient mice. In fact, in hematoxylin- and eosin-stained muscles, we note that sheets of condensed parallel fusiform nuclei with abundant myofibrillar tissue could be easily discerned in VAChT$^{wt/wt}$ and VAChT$^{wt/del}$ mice (Fig. 9A and B). In contrast, myofibrilar tissue was replaced with fragmented myofibrils in VAChT$^{del/del}$ mice (Fig. 9C). In some cases, there was a complete loss of normal architecture in mutant muscles, and degenerated myofibrils were replaced with fibrotic and fatty tissue (Fig. 6C). Relative to the controls, skeletal muscles from VAChT$^{del/del}$ mice showed marked atrophy. These findings suggest that in the absence of VAChT, despite the nerve terminals having increased ACh contents, the outcome for NMJ development was as severe as the lack of ACh synthesis.

DISCUSSION

The present work addresses the role of VAChT in sustaining the release of ACh. We found that VAChT is fundamental for ACh release in the brain and the NMJ. Moreover, in the absence of the vesicular transport of ACh, there are profound effects on axons, terminal numbers, and synaptic and muscle morphology at the NMJ. Indeed, VAChT-null mice, despite presenting fivefold-more ACh than control mice, recapitulate the NMJ phenotype found in mice that cannot synthesize ACh due to a lack of ChAT. These observations bear important consequences for understanding how developing synapses function and the mechanisms by which transmitter secretion during development regulates synaptic targeting.

VAChT knockout mice do not survive postnatally. The pharmacological inhibition of VAChT causes paralysis and death compatible with an NMJ blockade (5), indicating that interference with VAChT might be lethal. Given the observations that ChAT-null mice have abnormal NMJ development (4, 35), the question arises of whether it is just the presence of ACh that is required or if the VAChT-mediated storage of ACh during development is also important. Previous experiments with munc18-1 null mice, which have no regulated secretion of a neurotransmitter, also suggested that NMJ development is reg-

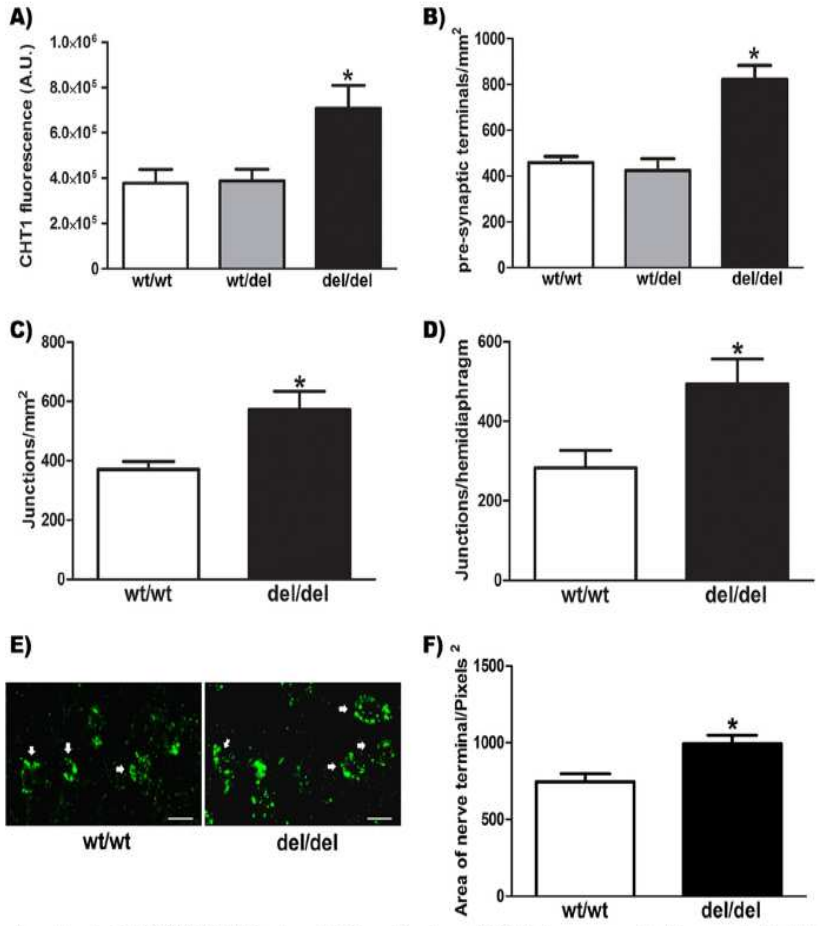

FIG. 7. Synaptic alteration in VAChT$^{del/del}$ E18.5 mice. (A) Quantification of CHT1 fluorescence (arbitrary units [A.U.]) in nerve terminals. An asterisk indicates a statistically significant difference (one-way ANOVA with Bonferroni post hoc test) [$F(2,20 = 5.632)$]. (B) Density of nerve terminals immunolabeled for CHT1 in hemidiaphragms from VAChT$^{wt/wt}$, VAChT$^{wt/del}$, and VAChT$^{del/del}$ mice. *, statistically different by ANOVA with Bonferroni post hoc test [$F(2,17) = 18.43$]. (C) Density of nerve terminals stained with FM1-43fx in hemidiaphragms of VAChT$^{wt/wt}$ and VAChT$^{del/del}$ mice (*, $P = 0.0218$ for VAChT$^{wt/wt}$ versus VAChT$^{del/del}$ mice by unpaired t test; $n = 6$). (D) Number of nerve terminals stained with FM1-43fx per hemidiaphragm (*, $P = 0.0260$ for VAChT$^{wt/wt}$ versus VAChT$^{del/del}$ mice by unpaired t test; $n = 6$). (E) Representative images of NMJs stained with FM1-43fx in hemidiaphragms of VAChT$^{wt/wt}$ and VAChT$^{del/del}$ mice (scale bar, 10 μm). (F) Average area of single nerve terminals in mouse hemidiaphragms stained with FM1-43fx (*, $P = 0.0018$ for VAChT$^{wt/wt}$ versus VAChT$^{del/del}$ mice by unpaired t test). At least 30 end plates were analyzed for each genotype.

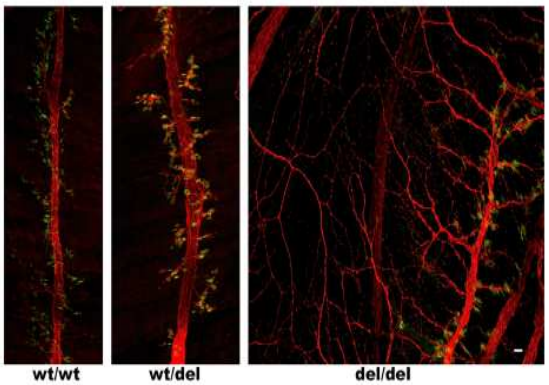

FIG. 8. Altered morphology at the NMJ of VAChT$^{del/del}$ E18.5 mice. Whole diaphragms were stained with anti-neurofilament antibody (red), and nAChRs were labeled with α-bungarotoxin (green). Confocal stacks were obtained, and maximal projections are shown in the images. The image is representative of three experiments. Note the large increase in axonal sprouting in VAChT-null mice.

ulated by synaptic vesicle exocytosis, although for these mutants, it has not been established whether ACh synthesis and storage are affected (28). A number of previously reported studies suggested that distinct pathways of ACh secretion might exist at cholinergic synapses (56, 60, 61, 64). Moreover, vesamicol-independent ACh release, presumably from synaptic vesicles, can be detected in response to pharmacological treatments (2, 7, 10, 11, 46). Hence, if VAChT-independent mechanisms of ACh release have functional significance, they might partially compensate for the lack of the transporter in at least some of its physiological roles.

Interestingly, experiments with an independent mouse line, VAChT KD^{HET} mice, that have close to a 40% reduction in VAChT expression levels showed that a moderate reduction in the level of VAChT causes no neuromuscular phenotype and only small changes in neuromuscular neurotransmission (47). Similar results were obtained with VAChT$^{wt/del}$ mice in the present report, suggesting an important safety mechanism at

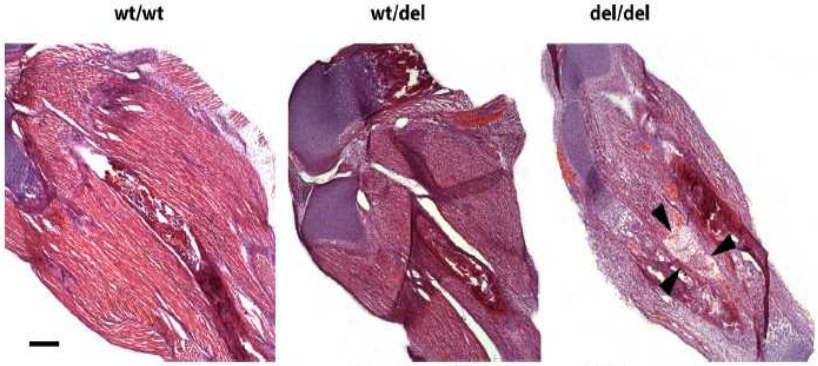

FIG. 9. Muscle morphology of E18.5 embryos from VAChT$^{wt/wt}$, VAChT$^{wt/del}$, and VAChT$^{del/del}$ genotypes. Skeletal muscles (gastrocnemius) were stained with hematoxylin and eosin. Black arrows indicate a loss of normal myofibrillar architecture. Bar, 250 μm.

the NMJ that allows decreased VAChT expression to be compensated. However, VAChT KD^{HOM} mice, with close to a 70% decrease in VAChT protein levels, do show alterations in neuromuscular neurotransmission and motor function (47). It should be noted, however, that synapses in the central nervous system are more sensitive to reductions in VAChT expression, and both VAChT KD^{HET} mice (47) and VAChT$^{wt/del}$ mice (our unpublished observations) present selective cognitive deficits in object recognition memory.

Despite this substantial compensation, the rapid postnatal death of VAChT$^{del/del}$ mice argues that the active storage of ACh by this transporter is critical at the NMJ, as the mice succumb to respiratory failure. In agreement with this conclusion, synaptosomes from VAChT$^{del/del}$ mice do not release newly synthesized ACh in response to depolarization. Lethal mutants of VAChT have also been generated in *Drosophila melanogaster*. These mutants are apparently expressed as well as wt alleles, but they have affected VAChT transport activity (31). Lethal alleles of *unc-17* in *C. elegans* have also been identified, indicating that VAChT is critical for survival in several organisms (1).

VAChT regulates cholinergic synaptic development. Whereas it is clear that ACh storage by VAChT is important for motor function, it is possible that during development, other mechanisms of ACh release, which are independent of this transporter, might become relevant. In nerve-muscle cocultures, a nonquantal release of ACh can be detected in developing growth cones (56). Moreover, compelling genetic evidence from *Drosophila* suggests that the correct axonal targeting of photoreceptors depends on ACh synthesis but not on the expression of VAChT or on synaptic vesicle exocytosis (64). Hence, at least in *Drosophila*, a VAChT-independent mechanism of secretion appears to be important during development. In the light of these findings, we examined whether neuromuscular development in mouse embryos depends on the VAChT-mediated storage of ACh.

Surprisingly, recordings from the diaphragm of VAChT$^{del/del}$ mice revealed small MEPPs, raising the possibility that they arise from small quanta of ACh. Experiments with curare confirmed that these MEPPs were due to the activation of nAChR. We tested the possibility that CHT1 can transport ACh, which might have explained the transport of ACh in vesicles lacking VAChT. A functional mutant of CHT1 retained on the cytoplasmic membrane was expressed in HEK293 cells, and the transfected cells were tested for an enhanced uptake of ACh. None was detected. Moreover, at the low internal pH of synaptic vesicles, CHT1 probably cannot transport substrates (30). We cannot completely eliminate the possibility that ATP or another vesicular constituent is released and activates nicotinic receptors, although the blockade of the small MEPP by curare indicates that ACh itself is the agent.

Early work on vesicles isolated from *Torpedo* electric organs identified a passive accumulation of ACh that could account for up to one-third of the total transport (8). More recent unpublished data indicate that isolated synapse-like microvesicles loaded with radiolabeled ACh lose their neurotransmitter by a VAChT-independent pathway (S. M. Parsons, personal communication). The experiments suggest that ACh can permeate vesicular membranes in the absence of active transport. Given that levels of intracellular ACh are increased fivefold in VAChT$^{del/del}$ mice, creating a very large gradient between the cytoplasm and the lumen of synaptic vesicles, we favor the possibility that the small MEPPs detected in VAChT$^{del/del}$ NMJs result from the passive entry of ACh into vesicles. In fact, vesicles from VAChT$^{del/del}$ NMJs can be loaded with FM1-43, confirming that "empty" vesicles undergo exocytosis-endocytosis (9, 40). However, a stimulated release of newly synthesized ACh from brain synaptosomes obtained from VAChT$^{del/del}$ mice did not occur, indicating that this putative passive transport is much less efficient and may require much more time than the active VAChT-mediated transport.

It seems unlikely that the VAChT-independent secretion of ACh, as recently detected for *Drosophila* (64), has a major role during the development of the mammalian NMJ based on our assessment of muscle morphology, axonal patterning, MN survival, and synaptogenesis in VAChT$^{del/del}$ mice. It is well established that the survival of MN, as well as proper axonal and synaptic targeting, depends on effective competition for neurotrophic support that can be modulated by muscle activity during embryogenesis. ACh has been recognized to act as a signal that induces proper axonal branching, nerve terminal size, and number and maturation of synapses. It likely generates muscle activity leading to the secretion of neurotrophic factors during embryonic development (4, 35). The programmed cell death of MNs is also regulated by ACh, and

ChAT-null mice have an increased number of MNs (4, 6, 35). These results are consistent with the well-known phenomenon of increased survival of MNs after a pharmacological blockade of muscle nAChR during development (38, 39, 42). Our observation that VAChT$^{del/del}$ mice, despite having a fivefold increase in tissue ACh levels, have alterations in neuromuscular development similar to that seen for ChAT-deficient mice strongly suggests that passive uptake by vesicles or even a leakage of ACh from nerve terminals cannot compensate for the lack of VAChT. In fact, the increase in ChAT, CHT1, and ACh contents should conspire to facilitate ACh leakage in VAChT$^{del/del}$ mice but apparently to no avail. It is curious, however, that the VAChT-independent ACh secretion described previously for *Drosophila* (64) does not operate in the mammalian NMJ. The difference between mice and flies may relate to the fact that ACh in *Drosophila* photoreceptors is not the chemical transmitter of these synapses as it is for the mammalian NMJ (64); rather, ACh in the fly photoreceptor seems to function as a developmental cue, whereas histamine is the actual neurotransmitter.

Cytoplasmic ACh in the absence of VAChT. We also find that the removal of the VAChT gene, which is embedded in the first intron of the ChAT gene, causes several neurochemical alterations in cholinergic synapses. The large increase in the ACh content is opposite from what happens in mice null for vesicular monoamine transporter 2, as they have a decrease in intracellular monoamine contents (62). *C. elegans* carrying a blocking mutation of VAChT also has an increase in ACh contents (29, 65).

The increase in the ACh content in mutant mice is likely due to increased levels of expression of ChAT and CHT1. The change in ChAT expression may be related to a compensatory mechanism due to the lack of ACh release, but it might also arise from the physical removal of a large fragment of the ChAT gene, which includes a large part of the first intron (after the R exon), the N exon, and part of the second intron. This deletion physically places the M promoter of ChAT close to the promoter for VAChT and potentially could increase the level of expression of ChAT mRNAs. However, given the fact that the CHT1 expression level is also increased, it is possible that the lack of evoked ACh release triggers signals that upregulate the ACh synthesis machinery. Moreover, the increase in the number of MNs can also contribute to the increased levels of CHT1 and ChAT in the spinal cord. Given that individual synaptic terminals at the NMJ show increased CHT1 expression levels by immunofluorescence, we favor the possibility that both increased expression levels and the increased number of neurons contribute to the higher levels of CHT1 and ChAT. It remains to be determined if cholinergic neurons in the brain present similar changes in morphology and sprouting.

Our data suggest that changes in levels of expression of ChAT and CHT1 "in vivo" can effectively increase the ACh content in cholinergic terminals. Moreover, it seems that the excess ACh in the cytoplasm can be accumulated without degradation, suggesting that "in vivo," this excessive amount of ACh does not impair ACh synthesis. These results agree with data from previously reported experiments performed in the presence of the VAChT inhibitor vesamicol, which, in the superior cervical ganglion, impairs ACh release and allows an accumulation of cytoplasmic ACh (13). These data suggest that ACh synthesis is not regulated by mass action, as previously proposed by a number of investigators (25, 57, 58), because in the absence of ACh release, the transmitter continues to accumulate.

Previous results indicated that both the exocytosis-endocytosis of synaptic vesicles and the quantal release of the neurotransmitter occur in developing axons (24, 34). Our experiments indicate that VAChT regulates a key step for physiologically relevant neurotransmission during the development of the NMJ.

ACKNOWLEDGMENT

We are indebted to Scott Zeitlin (Department of Neuroscience, University of Virginia School of Medicine) for the gift of Cre mice, Stanley Parsons (UCSB) for sharing unpublished data and for excellent suggestions for editing the manuscript, and Brian Collier (McGill University) for comments on the manuscript.

Research in our laboratory is supported by NIH-Fogarty grant R21 TW007800-02 (M.A.M.P., I.I., V.F.P., and M.G.C.), NIH grant RO1 NS53527 (R.W.O.), CIHR (MOP-89919 [V.F.P., R.J.R., and M.A.M.P.]), PRONEX-Fapemig (M.A.M.P. and V.F.P.), FINEP (M.A.M.P.), CNPq (Aging and Mental Health Programs [M.A.M.P., V.F.P., I.I., and M.C.]), FAPEMIG (V.F.P.), and Instituto do Milenio Toxins/MCT (M.V.G., M.A.M.P., and V.F.P.). C.M.-S. and C.M. received postdoctoral fellowships from DFAIT-Canada (Department of Foreign Affairs and International Trade Postdoctoral Fellowship Program). B.M.D.C., X.D.J., and R.L.F. received predoctoral student fellowships from CAPES and CNPq (Brazil).

M.G.C., M.A.M.P., V.F.P., I.I., C.M.-S., and B.M.D.C. have deposited a patent to cover the use of VAChT mutant mice in drug discovery.

REFERENCES

1. **Alfonso, A., K. Grundahl, J. S. Duerr, H. P. Han, and J. B. Rand.** 1993. The Caenorhabditis elegans unc-17 gene: a putative vesicular acetylcholine transporter. Science **261:**617–619.
2. **Barbosa, J., Jr., A. D. Clarizia, M. V. Gomez, M. A. Romano-Silva, V. F. Prado, and M. A. Prado.** 1997. Effect of protein kinase C activation on the release of [3H]acetylcholine in the presence of vesamicol. J. Neurochem. **69:**2608–2611.
3. **Bradford, M. M.** 1976. A rapid and sensitive method for the quantitation of microgram quantities of protein utilizing the principle of protein-dye binding. Anal. Biochem. **72:**248–254.
4. **Brandon, E. P., W. Lin, K. A. D'Amour, D. P. Pizzo, B. Dominguez, Y. Sugiura, S. Thode, C. P. Ko, L. J. Thal, F. H. Gage, and K. F. Lee.** 2003. Aberrant patterning of neuromuscular synapses in choline acetyltransferase-deficient mice. J. Neurosci. **23:**539–549.
5. **Brittain, R. T., G. P. Levy, and M. B. Tyers.** 1969. The neuromuscular blocking action of 2-(4-phenylpiperidino)cyclohexanol (AH 5183). Eur. J. Pharmacol. **8:**93–99.
6. **Buss, R. R., T. W. Gould, J. Ma, S. Vinsant, D. Prevette, A. Winseck, K. A. Toops, J. A. Hammarback, T. L. Smith, and R. W. Oppenheim.** 2006. Neuromuscular development in the absence of programmed cell death: phenotypic alteration of motoneurons and muscle. J. Neurosci. **26:**13413–13427.
7. **Cabeza, R., and B. Collier.** 1988. Acetylcholine mobilization in a sympathetic ganglion in the presence and absence of 2-(4-phenylpiperidino)cyclohexanol (AH5183). J. Neurochem. **50:**112–121.
8. **Carpenter, R. S., R. Koenigsberger, and S. M. Parsons.** 1980. Passive uptake of acetylcholine and other organic cations by synaptic vesicles from Torpedo electric organ. Biochemistry **19:**4373–4379.
9. **Ceccarelli, B., and W. P. Hurlbut.** 1975. The effects of prolonged repetitive stimulation in hemicholinium on the frog neuromuscular junction. J. Physiol. **247:**163–188.
10. **Clarizia, A. D., M. V. Gomez, M. A. Romano-Silva, S. M. Parsons, V. F. Prado, and M. A. Prado.** 1999. Control of the binding of a vesamicol analog to the vesicular acetylcholine transporter. Neuroreport **10:**2783–2787.
11. **Clarizia, A. D., M. A. Romano-Silva, V. F. Prado, M. V. Gomez, and M. A. M. Prado.** 1998. Role of protein kinase C in the release of [H-3]acetylcholine from myenteric plexus treated with vesamicol. Neurosci. Lett. **244:**115–117.
12. **Clarke, P. G., and R. W. Oppenheim.** 1995. Neuron death in vertebrate development: in vitro methods. Methods Cell Biol. **46:**277–321.
13. **Collier, B., S. A. Welner, J. Ricny, and D. M. Araujo.** 1986. Acetylcholine synthesis and release by a sympathetic ganglion in the presence of 2-(4-phenylpiperidino)cyclohexanol (AH5183). J. Neurochem. **46:**822–830.
14. **Dan, Y., and M. M. Poo.** 1992. Quantal transmitter secretion from myocytes loaded with acetylcholine. Nature **359:**733–736.
15. **de Castro, B. M., G. S. Pereira, V. Magalhães, J. I. Rossato, X. De Jaeger, C.**

Martins-Silva, B. Leles, P. Lima, M. V. Gomez, R. R. Gainetdinov, M. G. Caron, I. Izquierdo, M. Cammarota, V. F. Prado, and M. A. Prado. 2009. Reduced expression of the vesicular acetylcholine transporter causes learning deficits in mice. Genes Brain Behav. **8:**23–35.
16. **Dobransky, T., and R. J. Rylett.** 2005. A model for dynamic regulation of choline acetyltransferase by phosphorylation. J. Neurochem. **95:**305–313.
17. **Dragatsis, I., and S. Zeitlin.** 2000. CaMKIIalpha-Cre transgene expression and recombination patterns in the mouse brain. Genesis **26:**133–135.
18. **Edwards, R. H.** 2007. The neurotransmitter cycle and quantal size. Neuron **55:**835–858.
19. **Estrella, D., K. L. Green, C. Prior, J. Dempster, R. F. Halliwell, R. S. Jacobs, S. M. Parsons, R. L. Parsons, and I. G. Marshall.** 1988. A further study of the neuromuscular effects of vesamicol (AH5183) and of its enantiomer specificity. Br. J. Pharmacol. **93:**759–768.
20. **Falk-Vairant, J., P. Correges, L. Eder-Colli, N. Salem, E. Roulet, A. Bloc, F. Meunier, B. Lesbats, F. Loctin, M. Syngelakis, M. Israel, and Y. Dunant.** 1996. Quantal acetylcholine release induced by mediatophore transfection. Proc. Natl. Acad. Sci. USA **93:**5203–5207.
21. **Ferguson, S. M., M. Bazalakova, V. Savchenko, J. C. Tapia, J. Wright, and R. D. Blakely.** 2004. Lethal impairment of cholinergic neurotransmission in hemicholinium-3-sensitive choline transporter knockout mice. Proc. Natl. Acad. Sci. USA **101:**8762–8767.
22. **Ferguson, S. M., V. Savchenko, S. Apparsundaram, M. Zwick, J. Wright, C. J. Heilman, H. Yi, A. I. Levey, and R. D. Blakely.** 2003. Vesicular localization and activity-dependent trafficking of presynaptic choline transporters. J. Neurosci. **23:**9697–9709.
23. **Ferguson, S. S., and M. G. Caron.** 2004. Green fluorescent protein-tagged beta-arrestin translocation as a measure of G protein-coupled receptor activation. Methods Mol. Biol. **237:**121–126.
24. **Girod, R., S. Popov, J. Alder, J. Q. Zheng, A. Lohof, and M. M. Poo.** 1995. Spontaneous quantal transmitter secretion from myocytes and fibroblasts: comparison with neuronal secretion. J. Neurosci. **15:**2826–2838.
25. **Glover, V. A., and L. T. Potter.** 1971. Purification and properties of choline acetyltransferase from ox brain striate nuclei. J. Neurochem. **18:**571–580.
26. **Gomez, R. S., M. V. Gomez, and M. A. Prado.** 1996. Inhibition of Na+, K+-ATPase by ouabain opens calcium channels coupled to acetylcholine release in guinea pig myenteric plexus. J. Neurochem. **66:**1440–1447.
27. **Gomez, R. S., M. A. Prado, F. Carazza, and M. V. Gomez.** 1999. Halothane enhances exocytosis of [3H]-acetylcholine without increasing calcium influx in rat brain cortical slices. Br. J. Pharmacol. **127:**679–684.
28. **Heeroma, J. H., J. J. Plomp, E. W. Roubos, and M. Verhage.** 2003. Development of the mouse neuromuscular junction in the absence of regulated secretion. Neuroscience **120:**733–744.
29. **Hosono, R., T. Sassa, and S. Kuno.** 1987. Mutations affecting acetylcholine levels in the nematode Caenorhabditis elegans. J. Neurochem. **49:**1820–1823.
30. **Iwamoto, H., R. D. Blakely, and L. J. De Felice.** 2006. Na+, Cl−, and pH dependence of the human choline transporter (hCHT) in Xenopus oocytes: the proton inactivation hypothesis of hCHT in synaptic vesicles. J. Neurosci. **26:**9851–9859.
31. **Kitamoto, T., X. Xie, C. F. Wu, and P. M. Salvaterra.** 2000. Isolation and characterization of mutants for the vesicular acetylcholine transporter gene in Drosophila melanogaster. J. Neurobiol. **42:**161–171.
32. **Leao, R. M., M. V. Gomez, B. Collier, and M. A. Prado.** 1995. Inhibition of potassium-stimulated acetylcholine release from rat brain cortical slices by two high-affinity analogs of vesamicol. Brain Res. **703:**86–92.
33. **Marchbanks, R. M., S. Wonnacott, and M. A. Rubio.** 1981. The effect of acetylcholine release on choline fluxes in isolated synaptic terminals. J. Neurochem. **36:**379–393.
34. **Matteoli, M., K. Takei, M. S. Perin, T. C. Sudhof, and P. De Camilli.** 1992. Exo-endocytotic recycling of synaptic vesicles in developing processes of cultured hippocampal neurons. J. Cell Biol. **117:**849–861.
35. **Misgeld, T., R. W. Burgess, R. M. Lewis, J. M. Cunningham, J. W. Lichtman, and J. R. Sanes.** 2002. Roles of neurotransmitter in synapse formation: development of neuromuscular junctions lacking choline acetyltransferase. Neuron **36:**635–648.
36. **Nakata, K., T. Okuda, and H. Misawa.** 2004. Ultrastructural localization of high-affinity choline transporter in the rat neuromuscular junction: enrichment on synaptic vesicles. Synapse **53:**53–56.
37. **Nguyen, M. L., G. D. Cox, and S. M. Parsons.** 1998. Kinetic parameters for the vesicular acetylcholine transporter: two protons are exchanged for one acetylcholine. Biochemistry **37:**13400–13410.
38. **Oppenheim, R. W., J. Caldero, D. Cuitat, J. Esquerda, J. J. McArdle, B. M. Olivera, D. Prevette, and R. W. Teichert.** 2008. The rescue of developing avian motoneurons from programmed cell death by a selective inhibitor of the fetal muscle-specific nicotinic acetylcholine receptor. Dev. Neurobiol. **68:**972–980.
39. **Oppenheim, R. W., D. Prevette, A. D'Costa, S. Wang, L. J. Houenou, and J. M. McIntosh.** 2000. Reduction of neuromuscular activity is required for the rescue of motoneurons from naturally occurring cell death by nicotinic-blocking agents. J. Neurosci. **20:**6117–6124.
40. **Parsons, R. L., M. A. Calupca, L. A. Merriam, and C. Prior.** 1999. Empty synaptic vesicles recycle and undergo exocytosis at vesamicol-treated motor nerve terminals. J. Neurophysiol. **81:**2696–2700.
41. **Parsons, S. M.** 2000. Transport mechanisms in acetylcholine and monoamine storage. FASEB J. **14:**2423–2434.
42. **Pittman, R., and R. W. Oppenheim.** 1979. Cell death of motoneurons in the chick embryo spinal cord. IV. Evidence that a functional neuromuscular interaction is involved in the regulation of naturally occurring cell death and the stabilization of synapses. J. Comp. Neurol. **187:**425–446.
43. **Pittman, R. H., and R. W. Oppenheim.** 1978. Neuromuscular blockade increases motoneurone survival during normal cell death in the chick embryo. Nature **271:**364–366.
44. **Prado, M. A., T. Moraes-Santos, R. N. Freitas, M. A. Silva, and M. V. Gomez.** 1990. Choline oxidase chemiluminescent assay, after removal of eserine from medium, of acetylcholine released in vitro from brain slices. J. Neurosci. Methods **31:**193–196.
45. **Prado, M. A. M., M. V. Gomez, and B. Collier.** 1992. Mobilization of the readily releasable pool of acetylcholine from a sympathetic-ganglion by tityustoxin in the presence of vesamicol. J. Neurochem. **59:**544–552.
46. **Prado, M. A. M., M. V. Gomez, and B. Collier.** 1993. Mobilization of a vesamicol-insensitive pool of acetylcholine from a sympathetic-ganglion by ouabain. J. Neurochem. **61:**45–56.
47. **Prado, V. F., C. Martins-Silva, B. M. de Castro, R. F. Lima, D. M. Barros, E. Amaral, A. J. Ramsey, T. D. Sotnikova, M. R. Ramirez, H. G. Kim, J. I. Rossato, J. Koenen, H. Quan, V. R. Cota, M. F. Moraes, M. V. Gomez, C. Guatimosim, W. C. Wetsel, C. Kushmerick, G. S. Pereira, R. R. Gainetdinov, I. Izquierdo, M. G. Caron, and M. A. Prado.** 2006. Mice deficient for the vesicular acetylcholine transporter are myasthenic and have deficits in object and social recognition. Neuron **51:**601–612.
48. **Prado, V. F., M. A. M. Prado, and S. M. Parsons.** 2008. VAChT. UCSD-Nature Molecule Pages. doi:10.1038/mp.a002796.01.
49. **Rempe, D., G. Vangeison, J. Hamilton, Y. Li, M. Jepson, and H. J. Federoff.** 2006. Synapsin I Cre transgene expression in male mice produces germline recombination in progeny. Genesis **44:**44–49.
50. **Ribeiro, F. M., J. Alves-Silva, W. Volknandt, C. Martins-Silva, H. Mahmud, A. Wilhelm, M. V. Gomez, R. J. Rylett, S. S. Ferguson, V. F. Prado, and M. A. Prado.** 2003. The hemicholinium-3 sensitive high affinity choline transporter is internalized by clathrin-mediated endocytosis and is present in endosomes and synaptic vesicles. J. Neurochem. **87:**136–146.
51. **Ribeiro, F. M., S. A. Black, S. P. Cregan, V. F. Prado, M. A. Prado, R. J. Rylett, and S. S. Ferguson.** 2005. Constitutive high-affinity choline transporter endocytosis is determined by a carboxyl-terminal tail dileucine motif. J. Neurochem. **94:**86–96.
52. **Ribeiro, F. M., S. A. Black, V. F. Prado, R. J. Rylett, S. S. Ferguson, and M. A. Prado.** 2006. The "ins" and "outs" of the high-affinity choline transporter CHT1. J. Neurochem. **97:**1–12.
53. **Richards, D. A., C. Guatimosim, S. O. Rizzoli, and W. J. Betz.** 2003. Synaptic vesicle pools at the frog neuromuscular junction. Neuron **39:**529–541.
54. **Song, H., G. Ming, E. Fon, E. Bellocchio, R. H. Edwards, and M. Poo.** 1997. Expression of a putative vesicular acetylcholine transporter facilitates quantal transmitter packaging. Neuron **18:**815–826.
55. **Sudhof, T. C.** 2004. The synaptic vesicle cycle. Annu. Rev. Neurosci. **27:**509–547.
56. **Sun, Y. A., and M. M. Poo.** 1985. Non-quantal release of acetylcholine at a developing neuromuscular synapse in culture. J. Neurosci. **5:**634–642.
57. **Tucek, S.** 1985. Regulation of acetylcholine synthesis in the brain. J. Neurochem. **44:**11–24.
58. **Vaca, K., and G. Pilar.** 1979. Mechanisms controlling choline transport and acetylcholine synthesis in motor nerve terminals during electrical stimulation. J. Gen. Physiol. **73:**605–628.
59. **Van der Kloot, W.** 1986. 2-(4-Phenylpiperidino)cyclohexanol (AH5183) decreases quantal size at the frog neuromuscular junction. Pflugers Arch. **406:**83–85.
60. **Van der Kloot, W.** 2003. Loading and recycling of synaptic vesicles in the Torpedo electric organ and the vertebrate neuromuscular junction. Prog. Neurobiol. **71:**269–303.
61. **Vyskocil, F., and P. Illes.** 1977. Non-quantal release of transmitter at mouse neuromuscular junction and its dependence on the activity of Na+-K+ ATP-ase. Pflugers Arch. **370:**295–297.
62. **Wang, Y. M., R. R. Gainetdinov, F. Fumagalli, F. Xu, S. R. Jones, C. B. Bock, G. W. Miller, R. M. Wightman, and M. G. Caron.** 1997. Knockout of the vesicular monoamine transporter 2 gene results in neonatal death and supersensitivity to cocaine and amphetamine. Neuron **19:**1285–1296.
63. **Whitton, P. S., I. G. Marshall, and S. M. Parsons.** 1986. Reduction of quantal size by vesamicol (AH5183), an inhibitor of vesicular acetylcholine storage. Brain Res. **385:**189–192.
64. **Yang, H., and S. Kunes.** 2004. Nonvesicular release of acetylcholine is required for axon targeting in the Drosophila visual system. Proc. Natl. Acad. Sci. USA **101:**15213–15218.
65. **Zhu, H., J. S. Duerr, H. Varoqui, J. R. McManus, J. B. Rand, and J. D. Erickson.** 2001. Analysis of point mutants in the Caenorhabditis elegans vesicular acetylcholine transporter reveals domains involved in substrate translocation. J. Biol. Chem. **276:**41580–41587.

2.3 – Artigo número 3

Ouabain evokes exocytosis dependent on ryanodine and mitochondrial calcium stores that is not followed by compensatory endocytosis at the neuromuscular junction.

AMARAL, E.; LEITE, L. F.; GOMEZ, M. V.; PRADO, M. A.; GUATIMOSIM, C.

Neurochemystry International, v. 55, n. 6, p. 406-13, 2009.

Neurochemistry International 55 (2009) 406–413

Contents lists available at ScienceDirect

Neurochemistry International

journal homepage: www.elsevier.com/locate/neuint

Ouabain evokes exocytosis dependent on ryanodine and mitochondrial calcium stores that is not followed by compensatory endocytosis at the neuromuscular junction

Ernani Amaral [a], Luciana F. Leite [a], Marcus V. Gomez [b], Marco A.M. Prado [c], Cristina Guatimosim [a,*]

[a] Department of Morphology, Cell Biology Program, Biological Sciences Institute, Federal University of Minas Gerais, Belo Horizonte, MG, Brazil
[b] Laboratory of Neuroscience, School of Medicine, Federal University of Minas Gerais, Belo Horizonte, MG, Brazil
[c] Molecular Brain Research Group, Robarts Research Institute, Departments of Physiology and Pharmacology/Anatomy and Cell Biology, University of Western Ontario, Robarts Research Institute, London, ON, Canada

ARTICLE INFO

Article history:
Received 13 March 2009
Accepted 20 April 2009
Available online 3 May 2009

Keywords:
Neuromuscular junction
Ouabain
Intracellular calcium
FM1–43
Exocytosis
Endocytosis
Microscopy

ABSTRACT

Ouabain is a cardiotonic glycoside that inhibits the sodium potassium ATPase pump leading to sodium accumulation in nerve terminals. At the frog neuromuscular junction, ouabain induces acetylcholine release and a rapid depletion of synaptic vesicles. In the present work, we used FM1–43 vital labeling to dissect the effect of ouabain on synaptic vesicles recycling. We first examined images of nerve-muscle preparations that were stained with FM1–43 by electrical stimulation of the nerve and destained with ouabain. We observed that ouabain induced exocytosis of synaptic vesicles independently of extracellular calcium, implying a mechanism of exocytosis that can bypass the requirement for extracellular calcium. We therefore tested the hypothesis that ouabain induces exocytosis by mobilizing intracellular calcium and we report that calcium release from endoplasmic reticulum through ryanodine receptors is necessary for ouabain-evoked exocytosis. In addition, the ouabain-evoked exocytosis was dependent on calcium released from mitochondria. We also investigated if exocytosis evoked by ouabain is followed by compensatory endocytosis. We observed that muscles incubated with FM1–43 in the presence of ouabain did not present significant staining. In conclusion, our data demonstrate that exocytosis evoked by ouabain is independent on extracellular calcium but dependent on calcium release from endoplasmic reticulum and mitochondrial stores. In addition, we suggest that ouabain can be used as a pharmacological tool to uncouple synaptic vesicles exocytosis from endocytosis at the neuromuscular junction.

1. Introduction

One of the most defining features of a synapse is the presence of synaptic vesicles at the presynaptic axon terminal. These organelles are directly involved in one essential presynaptic function: the release of chemical messengers. Synaptic vesicles store neurotransmitters in their lumen and secrete their content by fusion with the plasma membrane in response to calcium influx (reviewed by Südhof, 2004). A crucial step for maintaining neurotransmission, especially during sustained activity, involves the ability of synaptic vesicles to undergo repetitive cycles of exo-endocytosis to avoid vesicle depletion and consequently, paralysis of neurotransmission. Therefore, many studies have focused on understanding synaptic vesicle recycling using distinct pharmacological tools to evoke neurotransmitter release. One tool is ouabain, a cardiac glycoside extracted from the seeds of the African tree *Strophanthus gratus*. It is a potent cardiotonic glycoside that inhibits Na^+, K^+-ATPase and, by increasing intracellular sodium levels, evokes neurotransmitter release that is usually independent on extracellular calcium and dependent on intracellular calcium store (Birks, 1963; Elmqvist and Feldman, 1965a,b; Paton et al., 1971; Vizi, 1972; Baker and Crawford, 1975; Gomez et al., 1975; Vizi and Vyskocil, 1979; Meyer and Cooper, 1981; Vyas and Marchbanks, 1981; Adam-Vizi and Ligeti, 1984; Adam-Vizi et al., 1991; Mulkey and Zucker, 1992; Prado et al., 1993; Casali et al., 1995; Gomez et al., 1996; Lomeo et al., 2003; Pivovarov and Drozdova, 2003). However, the intracellular target for ouabain action remains unknown, at least for the neuromuscular junction.

* Corresponding author at: Department of Morphology, Cell Biology Program, Biological Sciences Institute, Federal University of Minas Gerais, Av. Antonio Carlos 6627, Belo Horizonte, MG 31270-901, Brazil. Tel.: +55 31 34992824; fax: +55 31 34992810.
E-mail address: cguati@icb.ufmg.br (C. Guatimosim).

0197-0186/$ – see front matter © 2009 Elsevier Ltd. All rights reserved.
doi:10.1016/j.neuint.2009.04.009

In the present study, we investigated the effect of ouabain on the synaptic vesicle cycle using vital labeling of the frog neuromuscular junction with FM1–43 (Betz and Bewick, 1992a; Betz et al., 1992b). The FM family of activity-dependent fluorescent dyes has been useful for the study of exocytosis, endocytosis and vesicle trafficking in *ex vivo* preparations such as the neuromuscular junction (Betz and Bewick, 1992a; Betz et al., 1992b; Ribchester et al., 1994; Brumback et al., 2004). This dynamic approach allowed us to visualize synaptic vesicles recycling evoked by ouabain and to identify the intracellular calcium stores involved at ouabain-evoked synaptic vesicles exocytosis at the neuromuscular junction. In addition, we showed that ouabain selectively inhibits compensatory endocytosis and therefore we suggest that this glycoside might be used as a tool to uncouple exocytosis from endocytosis.

2. Materials and methods

2.1. Drugs and chemicals

FM1–43 was purchased from Invitrogen™; ouabain, *d*-tubocurarine, EGTA-AM, 2-APB, azumolene, oligomycin, and CCCP were purchased from Sigma–Aldrich. CGP37157 was obtained from Calbiochem, NJ, USA. All other chemicals and reagents were of analytical grade.

2.2. Experimental procedures

2.2.1. Staining and destaining with FM1–43

All procedures were approved by the local animal care committee (CETEA-UFMG). Briefly, Frog cutaneous pectoris nerve-muscle preparations were dissected from *Rana catesbeiana* (~60 g) and mounted in a sylgard-lined chamber containing frog Ringer solution (115 mM NaCl, 2.5 mM KCl, 1.8 mM $CaCl_2$, 5 mM Hepes, pH7.2). FM1–43 was used at 4 μM to stain the recycling pool of synaptic vesicles (Betz et al., 1992b). FM1–43 stains the extracellular membrane and upon stimulation, dye is internalized during cycles of exo-endocytosis. After washing out excess dye, endocytosed vesicles can be destained by a second round of stimulation (Betz and Bewick, 1992a). Frog nerve terminals stained with FM1–43 by tetanic stimulation (20 Hz, 10 min) present the typical pattern of fluorescent spots over the terminal length (Betz et al., 1992b). Each spot corresponds to a cluster of synaptic vesicles containing FM1–43 inside them (Henkel et al., 1996; Richards et al., 2000).

The muscles were incubated with *d*-tubocurarine (16 μM) to prevent contractions during electrical stimulation or image acquisition and thereafter they were stimulated by the nerve for 10 min with tetanic stimulus (20 Hz, 0.5 ms, square wave pulses, 4 V) fired by a suction electrode in the presence of FM1–43 (4 μM). After electrical stimulation, the preparation was maintained at rest for 15 min to guarantee maximal FM1–43 uptake. The excess of FM1–43 adhered to the muscle membrane was removed during a washing period in frog Ringer without the probe for at least 60 min. To investigate the ouabain effect on synaptic vesicles exocytosis, the glycoside was added to the frog Ringer in concentrations ranging from 1 μM to 100 μM and the destaining of motor nerve terminals labeled with FM1–43 was followed for 60 or 90 min. Images were acquired in intervals of 10 min until the end of the experiments.

Experiments investigating the role of extracellular Na^+ and Ca^{2+} ions on the exocytosis induced by ouabain were performed in modified Ringer solutions with equimolar substitution of NaCl for LiCl and equimolar substitution of $CaCl_2$ for $MgCl_2$, respectively. EGTA (2 mM), an extracellular calcium chelator, was added to the modified Ringer without Ca^{2+}. The preparations were incubated in modified Ringers for 1 h before treatment with ouabain.

Modified Ringer with equimolar substitution of $CaCl_2$ for $MgCl_2$ was also used to investigate the participation of intracellular Ca^{2+} stores on the vesicular release evoked by ouabain. The muscles were incubated for 60 min in the modified Ringer in the presence of EGTA-AM (50 μM), an intracellular calcium chelator, before exposure to ouabain. To elucidate the source of intracellular calcium ions related to exocytosis evoked by ouabain, the preparations were pre-incubated for 60 min in modified Ringer without Ca^{2+} in which was added 2-APB (100 μM), azumolene (100 μM) or CGP37157 (50 μM), inhibitors of inositol triphosphate receptors (IP3R), ryanodine receptors (RyR) and mitochondrial Na^+/Ca^{2+} exchanger, respectively.

The effects of ouabain on compensatory endocytosis were investigated by following FM1–43 active uptake. Preparations were incubated for 30 min in frog Ringer containing ouabain (100 μM) and FM1–43. The images were acquired after the washing period. The same protocol was used to investigate the effect of CCCP on compensatory endocytosis. In another set of experiments, muscles were pre-incubated with oligomycin (8 μg/ml) for 60 min and then electrically stimulated by the nerve (20 Hz, 10 min) in the presence of FM1–43 and oligomycin. The images were collected after the washing period.

2.2.2. Fluorescence microscopy and imaging analyses

Images were acquired using a fluorescence microscope (Leica DM2500) coupled to a CCD camera (12 bits, Micromax) and visualized in a computer. The fluorescence microscope was equipped with water immersion objectives (63×, 0.95 NA and 40×, 0.75 NA) and standard fluorescein optics (excitation 480 nm, dichroic 505 nm, emission 535 nm long pass). Excitation light came from a 100 W Hg lamp. The experimental parameters for collection of images were always identical in control and test contralateral muscles in a given trial.

Image analysis was performed using the software Metamorph Imaging System 7.0 which allows to draw lines around regions of interest and can be used to measure the brightness levels emitted from each fluorescent spot. The mean fluorescence intensity was determined for each group of spots and plotted against the time as percentage of its mean initial fluorescence using the softwares Microsoft Excel and Sigma Plot 9.0. Statistical analysis was performed using paired students *t*-test. P values < 0.05 were considered statistically significant.

3. Results

3.1. Ouabain-evoked destaining of nerve terminals

Several reports suggest that ouabain induces neurotransmitters release in distinct experimental models (Vizi, 1972; Baker and Crawford, 1975; Gomez et al., 1975; Haimann et al., 1985; Prado et al., 1993; Casali et al., 1995; Lomeo et al., 2003). To investigate the effect of Na^+/K^+-ATPase inhibition induced by ouabain on synaptic vesicles recycling, frog cutaneous pectoris motor nerve terminals were stained with FM1–43 by electrical stimulation of the nerve (Betz et al., 1992b). Fig. 1A, C and E shows representative images of nerve terminals with a typical pattern of staining, i.e., fluorescent spots over the terminal length. Upon electrical stimulation (20 Hz, 10 min), muscle-nerve preparations stained with FM1–43 destained (Fig. 1F), reflecting dye release from recycling vesicles. Incubation with ouabain (100 μM, 60 min) also induced destaining in terminals that were previously stained with FM1–43 by electrical stimulation (Fig. 1D). Control for photobleaching due to repetitive illumination was performed and there was some fluorescence decay in terminals that were illuminated for 60 min (Fig. 1B). To quantify the decrease in brightness that occurred due to photobleaching, ouabain (1, 10, 50 and 100 μM) and electrical stimulation, the mean fluorescence intensity of areas of interest was collected as grey levels (12 bits 4096 levels) and plotted against time (Fig. 1G). The rate of destaining of fluorescent spots was much faster when evoked by electrical stimulation than that evoked by ouabain, suggesting distinct mechanisms of synaptic vesicles release. The effect of ouabain was dose-dependent, with concentrations above 10 μM already inducing significant exocytosis. Photobleaching-evoked loss of fluorescence was statistically significant lower than that evoked by electrical stimulation or ouabain (10–100 μM, Fig. 1G).

Deri and Adam-Vizi (1993) showed that ouabain induces a gradual increase in intracellular sodium concentration in synaptosomes. To investigate if exocytosis of FM1–43 stained synaptic vesicles induced by ouabain is dependent on sodium, nerve-muscle preparations were incubated in modified frog Ringer with equimolar substitution of sodium for lithium in the presence of ouabain (100 μM) for 30 min. We detected no destaining by ouabain in this condition ($p = 0.522$, black arrow in Fig. 2J), and the small decrease in fluorescence was similar to photobleaching (Fig. 2J). However, when we exchanged the modified frog Ringer by a normal Ringer containing sodium with ouabain (100 μM) and followed the destaining of fluorescent spots from the same nerve terminal, now we could detect significant fluorescence loss ($p = 0.002$, Fig. 2I and J). The amount of destaining was equivalent to that obtained in nerve terminals exposed to normal sodium frog Ringer containing ouabain for 90 min (Fig. 2F and J). Thus, the results so far show that at the neuromuscular junction, ouabain induces exocytosis of FM1–43 stained synaptic vesicles and this effect is dependent on extracellular sodium.

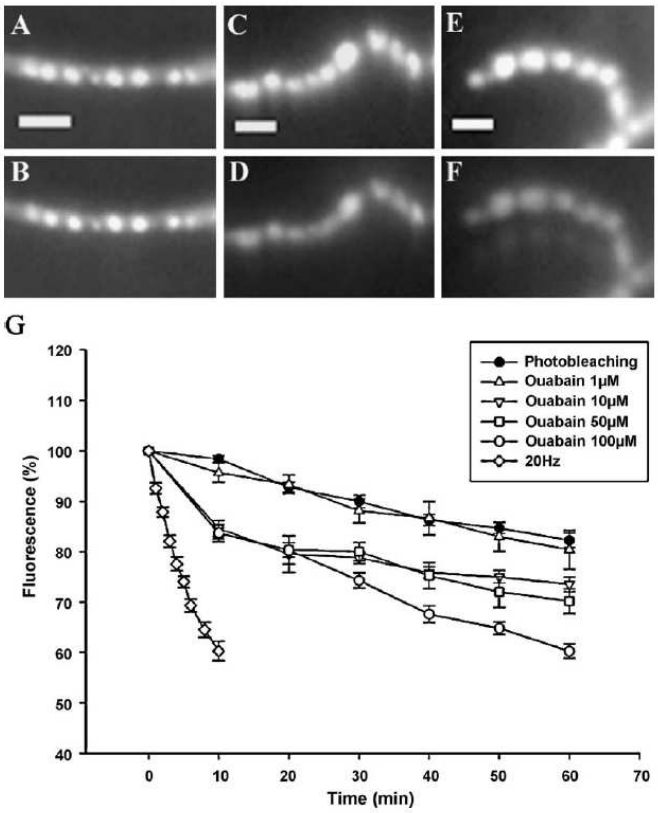

Fig. 1. Ouabain promotes synaptic vesicle release and FM1–43 destaining. (A) Representative frog neuromuscular junction stained with FM1–43 after electrical stimulation (20 Hz, 10 min). Note the punctuate pattern of synaptic vesicles clusters stained with the fluorescent probe. (B) Images acquired at 10 min intervals for a total experiment period of 60 min. The reduction in fluorescent spots intensity was due to photobleaching. (C) Motor nerve terminal stained with FM1–43 before addition of ouabain. (D) After 1 h of incubation with ouabain (100 μM), the terminal shows a significant reduction in fluorescence reflecting vesicular release. (E) Frog motor nerve terminal stained with FM1–43. (F) The same motor terminal seen in the previous panel submitted to 10 min of tetanic stimulation (20 Hz). (G) Time-course of destaining evoked by ouabain (1, 10, 50 and 100 μM) and by electrical stimulus (20 Hz, 10 min). Note that the ouabain-evoked destaining has a slower kinetic than tetanic stimulation. The photobleaching curve is plotted for control purposes. (Scale bar for all images: 10 μm.) The dose-response curves and the photobleaching plotted in (G) represent the mean of at least three independent experiments in which were considered 15 spots for analysis in each condition. The destaining with 20 Hz is a representative experiment. Error bars: ±S.E.M. At the end of 60 min, $p < 0.05$ for 10, 50 and 100 μM of ouabain.

3.2. Calcium dependence of exocytosis evoked by ouabain

Cardiotonic glycosides such as ouabain induce rapid spontaneous acetylcholine release by mobilizing intracellular calcium in motor nerve terminals (Elmqvist and Feldman, 1965a,b; Baker and Crawford, 1975). However, the intracellular calcium source involved in this process is still unknown. Here, we investigated the calcium-dependence of ouabain effect on FM1–43 destaining at the neuromuscular junction. Fig. 3A and B are representative images acquired at the beginning and the end of a control photobleaching experiment, respectively. Fig. 3C and D are representative images of a destaining evoked by ouabain (100 μM) in normal Ringer. Fig. 3E shows a representative motor nerve terminal stained with FM1–43 and Fig. 3F shows the same terminal after 60 min of incubation with calcium-free Ringer containing EGTA and ouabain (100 μM). As we can see in Fig. 3I, the destaining curve for ouabain in calcium-free medium overlaps with that obtained in normal Ringer. In fact, if we subtract the photobleaching, the amount of FM1–43 destaining was, on average, 21.97% and 20.88% for ouabain and ouabain plus EGTA respectively ($p = 0.877$), suggesting that at least for cholinergic motor neurons from the neuromuscular junction, exocytosis evoked by ouabain is independent on extracellular calcium. We performed experiments using the intracellular calcium chelator BAPTA-AM in the nerve-muscle preparation stained with FM1–43, however, this chelator quenched the fluorescence of FM1–43 (not shown). Therefore, we relied in the slower calcium chelator EGTA-AM. Fig. 3G shows a nerve terminal that was stained with FM1–43 and incubated with frog Ringer containing EGTA-AM (50 μM) for 60 min. After the incubation period, ouabain (100 μM) was added to the solution and after 60 min, the same terminal was imaged (Fig. 3H). We observed a reduction in FM1–43 destaining evoked by ouabain in the presence of EGTA-AM (5.10%) when compared with the destaining evoked by ouabain plus EGTA (20.88%, Fig. 4A). Vizi (1972) describes that the inhibition of the Na^+,K^+-ATPase by ouabain leads to an increase in intracellular sodium levels, a loss of intracellular potassium and possibly changes in intracellular calcium concentration. The inhibition of FM1–43 destaining by EGTA-AM prompted us to seek for the intracellular calcium source(s) for the ouabain effect. We first used 2-APB and

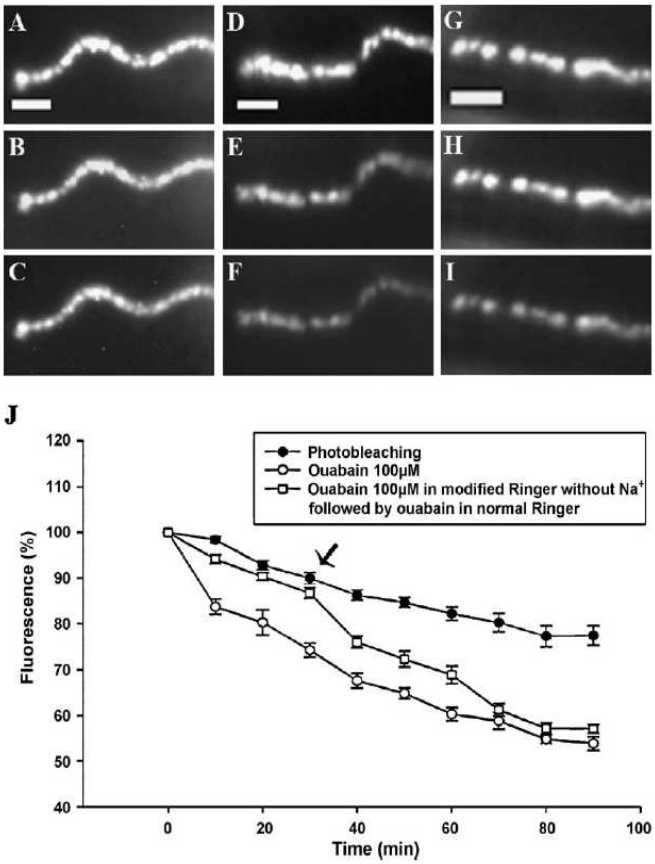

Fig. 2. Vesicular release evoked by ouabain is dependent on sodium ions. (A) Frog neuromuscular junction stained with FM1–43 at the beginning of a control experiment. (B) Decrease of spots fluorescence intensity due to photobleaching after 30 min. (C) Photobleaching observed at the end of 90 min. (D) Motor terminal stained with FM1–43 before addition of ouabain (100 μM). (E) The same terminal seen in (D) after 30 min of incubation with ouabain. (F) Destainning induced by ouabain after 90 min. (G) Motor terminal stained with FM1–43 and pre-incubated for 60 min in a modified Ringer in which Na^+ ions were replaced by Li^+. (H) The same terminal after 30 min of exposure to ouabain (100 μM) in the modified Ringer lacking Na^+. Note that the fluorescent spots presented little destaining. (I) Modified Ringer lacking Na^+ was exchanged by normal frog Ringer (black arrow in (J)). Ouabain evoked a significant FM1–43 destaining 60 min after medium exchange. (J) Time-course of experiments similar to that described in (A–I). (Scale bars: 10 μm. Curves in (J) represent, the mean of at least three independent experiments in which were considered 15 spots for analysis. Error bars: ±S.E.M.)

azumolene that are inhibitors of endoplasmic reticulum IP3R and RyR, respectively (Maruyama et al., 1997; Tian et al., 1991). Nerve terminals were stained with FM1–43 and pre-treated with frog Ringer containing 2-APB (100 μM) for 60 min. After this period, the medium was exchanged by a fresh one containing 2-APB and ouabain (100 μM) and images were obtained every 10 min during 60 min. FM1–43 destaining evoked by ouabain in the presence of 2-APB was not statistically different from that obtained in the absence of this drug (Fig. 4A). However, nerve terminals that were exposed to ouabain in the presence of azumolene (100 μM) presented only 7.86% of destaining which was statistically different from that obtained with ouabain alone ($p < 0.001$), suggesting that calcium released through RyR at the endoplasmic reticulum may be involved in the mechanism of action of ouabain.

At the presynaptic nerve terminals it has been shown that mitochondria have a major role in intracellular calcium handling and neurotransmitter release (Alnaes and Rahamimoff, 1975; Rahamimoff et al., 1978; David et al., 1998; David, 1999). To investigate if ouabain-evoked synaptic vesicle exocytosis recruits mitochondrial calcium stores, muscle-nerve preparations stained with FM1–43 were incubated for 60 min in frog Ringer containing CGP37157 (50 μM), a blocker of mitochondrial Na^+/Ca^{2+} exchanger and then exposed to ouabain (100 μM) in the presence of CGP37157. Fig. 4A shows averaged data from three individual preparations exposed to ouabain in the presence of CGP37157. We noticed that CGP37157 inhibits FM1–43 destaining induced by ouabain in similar way to that observed with EGTA-AM (Fig. 4A). In fact, destaining evoked by ouabain in the presence of CGP37157 was not statistically different from that obtained in the presence of EGTA-AM ($p = 0.305$).

In search for more evidences that could relate mitochondrial calcium stores with the synaptic vesicles exocytosis induced by ouabain, we compared FM1–43 destaining evoked by ouabain with that evoked by pharmacological agents that disrupt mitochondrial function. We therefore tested the effect of the protonophore CCCP (2 μM), a metabolic uncoupler that inhibits ATP synthesis and increases intracellular calcium levels by inducing calcium efflux from mitochondria (Baker and Schlaepfer, 1978; Molgó and Pecot-Dechavassine, 1988). We found that CCCP (2 μM) induced FM1–43 destaining with a time-course very similar to that evoked by ouabain. This is illustrated in Fig. 4B which shows that FM1–43 destaining obtained after 60 min of treatment with ouabain or CCCP were similar on average (20.88% for ouabain and 24.40% for CCCP, $p = 0.489$). We also tested the effect of oligomycin (8 μg/ml),

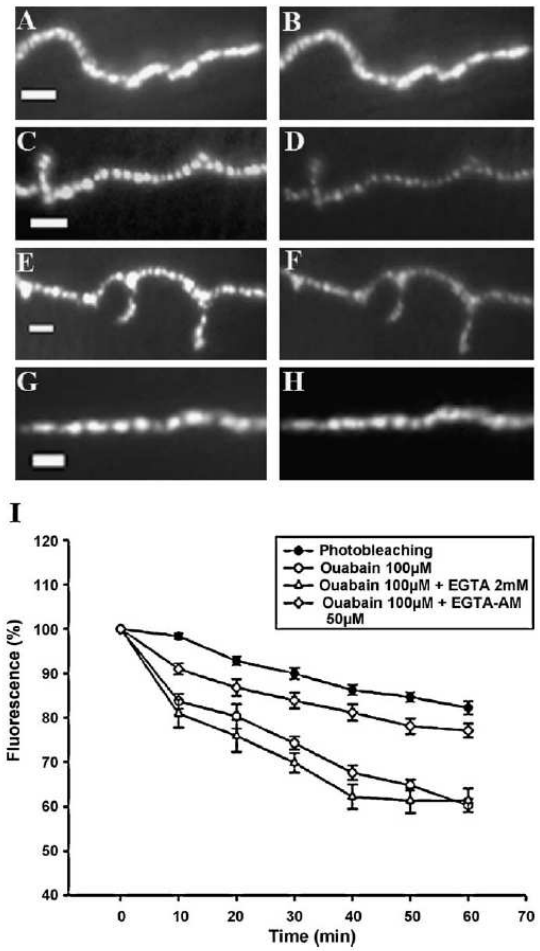

Fig. 3. Vesicular release induced by ouabain is independent on extracellular Ca^{2+} ions but seems to recruit intracellular Ca^{2+} stores. (A) A representative image of a motor nerve terminal stained with FM1–43. (B) Photobleaching observed at the end of a control experiment. (C) Motor terminal stained with FM1–43 before addition of ouabain (100 μM). (D) Destaining induced by ouabain after 60 min. (E) Terminal stained with FM1–43 and incubated for 60 min in modified Ringer in which Ca^{2+} ions were replaced by Mg^{2+} and with EGTA (2 mM). (F) After incubation with Ouabain (100 μM) for 60 min, the glycoside induced destaining of fluorescent spots even in the absence of extracellular Ca^{2+} ions. (G) Motor nerve terminal stained with FM1–43 and incubated for 60 min in the modified Ringer supplemented with EGTA-AM (50 μM). (H) The same terminal seen in (G) after incubation with ouabain (100 μM) for 60 min in modified Ringer containing EGTA-AM. Just a little destaining of fluorescent spots was observed. (I) Time-course curves of the destaining evoked by ouabain in the absence or in the presence of EGTA or EGTA-AM. Intracellular Ca^{2+} sequestration inhibits vesicular release by ouabain. (Scale bars: 10 μm. Curves in (I) represent the mean of at least three independent experiments in which were considered 15 spots for analysis. Error bars: ±S.E.M.)

another metabolic uncoupler that inhibits mitochondrial ATP synthesis without inducing calcium release from this organelle (Budd and Nicholls, 1996; Calupca et al., 2001) on FM1–43 destaining. Fig. 4B shows that oligomycin did not induce statistically significant FM1–43 destaining. Taken together, these results suggest that mitochondrial calcium release might strongly contribute for ouabain-evoked exocytosis of FM1–43 stained synaptic vesicles.

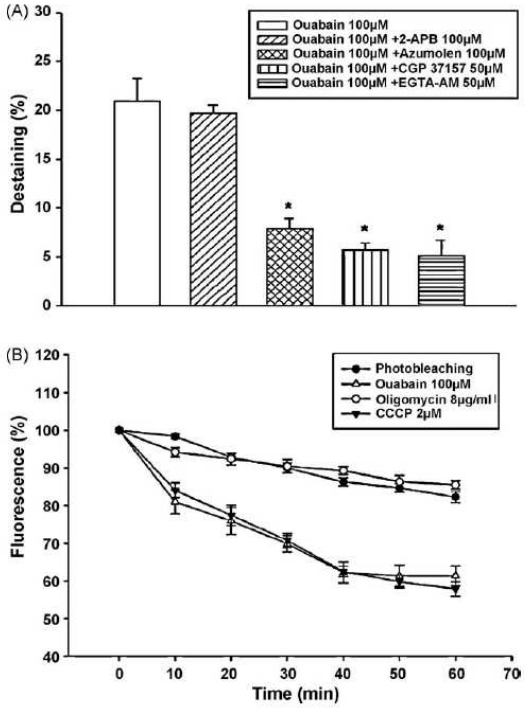

Fig. 4. Ouabain promotes vesicular release mobilizing Ca^{2+} ions stored in mitochondria and endoplasmic reticulum. (A) Graph comparing the destaining induced by ouabain in motor terminals stained with FM1–43 after 1 h of pre-incubation with 2-APB, azumolene, CGP37157 (inhibitors of IP_3R, RyR and mitochondrial Na^+/Ca^{2+} exchanger, respectively) or EGTA-AM. The photobleaching values were subtracted from the ouabain-induced FM1–43 destaining in each condition. These experiments were conducted in modified Ringer in which Ca^{2+} ions were replaced by Mg^{2+}. (B) Comparative analysis of the destaining induced by ouabain, oligomycin (an inhibitor of ATPsynthase) or CCCP (a protonophore which disrupts mitochondrial Ca^{2+} uptake mechanisms). The vesicular release evoked by ouabain has a time-course similar to that induced by CCCP. However, oligomycin could not evoke vesicular release and FM1–43 destaining. (Bar graph in (A) and curves in (B) represent the mean of at least three independent experiments for each condition in which were considered 15 spots for analysis. Error bars: ±S.E.M. $^*p < 0.05$.)

3.3. Ouabain evokes synaptic vesicles exocytosis that is not followed by compensatory endocytosis at frog neuromuscular junction

Haimann et al. (1985), by performing an ultrastructural analysis of frog motor terminals exposed to ouabain, reported a depletion of vesicular pools and an increase in the terminal area, suggesting an impairment of endocytosis in nerve terminals treated with the glycoside. To determine whether the depletion of synaptic vesicles observed with ouabain was due to impairment of vesicle recycling, we therefore tested directly this paradigm by visualizing FM1–43 internalization evoked by ouabain. Nerve-muscle preparations were incubated for 30 min in frog Ringer solution with ouabain (100 μM) and FM1–43. On this condition, we did not observe the typical punctuate staining of FM1–43 fluorescent spots (Fig. 5A). To confirm the disruption of endocytosis due to ouabain treatment, nerve-muscle preparations were pre-incubated with the glycoside for 60 min and subsequently submitted to tetanic stimulation (20 Hz, 10 min) in the presence of FM1–43. Pre-incubation with ouabain inhibited FM1–43 uptake and the terminals did not present the typical punctuate pattern of staining. Instead, they had

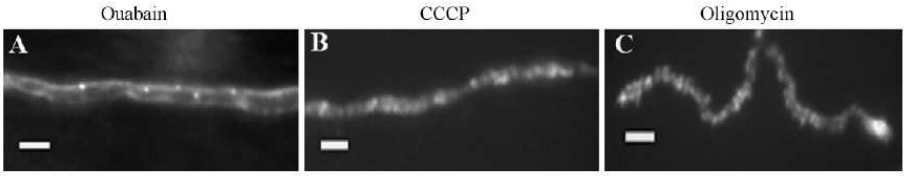

Fig. 5. Exocytosis evoked by ouabain is not followed by compensatory endocytosis. (A) A representative nerve terminal exposed to FM1–43 during 30 min of incubation with ouabain. (B) A representative nerve terminal from a nerve-muscle preparation that was exposed to FM1–43 for 60 min in the presence of CCCP (2 μM). Despite of promoting vesicular release, ouabain and CCCP do not induce FM1–43 uptake by compensatory endocytosis. (C) Another representative nerve terminal from a preparation that was pre-incubated with oligomycin (8 μg/ml) for 60 min and then exposed to FM1–43 during tetanic stimulation (20 Hz, 10 min) to evoke synaptic vesicles exocytosis. The same lack of staining with FM1–43 was observed. (Scale bars: 10 μm. Every experiment was repeated for, at least, three times.)

just a weak punctuate aspect (not shown). In addition, even when preparations pre-incubated with ouabain were later submitted to a washing time for 1 h in frog Ringer to remove the glycoside, the terminals presented no significant FM1–43 uptake when submitted to tetanic stimulation (not shown), suggesting that ouabain might block endocytosis irreversibly. Based on the observation that at the ultrastructural level, nerve terminals that were treated with CCCP are depleted of synaptic vesicles (Molgó and Pecot-Dechavassine, 1988) and show alterations that are qualitatively similar to those reported for ouabain (Haimann et al., 1985), we therefore analyzed the pattern of FM1–43 staining obtained in the presence of this protonophore. Nerve-muscle preparations that were submitted to staining with FM1–43 in the presence of CCCP (2 μM) show no uptake of the fluorescent dye (Fig. 5B). Interestingly, the same lack of staining was observed when muscles were pre-incubated with oligomycin (8 μg/ml), which also collapses mitochondrial energetic but does not cause calcium leaking from mitochondria (Fig. 5C).

4. Discussion

In the present work, we optically showed the effects of ouabain on synaptic vesicle recycling at the frog neuromuscular junction. Using the fluorescent dye FM1–43, we provided direct evidences that ouabain evokes synaptic vesicles exocytosis that is dependent on intracellular calcium stores (endoplasmic reticulum and mitochondria). According to Adam-Vizi (1992), there are three possibilities of calcium independent vesicle release: (1) exocytosis independent of extracellular calcium ions but mediated by recruitment of intracellular calcium stores. (2) Exocytosis completely independent of calcium ions, which uses the same molecular machinery employed in the calcium fired vesicle release. This hypothesis is related to the possibility of exocytosis evoked by an increase in intracellular ions other than calcium like, for example, sodium ions (Nordmann and Stuenkel, 1991; Nordmann et al., 1992; Meunier et al., 1997). (3) Vesicular release completely independent of calcium ions, which uses molecular machinery distinct from that employed in calcium fired exocytosis. Several pharmacological agents can evoke vesicular release in a calcium free environment in a way similar to that evoked by ouabain. Indeed, this was observed using sodium ionophores, veratridine, ethanol, α-latrotoxin, hypoxic conditions and unsaturated fat acids. All these conditions share common aspects like: (a) slower kinetic than that observed with calcium fired exocytosis and (b) a smaller dependence from membrane potential (reviewed by Adam-Vizi, 1992).

Even though there were evidences for motor nerve terminals that cardiotonic glycosides such as ouabain induce rapid spontaneous acetylcholine release by mobilizing intracellular calcium, the intracellular calcium source involved in this process was still unknown (Elmqvist and Feldman, 1965a,b; Baker and Crawford, 1975). In this work, to identify the calcium sources recruited by ouabain, we used azumolene and 2-APB, inhibitors of RyR and IP3R, respectively. Azumolene inhibited ouabain induced exocytosis, but 2-APB did not interfere with ouabain induced FM1–43 destaining. Experiments with TMB-8, another RyR inhibitor also provided similar results to that obtained with azumolene (data not shown), suggesting that ouabain might mobilize calcium ions stored in endoplasmic reticulum via RyR. Mitochondria also modulate homeostasis of the cytosolic calcium concentration. In neurons and chromaffin cells, mitochondria can act as rapid and reversible calcium buffer (Werth and Thayer, 1994; Herrington et al., 1996; Babcock et al., 1997). Montero et al. (2000) found a tight functional coupling of voltage dependent calcium channels on the plasma membrane, RyR on the endoplasmic reticulum and mitochondria. They reported that protonophores, which abolish mitochondrial calcium uptake, can increase secretion of catecholamine by controlling calcium levels available for exocytosis. It was mentioned previously that ouabain inhibits Na^+/K^+ATPase and creates a condition favorable to intracellular Na^+ accumulation. High intracellular levels of sodium ions could promote calcium extrusion from mitochondria via its Na^+/Ca^{2+} exchanger. To check the possibility that at the neuromuscular junction, ouabain might recruit mitochondrial calcium for vesicle release, we used CGP37157. Fig. 4A shows that CGP37157 strongly inhibited ouabain induced FM1–43 destaining and consequently vesicle release. Moreover, in the absence of sodium ions, ouabain could not evoke exocytosis significantly (Fig. 2J). Narita et al. (1998) reported that the influx of calcium ions through the presynaptic terminal can recruit internal calcium stores via RyR. This mechanism of Ca^{2+} induced Ca^{2+} release (CICR) is coupled to voltage-dependent calcium channels and amplifies the impulse-induced rise in $[Ca^{2+}]_i$, enhancing neurotransmitter exocytosis. Therefore CICR is a type of short-term plasticity (Narita et al., 2000). In our investigation, we observed that calcium stored in mitochondria and endoplasmic reticulum is involved in the ouabain-evoked exocytosis which occurs even in the absence of extracellular calcium. We speculate that an intracellular mechanism similar to CICR involving different organelles could operate during ouabain treatment. Calcium ions which leak from mitochondria via Na^+/Ca^{2+} exchanger due to intracellular accumulation of sodium ions after ouabain treatment might activate RyR on endoplasmic reticulum leading to an increase in $[Ca^{2+}]_i$ sufficient to fire spontaneous vesicle release and FM1–43 destaining.

We dynamically demonstrated that ouabain evokes synaptic vesicles exocytosis that is not followed by compensatory endocytosis. This result is in agreement with Haimann et al. (1985) who reported absence of HRP internalization at neuromuscular junction submitted to treatment with ouabain. They also describe the appearance of membrane infoldings at the presynaptic terminal. Molgó and Pecot-Dechavassine (1988) reported that CCCP, a protonophore and a respiratory chain uncoupler which also leads to calcium leaking from mitochondria, increases

MEPPs frequency and promotes depletion of synaptic vesicle clusters at neuromuscular junctions independently of extracellular calcium ions. Moreover this protonophore caused an expressive mitochondrial swelling and disruption of mitochondrial crests. These alterations in mitochondrial structure are very similar to that noticed by Haimann et al. (1985) after treatment of frog neuromuscular junctions with ouabain. Our data suggest a similarity between the effects of ouabain and CCCP on the synaptic vesicle cycle. FM1–43 destaining induced by CCCP had a kinetic equivalent to that plotted for ouabain (Fig. 4B). Another evidence that ouabain causes a collapse of mitochondrial function is provided by Whittam and Blond (1964) who reported a reduction in oxygen consumption at brain cortical slices that were previously incubated with ouabain. In addition, Wang et al. (2004), working with a drosophila temperature sensitive mutant in phosphoglycerate kinase, an enzyme required for ATP generation, reported that endocytotic pathways may be more sensitive to altered ATP levels than those used for exocytosis. Considering all these data, ouabain, as was observed with CCCP, seems to cause an energetic collapse which is associated to calcium leaking from mitochondria that might promote vesicular release and selectively endocytosis block. Further experiments should be performed to test directly the effect of ouabain on ATP consumption at motor nerve terminals.

Although ouabain acts inhibiting a membrane protein (Na^+/K^+ATPase), this glycoside is a steroid derivate and we could not discard the existence of intracellular targets for ouabain. It was reported the association between ouabain and a protein of 31,5KD on T tubules of cat cardiomiocytes named NORP (*new31,5KD ouabain receptor protein*). This interaction would be related with the inotropic effect of the glycoside (Fujino and Fujino, 1995). Moreover, a better understanding of the mechanism of action of ouabain has gained more importance with the discovery of endogenous compounds with similar structure to ouabain in mammal tissues (Hamlyn et al., 1991; Schneider et al., 1998; Boulanger et al., 1993) raising the possibility of this compounds to be involved in physiological processes.

In summary, this work identifies the endoplasmic reticulum (RyR) and mitochondrial calcium stores as possible targets for ouabain effect on synaptic vesicles exocytosis at the neuromuscular junction. In addition, we showed that ouabain evokes exocytosis that is not followed by compensatory endocytosis. We propose that ouabain can be used as a pharmacological tool to uncouple synaptic vesicles exocytosis from endocytosis and can be applied in studies that aim to investigate these two processes independently.

Acknowledgment

This work was supported by grants from CAPES, FAPEMIG and CNPq.

References

Adam-Vizi, V., Ligeti, E., 1984. Release of acetylcholine from rat brain synaptosomes by various agents in the absence of external calcium ions. J. Physiol. 353, 505–521.

Adam-Vizi, V., Deri, Z., Vizi, E.S., Sershen, H., Lajtha, A., 1991. Ca2+o-independent veratridine-evoked acetylcholine release from striatal slices is not inhibited by vesamicol (AH5183): mobilization of distinct transmitter pools. J. Neurochem. 56, 52–58.

Adam-Vizi, V., 1992. External $Ca^{(2+)}$-independent release of neurotransmitters. J. Neurochem. 58, 395–405.

Alnaes, E., Rahamimoff, R., 1975. On the role of mitochondria in transmitter release from motor nerve terminals. J. Physiol. 248, 285–306.

Babcock, M., de Silva, D., Oaks, R., Davis-Kaplan, S., Jiralerspong, S., Montermini, L., Pandolfo, M., Kaplan, J., 1997. Regulation of mitochondrial iron accumulation by Yfh1p, a putative homolog of frataxin. Science 276, 1709–1712.

Baker, P.F., Crawford, A.C., 1975. A note of the mechanism by which inhibitors of the sodium pump accelerate spontaneous release of transmitter from motor nerve terminals. J. Physiol. 247, 209–226.

Baker, P.F., Schlaepfer, W., 1978. Uptake and binding of calcium by axoplasm isolated from giant axons of Loligo and Myxicola. J. Physiol. 276, 103–125.

Betz, W.J., Bewick, G.S., 1992a. Optical analysis of synaptic vesicle recycling at the frog neuromuscular junction. Science 255, 200–203.

Betz, W.J., Mao, F., Bewick, G.S., 1992b. Activity dependent fluorescent staining and destaining of living vertebrate motor nerve terminals. J. Neurosci. 12, 363–375.

Birks, R.I., 1963. The role of sodium ions in the metabolism of acetylcholine. Can. J. Biochem. Physiol. 41, 2573–2597.

Boulanger, B.R., Lilly, M.P., Hamlyn, J.M., Laredo, J., Shurtleff, D., Gann, D.S., 1993. Ouabain is secreted by the adrenal gland in awake dogs. Am. J. Physiol. 264, 413–419.

Brumback, A.C., Lieber, J.L., Angleson, J.K., Betz, W.J., 2004. Using FM1–43 to study neuropeptide granule dynamics and exocytosis. Methods 33, 287–294.

Budd, S.L., Nicholls, D.G., 1996. A reevaluation of the role of mitochondria in neuronal Ca^{2+} homeostasis. J. Neurochem. 66, 403–411.

Calupca, M.A., Prior, C., Merriam, L.A., Hendricks, G.M., Parsons, R.L., 2001. Presynaptic function is altered in snake K+-depolarized motor nerve terminals containing compromised mitochondria. J. Physiol. 532, 217–227.

Casali, T.A., Gomez, R.S., Moraes-Santos, T., Gomez, M.V., 1995. Differential effects of calcium channel antagonists on tityustoxin and ouabain-induced release of [3H]acetylcholine from brain cortical slices. Neuropharmacology 34, 599–603.

David, G., Barrett, J.N., Barrett, E.F., 1998. Evidence that mitochondria buffer physiological Ca^{2+} loads in lizard motor nerve terminals. J. Physiol. 15, 59–65.

David, G., 1999. Mitochondrial clearance of cytosolic $Ca^{(2+)}$ in stimulated lizard motor nerve terminals proceeds without progressive elevation of mitochondrial matrix [$Ca^{(2+)}$]. J. Neurosci. 19, 7495–7506.

Deri, Z., Adam-Vizi, V., 1993. Detection of intracellular free Na^+ concentration of synaptosomes by a fluorescent indicator, $Na^{(+)}$-binding benzofuran isophthalate: the effect of veratridine, ouabain, and alpha-latrotoxin. J. Neurochem. 61, 818–825.

Elmqvist, D., Feldman, D.S., 1965a. Calcium dependence of spontaneous acetylcholine release at mammalian motor nerve terminals. J. Physiol. 181, 487–497.

Elmqvist, D., Feldman, D.S., 1965b. Effects of sodium pump inhibitors on spontaneous acetylcholine release at the neuromuscular junction. J. Physiol. 181, 498–505.

Fujino, M., Fujino, S., 1995. An immunohistochemical study of the significance of a new 31,5-KD ouabain receptor protein isolated from cat cardiac muscle. Jpn. J. Pharmacol. 67, 125–135.

Gomez, M.V., Diniz, C.R., Barbosa, T.S., 1975. A comparison of the effects of scorpion venom tityustoxin and ouabain on the release of acetylcholine from incubated slices of rat brain. J. Neurochem. 24, 331–336.

Gomez, R.S., Gomez, M.V., Prado, M.A., 1996. Inhibition of Na+,K+-ATPase by ouabain opens calcium channels coupled to acetylcholine release in guinea pig myenteric plexus. J. Neurochem. 66, 1440–1447.

Haimann, C., Torri-Tarelli, F., Fesce, R., Ceccarelli, B., 1985. Measurement of quantal secretion induced by ouabain and its correlation with depletion of synaptic vesicles. J. Cell. Biol. 101, 1953–1965.

Hamlyn, J.M., Blaustein, M.P., Bova, S., Du Charme, D.W., Harris, D.W., Mandel, F., Mathews, W.R., Ludens, J.H., 1991. Identification and characterization of a ouabain-like compound from human plasma. Proc. Natl. Acad. Sci. U.S.A. 88, 6259–6263.

Henkel, A.W., Lübke, J., Betz, W.J., 1996. FM1- 43 dye ultrastructural localization in and release from frog motor nerve terminals. Proc. Natl. Acad. Sci. U.S.A. 93, 1918–1923.

Herrington, J., Park, Y.B., Babcock, D.F., Hille, B., 1996. Dominant role of mitochondria in clearance of large Ca^{2+} loads from rat adrenal chromaffin cells. Neuron 16, 219–228.

Lomeo, R.S., Gomez, R.S., Prado, M.A., Romano-Silva, M.A., Massensini, A.R., Gomez, M.V., 2003. Exocytotic release of [3H]-acetylcholine by ouabain involves intracellular Ca^{2+} stores in rat brain cortical slices. Cell. Mol. Neurobiol. 23, 917–927.

Maruyama, T., Kanaji, T., Nakade, S., Kanno, T., Mikoshiba, K., 1997. 2APB, 2-aminoethoxydiphenyl borate, a membrane-penetrable modulator of Ins(1,4,5)P3-induced Ca^{2+} release. J. Biochem. 122, 498–505.

Meunier, F.A., Colasante, C., Molgo, J., 1997. Sodium-dependent increase in quantal secretion induced by brevetoxin-3 in Ca^{2+}-free medium is associated with depletion of synaptic vesicles and swelling of motor nerve terminals in situ. Neuroscience 78, 883–893.

Meyer, E.M., Cooper, J.R., 1981. Correlations between Na^+-K^+ ATPase activity and acetylcholine release in rat cortical synaptosomes. J. Neurochem. 36, 467–475.

Molgó, J., Pecot-Dechavassine, M., 1988. Effects of carbonyl cyanide mchlorophenylhydrazone on quantal transmitter release and ultrastructure of frog motor nerve terminals. Neuroscience 24, 695–708.

Montero, M., Alonso, M.T., Carnicero, E., Cuchillo-Ibáñez, I., Albillos, A., García, A.G., García-Sancho, J., Alvarez, J., 2000. Chromaffin-cell stimulation triggers fast millimolar mitochondrial Ca^{2+} transients that modulate secretion. Nat. Cell. Biol. 2, 57–61.

Mulkey, R.M., Zucker, R.S., 1992. Posttetanic potentiation at the crayfish neuromuscular junction is dependent on both intracellular calcium and sodium ion accumulation. J. Neurosci. 12, 4327–4336.

Narita, K., Akita, T., Osanai, M., Shirasaki, T., Kijima, H., Kuba, K., 1998. A Ca^{2+}-induced Ca^{2+} release mechanism involved in asynchronous exocytosis at frog motor nerve terminals. J. Gen. Physiol. 112, 593–609.

Narita, K., Akita, T., Hachisuka, J., Huang, S., Ochi, K., Kuba, K., 2000. Functional coupling of $Ca^{(2+)}$ channels to ryanodine receptors at presynaptic terminals. Amplification of exocytosis and plasticity. J. Gen. Physiol. 115, 519–532.

Nordmann, J.J., Stuenkel, E.L., 1991. $Ca^{(2+)}$-independent regulation of neurosecretion by intracellular Na^+. FEBS Lett. 292, 37–41.

Nordmann, J.J., Lindau, M., Stuenkel, E.L., 1992. Sodium, calcium and exocytosis: confessions of calcified scientists. J. Physiol. Paris. 86, 15–21.

Paton, W.D., Vizi, E.S., Zar, M.A., 1971. The mechanism of acetylcholine release from parasympathetic nerves. J. Physiol. 215 (3), 819–848.

Pivovarov, A.S., Drozdova, E.I., 2003. Regulation of post-tetanic increases in the cholinosensitivity of neurons in the common snail by the Na,K pump: the role of Na/Ca exchange and calcium mobilization. Neurosci. Behav. Physiol. 33, 929–932.

Prado, M.A., Gomez, M.V., Collier, B., 1993. Mobilization of a vesamicol-insensitive pool of acetylcholine from a sympathetic ganglion by ouabain. J. Neurochem. 61, 45–56.

Rahamimoff, R., Erulkar, S.D., Lev-Tov, A., Meiri, H., 1978. Intracellular and extracellular calcium ions in transmitter release at the neuromuscular synapse. Ann. N. Y. Acad. Sci. 307, 583–598.

Ribchester, R.R., Mao, F., Betz, W.J., 1994. Optical measurements of activity-dependent membrane recycling in motor nerve terminals of mammalian skeletal muscle. Proc. R. Soc. Lond. B: Biol. Sci. 255, 61–66.

Richards, D.A., Guatimosim, C., Betz, W.J., 2000. Two endocytic recycling routes selectively fill two vesicle pools in frog motor nerve terminals. Neuron 27, 551–559.

Schneider, R., Wray, V., Nimtz, M., Lehmann, W.D., Kirch, U., Antolovic, R., Schoner, W., 1998. Bovine adrenals contain, in addition to ouabain, a second inhibitor of the sodium pump. J. Biol. Chem. 273, 784–792.

Südhof, T.C., 2004. The synaptic vesicle cycle. Annu. Rev. Neurosci. 27, 509–547.

Tian, Q., Katz, A.M., Kim, D.H., 1991. Effects of azumolene on doxorubicin-induced Ca^{2+} release from skeletal and cardiac muscle sarcoplasmic reticulum. Biochim. Biophys. Acta 1094, 27–34.

Vizi, E.S., 1972. Stimulation, by inhibition of $(Na^+–K^+–Mg^{2+})$-activated ATP-ase, of acetylcholine release in cortical slices from rat brain. J. Physiol. 226, 95–117.

Vizi, E.S., Vyskocil, F., 1979. Changes in total and quantal release of acetylcholine in the mouse diaphragm during activation and inhibition of membrane ATPase. J. Physiol. 286, 1–14.

Vyas, S., Marchbanks, R.M., 1981. The effect of ouabain on the release of [14C]acetylcholine and other substances from synaptosomes. J. Neurochem. 37, 1467–1474.

Wang, P., Saraswati, S., Guan, Z., Watkins, C.J., Wurtman, R.J., Littleton, J.T., 2004. A Drosophila temperature-sensitive seizure mutant in phosphoglycerate kinase disrupts ATP generation and alters synaptic function. J. Neurosci. 24, 4518–4529.

Werth, J.L., Thayer, S.A., 1994. Mitochondria buffer physiological calcium loads in cultured rat dorsal root ganglion neurons. J. Neurosci. 14, 348–356.

Whittam, R., Blond, D.M., 1964. Respiratory control by an adenosine triphosphatase involved in active transport in brain cortex. Biochem. J. 92, 147–158.

2.4 – Artigo número 4

Membrane cholesterol regulates synaptic vesicle exo/endocytosis at the frog neuromuscular junction

AMARAL, E.; LIMA, R.; RODRIGUES, H. A.; FONSECA, M.C.; KUSHMERICK, C.; NAVES, L.; GOMEZ, M. V.; PRADO, M. A. M.; GUATIMOSIM, C.

(Artigo em preparação para submissão)

Membrane cholesterol regulates synaptic vesicle exo/endocytosis at the frog neuromuscular junction

AMARAL, E[1**].; LIMA, R[2].; RODRIGUES, H. A[1].; FONSECA, M.C[1].; KUSHMERICK[2], C.; NAVES, L[2].; GOMEZ, M. V[3].; PRADO, M. A. M[4].; GUATIMOSIM, C[1*].

Departments of Morphology[1], Physiology and Biophysics[2]- Federal University of Minas Gerais, Belo Horizonte, Brasil ; Núcleo Santa Casa de Pós-Graduação[3], Belo Horizonte, Brasil; [4] Molecular Brain Research Group, Robarts Research Institute and Department of Physiology & Pharmacology and Anatomy & Cell Biology, University of Western Ontario, London, ON

***Corresponding author**
Cristina Guatimosim
Associated Professor
Departamento de Morfologia, ICB
Federal University of Minas Gerais
Av. Antônio Carlos, 6627
Belo Horizonte, MG
31270-901
Email: cguati@icb.ufmg.br

**** Present address: Instituto de Ciências e Tecnologia, Universidade Federal dos Vales do Jequitinhonha e Mucuri, Diamantina, Brasil.**

Amaral et al., em preparação.

Abstract

Cholesterol is an abundant component of animal cell membranes and it regulates membrane fluidity. In association with sphingolipids and glycolipids, cholesterol also participates on the assembly of specific domains resistant to nonionic detergents at 4ºC. Initially, these microdomains were named lipid rafts but more recently they have been renamed as membrane rafts since they are associated to many proteins including those involved on synaptic vesicle cycle like SNAREs and some calcium channels isoforms. In this work, we investigated the role of cholesterol on synaptic vesicles recycling at the frog neuromuscular junctions. Cholesterol removal by methyl-ß-cyclodextrin (MßCD) induced fusion of synaptic vesicle pools labeled with the styryl dye FM1-43 and increased MEPPs frequency and amplitude. Cholesterol removal by MßCD did not have any effect on acetylcholinesterase and did not induce any morphological alteration on nicotinic acetylcoline receptors clusters, suggesting a presynaptic rather than a postsynaptic action. MßCD inhibited K^+-evoked exocytosis and FM1-43 uptake and ultrastructural analyses confirmed this observation and shows that cholesterol removal disrupts evoked synaptic vesicle recycling but stimulates spontaneous recycling. In summary, our results provide additional evidences that membrane cholesterol acts on the modulation of synaptic vesicle cycle and seems to be essential for the balance between evoked and spontaneous release. Moreover, our results may reinforce the possibility of coexistence of a synaptic vesicle pool mobilized by evoked exocytosis and another pool of vesicles that fuses spontaneously.

Introduction

According to the mosaic fluid model proposed by Singer and Nicolson (1972), phospholipids and proteins were globally dispersed through cell membrane. However, in the last two decades many researchers have reported the presence of membrane microdomains with elevated proportions of cholesterol, sphingolipids and glycolipids (for a review see Lingwood *et al.*, 2009). These microdomains, named lipid rafts, are resistant to Triton X-100 at 4ºC and they are associated to many proteins like GPI-anchored proteins and tyrosine kinases of the Src-family (Simons and van Meer, 1988; Brown and Rose, 1992; Simons and Ikonen, 1997). More recently, a new definition for membrane domains to be classified as rafts was proposed and the term 'lipid raft' was replaced by 'membrane raft', as it is now widely acknowledged that rafts do not form solely by lipid-driven interactions but involve also proteins (Pike, 2006). Therefore, the ultimate definition of membrane raft describes it as small (10–200 nm), heterogeneous, highly dynamic, sterol- and sphingolipid-enriched domains that compartmentalize cellular processes. Small rafts can sometimes be stabilized to form larger platforms through protein–protein and protein–lipid interactions (Pike, 2006; reviewed by Rohrbough and Broadie, 2005 and Lang, 2007).

Over the years, more than 200 components have been assigned to rafts (Foster *et al.*, 2003) including those related to the control of the synaptic vesicle cycle, which is a key step for neurotransmitter release into the synapse. Synaptic vesicles exocytosis is regulated by a set of proteins, among them we highlight the SNARE complex which mediates the fusion of synaptic vesicles with the presynaptic membrane at active zones (reviewed by Murthy and De Camilli, 2003; Sudhoff, 2004). Noteworthy, cholesterol has a strong impact on synaptic transmission. Zamir and Charlton (2006) reported that cholesterol acute depletion with methyl-ß-cyclodextrin (MßCD) blocked action

potential conductance in crayfish neuromuscular junction and increased MEPPs frequency. In hippocampal neurons, Wasser *et al.* (2007) observed that removal of synaptic vesicle cholesterol with MßCD resulted in an increase in the frequency of MEPSC events and a decrease in evoked vesicle fusion. These findings suggest that the presence of cholesterol inhibits spontaneous fusion and favors regulated evoked synaptic vesicles fusion.

Considering that at present there is little data showing how synaptic plasma membrane rafts regulate functional aspects of neurotransmission, in this work we proposed to dynamically investigate the role of acute cholesterol depletion on exo/endocytois at the frog neuromuscular junction. Our data provides additional evidences that cholesterol enriched microdomains have crucial roles on synaptic vesicle cycle. Using the fluorescent probe FM1-43 we could dynamically confirm that cholesterol sequestration facilitates spontaneous synaptic vesicles release but inhibits evoked exocytosis. We also show at the ultrastructural level that cholesterol removal impairs recycling of synaptic vesicles that are mobililized during evoked stimulation but induces recycling of those vesicles that fuses spontaneously. Finally, our electrophysiological findings indicate that membrane cholesterol interferes with the amplitude and area of miniature end plate potentials (MEPPS) which were not due to postsynaptic effects. Taken together, our work reinforces the hypothesis that cholesterol presented at membrane rafts might be responsible for restraining vesicles from fusing spontaneously. We suggest that our work contributes to a better understanding of a paradigm on synaptic transmission field which is how spontaneous and evoked neurotransmission are regulated.

Material and Methods

Drugs and Chemicals

FM1-43, Vybrant Lipid Raft Kit and α-bungarotoxin-Alexa 594 were purchased from Invitrogen™; methyl-ß-cyclodextrin (MßCD), hidroxi-propil-γ-cyclodextrin (HγCD), *d*-tubocurarine were purchased from Sigma-Aldrich. All other chemicals and reagents were of analytical grade.

Experimental Procedures

Staining and destaining with FM1-43

All procedures were approved by the local animal care committee (CETEA-UFMG) and followed the guidelines for the Use and Care of Animals for Research issued by the NIH. Experiments with FM1-43 were done according to protocol described by Betz *et al.* (1992) and Guatimosim *et al.* (1998). Briefly, frog cutaneous pectoris nerve-muscle preparations were dissected from *Rana catesbeiana* (~60g) and mounted in a sylgard-lined chamber containing frog Ringer solution (115mM NaCl, 2.5mM KCl, 1.8mM $CaCl_2$, 5mM HEPES, pH7.2). FM1-43 was used at 4μM to label the recycling pool of synaptic vesicles (Betz *et al.*, 1992). FM1-43 stains the extracellular membrane and upon stimulation, the dye is internalized during cycles of exo/endocytosis. After washing out excess dye, endocytosed vesicles can be destained by a second round of stimulation (Betz and Bewick, 1992).

Frog muscle-nerve preparations were stained with FM1-43 by stimulation with high K^+ solution (KCl 60mM) for 10min. The muscles were incubated with *d*-tubocurarine 16μM to prevent contractions during the stimulus with KCl or image acquisition. After K^+-stimulation, preparations were maintained in rest for 15min to guarantee maximal FM1-43 uptake. The excess of FM1-43 adhered to the muscle cells

membrane was removed during a washing period in frog Ringer without the probe for at least one hour. After staining, frog neuromuscular junctions examined in a fluorescence microscope presented the typical pattern of fluorescent spots over the nerve terminal length. Each spot corresponding to a cluster of synaptic vesicles labeled with FM1-43 (Betz *et al.*, 1992; Henkel *et al.*, 1996; Richards *et al*., 2001).

To investigate the effects of cholesterol sequestration over the synaptic vesicle clusters, preparations labeled with FM1-43 were treated with concentrations of methyl-ß-cyclodextrin (MßCD) ranging from 1 to 10mM for 60min.

The role of membrane cholesterol on endocytosis was investigated through the analyses of FM uptake during stimulation with KCl (60mM) after preincubation with MßCD (10mM) for 30min.

The effects of MßCD over exo/endocytosis were compared to the effects of hidroxi-propil-γ-cyclodextrin (HγCD – 10mM), a cyclodextrin which has low affinity for cholesterol. Experimental schemes using HγCD were identical to that described for MßCD.

Staining of lipid rafts in frog nerve terminals

To stain lipid rafts in frog motor nerve terminals, it was used the fluorescent subunit B from cholera toxin (CTxB-Alexa 488) available in the Vybrant Lipid Raft Kit (Invitrogen™). The experimental protocol was elaborated according to the guidelines of the product. In summary, preparations of frog neuromuscular junctions were incubated for 15min in Ringer containing CTxB-Alexa 488 (1μg/ml). This toxin has affinity for the ganglyoside GM1 inserted in lipid rafts. After staining with fluorescent CTxB, the preparations were incubated for more 15min with the antibody anti-CTxB and then fixed with paraformaldehyde 4% at 4ºC during 40min.

To investigate the consequences of cholesterol sequestration on the lipid rafts structure at frog neuromuscular junction, preparations were preincubated with MßCD (10mM) or HγCD (10mM) for 30min before labeling with CTxB-Alexa 488. The staining was compared to that obtained in control condition.

Staining of nicotinic receptors at frog neuromuscular junctions

In control experiments, nicotinic receptors for acetylcholine at frog neuromuscular junctions were stained with α-bungarotoxin-Alexa 594 during 20min of incubation of cutaneous pectoris muscle in Ringer containing 4µg/ml of the toxin. After labeling, preparations were fixed with paraformaldehyde 4% at 4ºC. To investigate the effects of cholesterol sequestration on morphological aspect of nAChRs clusters, frog neuromuscular junctions were preincubated with MßCD (10mM) for 30min before labeling with α-bungarotoxin.

Fluorescence microscopy and image analyses

Images of frog neuromuscular junctions stained with FM1-43 were acquired in a fluorescence microscope (Leica DM2000) coupled to a CCD camera (12 bits, Micromax) and visualized on a computer screen. The microscope was equipped with water-immersion objectives (63x, 0.95 NA and 40x, 0.75 NA). Excitation light came from a 100 W Hg lamp and passed through filters to select the fluorescein spectrum of excitation/emission. Image analysis was performed using the software Image J which permits to quantify the brightness levels emitted by regions of interest. The mean fluorescence intensity was determined for each group of spots and plotted as percentage of its mean initial fluorescence using the softwares Microsoft Excel, Sigma Plot 10.0 and GraphPad Prism 4.0.

Images of frog motor terminals labeled with CTxB-Alexa 488 and α-bungarotoxin-Alexa 594 were collected in a confocal microscope (Leica SP5) using a

63x water-immersion objectives. Argon laser (488nm) was used for excitation of terminals stained with CTxB-Alexa 488 and the emission spectrum was set from 510 to 620nm. For terminals marked with α-bungarotoxin, it was used a 594nm laser and the emission spectrum was set from 610 to 710. Images collected in the confocal microscope were analyzed using the same softwares cited for image analyses in conventional fluorescence microscopy.

For all experiments, statistical analysis was performed through the application of paired students *t*-test. P values <0.05 were considered statistically significant.

Electrophysiological recordings

The experiments were performed at room temperature (22-24°C) using the cutaneous pectoris from *Rana catesbeiana*. The muscle was pinned to a silicon pad in a 5 ml acrylic chamber with ringer solution containing (in mM): NaCl 115, KCl 2.5, $CaCl_2$ 1.8, HEPES 5, and pH 7.2 (adjusted with NaOH). Standard intracellular recording techniques were used to record MEPPs with an Axioclamp model Axoclamp-2A amplifier. Recordings were band-pass filtered (0.1 Hz - 10 KHz) and amplified 100X prior to digitization and acquisition on a computer running WinEDR (John Dempster, University of Strathclyde). Microelectrodes were fabricated from borosilicate glass and had resistances of 8-15MΩ when filled with 3M KCl. To avoid contractions during MEPPs recording we used tetrodotoxin (0.3 μM). The DC membrane potential was also recorded and used to correct amplitudes and areas to a standard resting potential of -80 mV using the method of Katz and Thesleff (1957). The drugs were added directly to the bath from a ringer stock solution to the final concentrations given in the text.

Electron Microscopy

For ultrastructural studies, preparations were fixed in ice-cold fixative solution (1.6% paraformaldehyde and 2.0% glutaraldehyde at 4°C) for 30 min. After washing

with phosphate buffer (PB; 0.1 M), each muscle was cut into four pieces, postfixed in osmium (2% osmium in 0.1 M PB) at 4°C, and dehydrated through an ascending series of ethanol solutions. After dehydration the muscles were stained *en bloc* with uranyl acetate (4% uranyl acetate in 50% ethanol) and embedded in EPON. The blocks were sectioned, and gray-gold sections (80-90 nm) were collected and viewed with a Tecnai-G2-Spirit-FEI/Quanta microscope (120 kV Philips) located at the Centro de Microscopia da UFMG.

Results

Cholesterol depletion induces FM1-43 destaining at frog neuromuscular junctions

During the last ten years, many works have pointed relations between cholesterol-enriched microdomains and proteins that regulate synaptic vesicle exo-endocytosis (Thiele *et al.*, 2000; Rodal *et al.*, 1999; Salaun *et al.*, 2005; Yoshinaka *et al.*, 2004; Lang *et al.*, 2001). Some authors have also reported that a reduction in cholesterol content on plasma and vesicular membrane causes an increase in MEPPs frequency (Zamir and Charlton, 2006; Wasser *et al.*, 2007). These data stimulated us to investigate the effects of cholesterol sequestration on synaptic vesicles recycling at the neuromuscular junction. Frog neuromuscular junctions previously labeled with FM1-43 during K^+-stimulation (KCl 60mM, 10min) destained when incubated with methyl-ß-cyclodextrin (MßCD - FIG. 1B to 1C). At concentrations of 2.5mM, 5mM and 10mM, MßCD induced a significant decrease in the fluorescent signal emitted by clusters of synaptic vesicles stained with FM1-43 when compared to the photobleaching (FIG. 1C).

To test if the FM1-43 destaining was due to cholesterol sequestration, neuromuscular preparations were stained with FM1-43 and then incubated with Hydroxi-propyl-γ-cyclodextrin (HγCD – 10mM), which has low affinity for cholesterol. Figures 2B, 2B'and 2C showed that HγCD did not promote significant FM1-43 destaining. To investigate if MßCD can actually interfere with membrane rafts, we used the fluorescent subunit B from Cholera toxin (CTxB-Alexa 488) which has affinity for the ganglyoside GM1 at membrane rafts. Preincubation of neuromuscular preparations with HγCD (10mM- 30min) did not cause any significant alteration in CTxB labeling of motor terminals (compare FIG. 2D to FIG. 2E). On the other hand, preincubation with MßCD (10mM – 30min) significantly inhibited staining with fluorescent CTxB (FIG.

2F see also Fig 2G for quantification). Taken together, these data suggest that in our system, the effects of MßCD were resultant from cholesterol sequestration.

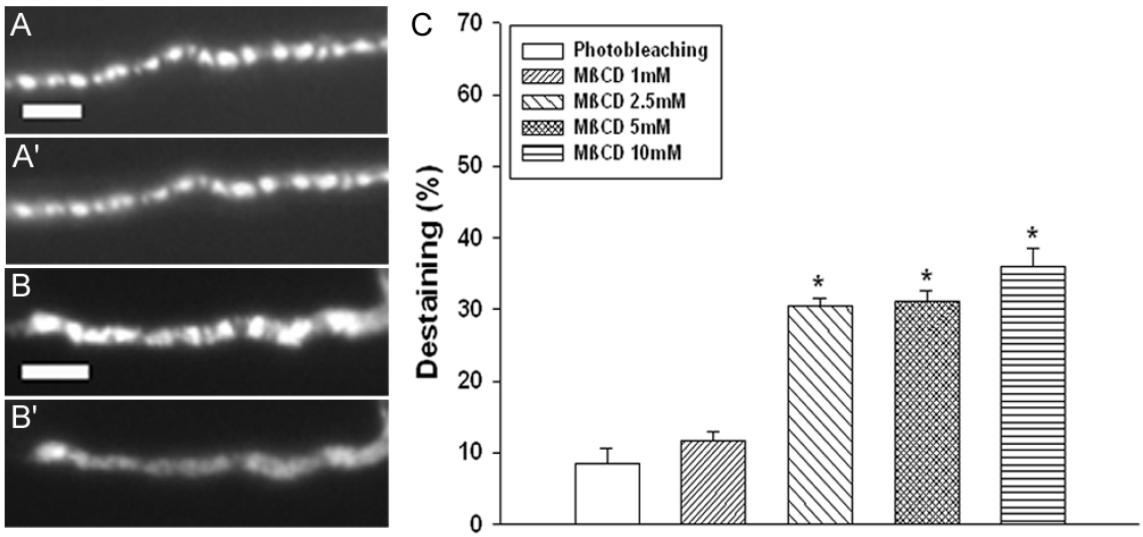

Figure 1: MβCD induced synaptic vesicle release and FM1-43 destaining. **A and A')** Frog motor terminal stained with FM1-43 at the beginning and the end of a control experiment, respectively. Each fluorescent spot represents synaptic vesicle clusters (scale bar: 10μm). The decrease in fluorescence was due to photobleaching. **B and B')** Motor Terminal stained with FM1-43 before and after 60min of incubation with MβCD (10mM), respectively (scale bar: 10μm). The destaining was much more expressive than that observed in control experiment. **C)** Percentual destaining induced by different doses of MβCD after 60min of incubation with the cyclodextrin (error bars: S.E.M; n=3; *$p<0.05$).

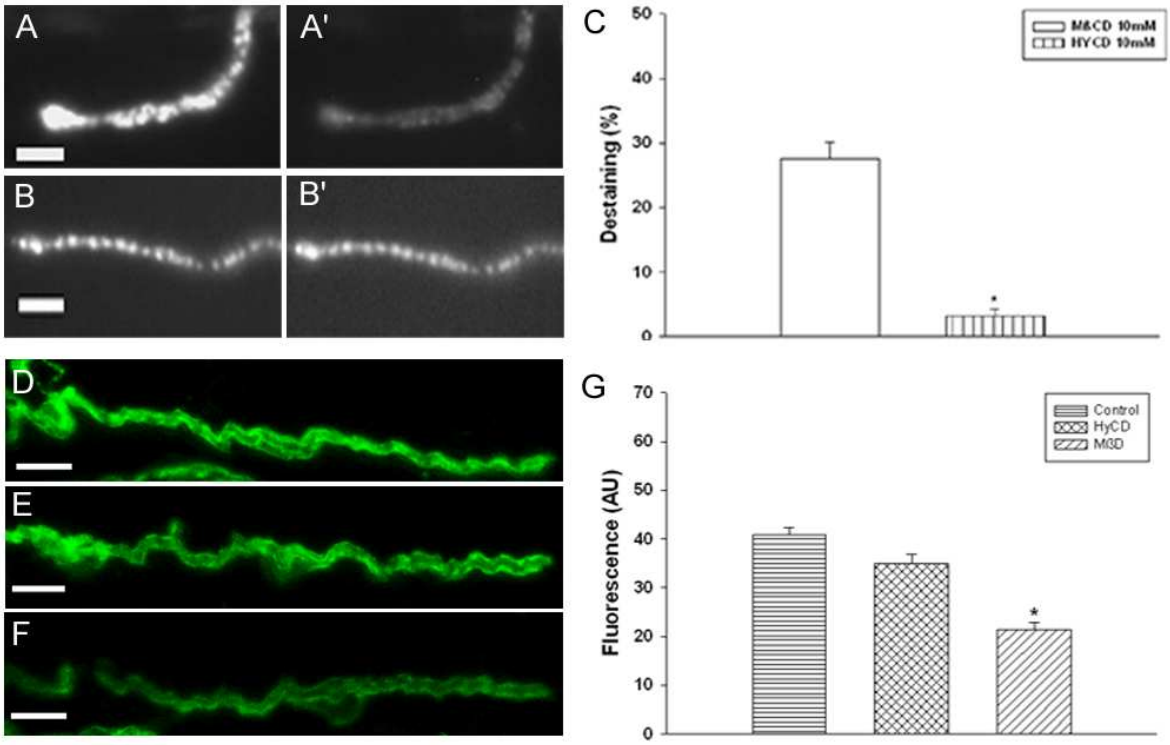

Figure 2: Effects of MβCD were resultant from cholesterol sequestration. **A and A')** Motor terminal stained with FM1-43 before and after 60min of incubation with MβCD (10mM), respectively. **B and B')** Motor terminal stained with FM1-43 before and after 60min of incubation with Hidroxi-propil-γ-ciclodextrin (HγCD – 10mM), respectively. This cyclodextrin has low affinity for cholesterol. **C)** Quantification of the destaining induced by MβCD and HγCD (*p<0.05; error bars: S.E.M; n=3). **D)** Motor terminal labeled with fluorescent B subunit of cholera toxin (CTxB-Alexa 488), a marker for membrane rafts. **E)** Motor terminal stained with CTxB-Alexa 488 after 30min of preincubation with HγCD (10mM). **F)** Motor terminal labeled with CTxB-Alexa 488 after 30min of preincubation with MβCD (10mM). **G)** Quantification of the fluorescent signal emitted by motor terminals stained with CTxB-Alexa 488 in control condition or after 30min of preincubation with MβCD or HγCD. Cholesterol sequestration inhibited labeling of membrane rafts (n=3. *p<0.05). All scale bars in this figure represent 10µm.

Cholesterol removal by MßCD modify electrophysiological parameters at the frog neuromuscular junctions

Previous works have shown that cholesterol removal from the plasma (Zamir and Charlton, 2006) and synaptic vesicle membrane (Wasser *et al*., 2007) increases spontaneous synaptic vesicle release. We therefore asked if MßCD-induced FM1-43 destaining at frog neuromuscular junctions was due to an increase in spontaneous synaptic vesicles fusion with the plasma membrane. We measured MEPPs in preparations that were treated with MßCD but we observed that high concentrations of MßCD (10mM) led to a significant drop in membrane potential and muscles twitches (table 1). These MßCD (10mM) effects made any electrophysiological analyses of vesicle release impracticable. However, low doses of MßCD (2.5mM) had no influence on membrane potential and induced a significant increase in MEPPs frequency (FIG. 3A to 3D - control = 0.97± 0.08; HγCD 10mM = 0.84±0.05; MßCD 2.5 mM 1.59±0.26; MßCD 10 mM 18.02±1.0). In addition, this increase in MEPPs frequency augmented along time (FIG. 3E - 0-5 min 1.59±0.26; 5-10 min 5.38±0.42; 10-15 min 7.15±0.56).

Interestingly, at frog neuromuscular junction we observed that MßCD treatment increased MEPPs amplitude and MEPPs area (FIG. 4A and 4A'), which was not observed at the crayfish neuromuscular junction (Zamir and Charlton, 2006) and hippocampal cultures (Wasser *et al*., 2007). Considering that these two experimental models mentioned above are glutamatergic synapses, we wondered if these MßCD effects on MEPPs amplitude and area were specifically cholinergic. To address this point, we first examined if cholesterol sequestration interfered with acetylcholine degradation at synaptic cleft. Molecules of acetylcholinesterase are anchored on the postsynaptic membrane so they could have its distribution or its functionality disrupted after cholesterol sequestration. To investigate this possibility, we analyzed cumulative

frequency curves comparing the effects of neostigmin, an acetylcholinesterase inhibitor, to the effects of MßCD over MEPPs kinetic parameters. Figures 4B and 4B' show that cholesterol sequestration by MßCD increased MEPPs amplitude and area even in the presence of neostigmin (10μM). Therefore this increase in amplitude of spontaneous events was not due to changes in the functionality of acetylcholinesterase after cholesterol sequestration.

Another possible explanation for the increase in MEPPs amplitude and area after MßCD may be related to changes on proper clustering of nicotinic acetylcholine receptors (nAChRs) at the neuromuscular junction. For example, cholesterol sequestration could disperse nicotinic receptors over the postsynaptic membrane length. However, staining of nAChRs clusters with α-bungarotoxin-Alexa 594 after preincubation with MßCD (10mM) revealed no morphological alterations in comparison to that obtained in control condition (FIG. 4C). Although treatment with MßCD presented a small tendency to increase the intensity of labeling with fluorescent bungarotoxin, this might be a consequence of a better accessibility of the toxin to the nAChRs clusters after cholesterol sequestration. We cannot rule out functional alterations on nAChRs after cholesterol sequestration and more refined electrophysiological techniques like electrotonic induction of vesicle release might help to clarify if MßCD has an influence on the functionality of nicotinic receptors at neuromuscular junctions. Nonetheless, we suggest that cholesterol removal by MßCD interferes with MEEP amplitude and area probably due to a presynaptic rather than a postsynaptic effect.

Table 1 – Effects of MßCD and HγCD over membrane potential (MP) after 5 minutes of incubation with the cyclodextrins (n=3, *p<0.05)

	Basal MP (mV)	Relative MP
MßCD 10mM	-82.18±4.1	0.56±0.05*
MßCD 2.5mM	-79.32±1.45	0.99±0.08
HγCD 10mM	-81.97±5.8	0.97±0.04

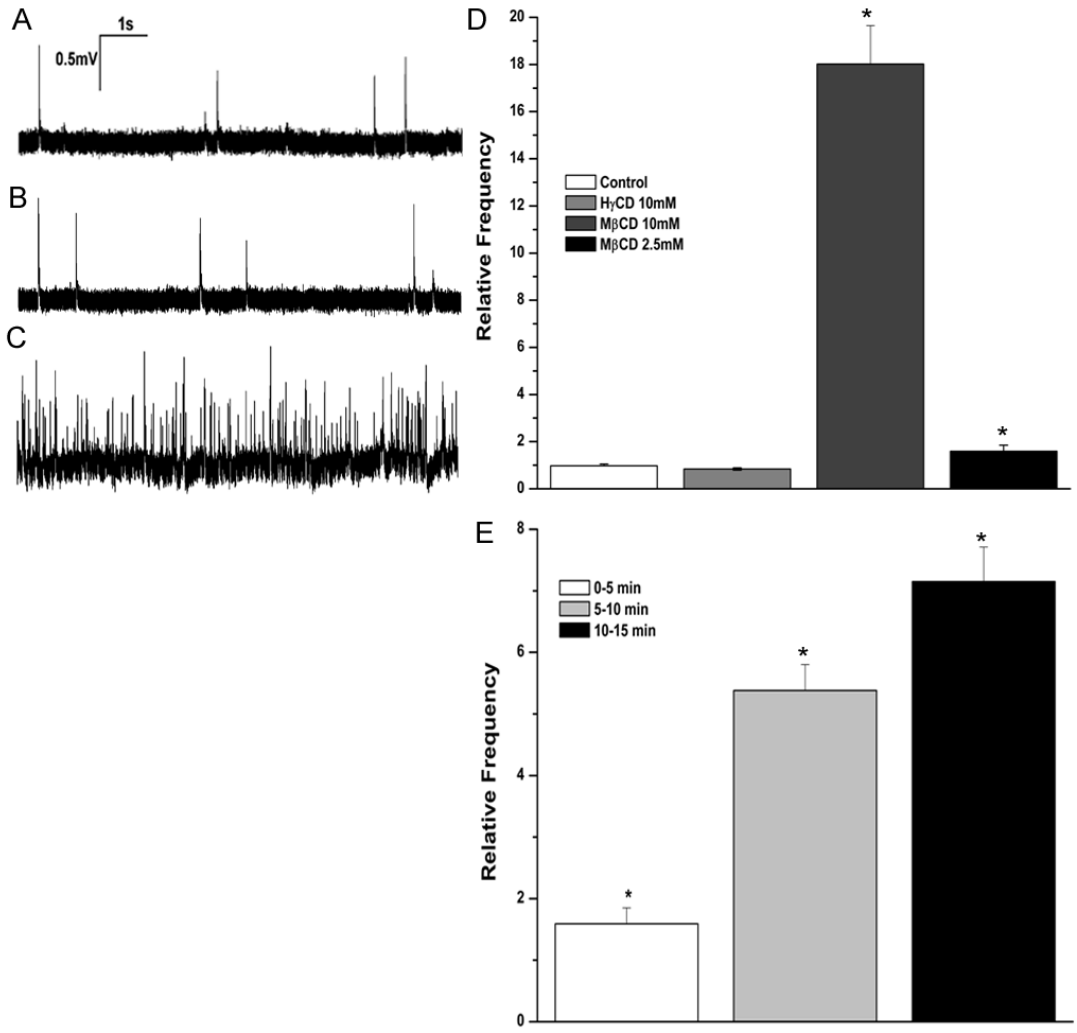

Figure 3: MβCD increased spontaneous vesicle release. **A)** MEPPs frequency recorded at a frog motor terminal in resting condition. **B)** MEPPs frequency recorded after 5min of incubation with HγCD (10mM). **C)** MEPPs frequency recorded after 5min of MβCD (10mM). **D)** Histogram representing the effects of MßCD and HγCD on spontaneous vesicle release. Data plotted correspond to 5min of incubation with the cyclodextrins (n=3; *p<0.05). **E)** Even in doses that cause no significant alteration on membrane potential (MßCD 2.5mM - see table 1), methyl cyclodextrin can significantly increase MEPPs frequency over the time (n=3; *p<0.05).

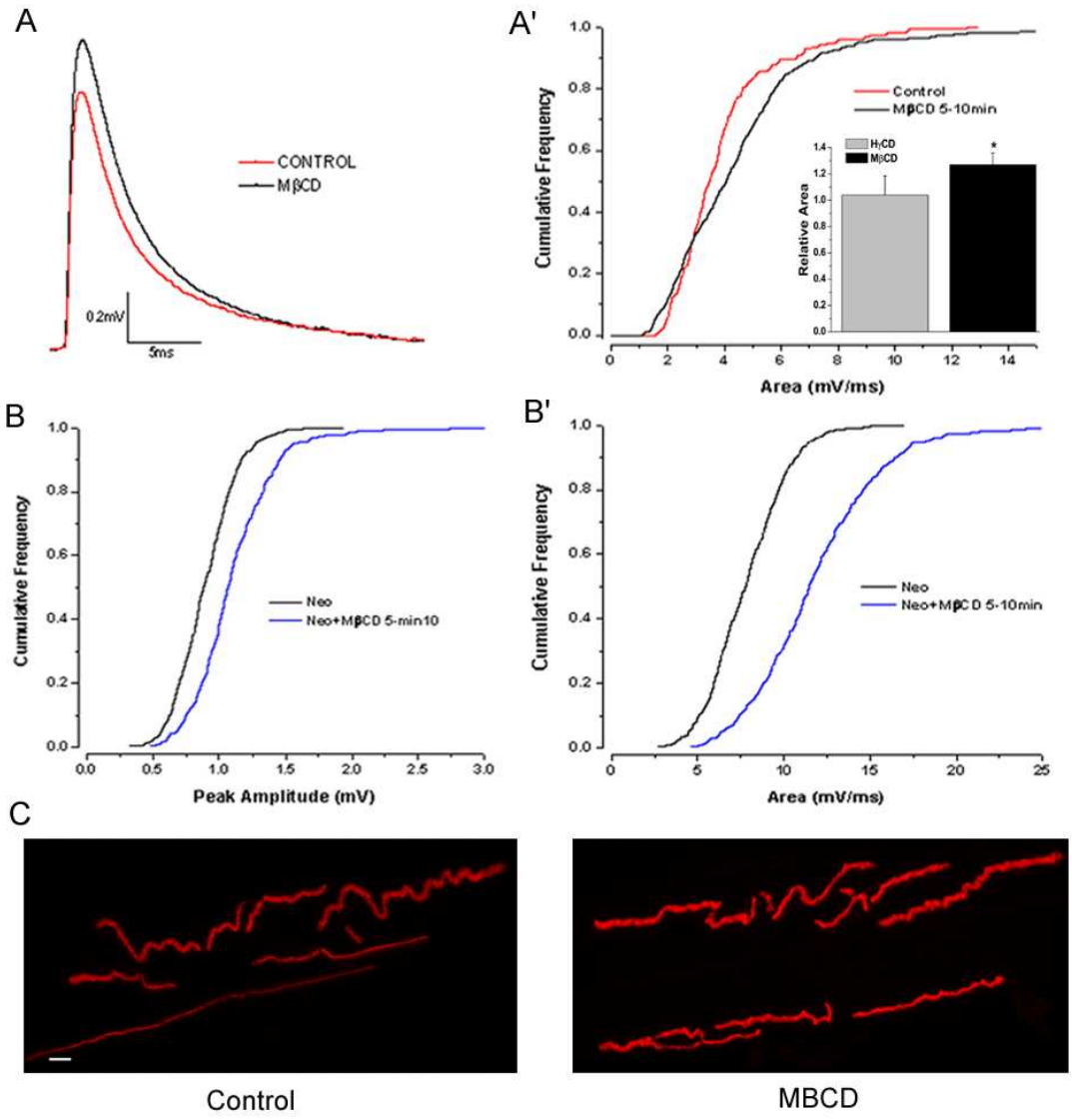

Figure 4: Cholesterol sequestration increased amplitude and area of spontaneous events A) Representative MEPPs in control conditions and after incubation with MßCD (2.5mM **A')** Cumulative frequency curves showing the effects of MßCD (2.5mM) over MEPPs area. **Inset:** MßCD (2.5mM), but not HγCD (10mM), increased relative area of MEPPs after 5min of incubation with the cyclodextrins (n=3, *p<0.05). **B and B')** Neostigmin, an acetylcholinesterase inhibitor, could not block the effects of MßCD (2.5mM) on MEPPs amplitude and area, respectively. Terminals were previously incubated with neostigmin (10µM) for 30min and then MßCD was added to the frog Ringer. Data were recorded before or 5, 10 and 15min after addition of the cyclodextrin (n=3). **C)** Nicotinic acetylcholine receptors (nAChRs) labeled with α-bungarotoxin conjugated to Alexa-594 in control condition or after 30min of preincubation with MßCD (10mM – scale bar:10µm).

Cholesterol sequestration with MßCD inhibits K^+-induced exocytosis and compensatory endocytosis

Depolarizing stimuli like tetanic pulses or high KCl concentrations evoke FM1-43 destaining and consequently synaptic vesicle fusion (Betz *et al.*, 1992; reviewed by Gaffield and Betz 2006). We therefore investigated the effects of MßCD on evoked synaptic vesicle release. Neuromuscular preparations that were previously labeled with FM1-43 were stimulated with high KCl (60mM) in the presence of MßCD (10mM) and we observed that cholesterol removal from the plasma membrane significantly inhibited K^+-evoked exocytosis (FIG 5A compare third and fourth bars). Figure 5B confirms at the ultrastructural level that MßCD inhibits exocytosis evoked by KCl (60mM). In addition, nerve terminals of control, MßCD and HγCD experimental conditions show a similar number of synaptic vesicles (FIG. 5B and 5C). Neuromuscular preparations that were exposed to KCl and bathed in cold fixative immediately after the end of stimuli presented nerve terminals with very few synaptic vesicles. By contrast, preparations that were treated with MßCD and submitted to the stimulation and fixation protocol described above presented terminals with a number of synaptic vesicle that was statistically different from that obtained by the treatment with KCl alone (FIG. 5C).

After exocytosis, synaptic vesicle pools are reorganized by compensatory endocytosis to guarantee maintenance of synaptic transmission (Ceccarelli *et al.*, 1973, Heuser and Reese, 1973; Richards *et al.*, 2001 reviewed by Royle and Lagnado, 2003). To investigate the consequences of cholesterol sequestration over synaptic vesicle endocytosis, preparations of frog neuromuscular junctions were preincubated with MßCD (10mM) or HγCD (10mM) before staining with FM1-43 under K^+- stimulation (KCl 60mM). Preincubation with MßCD inhibited FM1-43 uptake so the typical pattern

of staining with fluorescent spots could not be observed (compare FIG. 6A to 6C). On the other hand, motor terminals preincubated with HγCD presented the typical fluorescent spots with brightness equivalent to that observed in control preparations stained with FM1-43 (FIG. 6B). These results indicate that cholesterol sequestration inhibits FM1-43 uptake and compensatory endocytosis after K^+-evoked exocytosis.

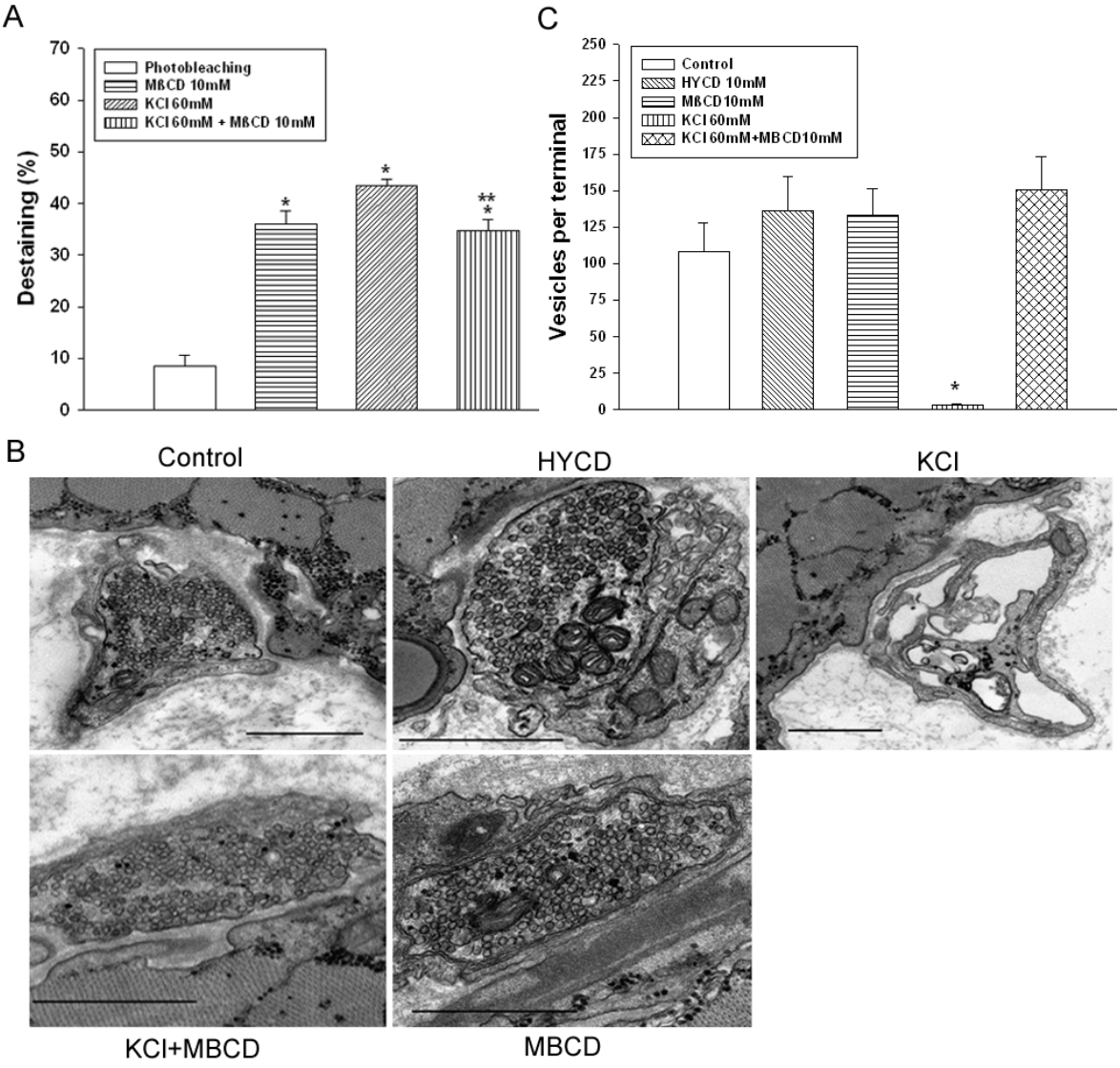

Figure 5: Cholesterol sequestration from membrane of motor terminals inhibited K^+-evoked synaptic vesicle release. A) Histogram representing FM1-43 destaining induced by MβCD, KCl and KCl+MβCD respectively (error bars: ±S.E.M.; n=3; *p<0.05; **p<0.05 in relation to KCl alone). **B)** Panel showing representative micrographs from frog motor terminals obtained in control condition or after 30min of incubation with MßCD (10mM), HγCD (10mM), KCl (60mM) and KCl (60mM)+MßCD(10mM). Scale bars:1µm. **C)** Average number of vesicles per terminal (error bars: ±S.E.M.; n=9; *p<0.05).

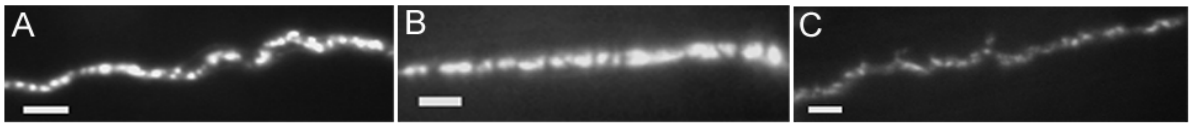

Figure 6: Cholesterol sequestration inhibits endocytosis and FM1-43 uptake. **A)** Nerve terminal labeled with FM1-43 during a high K^+ stimulus for 10min. Note the typical fluorescent spots of FM1-43 labeling. **B)** Motor terminal preincubated with HγCD (10mM – 30min), followed by a washing time of 15 minutes and subsequent staining with FM1-43 in a high K^+ medium. HγCD has low affinity for cholesterol and could not block endocytosis and FM1-43 uptake. **C)** Terminal preincubated with MβCD (10mM – 30min) followed by a washing time of 15min and subsequent staining with FM1-43 in a high K^+ medium. Even after a washing time, cholesterol removal still inhibited endocytosis of the probe. (Scale bars: 10μm for each image).

Discussion

Cholesterol and spontaneous synaptic vesicle exocytosis

In this work, we investigated the role of cholesterol upon synaptic vesicles recycling at motor nerve terminals of the frog neuromuscular junction. Using FM1-43 imaging and electrophysiology techniques, we showed that acute cholesterol depletion induces FM1-43 destaining and increases the frequency of MEPPS. Therefore, according to our data cholesterol sequestration from presynaptic membrane amplifies spontaneous vesicle release. Interestingly, although Zamir and Charlton (2006) reported no MßCD-induced effects on MEPPs amplitude and kinetic at crayfish neuromuscular junction, we could observe that cholesterol sequestration increased MEPPs amplitude and area of spontaneous events. Thus we inquired if these electrophysiological findings were specific to cholinergic synapses considering that the crayfish neuromuscular junction is glutamatergic. First we investigated if inhibition of acethylcholinesterase could interfere with the effects of cholesterol sequestration on MEPPs kinetic. However, even after incubation with neostigmin, MßCD still increased MEPPs frequency and MEPPs area (FIG. 4B and 4B'). Next we analyzed if cholesterol sequestration could alter the structure of nicotinic receptors clusters for acetylcholine on postsynaptic membrane. Some researchers have noticed that MßCD disperses nAChRs at myoblast cultures (Stetzkowski-Marden *et al.*, 2006). Thus we investigated if cholesterol sequestration would have any influence over nAChRs clusters at the mature frog neuromuscular junctions. Nonetheless, experiments with fluorescent α-bungarotoxin showed that preincubation with MßCD did not interfere with the staining of nAChRs (FIG. 4C) suggesting that the increase in MEPPs amplitude was not caused by a disruption of nAChRs clusters after cholesterol sequestration. Further investigations should be conducted to clarify how MßCD increases MEPPs amplitude and area.

Therefore, our data shows that that cholesterol removal by MßCD interferes with MEEP amplitude and area probably due to a presynaptic rather than a postsynaptic effect. Probably, cholesterol acts on more steps of synaptic cycle that go beyond the exo/endocytosis modulation. For example, Yoshinaka *et al*. (2004) identified VH^+-ATPase as the main protein component inserted in lipid rafts obtained from synaptic vesicle fraction. In addition, they observed that the ability of VH^+-ATPase to metabolize ATP and promote vesicle acidification is reduced after cholesterol sequestration. We hypothesize that membrane rafts might be important for synaptic vesicles refilling with neurotransmitter or might interfere with the trafficking of membrane proteins involved in the neurotransmitter cycle.

Cholesterol and evoked exocytosis

Our data shows that, at the frog neuromuscular junction, cholesterol sequestration inhibited KCl-evoked exocytosis. Depolarizing stimulus with high KCl is independent on activation of voltage gated sodium channels but promotes the opening of calcium channels which permits the influx of Ca^{2+} ions into presynaptic terminal. The rise in intracellular calcium levels fires synaptic vesicle release (reviewed by Murthy and De Camilli, 2003; Sudhof, 2004). Thus, to guarantee efficiency to exocytosis, calcium channels are strategically positioned near active zones and synaptic vesicle clusters (Robitaille *et al.*, 1990; reviewed by Zhai and Bellen, 2004). In addition, association between calcium channels isoforms and SNARE proteins on lipid rafts has been noticed (Taverna *et al.*, 2004). Such findings suggest that lipid rafts disruption through cholesterol sequestration would interfere on synchronic exocytosis fired by calcium influx. Therefore cholesterol enriched microdomains could act not only in the subcellular distribution of ionic pumps and channels but also participate in their

functional modulation. However, according to Zamir and Charlton (2006), the effects of cholesterol sequestration over synaptic vesicle release in neuromuscular junctions are independent on intra or extracellular calcium levels. Moreover, the effects of MßCD over synaptic vesicle release are reversible through the conjugate cholesterol-MßCD (Zamir and Charlton, 2006; Wasser *et al.*, 2007). These data suggest that the increase in spontaneous vesicle release and inhibition of K^+-evoked exocytosis are primary resultant from disorganization of the membrane microdomains which participate in the sorting of proteins that regulates synaptic vesicle cycle. Recently, it was reported that cholesterol removal disrupts synaptosomal porosomes, which are cup shaped lipoprotein structures that define the specific sites of vesicle docking and fusion. At each porosome, t-SNAREs are linked to N-type calcium channels and treatment with Triton/Lubrol breaks this interaction but cause no damage to the capacity of association between t-SNAREs and v-SNAREs (Cho *et al.*, 2007). Since synchronic vesicle release requires participation of SNARE complex and calcium channels, these findings might help to explain the inhibition K^+-evoked exocytosis at frog neuromuscular junction. We could speculate that some observations made after treatment with MßCD like the blocking of action potentials conductance (Zamir and Charlton, 2006), decrease on calcium influx into presynaptic terminal (Taverna *et al*., 2004) or drop on resting potential (table 1) would be only secondary phenomena due to modifications on microdomains that contain proteins involved on ionic balance.

Cholesterol and synaptic vesicles endocytosis

Endocytosis of synaptic vesicles occurs in defined plasma membrane regions in which preassembled lipid and protein constituents trigger the formation of the endocytic synaptic machinery (Rohrbough and Broadie, 2005). In fact, cholesterol plays

an important role on endocytosis since MßCD retarded or prevented clathrin mediated endocytosis of transferrin receptor internalization (Subtil et al., 1999). In PC12 cells, it was shown that the biding of specific proteins to cholesterol might aid clathrin mediated formation of new synaptic vesicles (Thiele *et al*., 2000). Wasser et al. (2007) observed decreased uptake of HRP and clear reduction in the number of synaptic vesicles after acute removal of vesicular cholesterol fraction from hippocampal cultured neurons. We tested this paradigm in our system by incubating frog neuromuscular junctions with MßCD followed by staining with FM1-43 and we failed to detect any significant staining (FIG 6), which suggests that the dye could not be internalized, maybe due to endocytosis inhibition. This finding is in agreement with other works that showed endocytosis impairment after cholesterol sequestration (for a review see Pichler and Riezman, 2004). In addition, HγCD did not alter significantly FM uptake. As the proteic machinery that regulates endocytosis is so complex as the one involved in exocytosis, cholesterol enriched microdomains may recruit the complex of proteins needed for endocytosis and may help to organize the sites of vesicle recycling. Moreover the kinetic of partioning/departioning of FM1-43 into membranes is not affected by cholesterol levels on the double layer of phospholipids (Wu *et al.* 2009), so the effects of MßCD over exo/endocytosis are resultant from alterations on membrane traffic but not on FM affinity for membranes.

Cholesterol, synaptic vesicle pools and modes of synaptic vesicles release

Most synaptic systems seem to rely on several pools of vesicles to maintain effective neurotransmission. At the frog neuromuscular junction, the main characteristics of vesicle pools can be described as follows: i) Readily releasable pools which comprises ~10,000 vesicles (0,4 % total); ii) Recycling pool corresponding to

~75,000 vesicles (14-19% total); iii) Reserve pool with ~400,000 vesicles (80 % total) (data extracted from a review by Rizzoli and Betz 2005). The precise pools location and vesicles intermixing and the molecular components that distinguish members of the pools have been under intense debate and investigation (Rizzoli and Betz, 2004). More recent, an attempt has been made to relate those vesicle pools with modes of release (Wasser *et al.*, 2007; Wasser and Kavalali, 2009).

As mentioned previously, our data shows that preparations that are cholesterol depleted failed to internalize FM1-43 after a depolarizing stimulus (FIG. 6C). Intriguing, at the ultrastructural level, nerve terminals that were treated with MßCD have many synaptic vesicles (FIG. 5B and 5C). This raised the question if those vesicles that fuse spontaneously belong to a distinct pool of vesicles, which is not part of the recycling pool of synaptic vesicles, do not stain with FM1-43 and is not recruited during evoked release. Indeed, Fredj and Burrone (2009) performed elegant studies in cultured hippocampal neurons showing that calcium-dependent evoked and spontaneous vesicle fusion recruits distinct pools of synaptic vesicles. They also show evidences that spontaneously released vesicles are mobilized from a resting pool, which was originally described as an activity independent set of vesicles that do not participate in vesicle cycling. These data agrees with the lack of FM1-43 internalization after treatment with MßCD (Fig 6C) contrasting with the normal number synaptic vesicles detected at the ultrastructural level (Fig 5B and 5C) observed in our experiments. Therefore, the present work provides additional evidence that spontaneous and evoked synaptic vesicles release require distinct synaptic vesicle pools and that at least for the neuromuscular junction, cholesterol might be responsible to segregate vesicles into these pools.

In conclusion, we have shown that membrane cholesterol acts on the modulation of synaptic vesicle cycle and seems to be essential for the balance between evoked and spontaneous release. Moreover, our results may reinforce the possibility of coexistence of a synaptic vesicle pool mobilized by evoked exocytosis and another pool spontaneously released.

Acknowledgments

This work was supported by grants from CNPq and FAPEMIG (CG). The authors would like to thank Prof. Patricia Martinelli for advice about EM protocols and Mr. Kinulpe Honorato for technical assistance during the acquisition of electron micrographs. We also thank the members of Centro de Microscopia da UFMG for all support.

References

Betz W. J., Bewick G. S. (1992) Optical analysis of synaptic vesicle recycling at the frog neuromuscular junction. *Science* **255(5041)**, 200-203.

Betz W. J., Mao F., Bewick G. S. (1992) Activity-dependent fluorescent staining and destaining of living vertebrate motor nerve terminals. *J Neurosci*. **12(2)**, 363-375.

Brown D. A., Rose K.J., (1992) Sorting of GPI-anchored proteins to glycolipid enriched membrane subdomains during transport to the apical cell surface. *Cell* **68**, 533–544.

Ceccarelli B., Hurlbut W. P., Mauro A. (1973) Turnover of transmitter and synaptic vesicles at the frog neuromuscular junction. *J Cell Biol*. **57(2)**, 499-524.

Cho W. J., Jeremic A., Jin H., Ren G., Jena B. P. (2007) Neuronal fusion pore assembly requires membrane cholesterol. *Cell Biol Int.* **31(11)**, 1301-1308.

Foster L. J., De Hoog C. L., Mann M. (2003) Unbiased quantitative proteomics of lipid rafts reveals high specificity for signaling factors. *Proc Natl Acad Sci U S A.* 100(10), 5813-8.

Fredj N. B., Burrone J. (2009) A resting pool of vesicles is responsible for spontaneous vesicle fusion at the synapse. *Nat Neurosci.* **12(6)**, 751-8.

Gaffield M. A., Betz W. J. (2006) Imaging synaptic vesicle exocytosis and endocytosis with FM dyes. *Nat Protoc*.**1(6)**, 2916-2921.

Guatimosim C., Romano-Silva M. A., Gomez M. V., Prado M. A. (1998) Recycling of synaptic vesicles at the frog neuromuscular junction in the presence of strontium. *J Neurochem.* **70(6)**, 2477-2483.

Henkel A. W., Lübke J., Betz W. J. (1996) FM1-43 dye ultrastructural localization in and release from frog motor nerve terminals. *Proc Natl Acad Sci U S A*. **93(5)**, 1918-23.

Heuser J. E., Reese T. S. (1973) Evidence for recycling of synaptic vesicle membrane during transmitter release at the frog neuromuscular junction. *J Cell Biol.* **57(2),** 315-344.

KATZ B., THESLEFF S. (1957) On the factors which determine the amplitude of the miniature end-plate potential. *J Physiol.* **137(2)**, 267-78.

Lang T., Bruns D., Wenzel D., Riedel D., Holroyd P., Thiele C., Jahn R. (2001) SNAREs are concentrated in cholesterol-dependent clusters that define docking and fusion sites for exocytosis. *EMBO J.* **20(9)**, 2202-2213.

Lang T. (2007) SNARE proteins and 'membrane rafts'. *J Physiol*. **585(3)**, 693-8.

Lingwood D., Kaiser H. J., Levental I., Simons K. (2009) Lipid rafts as functional heterogeneity in cell membranes. *Biochem Soc Trans*. **37(5)**, 955-960.

Murthy V. N., De Camilli P. (2003) Cell biology of the presynaptic terminal. *Annu Rev Neurosci.* **26**, 701-728.

Pichler H., Riezman H. (2004) Where sterols are required for endocytosis. *Biochim Biophys Acta.* **1666(1-2)**, 51-61.

Pike L. J. (2006) Rafts defined: a report on the Keystone Symposium on Lipid Rafts and Cell Function. *J Lipid Res*. **47(7)**, 1597-8.

Richards D. A., Guatimosim C., Betz W. J. (2001) Two endocytic recycling routes selectively fill two vesicle pools in frog motor nerve terminals. *Neuron* **27(3)**, 551-559.

Rizzoli S. O., Betz W. J. (2004) The structural organization of the readily releasable pool of synaptic vesicles. *Science*. **303(5666)**, 2037-9.

Rizzoli S. O., Betz W. J. (2005) Synaptic vesicle pools. *Nat Rev Neurosci.* **6(1)**, 57-69.

Robitaille R., Adler E. M., Charlton M. P. (1990) Strategic location of calcium channels at transmitter release sites of frog neuromuscular synapses. *Neuron* **5(6)**, 773-779.

Rodal S. K., Skretting G., Garred O., Vilhardt F., van Deurs B., Sandvig K. (1999) Extraction of cholesterol with methyl-beta-cyclodextrin perturbs formation of clathrin-coated endocytic vesicles. *Mol Biol Cell*. **10(4)**, 961-974.

Rohrbough J., Broadie K. (2005) Lipid regulation of the synaptic vesicle cycle. *Nat Rev Neurosci.* **6(2),** 139-50.

Royle S. J., Lagnado L. (2003) Endocytosis at the synaptic terminal. *J Physiol*. **553(2)**, 345-55.

Salaün C., Gould G. W., Chamberlain L. H. (2005) The SNARE proteins SNAP-25 and SNAP-23 display different affinities for lipid rafts in PC12 cells. Regulation by distinct cysteine-rich domains. *J Biol Chem.* **280(2),** 1236-40.

Simons K., van Meer G. (1988) Lipid sorting in epithelial cells. *Biochemistry* **27(17)**, 6197-202.

Simons K., Ikonen E. (1997) Functional rafts in cell membranes**.** *Nature* **387(6633)**, 569-72.

Singer S. J., Nicolson G. L. (1972) The fluid mosaic model of the structure of cell membranes. *Science* **175(23)**, 720-731.

Stetzkowski-Marden F., Gaus K., Recouvreur M., Cartaud A., Cartaud J. (2006) Agrin elicits membrane lipid condensation at sites of acetylcholine receptor clusters in C2C12 myotubes. *J Lipid Res*. **47(10)**, 2121-33.

Subtil A., Gaidarov I., Kobylarz K., Lampson M. A., Keen J. H., McGraw T. E. (1999) Acute cholesterol depletion inhibits clathrin-coated pit budding. *Proc Natl Acad Sci USA*. **96(12)**, 6775-680.

Sudhof T. C. (2004) The synaptic vesicle cycle. *Annu Rev Neurosci.* **27**, 509-547.

Taverna E., Saba E., Rowe J., Francolini M., Clementi F., Rosa P. (2004) Role of lipid microdomains in P/Q-type calcium channel (Cav2.1) clustering and function in presynaptic membranes. *J Biol Chem*. **279(7)**, 5127-5134.

Thiele C., Hannah M.J., Fahrenholz F., Huttner W. B. (2000) Cholesterol binds to synaptophysin and is required for biogenesis of synaptic vesicles. *Nat Cell Biol.* **2(1)**, 42-49.

Wasser C. R., Ertunc M., Liu X., Kavalali E. T. (2007) Cholesterol-dependent balance between evoked and spontaneous synaptic vesicle recycling. *J Physiol.* **579(2)**, 413-429.

Wasser C. R., Kavalali E. T. (2009) Leaky synapses: regulation of spontaneous neurotransmission in central synapses. *Neuroscience* **158(1)**, 177-88.

Wu Y., Yeh F. L., Mao F., Chapman E. R. (2009) Biophysical characterization of styryl dye-membrane interactions. *Biophys J.* **97(1)**, 101-109.

Yoshinaka K., Kumanogoh H., Nakamura S., Maekawa S. (2004) Identification of V-ATPase as a major component in the raft fraction prepared from the synaptic plasma membrane and the synaptic vesicle of rat brain. *Neurosci Lett.* **363(2)**, 168-172.

Zamir O., Charlton M. P. (2006) Cholesterol and synaptic transmitter release at crayfish neuromuscular junctions. *J Physiol*. **571(1)**, 83-99.

Zhai R. G., Bellen H. J. (2004) The architecture of the active zone in the presynaptic nerve terminal. *Physiology (Bethesda)* **19**, 262-270.

3 - Discussão

3.1 - Reciclagem de vesículas sinápticas em camundongos com alteração na expressão do transportador vesicular de acetilcolina

Na literatura existem relatos de que o bloqueio da expressão do transportador vesicular de glutamato (VGLUT1) em terminações axônicas determina redução no número de vesículas sinápticas (Fremeau *et. al.*, 2004). Entretanto, o *nocaute* do transportador vesicular de monoaminas (VMAT2) não desencadeou alteração significativa nos aglomerados vesiculares (Croft *et. al.,* 2005). Os experimentos referentes à captação de FM1-43 mostram que terminações motoras de animais *knockdown* homozigotos internalizam FM1-43 em quantidade semelhante às junções de animais selvagens de tal modo que não se observou diferença significativa durante a quantificação do sinal fluorescente emitido pelos grupos vesiculares marcados com FM1-43 (artigo nº 1 - Prado *et al*., 2006). Tal resultado indica que o número de vesículas que reciclam durante estímulo despolarizante com potássio é equivalente para os dois genótipos. Além disso, a análise de desmarcação dos aglomerados vesiculares contendo FM1-43 demonstrou que a exocitose de vesículas sinápticas se processa praticamente com a mesma intensidade e mesma cinética quando são comparados os animais *knockdown* homozigotos e selvagens (artiog nº 1 - Prado *et al.*, 2006). Portanto, uma diminuição da expressão do VAChT de 65% com conseqüente redução do conteúdo quântico das vesículas não interfere com a reciclagem e biogênese de vesículas sinápticas na junção neuromuscular.

Outros trabalhos nos quais os pesquisadores utilizaram inibidores do VAChT, da VH^+-ATPase ou promoviam o colapso de gradiente eletroquímico responsável pela captação de neurotransmissor também indicaram a ocorrência de reciclagem de vesículas com conteúdo quântico reduzido. Cousin e Nicholls (1997) realizaram experimentos com células granulares do cerebelo submetidas a tratamento com bafilomicina, agente inibidor da VH^+-ATPase, e metilamina, uma base fraca que depleta o componente ΔpH do gradiente eletroquímico transmembrana responsável pelo armazenamento de neurotransmissores no interior das vesículas sinápticas. Eles observaram que a captação e liberação de FM1-43 após pulsos despolarizantes estavam preservadas mesmo nas células tratadas com os agentes acima citados, indicando que

vesículas com conteúdo quântico reduzido ou depletado podem ser recicladas na terminação axônica.

Parsons *et. al.* (1999), realizando experimentos em junção neuromuscular, constataram que a captação e liberação de FM1-43 dos aglomerados vesiculares estavam preservadas após tratamento com vesamicol, um inibidor do transportador vesicular de acetilcolina. Van der Kloot *et. al*. (2001) e Hong (2001) observaram, por meio de estudo eletrofisiológico, a ocorrência de liberação de vesículas sinápticas com conteúdo quântico reduzido após pré-incubação de preparações de junção neuromuscular com cloreto de amônio (colapsa ΔpH), vesamicol, bafilomicina e concanamicina, esta última também promove inibição da VH^{+}-ATPase.

Croft *et al.* (2005) através de experimentos com FM1-43 e FM2-10 demonstraram que vesículas sinápticas de animais *knockout* para o VMAT2 sofrem endocitose e exocitose com cinética idêntica àquela observada em animais selvagens.

Os resultados discutidos nos parágrafos anteriores sugerem que o transporte de acetilcolina para o interior de vesículas durante reciclagem não constitui pré-requisito para ocorrência de exo/endocitose. Também em fetos de camundongos *nocaute* para o VAChT era possível observar marcação com FM1-43fx, indicando que os passos de exo/endocitose estão preservados. Contudo, nos animais *nocaute* não foram realizadas análises comparativas da intensidade da marcação e da cinética de desmarcação do FM1-43 em relação aos animais selvagens. Portanto, não podemos fazer inferências quanto os níveis de endocitose e cinética de exocitose dos dois genótipos.

Os animais *knockdown* homozigotos não apresentaram alterações na área e no número de junções neuromusculares presentes no diafragma em relação aos camundongos selvagens (figura suplementar 1, p. 27). É possível que mesmo uma redução de 65% na expressão do VAChT, capaz de interferir no preenchimento de vesículas com a acetilcolina, não seria suficiente para acarretar alterações significativas na sinaptogênese e organização morfológica das placas motoras.

Contudo, fetos *nocaute* para o VAChT apresentaram aumento no número e na áreas das terminações motoras quando comparados com fetos selvagens (artigo nº 2 - de Castro *et al*., 2009). Alterações compensatórias também foram observadas em outras linhagens com alterações genéticas no sistema colinérgico. A deleção da ChAT determinou localização aberrante dos receptores nicotínicos da acetilcolina (nAChR), gerou aumento no número de neurônios motores e ampliou o número de arborizações

axônicas em diafragma de animais *nocaute* (Misgeld *et al.*, 2002; Brandon et *al.,* 2003;).

É preciso salientar que os experimentos com FM1-43 permitem estimar taxas de endocitose e avaliar a cinética da exocitose das vesículas que reciclam. Contudo, somente experimentos envolvendo análise ultra-estrutural poderiam avaliar as conseqüências de alteração da expressão do VAChT sobre a morfologia, a distribuição e o número total de vesículas sinápticas. Além disso, a análise ultra-estrutural certamente traria novas informações sobre a organização da junção neuromuscular como, por exemplo, número de zonas ativas e disposição da dobras na membrana pós-sináptica.

Embora exista a possibilidade de liberação de neurotransmissor por mecanismos independentes do VAChT, reconhecidamente, a acetilcolina, juntamente com outros fatores, participa da modulação do desenvolvimento de junções neuromusculares. Ela atua no estabelecimento da arborização axônica, na definição da área e do número de placas motoras (Misgeld *et al.*, 2002; Brandon et *al.,* 2003). As alterações morfológicas observadas em camundongos *nocaute* para o VAChT indicam que outros mecanismos de secreção da acetilcolina não são suficientes para compensar a ausência do seu transportador vesicular. Portanto, a liberação de acetilcolina armazenada em vesículas sinápticas via VAChT constitui um mecanismo fisiológico relevante durante a sinaptogênese e desenvolvimento das junções neuromusculares.

3.2 - Participação de estoques intracelulares de cálcio na exocitose evocada pelo glicosídeo ouabaína

Segundo Adam-Vizi (1992), existem três possibilidades, à priori, de liberação vesicular independente do cálcio extracelular: (1) liberação independente de Ca^{2+} extracelular, mas dependente do recrutamento de reservas intracelulares desse íon como retículo endoplasmático e mitocôndria. (2) Liberação completamente independente de cálcio, mas que se processa através dos mesmos mecanismos e usufrua da mesma maquinaria molecular que a liberação evocada pelo cálcio. Isto remete a possibilidade de liberação vesicular disparada por outros íons como o sódio (Nordmann & Stuenkel, 1991; Nordmann *et al.*, 1992; Meunier *et al*, 1997). (3) Liberação completamente independente de cálcio e processada por meio de mecanismos distintos da liberação disparada por este íon.

Não é objetivo deste trabalho de tese revisar todas as formas de liberação vesicular independentes da presença de cálcio no meio. Contudo, são inúmeras as condições que, além da ouabaína, promovem liberação de neurotransmissores mesmo na ausência de cálcio extracelular como, por exemplo, ionóforos de sódio, veratridina, condições hipóxicas, etanol, ácidos graxos insaturados, α-latrotoxina. Interessante observar que todas essas condições apresentam aspectos em comum como: (a) uma cinética de liberação mais lenta que a observada na liberação disparada pelo cálcio e (b) uma menor dependência do potencial de membrana de modo que mesmo após pequenas alterações em relação ao potencial de repouso é possível registrar liberação de neurotransmissor. Este comportamento é diferente da liberação mediada pelo influxo de cálcio que demonstra a necessidade de ultrapassar limiares de despolarização mais altos para disparar a exocitose (revisado por Adam-Vizi, 1992).

Conforme apresentado no artigo anexado nº 3 (Amaral *et al.*, 2009), a ouabaína, em preparações de junção neuromuscular, promove liberação vesicular e desmarcação de aglomerados vesiculares previamente carregados com FM1-43. A exocitose evocada pela ouabaína ocorre independentemente do cálcio extracelular, porém depende do recrutamento de estoques intracelulares de cálcio. Para identificar as fontes de cálcio intracelular mobilizadas pela ouabaína, foram utilizados azumoleno e 2-APB, inibidores do receptor de rianodina e inositol trifosfato respectivamente. Azumoleno inibiu a exocitose evocada pelo glicosídeo cardiotônico, porém 2-APB não interferiu significativamente com a desmarcação de terminações motoras carregadas com FM1-43. Experimentos com TMB-8, outro inibidor do receptor de rianodina, também resultaram em inibição da liberação de vesículas marcadas com FM1-43 em junção neuromuscular de forma semelhante ao azumoleno (dado não mostrado). Esses achados indicam que a ouabaína promove liberação vesicular recrutando cálcio armazenado em retículo endoplasmático via receptor de rianodina.

As mitocôndrias também participam da modulação da concentração intracelular de cálcio. Em neurônios e células cromafins, as mitocôndrias agem rápida e reversivelmente, tamponando grandes variações na concentração de cálcio intracelular (Werth & Thayer, 1994; Herrington *et al*., 1996; Babcock *et al*., 1997). Montero *et al.* (2000) relataram a existência de um acoplamento preciso entre canais para cálcio sensíveis à voltagem, receptores de rianodina do retículo endoplasmático e as mitocôndrias. Eles relataram que protonóforos que abolem o tamponamento de cálcio pelas mitocôndrias podem aumentar a secreção de catecolaminas por interferirem com

os níveis de íons Ca^{2+} disponíveis para a exocitose. Yang *et al*. (2003) demonstraram que o bloqueio da liberação de cálcio mitocondrial via trocador Na^{+}/Ca^{2+} inibe a potenciação sináptica induzida por estímulo tetânico. Além disso, Gárcia-Charcon *et al.* (2006) relataram que a inibição do trocador Na^{+}/Ca^{2+} mitocondrial com CGP37157 prolongava o decaimento da concentração de cálcio mitocondrial após estimulação e reduzia a amplitude de potenciais evocados em placa motora após estimulação prévia. Esses dados indicam que a extrusão de cálcio armazenado em mitodcôndrias presentes em placas motoras contribui para a liberação pós-tetânica de neurotransmissor. Como já citado anteriormente, ouabaína inibe a Na^{+}/K^{+} ATPase favorecendo um acúmulo intracelular de íons Na^{+}. Altos níveis intracelulares de sódio podem promover a extrusão de cálcio mitocondrial via trocador Na^{+}/Ca^{2+} mitocondrial. Como foi demonstrado neste trabalho, CGP37157, bloqueador do trocador Na^{+}/Ca^{2+} mitocondrial, inibiu a liberação de vesículas sinápticas marcadas com FM1-43. Além disso, na ausência de íons Na^{+}, a ouabaína não promoveu liberação significativa de vesículas contendo FM1-43. Esses dados indicam a participação de cálcio armazenado em mitocôndrias na exocitose de vesículas sinápticas evocadas pela ouabaína.

Narita *et al.* (1998) observaram que o influxo de íons cálcio em terminações pré-sinápticas recrutava estoques intracelulares do referido íon via receptores de rianodina (RyR). Este mecanismo de liberação de cálcio intracelular induzida pela própria entrada de cálcio proveniente do meio externo (*calcium induced calcium release* – CICR) é resultante da ativação de canais para cálcio dependentes de voltagem e amplifica o as concentrações intracelulares do referido íon divalente. Portanto, CICR corresponde a um tipo de plasticidade de curta duração (Narita *et al.*, 2000). Os dados apresentados nesta tese demonstraram que a exocitose evocada pela ouabaína se processa através do recrutamento de cálcio armazenado em mitocôndrias e retículo endoplasmático, mesmo na ausência de cálcio extracelular. Especula-se, então, a possibilidade de existência de um mecanismo intracelular semelhante a CICR envolvendo diferentes organelas e que esteja operante durante tratamento com a ouabaína. Os íons cálcio que vazam das mitocôndrias via trocador Na^{+}/Ca^{2+} mitocondrial devido ao aumento intracelular de sódio poderiam ativar RyRs no retículo endoplasmático, levando a uma ascensão na concentração intracelular de Ca^{2+} suficiente para disparar a exocitose de vesículas e promover desmarcação de terminações carregadas com FM1-43.

Utilizando o FM1-43, foi possível demonstrar dinamicamente que a ouabaína promove liberação de vesículas sinápticas, mas inibe a endocitose. Esses resultados estão em consonância com o trabalho de Haimann *et al.* (1985) que observaram ausência na captação de HRP em junções neuromusculares submetidas à ouabaína. Eles também relatam o aparecimento de invaginações de membranas na terminação pré-sináptica. Molgó & Pecot-Dechavassine (1988) relatam que o CCCP, um desacoplador da fosforilação oxidativa que promove o vazamento de cálcio mitocondrial, promove um aumento na freqüência de eventos em miniatura (MEPPs) e depleção dos aglomerados vesiculares em junção neuromuscular independentemente da presença de íons Ca^{2+} no meio extracelular. Além disso, esse protonóforo leva a uma dilatação mitocondrial e desorganização das cristas mitocondriais. Essas alterações na estrutura mitocondrial são também descritas em junções neuromuscualres submetidas a tratamento com ouabaína (Haimann *et al.*, 1985). Os dados de desmarcação de aglomerados vesiculares contendo FM1-43 em junção neuromuscular sugerem uma similaridade no mecanismo de ação entre a ouabaína e o CCCP. A cinética de liberação vesicular induzida pelo CCCP é equivalente àquela observada com a ouabaína. Outra evidência de que a ouabaína pode interferir com a função mitocondrial foi fornecida por Whittam & Blonde (1964) que observaram uma redução no consumo de oxigênio em fatias corticais que foram incubadas com o glicosídeo. Wang *et al.* (2004) demonstraram que uma linhagem de *Drosophila* mutante para a fosfoglicerato cinase, enzima envolvida com a síntese de ATP, apresenta comprometimento seletivo da endocitose. Fato também observado com a ouabaína. Em suma, os dados apresentados nesse trabalho indicam que a ouabaína, assim como o CCCP, parece interferir com o funcionamento mitocondrial, levando a um vazamento de cálcio capaz de promover exocitose de vesículas sinápticas. Além disso, a ouabaína possivelmente gera um colapso energético, causando inibição da endocitose.

Embora a Ouabaína seja um derivado esteróide que atue inibindo a Na^+,K^+-ATPase, uma proteína de membrana, não se pode descartar a possibilidade de que este glicosídeo atue sobre sítios específicos no interior das células. Recentemente, associação entre uma proteína de 31,5 KD presente no sistema de túbulos T de cardiomiócitos de gato e ouabaína foi relatada. A interação do glicosídeo com seu receptor protéico intracelular batizado de NORP (*new 31,5-KD ouabain receptor protein*) teria relação com a potencialização do efeito inotrópico do glicosídeo (Fujino & Fujino, 1995). A existência de alvos intracelulares abre uma linha de investigação

que poderia, talvez, permitir melhor definição do mecanismo de ação da ouabaína sobre o ciclo de vesículas sinápticas. Além disso, a compreensão sobre o mecanismo de ação da oubaína ganha uma dimensão muito maior na medida em que compostos endógenos de estrutura idêntica à ouabaína foram isolados em tecidos de mamíferos (Hamlyn *et al.*, 1991; Scheneider *et al.*, 1998; Boulanger *et al.*, 1993), levantando a possibilidade de atuação desses compostos em mecanismos fisiológicos.

3.3 - Participação do colesterol de membrana na biogênese e reciclagem de vesículas sinápticas

Segundo os dados apresentados no artigo anexado nº 4 (Amaral *et al.*, em preparação), a incubação de terminações motoras com MßCD ampliou a freqüência de MEPPs e promoveu desmarcação de agrupamentos vesiculares previamente carregados com FM1-43. Assim sendo, o seqüestro do colesterol de membrana estimula liberação espontânea de vesículas sinápticas. Além de sua participação na organização espacial de microdomínios ricos em proteínas específicas, o colesterol regula a fluidez das membranas celulares. Portanto, o seqüestro de colesterol poderia facilitar a fusão de vesículas em sítios que não correspondam às zonas ativas, ampliando a liberação espontânea de vesículas (Wasser & Kavalali, 2009).

Embora tenha estimulado a liberação espontânea, o seqüestro do colesterol de membrana inibiu liberação evocada por KCl (artigo nº4 - Amaral *et al.*, em preparação). É bem definido que a exocitose evocada (sincrônica) é regulada por um conjunto amplo de proteínas, entre as quais, deve-se ressaltar o complexo SNARE que rege a ancoragem e a fusão das vesículas sinápticas com as zonas ativas das terminações pré-sinápticas (Revisado por Murthy & De Camilli, 2003; Sudhoff, 2004). Este complexo de proteínas está inserido em microdomínios de membrana ricos em colesterol e esfingolipídios (Thiele *et al.*, 1999; Rodal *et al.*, 1999; Lang *et al.*, 2001). Segundo Salaün *et al.* (2004), para que a exocitose regulada se processe eficientemente, a maquinaria protéica envolvida com a modulação da liberação vesicular deve estar espacialmente bem organizada. Isto implica, inclusive, na distribuição dos componentes do complexo SNARE e proteínas reguladoras da exocitose em microdomínios diferentes de membrana. Seria pouco funcional, por exemplo, a coexistência nos mesmos domínios de proteínas SNARES e MUNC-18, já que esta proteína se associa à sintaxina, impedindo o estabelecimento do complexo SNARE heterotrimérico com SNAP-25 e

sinaptobrevina. Chamberlain *et al.* (2001) demonstraram que MUNC-18, αSNAP, NSF e complexinas, proteínas envolvidas com a regulação da exocitose, não estão presentes em balsas lipídicas. Portanto, excluindo moléculas reguladoras da liberação vesicular, as balsas lipídicas poderiam criar um ambiente propício para a fusão mediada por SNAREs, promovendo o acúmulo desse complexo protéico em sítios específicos para a exocitose. Sendo assim, o seqüestro de colesterol poderia desorganizar a distribuição espacial de proteínas de membrana relacionadas com o ciclo sináptico, resultando em inibição da liberação evocada e sincrônica.

Como já citado, o seqüestro de colesterol inibiu a exocitose evocada por KCl, conforme demonstrado por microscopia de fluorescência utilizando FM1-43 e microscopia eletrônica (artigo nº4 - Amaral *et al.*, em preparação). O estímulo despolarizante com KCl não recruta canais para sódio dependentes de voltagem mas são dependentes da ativação de canais para cálcio que permitem o influxo de íons Ca^{2+} para o interior do elemento pré-sináptico. A ascensão dos níveis de cálcio intracelular leva ao disparo da liberação vesicular. (revisado por Murthy & De Camilli, 2003; Sudhof, 2004). Assim, para garantir eficiência à exocitose, os canais para cálcio estão estrategicamente posicionados de forma bem próxima às zonas ativas e aos agrupamentos vesiculares (Robitaille *et al.*, 1990; revisado por Zhai & Bellen, 2004). A associação entre isoformas de canais para cálcio ou proteínas SNARES com balsas lipídicas já foi previamente demonstrada (Taverna *et al.*, 2004). Tais achados sugerem que a desorganização das balsas lipídicas pelo seqüestro de colesterol poderia interferir na exocitose sincrônica disparada pelo influxo de cálcio. Portanto, microdomínios ricos em colesterol poderiam atuar não apenas na distribuição subcelular de bombas e canais iônicos, mas também poderiam participar da modulação funcional desses componentes protéicos da membrana.

Recentemente foi demonstrada a presença de estruturas chamadas de *porosomos* na membrana plasmática de células que promovem ancoragem e liberação de vesículas. Os porosomos neuronais correspondem a estruturas lipoprotéicas com aspecto de xícara ou cesta de basquete constituídas por colesterol e muitas proteínas como, por exemplo, canais para cálcio, proteínas SNAREs (sintaxina-1 e SNAP-25), actina, vimentina e NSF. O diâmetro dos porosomos varia entre 12 e 17nm, correspondendo aos pontos específicos de membrana nos quais ocorre liberação de neurotransmissores (Cho *et al.*, 2004; Jena, 2005). Cho *et al.* (2007) demonstraram que a remoção do colesterol de membrana de sinaptossomos desorganiza o complexo

protéico presente nos *porosomos*, inibindo a associação entre t-SNAREs e canais para cálcio. Embora interfira com a organização do *porosomo*, a remoção do colesterol da membrana não bloqueia a capacidade de associação entre t e v SNARES. Considerando que a liberação sincrônica de neurotransmissores exige a participação de SNAREs e canais para cálcio, estes achados citados por Cho *et al.* (2007) poderiam explicar a inibição da exocitose evocada pelo potássio na presença de MßCD (artigo nº 4 - Amaral *et al.*, em preparação) ou mesmo o comprometimento da plasticidade neuronal em situações em que há desequilíbrio na homeostase do colesterol (Koudinov and Koudinova, 2001).

Segundo Zamir & Charlton (2006), os efeitos do seqüestro de colesterol sobre a liberação espontânea de vesículas em junção neuromuscular são independentes dos níveis de cálcio extra e intracelular já que quelantes do cálcio extra e intracelular não alteraram a exocitose induzida pela MßCD. Além disso, os efeitos da MßCD sobre liberação de vesículas sinápticas são reversíveis quando o colesterol de membrana é reposto com o conjugado MßCD-colesterol (Zamir and charlton, 2006; Wasser *et al.*, 2007). Esses dados sugerem que a inibição da exocitose evocada pelo KCl e o aumento da liberação espontânea após seqüestro de colesterol são primordialmente resultantes da desorganização dos microdomínios de membrana que participam da seleção ou arranjo de proteínas que regem o ciclo sináptico. Portanto, alguns fatos observados após tratamento com MßCD como, por exemplo, o bloqueio de potenciais de ação (Zamir and Charlton, 2006), a redução no influxo de cálcio para a terminação pré-sináptica (Taverna *et al*., 2004) ou a queda no potencial de membrana (artigo nº 4, Amaral *et al.*, em preparação) sejam apenas fenômenos secundários decorrentes de modificações em microdomínios que contenham proteínas envolvidas com balanço iônico. Talvez os níveis de colesterol de membrana sejam importantes para a manutenção da funcionalidade de proteínas de membrana como canais iônicos e a própria Na^+/K^+ATPase.

Zamir and Charlton (2006) não observaram alterações na amplitude e na cinética de MEPPS após incubação com MßCD em preparações de junção neuromuscular de lagostim. Entretanto, em preparações de junção neuromuscular de rã, foi possível observar que o seqüestro de colesterol aumenta a amplitude e a área dos eventos espontâneos (artigo nº 4 - Amaral *et al.*, em preparação). Diante desses dados, tornava-se necessário investigar se os achados eletrofisiológicos em junção neuromuscular de rã eram específicos dessa preparação colinérgica já que a junção

neuromuscular de lagostim utilizada por Zamir and Charlton (2006) é glutamatérgica. Neostigmina, um inibidor da acetilcolinesterase presente na membrana pós-sináptica, não inibiu os efeitos da MßCD sobre a cinética e área dos MEPPs (artigo nº4 - Amaral *et al.*, em preparação). Portanto, o aumento da amplitude e da área dos MEPPs não era decorrente de uma alteração da funcionalidade ou da distribuição pós-sináptica de moléculas da acetilcolinesterase induzida pela MßCD. Posteriormente, avaliaram-se possíveis efeitos do seqüestro de cholesterol sobre a morfologia dos aglomerados de receptores nicotínicos da acetilcolina (nAChRs) presentes na membrana pós-sinaptica. Alguns pesquisadores relataram que a MßCD era capaz de dispersar agrupamentos de nAChRs em mioblastos em cultura (Stetzkowski-Marden *et al.*, 2006) Contudo, utilizando marcação com α-bungarotoxina fluorescente em preparações de juncão neuromuscular de rã, não se observou nenhuma interferência da MßCD sobre a morfologia dos agrupamentos de nAChRs (artigo nº4 - Amaral, *et al.*, em preparação), sugerindo que o aumento na amplitude e área dos MEPPs não era resultante da desorganização dos aglomerados de nAChRs. Portanto, novas investigações devem ser realizadas para esclarecer o mecanismo pelo qual o seqüestro de cholesterol amplia a área e amplitude dos MEPPs. Seria interessante investigar, por exemplo, as conseqüências do seqüestro de colesterol sobre a funcionalidade ou responsividade dos nAChRs. Não se pode descartar, também, a possibilidade de que o colesterol de membrana atue em outros passos do ciclo sináptico que vão além da modulação da exo/endocitose. Por exemplo, Yoshinaka *et al*. (2004) identificaram a VH^{+}-ATPase como sendo o principal componente proteíco inserido em balsas lipídicas da fração de vesículas sinápticas. Além disso, eles observaram que a capacidade da VH^{+}-ATPase em metabolizar ATP e promover acidificação vesicular estava reduzida após seqüestro de colesterol. Talvez as balsas lipídicas e o cholesterol tenham papéis importantes e pouco conhecidos na acidificação vesicular e no preenchimento das vesículas com neurotransmissores.

Em nossos experimentos, a incubação de preparações neuromusculares com MßCD inibiu captação de FM1-43 (artigo nº4 - Amaral *et al.*, em preparação), sugerindo a possibilidade de comprometimento da endocitose após seqüestro de colesterol. Contudo, HγCD, uma ciclodextrina de baixa afinidade pelo colesterol, não alterou significativamente a captação de FM. Outros pesquisadores também apontam que o colesterol de membrana tem importante papel na regulação da endocitose, principalmente na endocitose mediada por capa de clatrina. Rodal *et al.* (1999) e Subtil

et al. (1999) demonstraram que o seqüestro de colesterol pela MßCD parece interferir com a capacidade da clatrina deformar a membrana para formação de invaginações e vesículas sinápticas. Considerando que a maquinaria protéica que regula a endocitose é tão complexa quanto o conjunto protéico que rege a exocitose, microdomínios ricos em colesterol poderiam participar do recrutamento e da seleção de proteínas necessárias a endocitose e também poderiam ter participação na organização dos sítios de reciclagem vesicular. Além disso, Wu *et al.* (2009) demonstraram que a cinética de associação/liberação do FM1-43 com a membrana não é afetada pelos níveis de colesterol na dupla camada lipídica, portanto, esta constatação sugere que os efeitos da MßCD sobre endocitose são resultantes de alterações no ciclo de membrana e não têm relação com a afinidade do marcador pela membrana.

Embora a captação de FM1-43 tenha sido praticamente abolida após tratamento com MßCD, sugerindo inibição da endocitose, imagens de microscopia eletrônica mostraram terminações motoras submetidas ao seqüestro de colesterol com número elevado de vesículas sinápticas. Contudo, as imagens de microscopia eletrônica não esclarecem se os aglomerados vesiculares observados nas micrografias correspondem a vesículas espontaneamente liberadas e recicladas ou se representam agrupamentos vesiculares que não foram exocitados em decorrência do seqüestro de colesterol e inibição da exocitose evocada. Segundo Wasser & Kavalali (2009), o papel do colesterol de membrana como regulador da liberação vesicular ainda não é totalmente compreendido, principalmente no que diz respeito ao pronunciado aumento da liberação espontânea após seqüestro de colesterol. Na literatura, alguns cenários diferentes foram propostos para explicar a liberação espontânea. É possível que a liberação espontânea se processe em sinapses diferentes e independentes das sinapses em que ocorre liberação evocada. Existe ainda a possibilidade da liberação espontânea e da liberação evocada se processarem na mesma sinapse, porém mobilizando agrupamentos vesiculares distintos que reciclam independentemente – um agrupamento de liberação espontânea distinto do agrupamento de liberação evocada. Em outro cenário, levanta-se a possibilidade de que o agrupamento de liberação espontânea esteja presente na mesma sinapse em que ocorre liberação evocada, porém a exocitose e a reciclagem de vesículas liberadas espontaneamente aconteceriam em sítios ectópicos, diferentes das zonas ativas. Analisando os dados de microscopia de fluorescência, microscopia eletrônica e eletrofisiologia, tendo como base a exposição deste parágrafo, é possível que as vesículas liberadas e recicladas espontaneamente após seqüestro de

colesterol pertençam a agrupamentos diferentes dos aglomerados de liberação evocada. Isso poderia explicar a ausência de captação de FM1-43 após tratamento com MßCD, contrastando com o grande número de vesículas observadas ao microscópio eletrônico. Seria necessário, portanto, investigar qual a origem e a qual grupamento pertencem as vesículas observadas nas micrografias eletrônicas, bem como se sua reciclagem é dependente ou não de clatrina.

Em trabalho recente com cultura de neurônios hipocampais, Fredj & Burrone (2009) apresentaram uma forma de VAMP-2 *biotinilada* em seu domínio intraluminal chamada de *biosyn.* Quando vesículas são liberadas, o domínio intraluminal biotilinado da VAMP-2 é exposto e pode ser reconhecido por estreptoavidina fluorescente, permitindo estimar taxas de exocitose e tamanho dos aglomerados vesiculares mobilizados. Com a utilização da *biosyn*, foi possível demonstrar a existência de dois agrupamentos vesiculares em neurônios hipocampais. Um aglomerado vesicular liberado de forma dependente de Ca^{2+} mediante aplicação de potenciais de ação e um segundo agrupamento vesicular, liberado de forma espontânea e independente de Ca^{2+}. Os dados apresentados por Fredj & Burrone (2009) reforçam a possibilidade de existência de agrupamentos vesiculares distintos, mobilizados durante exocitose evocada e espontânea. Contudo, em junção neuromuscular, grupos vesiculares marcados com FM1-43 durante aplicação de estímulo despolarizante com K^+ foram exocitados após seqüestro de colesterol com MßCD (43 (artigo nº 4 - Amaral *et al.*, em preparação), situação que inibe a liberação evocada, mas amplia exocitose espontânea. Portanto, assumindo a co-existência de grupos vesiculares de liberação espontânea e evocada, é possível que o colesterol atue como modulador da neurotransmissão e agente que permita a existência dos agrupamentos vesiculares supracitados. Em níveis normais, o colesterol de membrana poderia atuar como organizador da maquinaria molecular necessária para a exocitose sincrônica e dependente de cálcio. Após seqüestro de colesterol e desorganização dos microdomínios de membrana relacionados com a liberação evocada, há um aumento significativo da liberação espontânea, permitindo inclusive a exocitose de vesículas que foram recicladas após estimulação e possivelmente uma mistura dos agrupamentos de liberação espontânea e evocada. Persiste, no entanto, uma indefinição quanto à natureza da maquinaria molecular necessária para liberação espontânea. Futuras investigações poderiam esclarecer se o mesmo conjunto de proteínas envolvidas com liberação evocada seria também

responsável pela exocitose espontânea ou se essas formas de liberação vesicular utilizam maquinaria molecular distintas.

4 - Perspectivas

O ciclo sináptico é, em termos morfológicos, relativamente simples. Contudo, sua regulação bioquímica é bastante complexa. Após décadas de estudos exaustivos, vários aspectos do ciclo de vesículas sinápticas encontram-se bem analisados e compreendidos. Entretanto, muitas controvérsias ainda persistem. Os três tópicos abordados nesse trabalho de tese ainda apresentam pontos a serem esclarecidos que exigirão investigações futuras.

Os experimentos com animais geneticamente modificados para o gene do transportador vesicular de acetilcolina (VAChT) sugerem que a redução na expressão do VAChT não influencia os passos de exo/endocitose de vesículas e não acarreta danos ao processo de desenvolvimento morfológico de terminações motoras (relembre artigo nº2 - Prado *et. al.,* 2006 e figura suuplementar 1). Por outro lado, a ausência de expressão do VAChT determinou importantes alterações morfológicas nos animais *nocaute* como a redução da área e da densidade de terminações motoras presentes no diafragma. Portanto, a remoção do VAChT prejudica a sinaptogênese e desenvolvimento morfológico normal de junções neuromusculares (artigo nº 2 - de Castro *et al.*, 2009). Entretanto, nos diafragmas de camundongos fetais desprovidos da expressão do VAChT, o ciclo sináptico não foi monitorado por completo. Uma vez que foi utilizada a forma fixável do FM1-43, o passo de exocitose nos animais *nocaute* não foi comparado à liberação vesicular em animais selvagens. Também não foi realizada comparação da intensidade da marcação com FM1-43 entre os animais de genótipo selvagem e os animais *nocaute* para o VAChT. Tal análise permitiria uma inferência sobre a endocitose e o número de vesículas aptas para a reciclagem. Talvez o a ausência de expressão do VAChT possa ter implicações na cinética de exo/endocitose de vesículas ou no tamanho dos agrupamentos vesiculares, parâmetros que poderão ser melhor investigados por técnicas de eletrofisiologia e microscopia eletrônica, respectivamente.

Quanto aos efeitos da ouabaína sobre o ciclo sináptico, os dados obtidos indicam que esse glicosídeo promove liberação vesicular independente de cálcio extracelular, porém esse derivado esteróide interfere com a dinâmica intracelular de cálcio de tal modo que a exocitose evocada pela ouabaína mostrou-se dependente do recrutamento de íons Ca^{2+} armazenados no retículo endoplasmático e nas mitocôndrias.

A possibilidade de que exista um mecanismo de liberação de cálcio induzida pelo próprio cálcio (*calcium induced calcium release*) que opere entre compartimentos intracelulares em virtude do acúmulo intracelular de sódio induzido pela ouabaína necessita ser mais bem dissecada. Talvez protocolos experimentais utilizando técnicas de eletrofisiologia ou indicadores intracelulares de cálcio em associação com bloqueadores de recepotres de rianodina, de inositol trifosfato e do trocador Na^{+}/Ca^{2+} mitocondrial possam corroborar os dados obtidos com FM1-43 e também trazer à tona novas proposições sobre o mecanismo de ação da ouabaína.

Além de interferir com a dinâmica intracelular de cálcio, ouabaína parece promover um colapso da função mitocondrial. Experimentos empregando marcadores da viabilidade mitocondrial ou avaliando alterações no consumo de ATP após incubação com o glicosídeo poderiam ser úteis para esclarecer os efeitos da ouabaína sobre o metabolismo mitocondrial.

Os dados relativos ao papel do colesterol de membrana no ciclo de vesículas sinápticas corroboraram por técnica de imagem muitos achados previamente citados na literatura em investigações que utilizavam técnicas de eletrofisiologia ou preparações fixadas. Entretanto, novos dados apresentados neste trabalho de tese apontam para a possibilidade de que os níveis de colesterol de membrana interfiram em etapas que vão além do tráfego de vesículas nos passos de exo/endocitose (artigo nº4 - Amaral *et al.*, em preparação). Talvez o colesterol na membrana seja importante na modulação do ciclo de neurotransmissores e tenha influência na acidificação ou no preenchimento de vesículas sinápticas. Portanto, futuramente, também seria muito interessante investigar o papel do colesterol de membrana sobre o trânsito de proteínas (VH^{+}-ATPase, CHT1, VAChT) entre a membrana da terminação axônica e os agrupamentos vesiculares. Talvez, de maior impacto ainda, seria investigar as implicações do seqüestro de colesterol sobre a funcionalidade das proteínas acima citadas. Marcação de proteínas da membrana vesicular poderiam também auxiliar na elucidação da existência de agrupamentos vesiculares distintos comprometidos com a exocitose evocada ou com a exocitose espontânea. Experimentos com *biosyn*, forma biotilinada de VAMP-2 reconhecida por estreptoavidina fluorescente (Fredj & Burrone, 2009), após seqüestro de colesterol, poderiam esclarecer se o colesterol de membrana é de fato o responsável pela existência de dois aglomerados vesiculares distintos nas terminações axônicas (agrupamentos de liberação evocada e espontânea, respectivamente) bem como pelo equilíbrio entre exocitose evocada e espontânea.

Em termos morfológicos, alguns aspectos também deverão ser analisados com maior profundidade. Marcadores de componentes da zona ativa poderiam indicar se há desorganização dos sítios de liberação no elemento pré-sináptico e se existe exocitose e reciclagem em sítios distintos das zonas ativas após seqüestro de colesterol. Tais investigações podem ser futuramente conduzidas e contribuirão para esclarecer o(s) papel(éis) do colesterol de membrana na organização morfofuncional do elemento pré-sináptico.

5 - Conclusões

Neste trabalho de tese, três importantes aspectos relacionados à biogênese e reciclagem de vesículas sinápticas foram abordados. Numa primeira etapa, foram investigadas as conseqüências da alteração na expressão do gene do transportador vesicular de acetilcolina (VAChT) sobre o ciclo de vesículas sinápticas em junções neuromusculares de camundongo. Os dados indicam que a redução da expressão do gene do VAChT não determina alterações significativas no número de vesículas sinápticas aptas para reciclagem em junção neuromuscular. O número e a área das terminações motoras presentes no músculo diafragma também não sofreram alterações após redução do VAChT. Além disso, os passos de exo/endocitose estão preservados nos animais *knockdow* homozigotos. Por sua vez, a anulação da expressão do VAChT determinou alterações compensatórias nos animais *nocaute*. Camundongos $VAChT^{del/del}$ apresentaram aumento no número e na área de terminações motoras observadas no músculo diafragma, indicando que a liberação de acetilcolina, armazenada em vesículas via VAChT, é fundamental para a sinaptogênese e desenvolvimento morfológico típico das junções neuromusculares. Mesmo em animais *nocaute* para o VAChT foi possível obter marcação com FM1-43, indicando ocorrência do ciclo exo/endocitose, embora a cinética desses passos não tenha sido avaliada.. Em conjunto, os dados obtidos sugerem que nestas linhagens de camundongos com alteração na expressão do VAChT o ciclo de vesículas sinápticas é independente do ciclo do neurotransmissor.

Em um segundo momento deste trabalho de tese, fez-se uma investigação sobre a participação de estoques intracelulares de cálcio na exocitose de vesículas sinápticas desencadeada pelo derivado esteróide ouabaína. Os dados obtidos demonstraram que a ouabaína promove, em junção neuromuscular de rã, desmarcação de aglomerados vesiculares contendo FM1-43, indicando a ocorrência de exocitose de vesículas sinápticas. A liberação de vesículas estimulada pela ouabaína, embora independente do cálcio extracelular, depende da presença de íons Na^+ e do recrutamento de íons Ca^{2+} armazenados no retículo endoplasmático e nas mitocôndrias através dos receptores de rianodina e trocador Na^+/Ca^{2+} mitocondrial, respectivamente. Além disso, a ouabaína inibe a endocitose compensatória. Os resultados descritos também fornecem evidências sugerindo que a oubaína, assim como o CCCP, possa comprometer a função mitocondrial, causando um colapso energético que poderia explicar a inibição seletiva

da endocitose. Sendo assim, a ouabaína constitui uma importante ferramenta farmacológica para estudos em que se deseja desacoplar a exocitose da endocitose.

Por fim, a investigação do papel do colesterol de membrana sobre o ciclo de vesículas sinápticas em junção neuromuscular de rã demonstrou que o seqüestro do colesterol pela metil-β-ciclodextrina (MβCD) determina aumento da liberação espontânea de vesículas sinápticas com conseqüente desmarcação de aglomerados vesiculares contendo FM1-43. Porém, MβCD inibe exocitose evocada pelo potássio, dependente da ativação de canais para cálcio. Além de promover aumento da freqüência de MEPPs, foi possível observar, de forma inédita, que seqüestro do colesterol de membrana determina alteração na amplitude e na cinética dos eventos espontâneos, sugerindo que o colesterol de membrana possa atuar não apenas no tráfego de membrana, mas também em etapas do ciclo do neurotransmissor como, por exemplo, durante o preenchimento das vesículas sinápticas. Embora facilite a liberação espontânea de vesículas sinápticas, o seqüestro de colesterol também parece inibir a endocitose compensatória. Em conjunto, os achados confirmam que o colesterol de membrana exerce importante efeito regulador sobre o ciclo sináptico e contribui para a organização morfofuncional das terminações nervosas.

Os dados obtidos com as investigações supracitadas contribuem para obtenção de princípios fundamentais sobre o funcionamento do sistema colinérgico e neurotransmissão em geral e poderão, no futuro, nortear novas investigações sobre o ciclo sináptico e subsidiar meios para intervenção farmacológica em disfunções da transmissão sináptica central e periférica.

6 – Referências Bibliográficas

ADAM-VIZI, V. External Ca(2+)-independent release of neurotransmitters. **Journal of Neurochemistry**, v. 58, n. 2, p. 395-405, 1992.

AIZMAN, O.; ULHEN, P.; LAL, M.; BRISMAR, H.; ASPERIA, A. Ouabain, a steroid hormone that signals with slow calcium oscillations. **Proceedings of the National Academy of Sciences USA**, v. 98, n. 23, p. 13420-24, 2001.

AMARAL, E.; LEITE, L. F.; GOMEZ, M. V.; PRADO, M. A.; GUATIMOSIM, C. Ouabain evokes exocytosis dependent on ryanodine and mitochondrial calcium stores that is not followed by compensatory endocytosis at the neuromuscular junction. **Neurochemystry International**, v. 55, n. 6, p. 406-13, 2009.

BABCOCK, D. F.; HERRINGTON, J.; GOODWIN, P. C.; PARK, Y. B.; HILLE, B. Mitochondrial participation in the intracellular Ca2+ network. **The Journal of Cell Biology**, v. 136, n. 4, p. 833-44, 1997.

BAKER, P. F.; CROWFORD, A. C. A note of the mechanism by which inhibitors of the sodium pump accelerate spontaneous release of transmitter from motor nerve terminals. **The Journal of Physiology**, v. 247, n. 1, p. 209-226, 1975.

BETZ, W. J.; MAO, F.; BEWICK, G. S. Activity dependent fluorescent staining and destaining of living vertebrate motor nerve terminals. **The Journal of Neuroscience,** v. 12, p.363-375, 1992.

BETZ, W. J.; MAO, F.; SMITH, Corey B. Imaging exocytosis and endocytosis. **Current Opinion in Neurobiology,** v. 6, p. 365-371, 1996.

BIRKS, R. I. The effects of a cardiac glycoside on subcellular structures within nerve cells and their processes in sympathetic ganglia and skeletal muscle. **Canadian Journal of Biochemistry and Physiology**, v. 40, p. 303-15, 1962.

BIRKS, R. I.; COHEN, M. W.; The action of sodium pumps inhibitors on neuromuscular transmission. **Proceedings of the Royal Society of London Series B: Biological Sciences,** v. 170, n. 21, p. 381-99, 1968.

BOULANGER, B. R.; LILLY, M. P.; HAMLYN, J. M.; LAREDO, J.; SHURTLEFF, D.; GANN, D. S. Ouabain is secreted by the adrenal gland in awake dogs. **The American Journal of Physiology: Endocrinology and Metabolism**, v. 264, n. 3, p. 413-419, 1993.

BRANDON, E. P.; MELLOTT, T.; PIZZO, D. P.; COUFAL, N.; D'AMOUR, K. A.; GOBESKE, K.; LORTIE, M.; LOPEZ-COVIELLA, I.; BERSE, B.; THAL, L. J.; GAGE, F. H.; BLUSZTAJN, J. K. Choline transporter 1 maintains cholinergic function in choline acetyltransferase haploinsufficiency. **The Journal of Neuroscience,** v. 24, n.24, p. 5459-66. 2004.

BRAVO, D.; PARSONS, S. M. Microscopic kinects and structure-function analysis in the vesicular acetylcholine transporter. **Neurochemistry International,** v. 41, p. 285-289, 2002.

BRUMBACK, A. C.; LIEBER, J. L.; ANGLESON, J. K.; BETZ, W. J. Using FM1-43 to study neuropeptide granule dynamics and exocytosis. **Methods,** v. 33, p. 287-294, 2004.

BURNS, M. E.; AUGUSTINE, G. J. Synaptic Structure and Function: Dynamic Organization Yields Architectural Precision. **Cell***,* v. 83, p. 187-194, 1995.

CASALI, T. A.; GOMEZ, R. S.; MORAES-SANTOS, T.; GOMEZ, M.V. Differential effects of calcium channel antagonists on tityustoxin and ouabain-induced release of [3H]acetylcholine from brain cortical slices. **Neuropharmacolog***y,* v. 34, n. 6, p. 599-603, 1995.

CECCARELLI, B.; HULBURT, W. P.; MAURO, A. Turnover of transmitter and synaptic vesicles at the frog neuromuscular junction. **The Journal of Cell Biology,** v. 57, p. 499-524. 1973.

CHAMBERLAIN, L. H.; BURGOYNE, R. D.; GOULD, G. W. SNARE proteins are highly enriched in lipid rafts in PC12 cells: implications for the spatial control of exocytosis. **Proceedings of the National Academy of Sciences USA**, v. 98, n.10, p. 5619-24, 2001.

CHAPMAN, E. R.; DAVIS, A. F. Direct interaction of a Ca2+-binding loop of synaptotagmin with lipid bilayers. **The Journal of Biological Chemitry**, v. 273, n. 22, p. 13995-4001, 1998.

CHAPMAN, E. R. How does synaptotagmin trigger neurotransmitter release? **Annual Review of Biochemistry**, v. 77, p. 615-41, 2008.

CHO, W. J.; JEREMIC, A.; JENA, B. P. Direct interaction between SNAP-23 and L-type Ca2+ channel. **Journal of Cellular and Molecular Medicine**, v. 9, n. 2, p. 380-6, 2005.

CHO, W. J.; JEREMIC, A.; JIN, H.; REN, G.; JENA, B. P. Neuronal fusion pore assembly requires membrane cholesterol. **Cell Biology International**, v. 31, n.11, p. 1301-8, 2007.

COUSIN, M. A.; NICHOLLS, D. G.; Synaptic vesicle recycling in cultured cerebellar granule cells: role of vesicular acidification and refilling. **Journal of Neurochemistry,** v. 69, n. 5, p. 1927-35, 997.

COUTEAUX, R. Remarks on the organization of axon terminals in relation to secretory processes at synapses. **Advances in Cytopharmacology**, v. 2, p. 369-79, 1974.

CROFT, B. G.; FORTIN, G. D., CORERA, A. T.; EDWARDS, R. H.; BEAUDET, A.; TRUDEAU, L. E.; FON, E. A. Normal biogenesis and cycling of empty synaptic vesicles in dopamine neurons of vesicular monoamine transporter 2 knockout mice. **Molecular Biology of the Cell,** v. 16, n. 1, p. 306-15, 2005.

DAVLETOV, B. A.; SÜDHOF, T. C. A single C2 domain from synaptotagmin I is sufficient for high affinity Ca2+/phospholipid binding. **The Journal of Biological Chemistry**, v. 268, n. 35, p. 26386-90, 1993.

DE CASTRO, B. M.; DE JAEGER, X.; MARTINS-SILVA, C.; LIMA, R. D.; AMARAL, E.; MENEZES, C.; LIMA, P; NEVES, C. M.; PIRES, R. G; GOULD, T. W.; WELCH, I.; KUSHMERICK, C.;, GUATIMOSIM, C.; IZQUIERDO, I.; CAMMAROTA, M; RYLETT, R. J.; GÓMEZ, M. V.; CARON, M. G.; OPPENHEIM, R. W.; PRADO, M. A.; PRADO, V. F. The vesicular acetylcholine transporter is required for neuromuscular development and function. **Molecular and Cellular Biology**, v.29, n.19, p. 5238-50, 2009.

DERI, Z.; ADAM-VIZI, V. Detection of intracellular free Na+ concentration of synaptosomes by a fluorescent indicator, Na(+)-binding benzofuran isophthalate: the effect of veratridine, ouabain, and alpha-latrotoxin. **Journal of Neurochemistry**, v. 61, n. 3, p. 818-25, 1993.

DESAKI, J.; UEHARA, Y. The overall morphology of neuromuscular junction as revealed by scanning electron microscopy. **Journal of Neurocytology**, v. 10, n. 1, p.101-110, 1981.

ELMQVIST, D.; FELDMAN, D. S. Effects of sodium pump inhibitors on spontaneous acetylcholine release at the neuromuscular junction. **The Journal of Physiology**, v. 181, n. 3, p. 498-505, 1965.

ELMQVIST, D.; FELDMAN, D. S. Calcium dependence of spontaneous acetylcholine release at mammalian motor nerve terminals. **The Journal of Physiology**, v. 181, n. 3, p. 487-97, 1965.

FERGUSON, S. M.; BAZALAKOVA, M.; SAVCHENKO, V.; TAPIA, J. C.; WRIGHT, J.; BLAKELY, R. D. Lethal impairment of cholinergic neurotransmission in hemicholinium-3-sensitive choline transporter knockout mice. **Proceedings of the National Academy of Science USA**, v. 101, n. 23, p. 8762-7, 2004.

FREDJ, N. B.; BURRONE, J. A resting pool of vesicles is responsible for spontaneous vesicle fusion at the synapse. **Nature Neuroscience**, v.12, n. 6, p. 751-8, 2009.

FREMEAU, R. T. Jr.; KAM, K.; QUERSHI, T.; JOHNSON, J.; COPENHAGEN, D. R.; STORM-MATHISEN, J.; CHAUDHRY, F. A.; NICOLL, R. A.; EDWARDS, R. H. Vesicular glutamate transporter 1 e 2 target to functionally distinct synaptic release sites. **Science**, v. 304, n. 5678, p. 1815-9, 2004.

FUJINO, M.; FUJINO, S. An immunohistochemical study of the significance of a new 31,5-KD ouabain receptor protein isolated from cat cardiac muscle. **Japanese Journal of Pharmacology**, v. 67, p. 125-135, 1995.

GANDHI, S. P.; STEVENS, C. F. Three modes of synaptic vesicular recycling revealed by single-vesicle imaging. **Nature** v. 423, n. 6940, p. 591-2, 2003.

GARCÍA-CHACÓN, L. E.; NGUYEN, K. T.; DAVID, G.; BARRETT, E. F. Extrusion of Ca2+ from mouse motor terminal mitochondria via a Na+-Ca2+ exchanger increases post-tetanic evoked release. **The Journal of Physiology**, v. 574, n. 3, p. 663-75, 2006.

GOMEZ, M. V; DINIZ, C. R.; BARBOSA, T. S. A comparison of the effects of scorpion venom tityustoxin and ouabain on the release of acetylcholine from incubated slices of rat brain. **Journal of Neurochemistry**, v. 24, n. 2, p. 331-336, 1975.

HAIMANN, C.; TORRI-TARELLI, F.; FESCE, R.; CECCARELLI, B.; Measurement of quantal secretion induced by ouabain and its correlation with depletion of synaptic vesicles. **The Journal of Cell Biology**, v. 101, p. 1953-65, 1985.

HALL, Z. W. **An Introduction to Molecular Neurobiology**. Sunderland, Massachusetts: Sinauer Associates. 1992.

HALL, Z. W.; SANES, J. R. Synaptic structure and development: the neuromuscular junction. **Cell/Neuron**, suplemento 72/10, p. 99-121, 1993.

HAMLYN, J. M.; BLAUSTEIN, M. P.; BOVA, S.; DU CHARME, D. W.; HARRIS, D. W.; MANDEL, F.; MATHEWS, W. R.; LUDENS, J. H. Identification and characterization of an ouabain-like compound from human plasma. **Proceedings of the National Academy of Science USA,** v. 88, p.6259-63, 1991.

HAMLYN, J. M.; LAREDO, J.; SHAH, J. R.; LU, Z. R.; HAMILTON, B. P. 11-Hydroxilation in the biosyntesis of endogeous ouabain: Multiple implications. **Annals of the New York Academy of Sciences**, v. 986, p. 685-93, 2003.

HARLOW, M.L.; RESS, D.; STOSCHEK, A.; MARSHALL, R. M.; MCMAHAN, U. J. The architecture of active zone material at the frog's neuromuscular junction. **Nature**, v. 409, n. 6819, p. 479-84, 2001.

HERRINGTON, J.; PARK, Y. B.; BABCOCK, D. F.; HILLE, B. Dominant role of mitochondria in clearance of large Ca2+ loads from rat adrenal chromaffin cells. **Neuron**, v. 16, n. 1, p. 219-28, 1996.

HEUSER, J. E.; REESE T. S. Evidence for recycling of synaptic vesicle membrane during transmitter release at the frog neuromuscular junction. **The Journal of Cell** *Biology*, v. 57, p. 315-344, 1973.

HONG, S. J. Reduction of quantal size and inhibition of neuromuscular transmission by bafilomycin A. **Neuropharmacology***,* v. 41, n. 5, p. 609-17, 2001.

JENA, B. P. Molecular machinery and mechanism of cell secretion. **Experimental Biology and Medicine (Maywood)**, v. 230, n. 5, p. 307-19, 2005.

KATZ, B.; MILEDI, R. Propagation of Electric Activity in Motor Nerve Terminals. **Proceedings of the Royal Society of London Séries B,** v. 161, p. 453-82, 1965.

KATZ, B. **Nerve, Muscle and Synapse**. New York: McGraw-Hill Book Company, 1966. 193p.

KATZ, B.; MILEDI, R. Spontaneous and evoked activity of motor nerve endings in calcium Ringer. **The Journal of Physiology**, v. 203, n. 2, p. 459-87, 1969.

KAWAMURA, A.; ABRELL, L. M.; MAGGIALI, F.; BEROVA, N; NAKANISHI, K.; LABUTTI, J.; MAGIL, S.; HAUPERT, G. T. Jr.; HAMLYN, J. M. Biological implication of conformational flexibility in ouabain: observations with two ouabain phosphate isomers. **Biochemistry**, v. 40, n. 19, p. 5835-44, 2001.

KOUDINOV, A. R.; KOUDINOVA, N. V. Essential role for cholesterol in synaptic plasticity and neuronal degeneration. **The FASEB Journal** v. 15, n. 10, p.1858-60, 2001.

LAFONT, F.; VERKADE, P.; GALLI, T.; WIMMER, C.; LOUVARD, D.; SIMONS, K. Raft association of SNAP receptors acting in apical trafficking in Madin-Darby canine Kidney cells. **Proceedings of the National Academy of Sciences USA,** v. 96, n. 7, p. 3734-8, 1999.

LANG, T.; BRUNS, D.; WENZEL, D.; RIEDEL, D.;HOLROYD, P.; THIELE, C.; JAHN, R. SNAREs are concentrated in cholesterol-dependent clusters that define docking and fusion sites for exocytosis. **EMBO Journal,** v. 20, n. 9, p. 2202-13, 2001.

LICHTMAN, J. W.; WILKINSON, R. S.; RICH, M. M. Multiple innervation of tonic endplates revelead by activity-dependent uptake of fluorescent probes. **Nature** v. 314 n. 6009, p. 357-9, 1985.

LINGWOOD, D.; KAISER, H. J.; LEVENTAL, I.; SIMONS, K. Lipid rafts as functional heterogeneity in cell membranes. **Biochemical Society Transactions**, v. 37, n. 5, 955-960, 2009.

LIU, Y.; EDWARDS, R. H. The role of vesicular transport proteins in synaptic transmission and neural degeneration. **Annual Review of Neuroscience**, v. 20, p.125-56, 1997.

LOMEO, R. S.; GOMEZ, R. S; PRADO, M. A.; ROMANO-SILVA, M. A; MASSENSINI, A. R.; GOMEZ, M. V. Exocytotic release of [3H]-acetylcholine by ouabain involves intracellular Ca2+ stores in rat brain cortical slices. **Cellular and Molecular Neurobiology**, v. 23, n. 6, p. 917-27, 2003.

MCFADDEN, S. C.; BOBICH, J. A.; ZHENG, Q. Double-labeled preparation for simultaneous measurement of [3H]-noradrenaline and [14C]-glutamic acid exocytosis from streptolysin-O (SLO)-perforated synaptosomes. **Journal of Neuroscience Methods**, v. 107, n. 1-2, p. 39-46, 2001.

MEUNIER, F. A.; COLASANTE, C.; MOLGO, J. Sodium-dependent increase in quantal secretion induced by brevetoxin-3 in Ca2+-free medium is associated with depletion of synaptic vesicles and swelling of motor nerve terminals in situ. **Neuroscience**, v. 78, n. 3, p. 883-93, 1997.

MISGELD, T.; BURGESS, R. W.; LEWIS, R. M.; CUNNINGHAM, J. M., LICHTMAN, J. W.; SANES, J. R. Roles of neurotransmitter in synapse formation: development of neuromuscular junctions lacking choline acetyltransferase. **Neuron**, v. 36, n. 4, p. 635-48, 2002.

MOLGÓ, J.; PECOT-DECHAVASSINE, M. Effects of carbonyl cyanide m-chlorophenylhydrazone on quantl transmitter release and ultrastructure of frog motor nerve terminals. **Neuroscience**, v. 24, n. 2, p.695-708, 1988.

MONTERO, M.; ALONSO, M. T.; CARNICERO, E.; CUCHILLO-IBÁÑEZ, I.; ALBILLOS, A.; GARCÍA, A. G.; GARCÍA-SANCHO, J.; ALVAREZ, J. Chromaffin-cell stimulation triggers fast millimolar mitochondrial Ca2+ transients that modulate secretion. **Nature Cell Biology**, v. 2, n. 2, p.57-61, 2000.

MURTHY, N. V; DE CAMILLI, P. Cell Biology of the Presynaptic Terminal**. Annual Review of Neuroscience**, v. 26, p. 701-728, 2003.

NARITA, K.; AKITA, T.; OSANAI, M.; SHIRASAKI, T.; KIJIMA, H.; KUBA, K. A Ca2+-induced Ca2+ release mechanism involved in asynchronous exocytosis at frog motor nerve terminals. **The Journal of General Physiology**, v.112, n. 5, p.593-609, 1998.

NARITA, K.; AKITA, T.; HACHISUKA, J.; HUANG, S.; OCHI, K.; KUBA, K. Functional coupling of Ca(2+) channels to ryanodine receptors at presynaptic terminals. Amplification of exocytosis and plasticity. **The Journal of General Physiology**, v. 115, n. 4, p. 519-32, 2000.

NGUYEN, M. L.; PARSONS, S. M. Effects of internal pH on the acetylcholine transporter of synaptic vesicles. **Journal of Neurochemistry**, v. 64, n. 3, p. 1137-42, 1995.

NGUYEN, M. L.; COX, G. D.; PARSONS, S M. Kinetic Parameters of the Vesicular Acetylcholine Transporter: Two Protons are Exchanged for One Acetylcholine. **Biochemistry,** v. 37**,** p. 13400-13410, 1998.

NORDMANN, J. J.; STUENKEL, E. L. Ca(2+)-independent regulation of neurosecretion by intracellular Na+. **FEBS Letters**, v. 292, n. 1-2, p. 37-41, 1991.

NORDMANN, J. J.; LINDAU, M.; STUENKEL, E. L. Sodium, calcium and exocytosis: confessions of calcified scientists. **The Journal of Physiology Paris**, v. 86, p. 15-21, 1992.

OZKAN, E. D.; UEDA, T. Glutamate Transport and Storage in Synaptic Vesicles. **Japanese Journal of Pharmacology** v. **77**, p. 1-10, 1998.

PARSONS, R. L.; CALUPCA, M. A.; MERRIAM, L. A.; PRIOR, C. Empty synaptic vesicles recycle and undergo exocytosis at vesamicol-treated motor nerve terminals. **Journal of Neurophysiology,** vol. 81, n. 6, p. 2696-700, 1999

PARSONS, R. L.; CALUPCA, M. A.; MERRIAM, L. A.; PRIOR, C.; PARSONS, S. M. Transport mechanisms in acetylcholine and monoamine storage. **FASEB Journal** v. 14, n.15, p.2423-34, 2000.

PERIN, M. S.; BROSE, N.; JAHN, R.; SÜDHOF, T. C. Domain structure of synaptotagmin (p65). **The Journal of Biological Chemistry**, v. 266, n. 1, p.:623-9, 1991.

PRADO, M. A., GOMEZ, M. V.; COLLIER, B. Mobilization of a vesamicol-insensitive pool of acetylcholine from a sympathetic ganglion by ouabain. **Journal of Neurochemistry,** v. 61. n. 1, p. 45-56. 1993.

PRADO, M. A. M.; REIS, R. A. M.; PRADO, V. F.; MELLO, M. C. de; GOMEZ, M. V.; MELLO, F. G**.** Regulation of acetylcholine synthesis and storage. **Neurochemistry International,** v. 41, p. 291-299, 2002.

PRADO, V. F.; MARTINS-SILVA, C.; DE CASTRO, B. M.; LIMA, R. F.; BARROS, D. M.; AMARAL, E.; RAMSEY, A. J.; SOTNIKOVA, T.D.; RAMIREZ, M. R.; KIM, H. G.; ROSSATO, J.I.; KOENEN, J.; QUAN, H.; COTA, V. R.; MORAES, M. F.; GOMEZ, M. V.; GUATIMOSIM, C.; WETSEL, W. C.; KUSHMERICK, C.; PEREIRA, G. S.; GAINETDINOV, R. R.; IZQUIERDO, I.; CARON, M. G.; PRADO, M. A. Mice deficient for the vesicular acetylcholine transporter are myasthenic and have deficits in object and social recognition. **Neuron**, v. 51, n. 5, p. 601-12, 2006.

PYLE, J. L.; KAVALALI, E. T.; PIEDRAS-RENTERIA, E. S.; TSIEN, R. W. Rapid reuse of readily releasable pool of vesicles at hippocampal synapses. **Neuron** v. 28, p. 221-231, 2000.

RIBCHESTER, R.R.; MAO F.; BETZ, W. J. Optical measurements of activity-dependent membrane recycling in motor nerve terminals of mammalian skeletal muscle. **Proceedings of the Royal Society B: Biological Sciences,** v. 255, n. 1342, p. 61-66, 1994

RIBEIRO, F. M.; BLACK, S. A. G.; PRADO, V. F.; RYLETT, R. J.; FERGUSON, S. S. G.; PRADO, M. A. M.. The "ins" and "outs" of the high-affinity choline transporter CHT1. **Journal of Neurochemistry,** v. 97, p. 1-12, 2006.

RICHARDS, D. A.; GUATIMOSIM, C.; BETZ, W. J. Two Endocytic Recycling Routes Selectively Fill Two Vesicle Pools in Frog Motor Nerve Terminals. **Neuron**, v. 27, p. 551-559, 2000.

RIZO, J.; SÜDHOF, T. C. Snares and Munc18 in synaptic vesicle fusion. **Nature Reviews. Neuroscience,** v. 3, n. 8, p. 641-53, 2002.

RIZZOLI, S. O.; BETZ, W. J. Synaptic Vesicle Pools. **Nature Reviews/Neuroscience** v. 6, p. 57-69, 2005.

ROBITAILLE, R.; ADLER, E. M.; CHARLTON, M. P. Strategic localization of calcium channels at transmitter release sites of frog neuromuscular synapses. **Neuron,** v. 5, p.773-779, 1990.

RODAL, S. K.; SKRETTING, G.; GARRED, O.; VILHARDT, F.; VAN DEURS, B.; SANDVIG, K. Extraction of cholesterol with metyl-β-cyclodextrin perturbs formation of clathrin-coated endocytic vesicles. **Molecular Biology of the Cell,** v. 10, p. 961-974, 1999.

ROYLE, S. G.; LAGNADO L. Endocytosis at the synaptic terminal. **The Journal of Physiology,** v. 553, n. 2, p. 345-355, 2003.

SALAUN, C.; JAMES, D. J.; CHAMBERLAIN, L. H. Lipid rafts and the regulation of exocytosis. **Traffic** v. 5, n. 4, p. 255-64, 2004.

SANES, J. R.; LICHTMAN, J. W. Induction, Assembly, Maturation and Maintenance of a Postsynaptic Apparatus. **Nature Reviews/Neuroscience**, v. 2, p.791-805, 2001.

SCHENEIDER, R.; VICTOR, W.; NIMTZ, M.; LEHMANNPAR, W. D.; KIRCH, U.; ANTOLOVI C, R.; SCHONER, W. Bovine adrenals contain, in addition to ouabain, a second inhibitor of the sodium pump. **The Journal of Biological Chemistry**, v. 273, n. 2, p. 784-92, 1998.

SIMONS, K.; IKONEN, E. Functional rafts in cell membranes. **Nature,** v. 387, n. 6633, p. 569-72, 1997.

SINGER, S. J.; NICOLSON, G. L. Fluid mosaic model of the structure of cell membranes. **Science** v. 175, n. 23, p. 720-731, 1972.

SÖLLNER, T.; BENNETT, M. K.; WHITEHEART, S. W.; SCHELLER, R. H.; ROTHMAN, J. E. A protein assembly-disassembly pathway in vitro that may correspond to sequential steps of synaptic vesicle docking, activation, and fusion. **Cell**, v. 75, n. 3, p. 409-18, 1993.

STETZKOWSKI-MARDEN, F.; GAUS, K.; RECOUVREUR, M.; CARTAUD, A.; CARTAUD, J. Agrin elicits membrane lipid condensation at sites of acetylcholine receptor clusters in C2C12 myotubes . **Journal of Lipid Research,** v. 47, n. 10, p. 2121-33, 2006.

STROBRAWA, S. M.; BREIDERHOFF, T.; TAKAMORI, S.; ENGEL, D.; MICHAELA, S.; ZDEBIK, A. A.; BOSI, M. R.; REUTHER, K.; JAHN, H.; DRAUGHN A.; JAHN, R.; SUBTIL, A.; GAIDAROV, I.; KOBYLARZ, K.; LAMPSON, M.; KEEN, J.; MCGRAW, T. Acute cholesterol depletion inhibits clathrin-coated pit budding. **Proceedings of the National Academy of Sciences USA,** v. 96, p. 6775-6780, 1999.

SUBTIL, A.; GAIDAROV, I.; KOBYLARZ, K.; LAMPSON, M.; KEEN, J.; MCGRAW, T. Acute cholesterol depletion inhibits clathrin-coated pit budding. **Proceedings of the National Academy of Sciences,** v. 96, p. 6775-6780, 1999.

SÜDHOF, T. C. The Synaptic Vesicle Cycle. **Annual Review of Neuroscience**, v.27, p. 509-547, 2004.

TAKEI, K.; MUNDIGL, O.; DANIELL, L.; DE CAMILLI, P. The synaptic vesicle cycle: a single vesicle budding step involving clathrin and dynamin. **The Journal of Cell Biology,** v. 133, p. 1237-1250, 1996.

THIELE, C.; HANNAH, M.; FARENHOLZ, F.; HUTTNER, W. Cholesterol binds to synaptophysin and is required for biogenesis of synaptic vesicles. **Nature Cell Biology**, v. 2, p. 42-49, 2000.

TORREJAIS, M. M.; SOARES, J. C.; MATHEUS, S. M. M.; CASSEL, F. D.; MELLO, J. M.; BASSO, N. A. Histochemical and SEM evaluation of the neuromuscular junctions from alcoholic rats. **Cell & Tissue**, v.34, n.2, p117-123, 2002.

VAN DER KLOOT, W.; COLASANTE. C.; CAMERON, R.; MOLGÓ, J. Recycling and refilling of transmitter quanta at the frog neuromuscular junction. **The Journal of Physiology**, v. 523, n4 , p. 247-58, 2000.

VAN DER KLOOT, W.; MOLGÓ, J.; CAMERON, R.; COLASANTE, C. Vesicle size and transmitter release at the frog neuromuscular junction when quantal acetylcholine content is increased or decreased. **The Journal of Physiology**, v. 541, n. 2, p. 385-93, 2002.

VAN DER KLOOT, W. A chloride channel blocker reduces acetylcholine uptake into synaptic vesicles at the frog neuromuscular junction. **Brain Research,** v. 961, p. 287-289. 2003.

VIZI, E. S. Stimulation, by inhibition of (Na + -K + -Mg 2+)-activated ATP-ase, of acetylcholine release in cortical slices from rat brain. **The Journal of Physiology**, v. 226, n.1, p. 95-117, 1972.

WANG, P.; SARASWATI, S.; GUAN, Z.; WATKINS, C. J.; WURTMAN, R. J.; LITTLETON, J. T. A Drosophila temperature-sensitive seizure mutant in phosphoglycerate kinase disrupts ATP generation and alters synaptic function. **The Journal of Neuroscience**, v. 24, n. 19, p. 4518-29, 2004.

WASSER, C. R.; ERTUNC, M.; LIU, X.; KAVALALI, E. T. Cholesterol-dependent balance between evoked and spontaneous synaptic vesicle recycling. **The Journal of Physiology,** v. 579, n. 2, p. 413-29, 2007.

WASSER, C. R.; KAVALALI, E. T. Leaky synapses: regulation of spontaneous neurotransmission in central synapses. **Neuroscience**, v. 158, n.1, p. 177-88, 2009.

WEBER, T.; ZEMELMAN, B. V.; MCNEW, J. A.; WESTERMANN, B.; GMACHL, M.; PARLATI, F.; SÖLLNER, T. H.; ROTHMAN, J. E. SNAREpins: minimal machinery for membrane fusion. **Cell**, v. 92, n. 6, p. 759-72, 1998.

WERTH, J. L.; THAYER, S. A. Mitochondria buffer physiological calcium loads in cultured rat dorsal root ganglion neurons. **The Journal of Neuroscience**, v. 14, n. 1, p. 348-56, 1994.

WHITTAM, R.; BLOND, D. M. Respiratory control by an adenosine triphosphatase involved in active transport in brain cortex. **The Biochemical Journal**, v. 92, n. 1, p. 147-58, 1964.

WU Y., YEH F. L., MAO F., CHAPMAN E. R. Biophysical characterization of styryl dye-membrane interactions. **Biophysical Journal**, v. 97, n. 1, p. 101-109, 2009.

YANG, F.; HE, X.; RUSSEL, J.; LU, B.. Ca^{2+} influx-independent synaptic potentiation mediated by mitochondrial Na^{+}-Ca^{2+} exchanger and protein kinase C. **The Journal of Cell Biology**, v. 163, n. 3, 2003.

YOSHINAKA, K.; KUMANOGOH, H.; NAKAMURA, S.; MAEKAWA, S. Identification of V-ATPase as a major component in the raft fraction prepared from the synaptic plasma membrane and the synaptic vesicle of rat brain. **Neuroscience Letters**, v. 363, n. 2, p. 168-72, 2004.

ZAMIR, O.; CHARLTON, M. P. Cholesterol and synaptic transmitter release at crayfish neuromuscular junction. **The Journal of Physiology,** v. 571, p. 83-99, 2006.

ZHAI, R. G.; BELLEN, H. J. The Architecture of the Active Zone in the Presynaptic Nerve Terminal. **Physiology**, v.19, p. 262-270, 2004.